

Characterization of the Pre-Lytic Active Egress of a Non-Enveloped Virus

Inauguraldissertation
der Philosophisch-naturwissenschaftlichen Fakultät
der Universität Bern

vorgelegt von
RAPHAEL WOLFISBERG

von Neuenkirch, LU

Leiter der Arbeit:

Prof. Dr. Christoph Kempf
and
PD Dr. Carlos Ros

Departement für Chemie und Biochemie

Characterization of the Pre-Lytic Active Egress of a Non-Enveloped Virus

Inauguraldissertation
der Philosophisch-naturwissenschaftlichen Fakultät
der Universität Bern

vorgelegt von

RAPHAEL WOLFISBERG

von Neuenkirch, LU

Leiter der Arbeit:

Prof. Dr. Christoph Kempf

and

PD Dr. Carlos Ros

Departement für Chemie und Biochemie

Von der Philosophisch-naturwissenschaftlichen Fakultät angenommen.

Bern,

Der Dekan:

Prof. Dr. Gilberto Colangelo

Abstract

The active egress of enveloped viruses is a well-characterized process and involves budding through host cell membranes. The release of non-enveloped viruses is considered a passive process because it is associated with cellular lysis. However, this basic principle in virology has recently been challenged by several studies suggesting that non-enveloped viruses may also egress by an active process but the mechanisms involved remain largely unknown. Due to their simplicity, the non-enveloped parvoviruses are strongly dependent on host cell functions for their replication and proliferation. Therefore, they are an ideal tool to study virus host-cell interactions. In order to gain insights into the mechanisms involved in the egress of parvoviruses, the late virus maturation steps preceding virus release were studied in two different cell lines.

Minute virus of mice (MVM) is a well-known model parvovirus. Assembly of structural capsid proteins occurs in the nucleus giving rise to icosahedral empty capsid (EC) precursors which are subsequently filled with the viral single-stranded DNA to generate full capsids (FC). By performing anion-exchange chromatography, intranuclear MVM progeny particles were separated based on their net surface charge. Apart from EC, two distinct FC progeny populations arose in the nuclei of infected cells. The first FC population to appear was infectious but was nuclear export deficient. In order to acquire egress potential, this early FC progeny underwent further maturations involving the exposure of the N-termini of the major capsid protein VP2 (N-VP2), as well as phosphorylations of surface residues. While the surface phosphorylations were strictly associated to nuclear export capacity, mutational analysis revealed that the phosphoserine-rich N-VP2 was dispensable. Mutants with a defective processing of N-VP2 showed less efficient delivery of the viral genome to the nucleus, revealing an important role of a precise N-VP2 processing during virus entry. The fact that only the mature phosphorylated population of FC was able to escape from the cells before detectable cell lysis confirms the existence of an active process of virus egress. For cell entry the reverse situation was observed since during endocytic trafficking, incoming virions lost both the N-VP2 termini and the additional surface phosphorylations.

Collectively, these temporally and spatially controlled changes in capsid surface phosphorylation would provide nuclear import and export potential required to complete the life cycle of the karyophilic virus.

Zusammenfassung

Behüllte Viren werden von ihrer Wirtszelle sezerniert, indem sie bei der Knospung Stücke von deren Zellmembran als Bestandteil in die Virushülle integrieren. Für behüllte Viren ist die aktive Freisetzung von Virionen aus infizierten Wirtszellen bereits gut dokumentiert. Die Freisetzung von unbehüllten Viren wird als passiver Vorgang beschrieben, bei dem die Zellmembran durch Zellyse aufgelöst wird, was zur Absonderung der neu gebildeten Virionen führt. Dieser Grundsatz der Virologie wurde in jüngster Zeit durch mehrere Studien in Frage gestellt, die für unbehüllte Viren einen aktiven Mechanismus zur Freisetzung der Virionen aufzeigten. Aufgrund ihrer Einfachheit sind die unbehüllten Parvoviren zur eigenen Vermehrung und Verbreitung stark von ihrer Wirtszelle abhängig. Daher eignen sie sich gut um die Interaktionen zwischen Viren und ihren Wirtszellen zu studieren. Um die Freisetzung von Parvoviren aus ihrer Wirtszelle besser zu verstehen, wurden späte Maturationsschritte im Kern von infizierten Zellen untersucht, welche der Absonderung der neu gebildeten Virionen unmittelbar bevorstehen. Zur Verstärkung der Aussagekraft wurden die Experimente an zwei verschiedenen Zelllinien durchgeführt.

Minute virus of mice (MVM) ist ein gut charakterisiertes Parvovirus, das sich als Modell für diese Studie eignet. Das Kapsid von Parvoviren wird aus Strukturproteinen, den sogenannten Kapsomeren, gebildet. Beim Vorgang der Selbstassemblierung lagern sich im Zellkern 60 solcher Kapsomere spontan und ohne Energieverbrauch zusammen und bilden ein Kapsid mit ikosaedrischer Symmetrie. Diese leeren Kapside werden anschliessend mit der einzelsträngigen viralen DNA bepackt. Neu generierte Virus Partikel wurden in dieser Studie mittels Anionenaustausch Chromatographie nach deren Oberflächenladungen aufgetrennt. Neben den leeren Kapsiden wurden auf diese Weise zusätzlich zwei unterschiedliche Populationen DNA-bepackte virale Partikel separiert. Die erste Population bepackter Viren im Zellkern war infektiös, wurde allerdings nicht ins Zytoplasma exportiert. Der Export aus dem Zellkern wurde der zweiten Population durch weitere Maturation ermöglicht. Die Maturationsschritte beinhalteten die Externalisierung der Amino-Termini des Hauptstrukturproteins VP2 (N-VP2) durch die Poren an den 5-fach Symmetriearchsen des Kapsids, sowie Phosphorylierungen von Aminosäuren auf der Oberfläche der Kapside. Die Phosphorylierungen auf der Kapsooberfläche wurden jeweils nur bei den Kapsiden beobachtet, die aus dem Kern exportiert wurden. Mutanten mit modifizierten N-VP2 Termini konnten hingegen ungehindert aus dem Zellkern exportiert werden. Dies impliziert, dass N-VP2 für diesen Vorgang entbehrlich ist. Es zeigte sich, dass N-VP2 vor allem zur Initierung

der viralen Infektion, sowie zur Reorganisation des Zytoskeletts während der Freisetzung der Viren erforderlich war. Die N-VP2 Mutanten wiesen einen erschwerten Transport des Kapsids zum Zellkern auf. Im Kern wurde weniger mutierte virale DNA quantifiziert was eine verzögerte Replikation zur Folge hatte. Zudem war die Zytolyse infizierter Zellen deutlich verzögert.

Weil vor der Zelltlyse ausschliesslich der vollständig maturierte Virus im Überstand der Zellkultur nachgewiesen wurde, konnte ein aktiver Mechanismus zur Freisetzung der neu gebildeten Virionen bestätigt werden. Obwohl zuerst eine Segregation beider DNA-bepackten Populationen beobachtet wurde konnte die frühe, unreife virale Population durch virus-induzierte Zelltlyse passiv freigesetzt werden. Interessanterweise wurde beim Eindringen der Viren in die Wirtszelle die umgekehrte Situation beobachtet. In den Endosomen wurde N-VP2 proteolytisch abgebaut und saure Phosphatasen entfernten die Phosphorylierungen auf der Kapsidoberfläche.

In dieser Arbeit wurden Phosphorylierungen auf der Kapsidoberfläche eines unbehüllten Virus identifiziert welche zeitlich und räumlich streng kontrolliert werden. Diese Modifikationen auf der Kapsidoberfläche könnten unbehüllten Viren den Import in den Zellkern, beziehungsweise deren Export aus dem Zellkern, ermöglichen. Der Transport in und aus dem Zellkern ist für karyophile Viren unabdingbar zur Vollendung ihres Lebenszyklus. Zur Identifizierung der entsprechenden Phosphorylierungen auf der Kapsidoberfläche sind in Zukunft weitere Untersuchungen notwendig. Zudem bleibt deren spezifischer Einfluss in der aktiven Freisetzung der neu generierten Virionen von der Wirtszelle weiterhin unklar.

Acknowledgements

The present thesis would not have been possible without the support and guidance that I received from many individuals. All of them contributed in one way or another and extended their valuable assistance during the preparation and completion of this study. It is a great pleasure to express my gratitude to all of them in my humble acknowledgement.

Foremost I want to thank Prof. Dr. Christoph Kempf for providing me with the opportunity to complete my PhD in his research group. Thank you very much for your active support and the freedom you gave me during the time in your lab.

I feel deeply indebted and honored to be mentored by PD Dr. Carlos Ros, my direct supervisor, who believed in my abilities and patiently guided me through the whole thesis. I am always grateful for his encouragement and for inspiring me with numerous clever experiments which helped to substantiate my scientific outlook. The joy and enthusiasm he has for our research was exemplary, contagious, and motivated me greatly during my PhD. I received constructive and competent feedback with regards to critical reading of papers as well as coherent presentation and rigorous interpretation of my results. His helpfulness and great sense of humor helped me to overcome experimental setbacks and provided a nice working atmosphere.

I would like to thank all the former and current co-workers in our laboratory: Aurélie Allemann, Chiarina Di Tommaso, Remo Leisi, Nico Ruprecht, Marcus von Nordheim, and Seline Zürcher. Our group has been a source of friendships as well as good collaboration. It was very pleasant to work in such a friendly and helpful environment.

I gratefully acknowledge the funding received towards my PhD from the University of Bern as well as CSL Behring AG.

Further thanks go to Achim Stocker and Walter Aeschimann for their advice and kind help with the ÄKTA chromatography system and for optimizing the chromatography protocols. It has been always interesting to gain further insight into the field of virology from totally different perspectives.

My time at the university of Bern was made enjoyable in large part due to the many friends at the department of chemistry and biochemistry (DCB). I am grateful for the time I spent

with you, for partying together and for the time we spent in the city, on the Gurten or down by the Aare. Special thanks go to Christof Wyss and his family for annually offering us a royal residence in their lovely chalet in Grindelwald during our memorable skiing vacations!

I want to thank Dr. Shweta Kailasan and Dr. Pamela Nicholson for critical review of parts of the present PhD thesis and for their helpful annotations in revising my English language.

Many thanks go to my best friends Martin Buob and Christian Schnyder for frequently distracting me from work and always giving me a warm welcome back at home in Neuenkirch. They always kept me well informed about the most recent happenings in Lucerne, thus I never felt fully disconnected. I really enjoyed the countless amazing moments I could share together with you whether it be just having a beer in a bar, enjoying the atmosphere at an open-air concert, or traveling around and discovering new places. In addition, I really appreciate the many barbecues I had together with you and our friends at Sagiweg 3 in Neuenkirch!

I would like to thank Stefan Hofstetter for pitching L^AT_EX to me and for rescuing me from the flaws of Microsoft word. I appreciate his invaluable advice and his patient help with the organization of the template file. It helped me definitely to save a lot of time, energy and pain!

I want to thank Markus Antener, my long-standing flat mate, for the funny time we had together and for bearing me for eight years! Thanks a lot for all the computer support and for providing me always with the latest software. I thank Marion Landolt for always arranging our flat with many flowers, paintings, pictures, and photos, thus making it a pleasant and comfortable place to live. I loved a lot her “bündnerische” nature and her crazy ideas. Thank you both for regularly taking me out and for all the relaxing activities we undertook together.

Last but definitely not least I would like to express my sincere gratitude to my lovely family. A special thanks to my parents Beat and Pia for all of the sacrifices that you have made on my behalf. Your faith in me was what sustained me thus far. Thanks for your thoughtfulness, encouragement, and financial support. You were all the time on hand with help and advice for me. I further thank Chantal, Nadine, and Anja for being the best sisters and for their warmth and words of advice. Thank you.

To my friends in Madrid

Un agradecimiento profundo al profesor José María Almendral del Río por su colaboración y por hacer posible mi breve estancia en el Centro de Biología Molecular Severo Ochoa (CBMSO) en la Universidad Autónoma de Madrid (UAM). Muchas gracias por hacer los días tan agradables en tu laboratorio y por periódicamente sacarnos a pasear para comer en el centro. Quedo en deuda contigo por haber puesto a mi disposición gran cantidad de material, anticuerpos y mutantes incluso, después de mi partida.

Especial mención merecen Nooshin Bayat y Lorena Gallego Villar por todas las chulas actividades que hicimos juntos en Madrid. Ha sido un verdadero placer conocerlos y descubrir parte de Madrid con vosotros. Fue muy divertido e interesante conocer Madrid, la comida rica, la cultura y las fiestas españolas! Muchas gracias por todos los buenos momentos que compartimos.

Quiero agradecer a mis queridos compañeros que trabajan en Madrid. A Carlos Dominguez Redondo, Jon Gil Ranedo, Josefa González Nicolás, Marta Pérez Illana y Aroa Tato de la Torre por haberme acogido tan amablemente en el grupo y por el ambiente de trabajo muy divertido y socorrido. Muchas gracias a Sandra Arduim Brasil, Celia Medrano Rodríguez, Alfonso Oyarzabal Sanz, Pablo Pérez Carillo y Patricia Yuste Checa por las conversaciones interesantes a la hora de comer y la paciencia que tuvieron con mi pobre español.

Raphael Wolfisberg
University of Bern
September 2015

Nomenclature

AAV	Adeno-associated virus	FCS	Fetal calf serum
AMDV	Aleutian mink disease virus	FGFR1	Fibroblast growth factor receptor 1
ATP	Adenosine triphosphate	FPV	Feline parvovirus
ATPase	Adenosine triphosphatase	GmDNV	Galleria mellonella densovirus
B19V	Human parvovirus B19	H1-PV	Parvovirus H1
BC	Basic cluster	HBoV	Human Bocavirus
Bp	Base pair	HGFR	Hepatocyte growth factor receptor
BPV	Bovine parvovirus	HIV	Human immunodeficiency virus
CD	Cytochalasin D	hpi	Hours post-infection
ChPV	Chicken parvovirus	HRP	Horseradish peroxidase
CLIC	Clathrin-independent carrier	HSPG	Heparan sulphate proteoglycan
CPV	Canine parvovirus	IF	Immunofluorescence microscopy
CRE	cAMP-responsive element	Ig	Immunoglobulin
cRF	Closed replicative form DNA	IgG	Immunoglobulin G
CRM1	Chromosome region maintenance 1	IP	Immunoprecipitation
CV	Column volume	ITR	Inverted terminal repeat
DCB	Department of Chemistry and Biochemistry	kb	Kilobase
DMEM	Dulbecco modified Eagle's medium	kDa	Kilodalton
DNA	Deoxyribonucleic acid	LamR	Laminin receptor
dRF	Dimeric replicative form DNA	LMB	Leptomycin B
dsDNA	Double-stranded DNA	m. u.	Map unit
EC	Empty capsid	mAb	Monoclonal antibody
EGFR	Epidermal growth factor receptor	mRF	Monomeric replicative form DNA
EM	Electron microscopy	mRNA	messenger RNA
ER	Endoplasmic reticulum		
FC	Full capsid		

MVM	Minute virus of mice	pre-mRNA	messenger RNA precursor
MVMi	Immunosuppressive strain of MVM	PTM	Post-translational modification
MVMP	Prototype strain of MVM	qPCR	Quantitative PCR
MW	Molecular weight	RF	Replicative form
ND	Nocodazole	RHR	Rolling hairpin replication
NHP	Nonhuman primate	RNA	Ribonucleic acid
NIH	National institutes of health	RSS	Runting-stunting syndrome
NLM	Nuclear localization motif	SA	Sialic acid
NLS	Nuclear localization signal	SAT	Small alternatively translated protein
NPC	Nuclear pore complex	SCID	Severe combined immunodeficiency
NS	Non-structural (protein)	SN	Supernatant
nt	Nucleotide	sPLA ₂	Secretory PLA ₂
ORF	Open reading frame	ssDNA	Single-stranded DNA
PARV4	Human parvovirus 4	SV40	Simian vacuolating virus 40 or Simian virus 40
PCNA	Proliferating cell nuclear antigen	TfR	Transferrin receptor
PCR	Polymerase chain reaction	TGN	Trans Golgi network
PDGFR	Platelet-derived growth factor	TuPV	Turkey parvovirus
PEC	Poult enteritis complex	VLP	Virus-like particle
PEMS	Poult enteritis mortality syndrome	VP	Viral protein
PFU	Plaque-forming unit	VP1u	VP1 unique region
PIF	Parvovirus initiation factor	WB	Western blotting
PLA ₂	Phospholipase A ₂		
PPV	Porcine parvovirus		

Contents

Abstract	I
Zusammenfassung	III
Acknowledgements	V
Nomenclature	IX
I. Introduction	1
1. Discovery and Brief History	3
2. Taxonomy	5
2.1. The Subfamily <i>Parvovirinae</i>	6
2.1.1. <i>Amdoparvovirus</i>	6
2.1.2. <i>Aveparvovirus</i>	7
2.1.3. <i>Bocaparvovirus</i>	7
2.1.4. <i>Copiparvovirus</i>	8
2.1.5. <i>Dependoparvovirus</i>	9
2.1.6. <i>Erythroparvovirus</i>	9
2.1.7. <i>Protoparvovirus</i>	10
2.1.8. <i>Tetraparvovirus</i>	10
3. Morphology	13
4. The Rugged Virion	15
4.1. Physicochemical Properties	15
4.2. Atomic Model	16
4.3. Structural Proteins	18

Contents

4.4.	Functional Domains	18
4.4.1.	The Phospholipase A ₂ Motif	19
4.4.2.	The Nuclear Localization Signal	20
4.4.3.	The Nuclear Localization Motif	21
5.	Genome Architecture	23
5.1.	The MVM Left- and Right-End Telomeres	23
5.1.1.	Terminal Resolution <i>versus</i> Asymmetric Junction Resolution	24
5.2.	Genetic Variability	25
6.	Host Range and Specificity	27
6.1.	Tissue Tropism Determinants	27
6.2.	Pathogenicity Determinants	28
6.3.	Comparison of Tissue Tropism and Pathogenicity Determinants among Parvoviurses	29
7.	The Parvovirus Life Cycle	31
7.1.	Receptor Binding	32
7.2.	Receptor-Mediated Endocytosis	34
7.3.	Endosomal Trafficking and Capsid Rearrangements	35
7.4.	Endosomal Escape	36
7.5.	Cytosolic Trafficking and Interactions with the Proteasome	37
7.6.	Nuclear Targeting	38
7.6.1.	Nuclear Translocation of the Incoming Virion	38
7.6.2.	Nuclear Translocation of the Structural Proteins	40
7.7.	Non-Structural Proteins	41
7.7.1.	Non-Structural Protein 1	41
7.7.2.	Non-Structural Protein 2	42
7.7.3.	Small Alternatively Translated Protein	42
7.8.	Replication	43
7.9.	Transcription and RNA Processing	45
7.10.	Assembly	48
7.11.	DNA Packaging	49
7.12.	Nuclear Export	50
7.13.	Egress	52

8. Aim of the Thesis and Experimental Strategy	53
8.1. Goals	53
8.2. Experimental Strategy	53
II. Methods	55
9. Standard Laboratory Protocols	57
9.1. Cell Cultures	57
9.1.1. Freezing and Thawing of Cells	57
9.2. Virus Stocks	57
9.2.1. Separation of Empty and Full Capsids	58
9.3. Freezing Bacteria Stocks in Glycerol	58
9.4. Fast Protein Liquid Chromatography	58
9.4.1. Anion-Exchange Chromatography	59
9.5. Quantitative PCR	60
9.6. Virus Infection	61
9.7. Transfection	62
9.8. Cell Fractionation	62
9.8.1. Nuclei Isolation	62
9.8.2. Extraction of the Cytoplasm	62
9.9. Immunoprecipitation	62
9.10. Dot Blot	63
9.11. SDS-PAGE and Western Blotting	63
9.12. Enzymatic Reactions	64
III. Results	65
10. Manuscript	67
Late Maturation Steps in the Nucleus Preceding Pre-Lytic Active Egress of Progeny Parvovirus	67
11. Supplementary Data	111
11.1. The Phosphoserine-Rich N-VP2 of MVM Facilitates Nuclear Targeting and Assists in Cytolysis	111
11.2. NS2-Crm1 Interaction is Required for Nuclear Export but Not for the Late Nuclear Maturation	114

Contents

11.3. The Role of Empty Capsids During the Infection	116
11.3.1. Isolation and Characterization of Empty Capsids	116
11.3.2. Empty Capsids Specifically Bind to Sialic Acid	116
11.3.3. Preferential Binding of Full Capsids to Murine Fibroblasts	118
11.3.4. Full Capsids have Better Binding Capacity to Sialic Acids than Empty Capsids	118
11.4. AEX as a Novel Tool to Study the Surface Conformation of Small Non-Enveloped Viruses	120
IV. Conclusion	125
V. Appendix	129
12. Materials	131
12.1. Infectious Clone of MVMp (pIC_MVMp)	131
12.1.1. Plasmid Map of pIC_MVMp	131
12.1.2. Complete Sequence of pIC_MVMp	132
12.2. Chemicals and Compounds	135
12.3. Buffers	138
12.3.1. General Buffers	138
12.3.2. Anion-Exchange Chromatography	139
12.3.3. Agarose Gel Electrophoresis	139
12.3.4. Western Blot	140
12.4. Kits	141
12.5. Enzymes	142
12.6. Antibodies	142
12.6.1. Primary Antibodies	142
12.6.2. Secondary Antibodies	143
12.7. Media	143
Bibliography	145
Declaration	170

List of Figures

2.1.	The Subfamily <i>Parvovirinae</i>	6
3.1.	Parvovirus Surface Topology Groups	13
4.1.	Structure of MVM	17
4.2.	The Cleavage Sites of Different Types of PLAs	19
4.3.	Nuclear Localization Signal	20
4.4.	Nuclear Localization Motif	21
5.1.	Genome Architecture of MVM	26
7.1.	Life Cycle of MVM	31
7.2.	Rolling Hairpin Replication	43
7.3.	Transcription Map of MVM	47
9.1.	Schematic Outline of the ÄKTA Chromatography System	58
S1.	Nuclear Import, Export, and Cytotoxicity During an Infection with 5SG Virions .	112
S2.	NS2-Crm1 Interaction is Required for Nuclear Export but Does Not Influence the Late Nuclear Maturation of MVM	115
S3.	Purification and Analysis of Full Capsids and Empty Capsids	117
S4.	Specific Binding of Full Capsids and Empty Capsids to Sialic Acid	117
S5.	Full Capsids Bind More Efficiently to Sialic Acid than Empty Capsids	119
S6.	N-VP2 Exposure Alone is not Sufficient for the Better Binding to Sialic Acid Moieties	121
S7.	Anion-Exchange Chromatography Performed with Other Parvoviruses	123
11.8.	Model of Nuclear Import and Export of MVM	128
12.1.	Plasmid Map of the Infectious Clone of MVMP	131

List of Tables

2.1.	Taxonomy for the Subfamily <i>Parvovirinae</i>	11
7.1.	Parvoviruses and their Receptors	33
9.1.	Cleaning of the Mono Q™ HR 5/5 AEX Column	59
9.2.	Master Mix for Quantitative PCR	60
9.3.	PCR Conditions	60
9.4.	Primers	61
12.1.	Chemicals and Compounds	135
12.2.	General Buffers	138
12.3.	Anion-Exchange Chromatography Buffers	139
12.4.	Agarose Gel Electrophoresis Buffers	139
12.5.	Western Blot Buffers	140
12.6.	Ready-to-Use Reaction Systems (Kits)	141
12.7.	Enzymes	142
12.8.	Primary Antibodies	142
12.9.	Secondary Antibodies	143
12.10.	Media	143

Part I

Introduction

1. Discovery and Brief History

Minute virus of mice (MVM) is a small, non-enveloped autonomous replicating parvovirus. Two variant forms of MVM that share 96 % nucleotide (nt) sequence identity [394] have been discovered. MVMP¹, the prototype strain, was isolated and characterized by Crawford in 1966. It originated from a contaminated murine adenovirus stock and was shown to replicate efficiently in mouse fibroblasts [138]. The virus was plaque purified in 1972 [440] and the resulting strain was designated MVM(p) for prototype [428]. Another strain was recovered from the culture fluid of infected murine EL-4 T-cell lymphoma cells by Bonnard and colleagues in 1976 [58]. This strain efficiently replicates in lymphocytes and is immunosuppressive for allogeneic mixed leukocyte cultures as it inhibits the generation of cytolytic T lymphocytes [163]. Therefore, it was referred to as immunosuppressive strain MVMi [305]. Both strains are well characterized and reciprocally restricted for growth in each other's murine host cell.

Since its discovery nearly 50 years ago, MVM served as an interesting model virus to dissect the molecular mechanisms of tissue tropism, capsid dynamics associated with endosomal trafficking, as well as viral deoxyribonucleic acid (DNA) replication and packaging. Furthermore, it gained increasing interest as an important tool for cancer therapy due to its oncolytic capabilities and currently represents a commonly accepted parvovirus model.

¹ MVMP was used as a model parvovirus in the present thesis. For the sake of simplicity MVM prototype (MVMP) will be referred to as MVM throughout this document with Chapter 6, pp. 27 - 29, as the only exception.

2. Taxonomy

The classification of the family *Parvoviridae* is based on morphological and functional characteristics. Parvoviruses are ubiquitous pathogens that belong to one of the smallest DNA-containing viruses. Hence, the prefix “parvum” that means small in Latin. The name “parvovirus” was first introduced to the literature by Carlos Brailovsky, in an early attempt to establish a latinized binomial taxonomy system for viruses, in 1966 [64]. The age of the family *Parvoviridae* may exceed 40 to 50 million years [39]. Apart from their ancient history, the genomes of parvoviruses were affirmed to display similar high mutation rates to ribonucleic acid (RNA) viruses [173, 185, 412, 413, 432, 487]. Such high mutation rates in conjunction with the long history might be a reason for the vast genetic divergence and extensive diversity seen within the family. The family *Parvoviridae* comprises of non-enveloped, isometric viruses that contain linear single-stranded DNA genomes. Indeed, parvoviruses are the only viruses in the known biosphere that have both single-stranded and linear DNA genomes. The encapsidated single genomic molecule is 4-6 kilobases (kb) in length and terminates in palindromic duplex hairpin telomeres. In general, there are two large open reading frames (ORF1 and ORF2) encoding for the non-structural (NS) protein(s) and the viral capsid protein(s) (VPs), respectively. In some cases, an additional ORF3 has been identified that encodes an accessory protein, such as NP1, a NS protein only found in members of the genus *Bocaparvovirus* and in porcine parvovirus (PPV) 4 a member of the genus *Copiparvovirus* [87, 90, 262]. As a consequence of such a simple genome, parvoviruses are highly dependent on their host for diverse functions in their reproduction [111, 452]. The terminal hairpins are fundamental for their unique replication strategy and serve as an invariant hallmark for classification. Members of the family *Parvoviridae* infect a wide variety of hosts, ranging from insects to primates. Depending on their host range, members of the family *Parvoviridae* are subdivided into the subfamilies *Parvovirinae* infecting vertebrates and *Densovirinae* infecting insects and other arthropods, respectively. The subfamily *Parvovirinae* is further subdivided into eight genera: *Amdoparvovirus*, *Aveparvovirus*, *Bocaparvovirus*, *Copiparvovirus*, *Dependoparvovirus*, *Erythroparvovirus*, *Protoparvovirus*, and *Tetraparvovirus* (see Figure 2.1, p. 6) [108]. The subdivision into the eight genera is based on differences in transcription maps, organization of the inverted terminal repeats (ITRs), the ability to replicate efficiently either autonomously or with helper virus, the sense of the single-stranded DNA (ssDNA) that is packaged into separate virions, and sequence homology amongst the subfamily *Parvovirinae* [241, 286]. The complete virus list encompassing all members of the subfamily *Parvovirinae* is summarized in Table 2.1, pp. 11 - 12.

2. Taxonomy

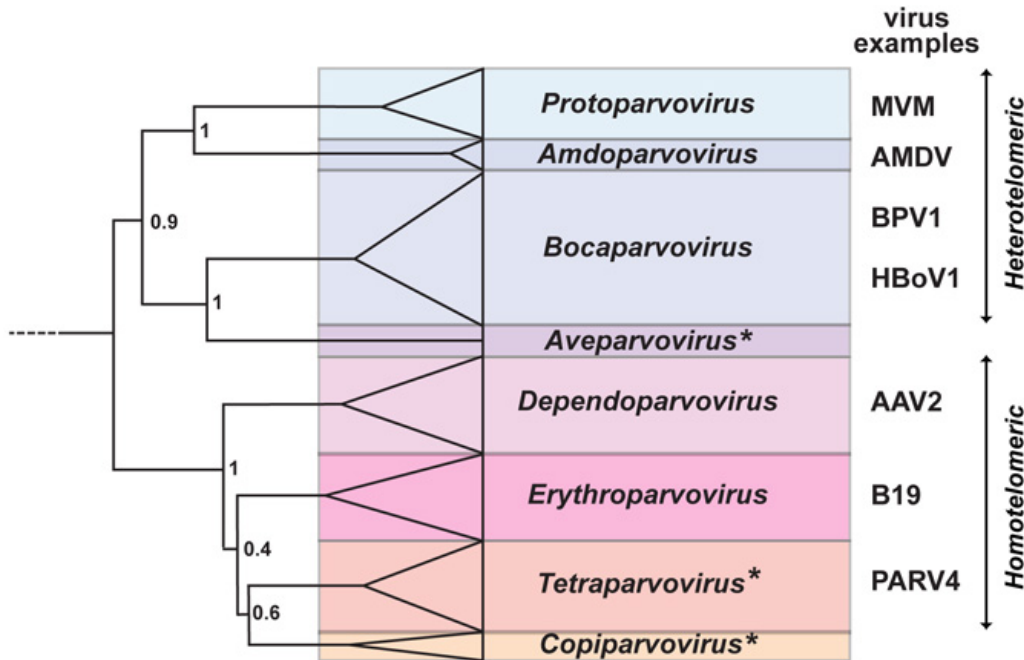


Figure 2.1.: The subfamily *Parvovirinae*. The genera of the subfamily *Parvovirinae* are depicted in a phylogenetic tree. Phylogenetic analysis is based on the amino acid sequence of NS1. The size of the color block for each genus indicates the relative number of species currently recognized, as an indicator of its diversity. Asterisks denote the names of new genera. This figure was adapted from reference [127].

2.1. The Subfamily *Parvovirinae*

2.1.1. *Amdoparvovirus*

Mature virions exclusively contain negative strand genomic DNA of approximately 4.8 kb in length harboring dissimilar palindromic sequences at each end [9, 53]. A single promoter located at map unit (m. u.)² 3 at the left end of the genome generates all messenger RNA (mRNA) transcripts of Aleutian mink disease virus (AMDV). Polyadenylation may occur at either the proximal site or at the distal site of the genome. Thus, the transcription profile of the genus *Amdoparvovirus* most closely resembles that of the genus *Erythroparvovirus* [377]. Only two distant species have been reported. Firstly, *Carnivore amdoparvovirus 1*, which comprises only AMDV and secondly, *Carnivore amdoparvovirus 2*, which encompasses solely gray fox amdovirus [268]. Permissive replication is tightly restricted to Crandell feline kidney cells. The virion surface displays three mounds elevated around the threefold icosahedral axis of symmetry. Several structure features were ascertained to be similar to those found in human parvovirus B19 (B19V), canine parvovirus (CPV), feline parvovirus (FPV), and MVM. Such appearance is comparable to those observed

² Map units are commonly accepted units that relate to the position in the genome. The parvoviral genomes are arbitrarily subdivided into 100 m. u.

2.1. The Subfamily *Parvovirinae*

for the genus *Dependoparvovirus* [303]. Remarkably, there is no evidence of a phospholipase 2A enzymatic core within the naturally truncated N-VP1 terminus of members belonging to the genus *Amdoparvovirus* as it is common to the other genera of the subfamily *Parvovirinae* [241].

2.1.2. *Aveparvovirus*

Aveparvovirus is a new genus within the subfamily *Parvovirinae* that comprises of the species chicken parvovirus (ChPV) and turkey parvovirus (TuPV). The name *Aveparvovirus* is derived from avian parvoviruses, referring to the hosts from which the members were isolated. Although these viruses were identified for years in the intestinal tracts of poultry [244, 245, 454], analysis of the complete sequence has been reported only recently. Phylogenetic study of the genomic sequences revealed that interestingly, ChPV and TuPV do not group phylogenetically with goose parvovirus and duck parvovirus, that are members of the genus *Dependoparvovirus*. It has been clearly demonstrated that ChPV, along with the closely related TuPV, represents the prototype of a novel genus within the subfamily *Parvovirinae* [248, 515]. Identical direct repeat sequences flank the genome at both the 3' and the 5' end. Each of which contains a 39 nt ITR that is predicted to form a hairpin structure. ChPV and TuPV feature an overall genome organization similar to that of members of the genus *Bocaparvovirus* [144]. Although it has been demonstrated that ChPV can induce clinical signs in broiler chickens that show characteristics of the runting-stunting syndrome (RSS) [243], the role of avian parvoviruses in the aetiology of enteric diseases in poultry still remains to be demonstrated. RSS, also referred to as malabsorption syndrome, is characterized by significantly decreased egg hatchability, poorly developed hatched chickens, serious growth retardation, diarrhoea, enteritis, disturbed feathering, low vitality, and bone disorders [184, 350, 363]. Currently, the pathogenicity of TuPV has not been investigated yet. The predominant enteric diseases in turkeys are known as poult enteritis complex (PEC) [27] or the more drastic poult enteritis mortality syndrome (PEMS) [395]. Understanding the role of avian parvoviruses in PEMS, PEC, and RSS is of great interest due to the economic losses resulting from enteric diseases in poultry. [515].

2.1.3. *Bocaparvovirus*

The name of the genus is derived from bovine and canine, referring to the two hosts of the first identified members of this genus. The genomes of members of the genus *Bocaparvovirus* are quite distinct from all other viruses in the subfamily *Parvovirinae*. As the members of the genera *Protoparvovirus* and *Amdoparvovirus* they contain non-identical imperfect palindromic sequences at both ends of their 5.5 kb genome. Mature virions contain mainly, but not exclusively, negative strand ssDNA [88, 404]. All RNA transcripts are generated from a single P4 promoter at the left-hand end of the genome. The transcripts are alternatively spliced and polyadenylated either at an internal site or at the 3'-end of the genome [378]. Noteworthy, bovine parvovirus

2. Taxonomy

(BPV), the main representative, encodes a 22.5 kilodalton (kDa) nuclear phosphoprotein, NP1, whose function still remains unknown. This protein is distinct from any other parvovirus-encoded polypeptide [262]. A human bocavirus (HBoV) was first described in 2005, when it was detected in nasopharyngeal aspirates of young children with respiratory tract infection [10, 11]. More recently, HBoV has been identified in diarrheal feces of children with gastroenteritis [467]. HBoV infection is associated with acute respiratory symptoms and is usually detected in children under 2 years of age [35, 295, 301]. HBoV infections have been reported world-wide and HBoV was often isolated in respiratory samples of diseased as well as asymptomatic patients sometimes long after the primary infection. Therefore, it can be frequently detected even though it is not likely acting as a pathogen, thus complicating the use of polymerase chain reaction (PCR) in diagnostics. Furthermore, long-term persistence may explain that HBoV infection among adults was predominantly reported in association with immunosuppression or immunodeficiency [256, 295].

2.1.4. *Copiparvovirus*

Based on phylogenetic analysis, the genus *Copiparvovirus* encompasses PPV4 and BPV2. PPV4 was identified in clinical samples from swine herds [50, 90, 218] and represents a distinct branch together with BPV2 [10]. The name *Copiparvovirus* refers to cows and pigs, the hosts from which members of that genus were isolated. PPV4 is unique in that it is phylogenetically most closely related to BPV2 but the coding capacity and genome organization resemble more those of viruses of the genus *Bocaparvovirus*. While the ORF3 encoded proteins of the three recognized *Bocaparvovirus* members share amino acid identities of 43.3-47.0 % among themselves, the PPV4 ORF3 encoded protein does not display homology with any protein in the GenBank database [90, 218]. Recently, two novel porcine parvoviruses, PPV5 and PPV6, were discovered [335, 500]. Characterization of their sequences revealed that their full-length genomes are approximately 6 kb in length. As a consequence of this capacious genome size, especially their capsid protein encoding genes are exceptionally large. Interestingly, the genomic organization of PPV5 and PPV6 is different from PPV4 in that they lack the extra ORF3 in the middle of the genome. Moreover, PPV5 as well as PPV6 possess the conserved putative secretory phospholipase A₂ (sPLA₂) motif which is present in the capsid protein of most parvoviruses but is lacking in PPV4. In spite of considerable differences in the genomic organization between BPV2, PPV5, and PPV6 on the one hand and PPV4 on the other hand, phylogenetic analysis revealed a close evolutionary relationship of these viruses, suggesting that they share the same immediate ancestor [335, 499]. Since members of the genus *Copiparvovirus* were discovered quite recently, their biological characteristics, relatedness to disease, and potential clinical manifestations are still not fully understood [90, 218, 335, 499]. Especially, Kresse strain of porcine parvovirus belonging to the genus *Protoparvovirus* is known to be an important pathogen responsible for

2.1. The Subfamily *Parvovirinae*

embryonic and fetal death in piglets, resulting in considerable losses in the pig industry worldwide [253, 307, 308, 464]. In order to clarify the precise role of the most recently discovered members of the genus *Copiparvovirus* as causative agents of reproductive failure in breeding animals, more comprehensive epidemiologic studies are required in the future [335].

2.1.5. *Dependoparvovirus*

Positive and negative strand ssDNA is distributed indifferently among mature virions belonging to the genus *Dependoparvovirus* [41, 389]. The 4.7 kb DNA molecule contains identical ITRs of 145 nt, the first 125 nt of which form a palindromic sequence [288]. Three mRNA promoters that are located at m. u. 5, 19, and 40 initiate transcription that can be terminated in two polyadenylation sites located at the right-hand end or alternatively, in the middle of the genome [188, 289]. Common for all currently accepted replication-defective members of the genus *Dependoparvovirus* is their strict dependence upon helper adenoviruses or herpesviruses [21, 74, 212]. Therefore, their host range tropism strongly depends on the one of the helper virus. The only exceptions are the autonomously replicating duck and goose parvoviruses which are also comprised within the genus *Dependoparvovirus* based on phylogenetic analysis [241]. The most important members of this genus are the adeno-associated viruses (AAV). They attract considerable interests since some of them, including AAV-2, have been reported to integrate site-specifically into the human genome [250–252, 399]. This characteristic makes AAV a promising candidate for creating viral vectors for gene therapy [143, 313]. As a well characterized member of the *Dependoparvoviruses*, AAV-2 represents the model virus among this genus.

2.1.6. *Erythroparvovirus*

Equivalent numbers of positive and negative sense ssDNA are packaged into infectious virions of the genus *Erythroparvovirus*. As in the case with the genus *Dependoparvovirus*, the 5.5 kb ssDNA molecule contains identical ITRs of 383 nt in length at both the 3' and the 5' end. The first 365 nt of those secondary elements form palindromic sequences [146]. Transcription is regulated by a single mRNA promoter located at m. u. 6 [153]. A distal polyadenylation site for use in termination of RNA synthesis is located at the far right side. Additionally, transcripts may be terminated at an unusual internal polyadanylation site in the middle of the genome [347]. Viruses belonging to this genus are highly erythrotropic, meaning that efficient replication only occurs in rapidly dividing erythroid progenitor cells, such as erythroblasts and megakaryocytes present in the bone marrow. B19V, a widespread human pathogen that causes fifth disease, polyarthropathia, anemic crises in children with underlying hematological diseases (e.g. sickle cell anemia or thalassemia) and intrauterine infections (with hydrops fetalis in some cases) [207] represents the model virus among the genus *Erythroparvovirus*.

2. Taxonomy

2.1.7. *Protoparvovirus*

Kilham Rat virus, a member of the genus *Protoparvoviruses* was the first member of the subfamily *Parvovirinae* to be discovered in 1959 [239]. Some members of the genus contain positive strand DNA in variable proportions up to 50 % [36]. However, in mature virions of most members, virtually only negative strand DNA occurs. What they have in common are their hairpin structures at both the 5' and 3' ends of the linear 5 kb ssDNA molecule that differ in both sequence and predicted structure [20]. Transcription of the genome is regulated by two mRNA promoters at m. u. 4 and 38 [368]. There is only one polyadenylation site at the 3' end. Viral replication provokes characteristic cytopathic effects in cell culture. Many species display hemagglutination with erythrocytes of one or several species, but not enforcedly of their natural host [194]. The genus *Protoparvovirus* is primarily represented by MVM [241, 441].

2.1.8. *Tetraparvovirus*

The genus *Tetraparvovirus* is a genus that has been recently described. To date, six species have been discovered, which were isolated from humans [227], chimpanzees, baboons [415], cows, pigs [2, 260, 266], as well as sheep [459]. RNA transcripts that encode the NS proteins or the VPs are generated from two promoters that are located at m. u. 6 and 38, respectively. Transcription can be terminated in two polyadenylation sites located at the right-hand end of the genome or alternatively, at an internal polyadenylation site. Since the full-length genome has not been sequenced yet, information of the terminal repeats is still lacking [284]. Analysis of the NS1 protein revealed a G2/M cell cycle arrest induced in NS1-expressing hematopoietic stem cells that clearly involved the predicted helicase motifs [225, 317, 473] of NS1. To date, no phospholipase A₂ (PLA₂)-like activity of expressed VP1 unique region (VP1u) polypeptides has been demonstrated for any member of the genus *Tetraparvovirus* [284]. Human parvovirus 4 (PARV4) is one of the only four groups of parvoviruses that is known to infect humans besides B19V, HBoV, and AAV. It was first reported in an intravenous drug user who was positive for hepatitis B virus infection in 2005. The patient suffered from arthralgia, confusion, diarrhea, fatigue, neck stiffness, night sweat, pharyngitis, and vomiting. PARV4 represents a phylogenetic deeply rooted lineage between avian dependoviruses and BPV type 3 [227]. So far, most evidence about PARV4 transmission comes from patients who had engaged in high risk behaviour for blood borne viral infections, where PARV4 infection basically was observed to be strongly associated with hepatitis C virus and human immunodeficiency virus (HIV) infection [296, 419, 506]. However, there are several reports of parenteral transmission in the absence of HIV, hepatitis B virus, or hepatitis C virus. PARV4 immunoglobulin G (IgG) has been documented independently from other blood borne viruses among injecting drug users [418], in haemophilia patients [414], and in patients who were subjected to intra-muscular injections in the past [261]. Currently, no definitive clinical syndrome has been associated with PARV4 infection and there is no evidence for a potential pathogenicity

2.1. The Subfamily *Parvovirinae*

of related members of the genus *Tetraparvovirus* in animals [260]. PARV4 viraemia appears to be asymptomatic [352] and co-existing blood borne viruses do not increase severity [506].

Table 2.1.: Taxonomy for the subfamily *Parvovirinae*

Genus	Species	Virus / virus variants	Abbr.	ACNO ³
<i>Amdoparvovirus</i>	<i>Carnivore amdoparvovirus 1</i>	Aleutian mink disease virus	AMDV	JN040434
	<i>Carnivore amdoparvovirus 2</i>	Gray fox amdovirus	GFAV	JN202450
<i>Aveparvovirus</i>	<i>Galliform aveparvovirus 1</i>	Chicken parvovirus	ChPV	GU214704
		Turkey parvovirus	TuPV	GU214706
<i>Bocaparvovirus</i>	<i>Carnivore bocaparvovirus 1</i>	Canine minute virus	CnMV	FJ214110
	<i>Carnivore bocaparvovirus 2</i>	Canine bocavirus 1	CBoV	JN648103
<i>Carnivore bocaparvovirus 3</i>		Feline bocavirus	FBoV	JQ692585
	<i>Pinniped bocaparvovirus 1</i>	California sea lion bocavirus 1	CslBoV1	JN420361
<i>Pinniped bocaparvovirus 2</i>		California sea lion bocavirus 2	CslBoV2	JN420366
	<i>Primate bocaparvovirus 1</i>	California sea lion bocavirus 3	CslBoV3	JN420365
<i>Primate bocaparvovirus 2</i>		Human bocavirus 1	HBoV1	JQ923422
		Human bocavirus 3	HBoV3	EU918736
<i>Primate bocaparvovirus 2</i>		Gorilla bocavirus	GBoV	HM145750
		Human bocavirus 2a	HBoV2a	FJ973558
<i>Primate bocaparvovirus 2</i>		Human bocavirus 2b	HBoV2b	FJ973560
		Human bocavirus 2c	HBoV2c	FJ170278
<i>Primate bocaparvovirus 2</i>		Human bocavirus 4	HBoV4	FJ973561
	<i>Ungulate bocaparvovirus 1</i>	Bovine parvovirus	BPV	DQ335247
<i>Ungulate bocaparvovirus 2</i>		Porcine bocavirus 1	PBoV1	HM053693
		Porcine bocavirus 2	PBoV2	HM053694
<i>Ungulate bocaparvovirus 3</i>		Porcine bocavirus 6	PBoV6	HQ291309
		Porcine bocavirus 5	PBoV5	HQ223038
<i>Ungulate bocaparvovirus 4</i>		Porcine bocavirus 7	PBoV7	HQ291308
		Porcine bocavirus 3	PBoV3	JF429834
<i>Ungulate bocaparvovirus 5</i>		Porcine bocavirus 4-1	PBoV4-1	JF429835
		Porcine bocavirus 4-2	PBoV4-2	JF429836
<i>Copiparvovirus</i>	<i>Ungulate copiparvovirus 1</i>	Bovine parvovirus 2	BPV2	AF406966
	<i>Ungulate copiparvovirus 2</i>	Porcine parvovirus 4	PPV4	GQ387499
<i>Dependoparvovirus</i>	<i>Adeno-associated dependoparvovirus A</i>	Adeno-associated virus-1	AAV1	AF063497
		Adeno-associated virus-2	AAV2	AF043303
		Adeno-associated virus-3	AAV3	AF028705
		Adeno-associated virus-4	AAV4	U89790
		Adeno-associated virus-6	AAV6	AF028704
		Adeno-associated virus-7	AAV7	AF513851
		Adeno-associated virus-8	AAV8	AF513852
		Adeno-associated virus-9	AAV9	AY753250
		Adeno-associated virus-10	AAV10	AY631965
		Adeno-associated virus-11	AAV11	AY631966
		Adeno-associated virus-12	AAV12	DQ813647
		Adeno-associated virus-13	AAV13	EU285562
		Adeno-associated virus-S17	AAVS17	AY695376
	<i>Adeno-associated dependovirus B</i>	Adeno-associated virus-5	AAV5	AF085716
		Bovine adeno-associated virus	BAAV	AY388617
<i>Anseriform dependoparvovirus 1</i>		Caprine adeno-associated virus	CapAAV	DQ335246
		Duck parvovirus	DPV	U22967
		Goose parvovirus-PT	GPV2	JF926695
<i>Avian dependovirus 1</i>		Goose parvovirus	GPV	U25749
		Avian adeno-associated virus	AAAV	AY186198
<i>Chiropteran dependoparvovirus 1</i>		Bat adeno-associated virus	BtAAV	GU226971
		California sea lion adeno-associated virus	CslAAV	JN420372
<i>Pinniped dependoparvovirus 1</i>		Snake adeno-associated virus	SAAV	AY349010
		Human parvovirus B19-Au	B19V-Au	M13178
<i>Erythroparvovirus</i>	<i>Primate erythroparvovirus 1</i>			

2. Taxonomy

Table 2.1 continued

Genus	Species	Virus / virus variants	Abbr.	ACNO ³
		Human parvovirus B19-J35	B19V-J35	AY386330
		Human parvovirus B19-W1	B19V-W1	M24682
		Human parvovirus B19-A6	B19V-A6	AY064475
		Human parvovirus B19-Lali	B19V-Lali	AY044266
		Human parvovirus B19-V9	B19V-V9	AJ249437
		Human parvovirus B19-D91	B19V-D91	AY083234
	<i>Primate erythroparvovirus 2</i>	Simian parvovirus	SPV	U26342
	<i>Primate erythroparvovirus 3</i>	Rhesus macaque parvovirus	RhMPV	AF221122
	<i>Primate erythroparvovirus 4</i>	Pig-tailed macaque parvovirus	PtMPV	AF221123
	<i>Rodent erythroparvovirus 1</i>	Chipmunk parvovirus	ChpPV	GQ200736
	<i>Ungulate erythroparvovirus 1</i>	Bovine parvovirus 3	BPV3	AF406967
<i>Protoparvovirus</i>	<i>Carnivore protoparvovirus 1</i>	Feline parvovirus	FPV	EU659111
		Canine parvovirus	CPV	M19296
		Mink enteritis virus	MEV	D00765
		Raccoon parvovirus	RaPV	JN867610
	<i>Primate protoparvovirus 1</i>	Bufavirus 1a	BuPV1a	JX027296
		Bufavirus 1b	BuPV1b	JX027295
		Bufavirus 2	BuPV2	JX027297
	<i>Rodent protoparvovirus 1</i>	H-1 parvovirus	H1	X01457
		Kilham rat virus	KRV	AF321230
		LuIII virus	LuIII	M81888
		Minute virus of mice (prototype)	MVMP	J02275
		Minute virus of mice (immunosuppressive)	MVMi	M12032
		Minute virus of mice (Missouri)	MVMm	DQ196317
		Minute virus of mice (Cutter)	MVMc	U34256
		Mouse parvovirus 1	MPV1	U12469
		Mouse parvovirus 2	MPV2	DQ196319
		Mouse parvovirus 3	MPV3	DQ199631
		Mouse parvovirus 4	MPV4	FJ440683
		Mouse parvovirus 5	MPV5	FJ441297
		Hamster parvovirus	HaPV	U34255
		Tumor virus X	TVX	In preparation
		Rat minute virus 1	RMV1	AF332882
	<i>Rodent protoparvovirus 2</i>	Rat parvovirus 1	RPV1	AF036710
	<i>Ungulate protoparvovirus 1</i>	Porcine parvovirus Kresse	PPV-Kr	U44978
		Porcine parvovirus NADL-2	PPV-NADL2	L23427
<i>Tetraparvovirus</i>	<i>Chiropteran tetraparvovirus 1</i>	Eidolon Helvum (bat) parvovirus	Ba-PARV4	JQ037753
	<i>Primate tetraparvovirus 1</i>	Human parvovirus 4 G1	PARV4G1	AY622943
		Human parv4 G2	PARV4G2	DQ873391
		Human parv4 G3	PARV4G3	EU874248
		Chimpanzee parv4	Ch-PARV4	HQ113143
	<i>Ungulate tetraparvovirus 1</i>	Bovine hokovirus 1	B-PARV4-1	EU200669
		Bovine hokovirus 2	B-PARV4-2	JF504697
	<i>Ungulate tetraparvovirus 2</i>	Porcine hokovirus	P-PARV4	EU200677
	<i>Ungulate tetraparvovirus 3</i>	Porcine Cn virus	CnP-PARV4	GU938300
	<i>Ungulate tetraparvovirus 4</i>	Ovine hokovirus	O-PARV4	JF504699

The type species for each genus is indicated in bold type. [108]

³ NIH GenBank accession number

3. Morphology

Parvoviruses belong to the smallest of isometric viruses. A linear single-stranded DNA genome of about 5 kb is packaged into the virus capsid [42, 139, 389]. They are non-enveloped and their diameters range from 215 Å (Penaeus stylirostris densovirus) to 255 Å (CPV) [241, 452].

The icosahedral nature of parvoviruses was shown unambiguously by a combination of electron microscopy (EM) and, latterly, X-ray crystallography [457]. Interpretation of the structural data gave rise to three distinct types of surface topology among parvoviruses (see Figure 3.1, p. 13) [349]. The icosahedral twofold axes and the protrusions surrounding the icosahedral threefold axes display profound surface topology differences between each group. Types I and III comprise members of the subfamily *Parvovirinae* described in Section 2.1, see p. 6. They share in common the following surface features: a protrusion at the 3-fold axis, depressed regions between the 3-fold elevated regions at the 2-fold axis, and another depressed region encircling the 5-fold axis. These two groups mainly differ in the shape of the 3-fold elevated region.

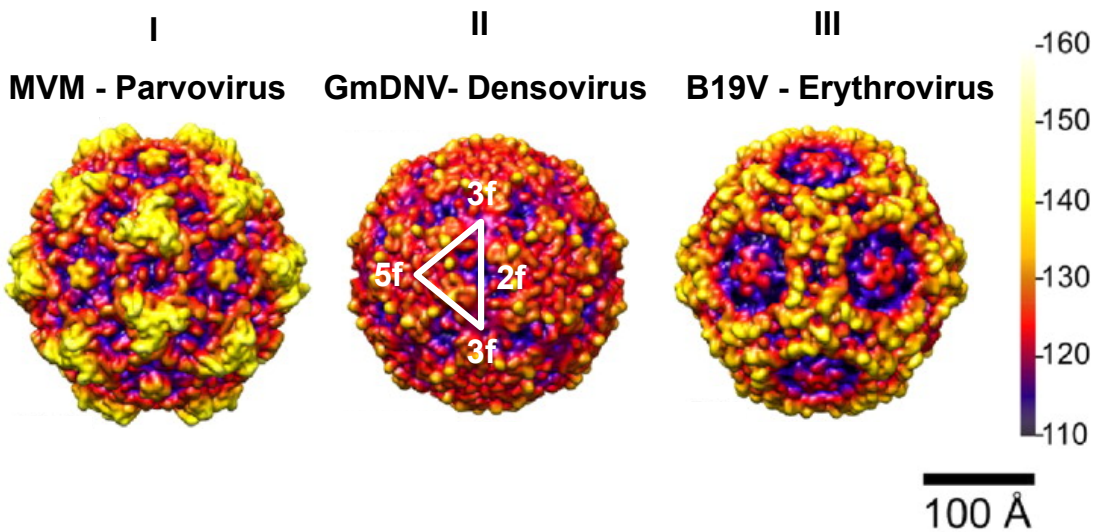


Figure 3.1.: Surface topology groups among members of the family *Parvoviridae*. Stereo, depth cued (blue-red-yellow-white), and space-filling capsid surface illustration of representative members of the two subfamilies of the parvoviruses. Type viruses representing the three surface topology groups (I-III) and the genus to which they belong are indicated. A viral asymmetric unit bound (white triangle) is shown by a 2-fold (2f), two 3-folds (3f) and a 5-fold (5f) axis on the GmDNV image. A horizontal scale bar (100 Å) for diameter measurement and a vertical color bar depicting color cueing as a function of particle radius in Å are shown on the right hand side. These images were computed from atomic coordinates using the UCSF-Chimera program [367], and all are rendered at the same resolution (7.9 Å) and magnification. The figure was adapted from reference [190].

3. Morphology

Members of the genus *Protoparvovirus*, as for example CPV, FPV, MVM, and PPV, represent the first topology group that is characterized by a single, relatively flat, pinwheel-shaped protrusion at the icosahedral threefold axes and a wider twofold dimple. The third topology group encompasses the AMDV, B19V, AAV2, AAV4, and AAV5 capsids, which show three distinct mounds at a distance of \sim 20-26 Å from the icosahedral threefold axes. In addition, the depression at the twofold axis appears to be slightly deeper, particularly for B19V [3, 190, 503]. In contrast to the vertebrate parvoviruses, no large surface protrusions or depressions are present in *Densovirus* capsids that appeared to be relatively spherical and featureless, adopting a second topology group [72, 421].

4. The Rugged Virion

4.1. Physicochemical Properties

The extracellular infectious virus entity is defined as virion. An infectious parvovirus virion only consists of two components, namely of about 75 % protein and 25 % DNA. Their molecular weight (MW) is approximately $5.5\text{-}6.2 \times 10^6$ dalton. The virion buoyant density is 1.39 to 1.43 gcm⁻³, measured in CsCl gradients [213, 397]. Since parvoviruses are devoid of a lipid envelope, mature virions are stable in the presence of lipid solvents. In particular, animal parvoviruses show considerable heat resistance. Most species resist alcohol or ether treatment, exposure to pH 3-10, or incubation at 60 °C for 60 min [54, 59, 80, 209, 210, 294, 400], hence they are clearly more stable compared to most other, especially enveloped, viruses. Only harsh conditions, such as treatment with formalin, β -propiolactone, hydroxylamine, ultraviolet light, and oxidizing agents as for example sodium hypochlorite, ensure effective virus inactivation [66, 203, 396, 405]. Accordingly, the capsid effectively protects the fragile, condensed genome from detrimental biological, chemical, and physical agents, thus ensuring efficient transmission of the virion through the extracellular environment.

4. The Rugged Virion

4.2. Atomic Model

Currently, there is no crystal structure available for MVMp DNA containing particles. Only baculovirus-expressed MVMp-like particles and empty capsids (EC) have been determined at a resolution of 3.25 Å and 3.75 Å, respectively [247]. For MVMi both DNA-containing full and empty particles were crystallized and determined at 3.5 Å resolution. The known CPV structure [287] was used as a phasing model with 52 % of the 587 amino acids in VP2 of MVMi being identical to CPV. Following molecular replacement and refinement, the resulting electron density map was interpreted with respect to the amino acid sequence of MVMi. The polypeptide chain of the major structural protein, VP2, could be traced from residue 39 to residue 587 at the C-terminus (see Figure 4.1, p. 17) [275]. The N-terminal extensions of VP1 and VP2 are not visible in the electron density map. The capsid displays a T=1 icosahedral symmetry, thus having a 5-3-2 point group symmetry containing 31 rotational symmetry axes that intersect at the center: six fivefolds, ten threefolds, and fifteen twofolds. The C-terminal part in common of the structural proteins has an eight-stranded (β B to β I) antiparallel β -barrel topology, referred to as jellyroll motif (reviewed in [202, 390]). This structural motif is frequently found in other virus capsid proteins. Additionally, like many other viruses, parvoviruses have a ninth β A-strand which is hydrogen-bonded to the β B-strand. The high structural conservation of the jellyroll motif among parvoviruses is remarkable considering the low sequence homology between members of this family. Large loops between the β -strands of the β -barrel that form the principal surface features, particularly the threefold spikes, confer the surface biological properties of the capsid, such as determination of host tropism [23, 360] and sites of antigenicity [52, 362]. Such loops were found to be quite dissimilar in different parvoviruses (see Figure 4.1, p. 17) [85].

The lack of the first 38 amino acids of VP2 indicates a highly disordered structure for N-VP2 [275]. Indeed, a glycine-rich conserved sequence at the N-terminal part of VP2 contributes to its flexibility. In virions, but not in EC, additional density seen within the fivefold channels was modeled and found to represent the predominantly poly-glycine conserved sequence [496, 502]. These findings suggest that the N-terminus of VP2 is highly dynamic as DNA packaging triggers externalization of one in five N-termini along the pores of the fivefold axis [4].

A substantial amount of electron density in the capsid interior was built as 10 DNA nucleotides which were located at equivalent positions to those previously found in the analysis of the structure of CPV [86, 458]. For MVM, 19 additional nucleotides were identified in a difference electron-density map with respect to the data of empty particles. Altogether, these 29 ordered, or partially ordered, nucleotides per icosahedral asymmetric unit imply that approximately 34 % of the total viral genome display icosahedral symmetry. These findings, and the conservation between the base-binding sites of MVMi and CPV, has led to the identification of a DNA-recognition site on the parvoviral capsid interior [4].

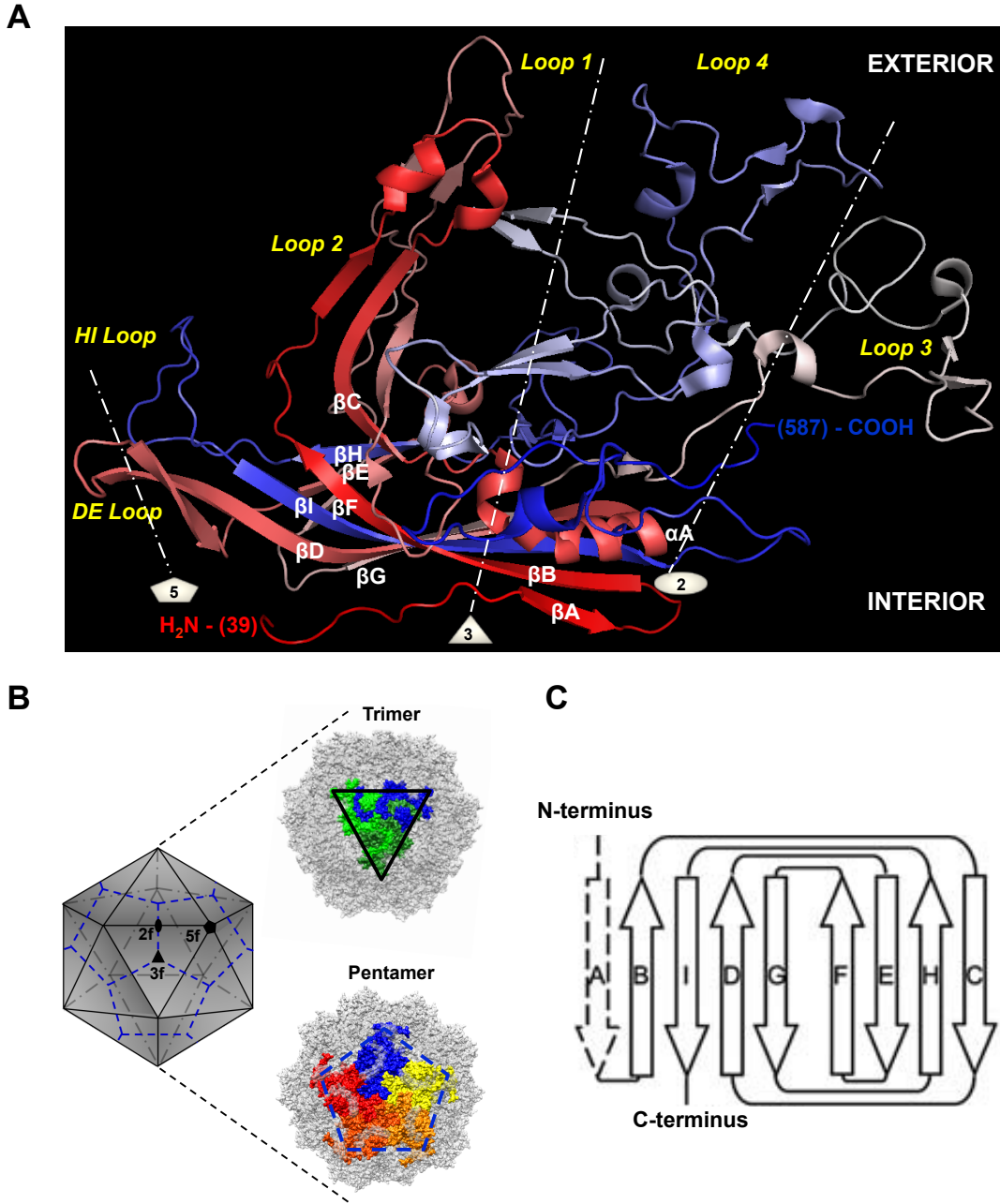


Figure 4.1.: Atomic model of MVM. **(A)** Ribbon diagram of MVMP VP2 illustrating β -strands, helical and loop regions. The amino acid sequence is gradually colored in a red-white-blue spectrum, beginning at residue 39 and ending at the C-terminal residue 587. The highly conserved α A-helix β -barrel motif, consisting of two antiparallel β -sheets (β ABIDG- β FEHC), are labeled. The icosahedral twofold (oval), threefold (triangle), and fivefold (pentagon) axes are indicated. Atomic coordinates for MVMP were obtained from RSCB protein database (PDB accession number 1Z14). The illustration was generated using the PyMol program [43]. **(B)** 60 copies of the capsid proteins form a T=1 icosahedral structure. Each triangle of the icosadeltahedron designates a virus capsid protein subunit. Rotational symmetry axes are referred to as 5f, 3f and 2f, representing 5-folds, 3-folds, and 2-folds, respectively. A VP trimer (assembly intermediate) and a VP pentamer are represented on the right hand side, superimposed on the capsid surface. The representation was generated using the UCSF-Chimera program [367] by computing the same atomic coordinates as mentioned in (A). **(C)** The connectivity of the antiparallel β strands (arrows) of the jellyroll β -barrel is schematically indicated. Strand A is dashed because it is conserved among parvoviruses and a number of other viruses but it is not present in all viruses. This illustration was adapted from reference [84]

4. The Rugged Virion

4.3. Structural Proteins

The MVM capsid is made up of 60 copies of a single polypeptide sequence. The virion contains structural proteins of three size classes (VP1-VP3) that constitute a nested set. These share the same C-terminal core structure, but differ in the sequence length on their N-termini. The capsid is assembled from about 10 copies per particle of VP1 (83 kDa), whereas VP2 (64 kDa) represents the major species [447]. In DNA containing virions, the N-terminal region of VP2 is cleaved during cell entry by intracellular proteolytic digestion to generate VP3 (60 kDa), which displays a truncation of approximately 25 amino acids at its N-terminus (see Section 7.3, p. 35) [100, 448, 460, 478]. The N-terminal cleavage of VP2 does not occur in EC, suggesting that DNA packaging into the particle allows the N-VP2 terminus to be externalized [111, 355, 448]. The processing of VP2 in full virions can be mimicked *in vitro* by digestion with tryptic proteases, as for instance chymotrypsin or trypsin. However, the proteolytic site *in vivo* is different to the chymotrypsin- or trypsin-sensitive site [355, 448, 460]. Although containing the identical amino acid sequence that is cleaved in VP2, VP1 does not appear to be cleaved at this position in either type of particle, *in vivo* or *in vitro*. VP2 is both necessary and sufficient for the assembly and encapsidation of viral ssDNA (see Sections 7.10 and 7.11, p. 48 - 49) [209]. However, VP1 is required to produce an infectious particle since capsids that lack VP1 were blocked subsequent to cell binding and prior to the initiation of DNA replication, thus they are unable to fulfill a complete viral life cycle [461]. Indeed, the 142 amino acid N-terminal extension of VP1 which is referred to as VP1 unique region (VP1u) harbors several important motifs to initiate viral infection. Two of which are a PLA₂ motif as well as a nuclear localization signal (NLS), elaborated in Section 4.4, p. 18. Since VP1u initially is sequestered within the viral shell, the incoming virion must undergo important structural changes *in vivo* in order to expose its functional domains on the capsid surface. By treatment of purified virions under controlled temperature or with urea, VP1u exposure could be demonstrated *in vitro* [131, 470].

4.4. Functional Domains

From the atomic model of parvoviruses it can be estimated that structural proteins of 25-30 kDa theoretically suffice to constitute a capsid to protect the viral genome. However, this minimum size is generally enlarged among parvoviruses. VP1 and VP2 exceed the minimum size more than twice as much. The additional parts of the structural proteins harbor essential functional motifs that mediate a number of processes in the infectious viral life cycle. These include host cell surface receptor recognition (see Section 7.1, p. 32), entry and escape from endosomes (see Sections 7.2 to 7.4, pp. 34 - 36), nuclear localization (see Section 7.6, p. 38), DNA packaging, nuclear export, tropism and pathogenicity determinants (see Chapter 6, pp. 27 - 29), immune surveillance and final maturation of particles to produce infectious virus progeny [453].

4.4.1. The Phospholipase A₂ Motif

In the VP1u region of all parvoviruses, except AMDV and the members of the genus *Brevidensovirus*, as well as *Tetraparvovirus*, a PLA₂ motif has been identified [508]. The calcium binding loop (YXGXG) and the catalytic histidine-aspartic acid dyad (HDXXY) of parvoviral phospholipases are related to Ca²⁺-dependent extracellular or secretory sPLA₂s which are found for example in bee and snake venoms. Unlike all previously characterized sPLA₂s, the viral sPLA₂ motifs show very weak sequence similarity and lack the characteristic multiple disulfide bonds, thus analogy is mainly restricted to the catalytic units. PLA₂s specifically catalyze the hydrolysis of phospholipid substrates at the 2-acyl ester (*sn*-2) position to release free fatty acids and lysophospholipids. The viral sPLA₂s hydrolyze all major classes of glycerophospholipids, except phosphatidylinositol, without displaying a preference for unsaturated *versus* saturated *sn*-2 fatty acyl chains [79]. The catalytic activity of the PLA₂ is dependent on Ca²⁺ in mM concentrations and reaches a maximum at a pH range 6-7, presumably associated with the deprotonation of the His residue in the catalytic dyad at such pH [37, 179].

The biological importance of the viral PLA₂ motif was demonstrated by mutational analyses with AAV2, MVM, and PPV [167, 429, 508]. Viruses lacking a functional PLA₂ motif were not infectious as they failed to escape from endosomes [155, 167, 183, 435].

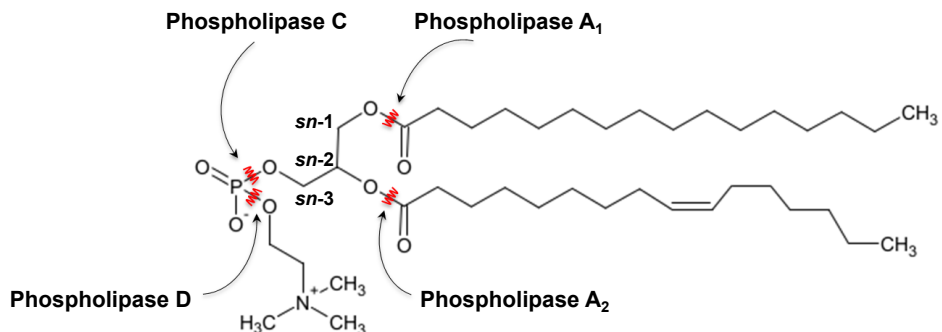


Figure 4.2.: The cleavage sites of the different PLAs are illustrated using phosphatidylcholine (PC), a common phospholipid, as an example. Phospholipase A₁, A₂, C, and D specifically cleave different ester bonds in the phospholipid. Their respective sites of attack are represented by red staggered lines.

4. The Rugged Virion

4.4.2. The Nuclear Localization Signal

In addition to the PLA₂ motif [508], the VP1u region of MVM contains four basic clusters (BCs) of amino acids, referred to as BC1 to BC4. These are highly conserved among parvoviruses and moreover, even in some other DNA viruses. BC1 and BC2 represent conventional NLS which are characterized by a short stretch of basic amino acids [229, 230]. BC3 and BC4, which are separated by a short spacing sequence in between, may rather be arranged as a bipartite NLS domain [385]. The clustered basic amino acids interact with transport receptors of the importin/karyopherin family which mediate nuclear import [300, 334, 483]. Nuclear transport activity has been demonstrated for BC1 in the context of a singly expressed VP1 protein [278] and as NLS-peptide coupled to an heterologous carrier protein [468]. Furthermore, it is proven to be essential for CPV infectivity [471] and for MVM to initiate infection [278]. In contrast, BC3 and BC4 did not show such capacity to import VP1 either expressed alone [468] or in the context of the complete MVM genome [278]. Alternatively, these BCs may be involved in the tethering of the ssDNA genome to the capsid inner surface. Such function has been demonstrated for two basic, significantly homologous DNA-binding domains of the protein J of the ϕ X174 bacteriophage [192].

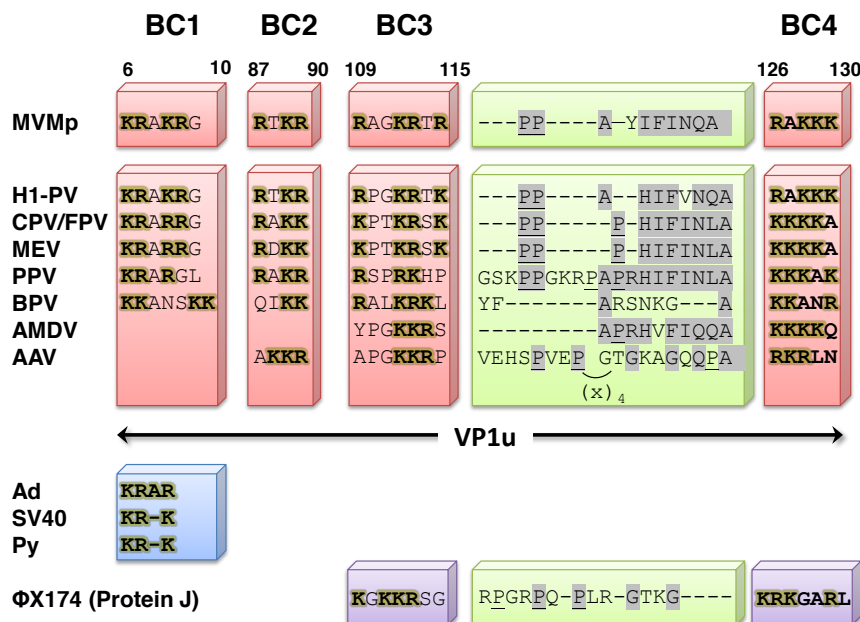


Figure 4.3.: VP1 nuclear targeting sequences. The alignment of BCs (BC1 to BC4), which are conserved in the VP1u region among parvoviruses, is boxed in red. Amino acid residues are abbreviated using the single letter code. Sequence homology between BC1 and other karyophilic double-stranded DNA (dsDNA) viruses is shaded in blue on the left-hand side. Conservation of BC3 and BC4 with the protein J of the ssDNA bacteriophage ϕ X174 is boxed in magenta on the right-hand side. Basic residues of the BC boxes are represented in bold face and possible homologous residues in the spacing region (boxed in green) between BC3 and BC4 are shadowed. Characteristic proline residues which are scattered along the space region are underlined. This illustration was adapted from references [278, 462].

4.4.3. The Nuclear Localization Motif

Since both VP1 and VP2 singly expressed proteins efficiently target the nucleus of transfected cells [278, 461] each protein must carry its own nuclear transport sequence. The common C-terminal sequence of VP1 and VP2 lacks a conventional consensus NLS. However, VP2 contains one single region which is enriched in basic amino acids (528-KGKLTMRRAKLRL-538) near its C-terminus (see Figure 4.4 B, p. 21). Based on the crystal structure [4, 457], analysis revealed that this sequence is structurally ordered as a β -sheet which forms the carboxy half of the β I strand (residues 520 to 538) of the eight-stranded antiparallel β -barrel (see Figure 4.1 A, p. 17). Moreover, the β I-strand shows marked amphiphatic characteristics, exposing all the basic amino acids to the solvent in the interior surface of the capsid while the hydrophobic residues face toward the protein core (see Figure 4.4 A, p. 21). Mutational analysis revealed that the basic nature of the exposed face of β I, as well as the hydrophobic residues on the opposite face, conferred a nuclear localization capacity to the VP2 protein. Accordingly, this sequence in β I which only functions under a precise conformation, but not in a linear form, is referred to as the VP2 nuclear localization motif (NLM) [277].

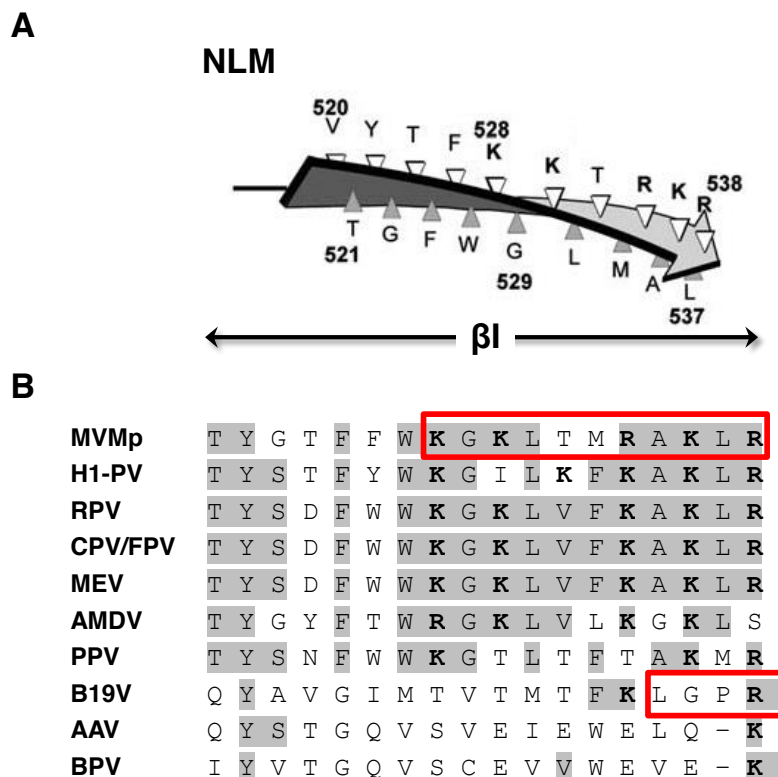


Figure 4.4.: Nuclear localization motif. (A) Schematic representation of the VP2 NLM of MVM as disposed on the β -strand I of the antiparallel, eight-stranded β -barrel topology in the common C-terminal part of VP1 and VP2. Basic amino acids which are exposed to the solvent are represented in bold. (B) Alignment of the NLM that is conserved among parvoviruses. Homologous positions are shadowed and basic residues are in bold. Sequences with proven nuclear localization capacity are boxed in red. This illustration was adapted from references [277, 462].

5. Genome Architecture

The MVM genome is a small, non-permuted, linear, single-stranded DNA molecule [18, 61, 446, 477] that is 5 085 nt in length for MVMi and 5 149 nt for MVMP [17]. The relatively long coding sequence of approximately 4.8 kb contains two major monosense ORFs which span most of the viral genome, with some sections having overlapping coding regions [20]. The ORFs encode a non-structural (NS) gene and a structural (VP) gene and they are, by convention, termed as occupying the “left” or the “right” half of the coding sequence, respectively. The NS gene encodes four proteins that are required for the replication of the viral genome and are referred to as NS1, NS2^P, NS2^Y, as well as NS2^L. The VP gene encodes an overlapping set of capsid proteins, VP1 the minor capsid protein and VP2 the major capsid protein [109, 228, 368]. A representation of the genomic organization of MVM is illustrated in Figure 5.1 A, p. 26.

5.1. The MVM Left- and Right-End Telomeres

The coding sequence is enclosed by short, imperfect palindromes which fold back on themselves to secondary structured duplex telomeres. Both telomeres differ considerably from each other in size, primary sequence and secondary structure [20]. Hence, they are physically and functionally dissimilar and also vary in their terminal resolution strategies at the two sites (see Section 5.1.1, p. 24), although the molecular principles that underlie both strategies are very similar [125].

The MVM left-end telomere is 121 nt in length and forms into a Y-shaped configuration, as depicted in Figure 5.1 B (left panel), p. 26. The stem region which contains 43 base pairs (bp) is only interrupted by a mismatched bubble sequence where a triplet GAA on the inboard arm is opposed to the dinucleotide sequence GA on the outboard arm. Additionally, an asymmetric thymidine residue is located within the stem on the outboard arm in the immediate proximity to the “ear” that are generated by small internal palindromes. These “ear”-like structures give rise to the Y-shaped configuration of the left-end terminus [16, 18, 20, 117]. A single DNA sequence, designated the “flip” sequence, is conserved in the progeny viral left-end telomere, as is observed *in vivo* [16].

The MVM right-end telomere is 248 nt in length and can be simply described as an almost perfect duplex stem structure of 121 bp (see Figure 5.1 D, p. 26). The palindrome is only interrupted by a triplet of unpaired nucleotides which form a small asymmetric bubble near the distal end of one strand, along with three unpaired bases which form the cross-link at the palindrome axis [16, 20].

5. Genome Architecture

As in homotelomeric parvoviruses, two distinct forms of the MVM right-end terminus, referred to as “flip” and “flop”, are generated in equimolar amounts *in vivo* (see Figure 5.1 D (i) and (ii), p. 26) [118, 125]. These two forms are the inverted complements of one another and both give rise to viral origins, called *oriR* [119, 128, 135]. A small internal palindrome, surrounding the three-nt bubble, thermodynamically enables an alternative, asymmetric cruciform configuration of the right-end telomere (see Figure 5.1 D (iii), p. 26) [19].

5.1.1. Terminal Resolution *versus* Asymmetric Junction Resolution

As is the case for most of the heterotelomeric parvoviruses, MVM shows packaging bias with minus strands preferentially encapsidated to plus strands by a 10-100-fold margin (see Section 7.11, p. 49) [111, 368]. This results from differences in the efficiency of their two DNA replication origins at both ends of their genomes, rather than any strand-specific packaging sequence. In particular, the efficient nick site of the *oriR* dictates the negative polarity of the packaged strand which is encapsidated in MVM virions [122].

In keeping with their homotelomeric counterparts, the right-end hairpin of MVM exists as an equimolar mix of flip and flop sequence orientations and is processed by a similar terminal resolution strategy. Nicking of the hairpin near the junction between palindromic and non-palindromic sequences and subsequent extension of the right-end terminus allows an efficient inversion of the palindrome (see step iii and iv in Figure 7.2, p. 43). On the contrary, the MVM left-end hairpin predominates in the flip orientation, indicating its generation by an asymmetric junction resolution mechanism [121]. Briefly, the asymmetric bubble sequence in the stem of the MVM left-end telomere (see Figure 5.1 B, p. 26) prevents assembly of an active nicking complex. Thus, the left-end telomere cannot function as a replication origin in its hairpin conformation [22]. During rolling hairpin replication (RHR) (see Section 7.8, p. 43), the hairpin is unfolded, extended, and copied to form the fully base-paired, imperfect palindromic junction sequence that bridges adjacent genomes in an intermediate dimer replicative form (dRF) (see Figure 5.1 B (right panel), p. 26). It was demonstrated that such junctions can initiate DNA replication in a NS1-dependent manner [115, 116]. Formation of the dimer junction effectively segregates two potential origins of DNA replication, one derived from each arm of the hairpin, on either side of the junction’s symmetry axis but only one of these origins is active. The activity is regulated by the sequence of the asymmetric bubble which serves as a precise spacer between the NS1 binding site and the parvovirus initiation factor (PIF). Binding of PIF stabilizes the interaction of NS1 with the active (TC) origin (*OriL_{TC}*) but not with the inactive (GAA) origin (*OriL_{GAA}*) [95]. The minimal left-end origin of replication is called *oriL* and shown in Figure 5.1 C, p. 26. It extends from two 5'-ACGT-3' motifs which represent binding sites for PIF [92–94], to a 5'-(ACCA)₂-3' binding site for the viral initiator nickase NS1 [129], and finally to the active nick site [116]. Recent studies have revealed that MVM tolerates both sequence and orientation changes in its left-end hairpin.

5.2. Genetic Variability

In which case it can be deduced that maintaining the flip orientation of the left-end telomere is a consequence of, but not the reason for, asymmetric dimer junction resolution. However, the same study indicated that asymmetric left-end processing is crucial for MVM replication [267].

In summary, the heterotelomeric hairpins, along with a few adjacent nucleotides, provide all of the *cis*-acting information required for efficient genome replication and encapsidation. In particular, these terminal nucleotides, representing less than 10 % of the entire genome, create the replication origins by providing nicking sites that are used as a primer for DNA synthesis and to effectively separate unit-length genomes for DNA packaging. Additionally, they function as flexible hinge regions used to establish and re-orient the replication fork, allowing it to roll back and forth along the linear viral DNA [118, 124, 324, 451].

5.2. Genetic Variability

When compared with cellular DNA, the genome of MVM has a relatively high GC-content (42 %) [20], partially reflecting its high density of regulatory elements [126]. The complexity of the viral genome is increased by transcriptional promoter sequences and various splicing signals that are embedded within the same primary sequence, beyond the encoded proteins which are organized in multiple overlapping ORFs. Following inoculation of clonal populations of MVMi stocks in mice, genetically different antibody-escape variants emerged *in vivo*. This indicates that viral replication appears to support the generation of heterogeneity [279]. The best studied example is represented by the emergent branch of CPV which evolved from FPV in 1978 allowing the virus to expand its host range to canines. The substitution rate of CPV resembles that seen in rapidly evolving RNA viruses, as for example HIV-1 and human influenza A virus [413]. Remarkably, such diversity occurred despite the fact that the viral genome is replicated using a subset of the host's DNA replication machinery [33, 106]. Hence, the mutation rates would be expected to be low [169, 402]. Probably, the unidirectional strand-displacement mechanism may exhibit lower fidelity compared to the bidirectional replication of eukaryotic genes. Additionally, the concatemeric duplex intermediates may allow for inter- and intramolecular recombination during replication of the viral DNA [126]. Moreover, there are several lines of evidence that MVM exploits the DNA damage response machinery early in infection in order to enhance its replication and to improve virus-induced cell cycle arrest in the S-phase [1]. Therefore, it seems possible that under such conditions the replication forks may be more error-prone. Finally, environmentally induced changes in the viral DNA sequence, such as depurination or deamination, cannot be corrected because virions contain ssDNA and hence do not provide a template for excision or mismatch repair systems. Nonetheless, the genetic complexity, a consequence of the constrained genome size, severely and selectively restricts the types of tolerated modifications [126].

5. Genome Architecture

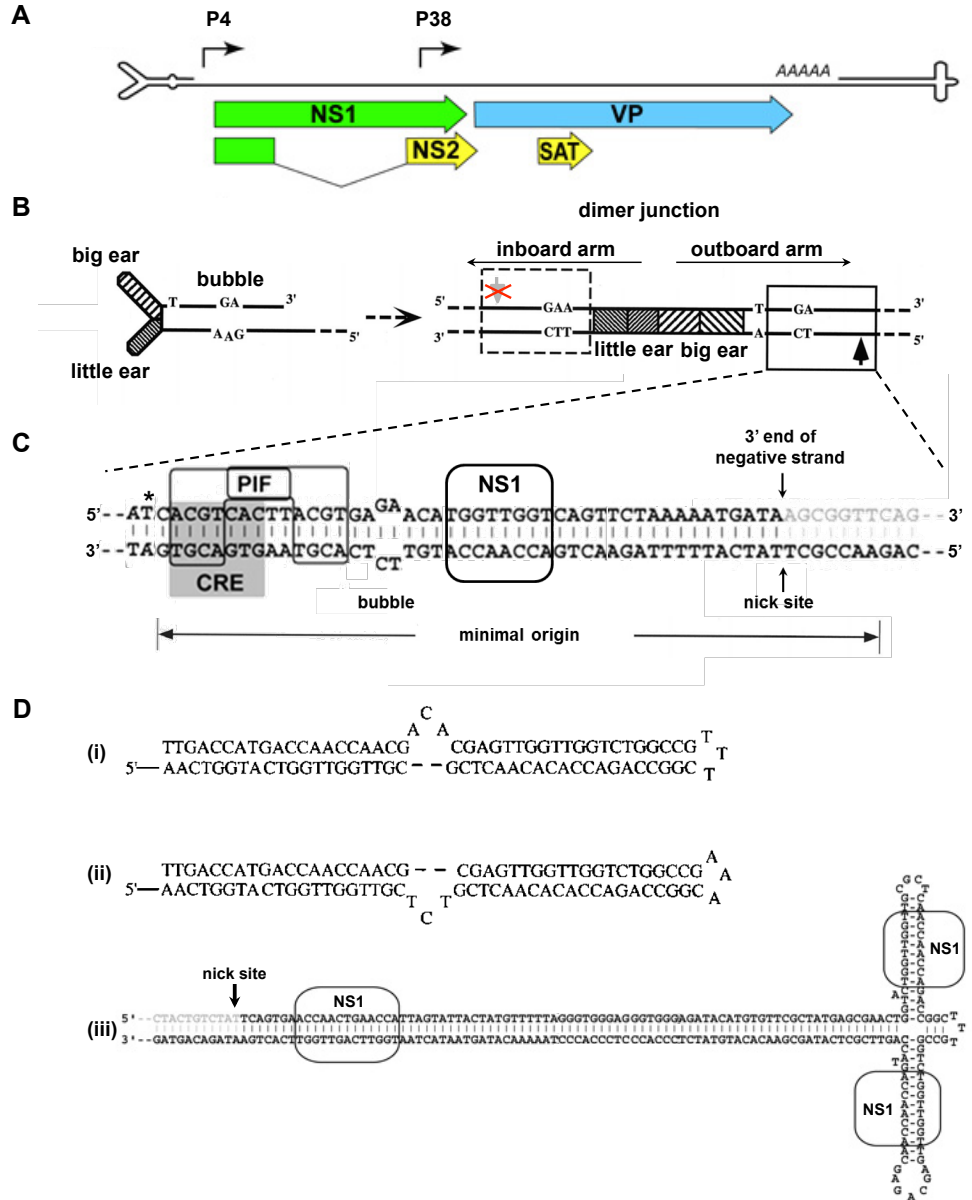


Figure 5.1: Genome architecture of MVM. (A) Schematic of the predicted structures of the terminal hairpins, scaled approximately 20× relative to the rest of the genome. Major ORFs are represented by arrowed boxes and alternative RNA splicing for NS2 is indicated. Proteins are shaded green for the major replication initiator protein (NS1), blue for the structural (VP) proteins of the capsid, and yellow for sequences unique to the ancillary NS proteins. The two transcriptional promoters, P4 and P38, are indicated by rightward arrows and the polyadenylation site by the AAAAA-sequence block [127]. (B) Diagram of the left-end hairpin of MVM and its dimer junction. Asymmetries, such as the “ear”-like structures, extra-helical T, and bubble sequence are indicated. The duplex, dimer junction, generated by RHR (see Section 7.8, p. 43), is shown on the right hand side. The short, palindromic sequences derived from the hairpin ears are represented by cross-hatched boxes. The active *OriL_{TC}* is boxed, with an arrow indicating the nick site. The equivalent sequence generated on the GAA side of the bubble is framed by a dashed box with an arrow at the potential nick site that is crossed out to indicate that *OriLGAA* is not active [76, 77]. (C) Sequence details of the active left-end origin (approx. 50 bp) are shown, with an arrow indicating the active nick site. The minimal sequence required for origin activity is indicated by the double-headed arrow. Sequences of the bubble and the PIF, cAMP-responsive element (CRE), and NS1 binding sites are indicated. An asterisk represents the position of the extra-helical T, now base paired, and the gray box below it indicates the CRE consensus sequence [76]. (D) Alternate conformations of the right-end hairpin sequences of MVM. The right-end terminus can form a hairpin structure in either the flip (i) or flop (ii) sequence orientation or a cruciform structure (iii). In the cruciform configuration, the binding sites for the replicator protein, NS1, are boxed and their site of nucleolytic cleavage is represented by a vertical arrow [106].

6. Host Range and Specificity

6.1. Tissue Tropism Determinants

Concerning their host range, most parvoviruses, such as MVM, CPV, and FPV, are tightly restricted to specific receptors of their particular hosts. However, some parvoviruses, as for example many of the AAVs, infect human cells by primary attachment to a variety of receptors (see Section 7.1, p. 32).

As outlined in Chapter 1 (see p. 3), two distinct strains of the parvovirus MVM have been described to occur in mice. On the one hand, MVMP, the prototype strain, replicates efficiently in mouse fibroblasts [138]. On the other hand, MVMi, the immunosuppressive strain, replicates in T lymphocytes [58, 305]. Both strains display disparate *in vitro* tropism and *in vivo* pathogenicity despite differing by only 14 amino acids in their capsid proteins [24], thus providing a useful model for in-depth characterization of the role of virus-receptor interaction (see Section 7.1, p. 32) in parvovirus infection. Beyond that, MVMP and MVMi are serologically indistinguishable, bind to sialic acid (SA), and are internalized in both fibroblasts and lymphocytes [427]. Consequently, it could be demonstrated that both viruses propagate in hybrids of the two cell types [442].

In order to map the allotropic determinants of MVM, chimeric viral genomes were constructed *in vitro* from infectious genomic clones of both strains. By mutagenesis and selective plaque assays, the major determinants for the acquisition of fibrotropism for MVMi have been mapped onto the capsid [14, 24, 104], in particular to the VP2 residues 317 and 321 [23, 302]. Both residues are located at the base of the threefold spike of the virion [14, 176, 177]. Interestingly, these two VP2 residues structurally localize nearby some of the important amino acids determining CPV, FPV, and PPV host range [186, 220, 466]. Further residues (VP2 residues 339, 399, 460, 553, and 558) were identified in MVMi to be able to confer fibrotropism to forward second-site mutants when either residues 317 or 321 are mutated. Those residues cluster around the twofold dimple-like depression [4]. In contrast, the switch to lymphotropism for MVMP is more complex and requires both an equivalent region of the major MVMi capsid protein gene VP2 and a segment of the NS protein genes [104].

6. Host Range and Specificity

6.2. Pathogenicity Determinants

MVMi appears to be more pathogenic in mice than MVMP. Oronasal inoculation of MVMi in most neonatal mice resulted in lethal phenotype or severe growth-retardation in survivors [240], as observed for other parvoviruses (see Section 2.1, p. 6). MVMP infection appears to be asymptomatic in newborn mice [71]. In contrast, MVMi infection in neonatal mice of some inbred strains caused renal papillary hemorrhage and viral replication in endothelia [70], hematopoietic precursors [406], and neuroblasts [380]. Following *in utero* inoculation of MVMi or MVMP into developing embryo, a broad set of cell types were infected that partially overlapped. Nevertheless, the tissue tropism of MVMP for fibroblasts and of MVMi for endothelium, as well as the higher virulence of MVMi was preserved [224]. By reason of the complexity of MVMi pathogenesis in the neonatal mouse, a more adequate model was required to investigate the virulence of MVMi *in vivo*.

Severe combined immunodeficiency (SCID) mice [60] represent such a model since they lack an antigen-specific immune response, thus allowing the study in adult mice and circumventing the complex situation of heterogenous viral multiplication in embryonic developing tissue. MVMi infection of adult SCID mice gave rise to the suppression of long-term repopulating hemopoietic stem cells in the bone marrow [408], leading to an acute lethal leukopenia and accelerated erythropoiesis [407]. In addition, it has been reported that MVMP evolved in intravenously inoculated SCID mice. Different variants, isolated from single plaques, carried only one of three single amino acid changes at position 325, 362, or 368 in the major VP2 capsid protein. These variants sustained their fibrotropism *in vitro*, but unlike MVMP, they propagated in mouse tissues following oronasal inoculation, eventually causing death [280, 391]. Two of the three invasive fibrotropic MVMP strains, I362S and I368R, were shown to induce lethal leukopenia in oronasal inoculated SCID mice. Emerging viral populations in leukopenic mice displayed altered sequences in the MVMi genotype at position 321 and 551 of VP2 for infections with the I362S variant or changes at position 551 and 575 in the K368R virus infections. In general, a high level of genomic heterogeneity in the DNA sequence encoding the VP2 protein was observed and was found to be clustered at the twofold depression of the viral capsid [281].

6.3. Comparison of Tissue Tropism and Pathogenicity Determinants among Parvoviurses

Significantly, the amino acids dictating *in vitro* tropism (317 and 321), *in vivo* pathogenicity (325, 362, and 368), fibrotropism on MVMi (339, 399, 460, 553, and 558), and those involved in the development of leukopenia (321, 551, and 575) were found to be located on, or near the capsid surface. Structurally, these residues cluster mainly by raised elements around the twofold axes of symmetry, in close vicinity of the SA binding pocket (see Section 7.1, p. 32) [280, 281].

Differences in the tissue tropisms and the pathogenic phenotypes have also been mapped to the capsid proteins of Aleutian mink disease parvovirus [51], PPV [40], CPV [83, 361], and FPV [456] in a capsid region analogous to that observed for MVM (reviewed in [3]). These pronounced *in vitro* tropism and *in vivo* pathogenicity disparities between the highly homologous viruses can occur at any of the various stages of the infectious viral life cycle, including cell receptor binding, internalization, capsid uncoating, DNA replication or transcription. Studies of the strain-specific tissue tropism conducted on members of other virus families have mainly shown that each strain recognizes a different specific cell surface receptor [168, 214, 319, 320, 423, 481, 482]. This receptor is only present on the target cell for that strain, but absent on the surface of other potential host cells. Although the same structural elements of parvoviruses are involved in mediating host and tissue tropisms, each appears to be affecting a different mechanism. Host ranges of CPV and FPV are controlled by receptor binding, as observed for many other viruses, whereas the cell tropisms of MVM appear to be due to restrictions of interactions with intracellular factors [4, 219, 427]. For MVM it was suggested that the point of restriction appeared after nuclear targeting and conversion of genomic ssDNA to replicative form (RF) intermediates but prior to viral genome replication. Most likely, the restraint occurs due to a block in capsid uncoating [216, 374].

As discussed in this section the functional regions among the subfamily *Parvovirinae* co-localize to similar capsid surface regions albeit three general parvovirus topology groups with characteristic local morphological surface differences emerged (see Chapter 3, p. 13). A profound understanding of functional domains that are involved in fundamental steps of the viral life cycle, particularly receptor attachment, *in vitro* tropism, *in vivo* pathogenicity, and antigenicity are essential for infection and disease control. Hence, showing great promise to allow genetic engineering of parvovirus capsids for the therapeutic delivery to be controlled or modified in gene therapy applications and to develop foreign antigens [3, 219].

7. The Parvovirus Life Cycle

As previously mentioned, parvoviruses are heavily dependent on their cellular systems to ensure productive infection. A plethora of molecular interactions between the virus and the host cell allow the recruitment of cellular machinery to provide an environment for optimal progeny morphogenesis. These numerous interactions include binding to the cell surface determining primary attachment and internalization, cytoplasmic interactions controlling intracellular trafficking and eventual maturation, and nuclear interactions regulating uncoating, replication, transcription, assembly, and packaging of progeny particles. Some of the viral mechanisms and interactions underlying the parvovirus life cycle are introduced in this chapter in further detail keeping MVM as the main focus.

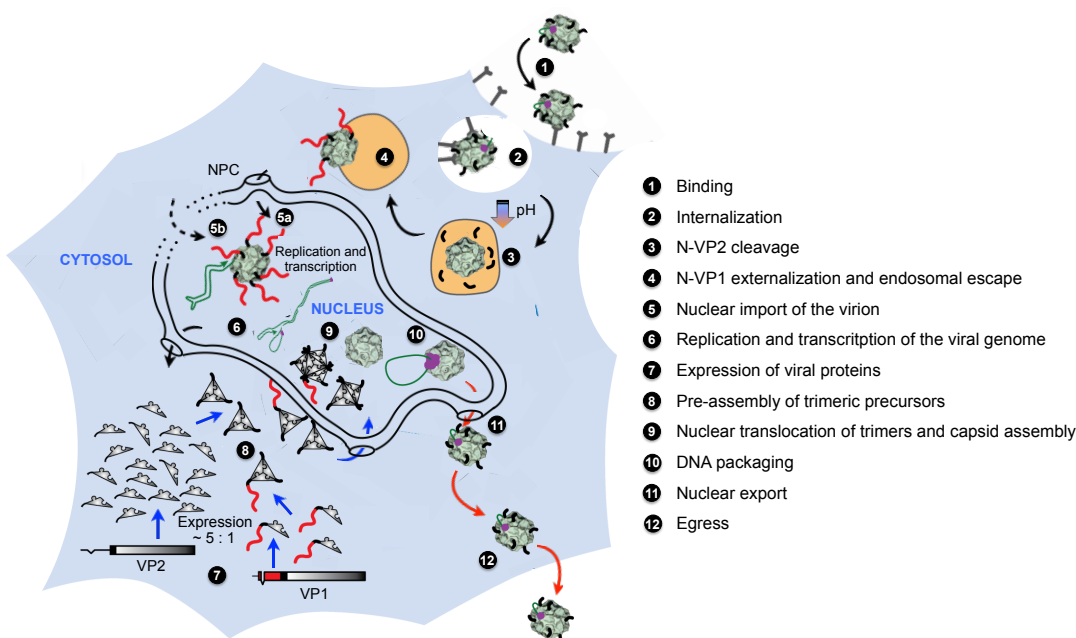


Figure 7.1.: Schematic view of the life cycle of MVM. Cell entry (black arrows), protein expression and progeny assembly (blue arrows), and DNA packaging, nuclear export and egress (red arrows) are illustrated. The unknown sialylated cell surface receptors are indicated as extended Y shapes and acidic late endocytic vesicles are colored in orange. Colored lines associated with virus particles represent the flexible N-VP2 termini (black), the VP1u region (red), and the viral genomic DNA (green). The number of externalized N-VP1 termini is not known and might vary between one and ten. Currently, nuclear targeting (step 5) of the virion is controversial and remains unclear. Due to its small size, MVM could physically traverse the nuclear pore complex (NPC) fully intact (step 5a). Alternatively, MVM was suggested to enter the nucleus in an NPC-independent manner by partial disruption of the nuclear envelope (step 5b). Horizontal bars represent primary VP gene transcripts and jigsaw triangles indicate the folded core containing the jellyroll motif common to all VP polypeptides. The multifunctional NS1 protein, which assists DNA replication and packaging, is represented as purple sphere. The amounts and the ratio of the represented viral proteins do not correspond to those of the natural capsids. This figure was adapted from reference [127].

7. The Parvovirus Life Cycle

7.1. Receptor Binding

Recognition of cell surface receptors by a virus enables the first step of infection and hence, represents a key parameter of tropism and pathogenesis (see Chapter 6, pp. 27 - 29). Different biomolecules, such as proteins, carbohydrates, and glycolipids can serve as primary attachment factors. To date, a variety of different receptor molecules with specific binding properties or functional activities have been identified for some members of the subfamily *Parvovirinae* (see Table 7.1, p. 33). Examples include the AMDV-binding protein for AMDV [170], the globoside erythrocyte P antigen, along with $\alpha_5\beta_1$ -integrin and Ku80 for B19V [69, 236, 323, 479, 480], transferrin receptors (TfRs) for CPV, FPV and mink enteritis virus [358, 359] and heparan sulfate proteoglycan (HSPG), $\alpha_V\beta_5$ -integrin, and growth factor receptors for AAVs [150, 235, 315, 376, 437, 438]. However, a recent study from our lab conducted on B19V failed to verify the interaction between B19V and $\alpha_5\beta_1$ -integrin. Instead, purified, recombinant VP1u was demonstrated to bind and internalize independently of the B19V capsid. VP1u binding and internalization was tightly restricted to only a few cell lines of the erythroid cell lineage only. These results, together with the ability of recombinantly expressed VP1u to efficiently prevent B19V endocytosis, indicate that an unknown receptor with an expression pattern confined to few erythroid cell types mediates B19V internalization [265].

For most of the parvoviruses only the glycan component of their specific receptor is known. Glycans are carbohydrate polymers and represent the major components of the cell surface. Thus they provide a vast collection of important cellular attachment factors for viruses in general. They may be conjugated with cell surface proteins or membrane lipid head groups to form glycoproteins and glycolipids, respectively, or constitute glycosaminoglycan chains attached to proteoglycans [344]. The extensive heterogeneity of the carbohydrate polymers which are expressed across different species, and even across different tissues within the same species, creates an immense variability in viral tissue tropism. This diversity is even further enlarged by various glycosidic linkage positions between each individual monosaccharide and by the high degree of chemical modifications of hydroxyl groups [13, 465]. Most commonly, SA or sulfated oligosaccharide motifs of glycosaminoglycans (e.g. heparan sulfate) form the distal and hence most surface exposed units of glycoepitopes [232].

Biochemical studies utilizing neuraminidase and proteinase K treatment have shown that SA is a common primary attachment factor for several parvoviruses infecting different species, as for example MVM [111, 280], parvovirus H1 (H1-PV) [12], BPV [45, 226, 450], PPV [57], AAV1 [497, 498], AAV4, AAV 5 [89, 231, 409, 474], CPV and FPV [26, 32]. However, SA-CPV and SA-FPV interactions are not sufficient for infectivity but require additional binding to their respective TfRs on canine and feline cells [26, 221, 351, 358]. More than 60 analogues of SA occur in nature which result from modifications to the nine-carbon backbone [232] and are estimated to be present at 5×10^5 copies per cell on A9 mouse fibroblasts [270, 427]. The SA binding pocket

7.1. Receptor Binding

of MVM was identified by analysis of SA soaked into preformed crystals of virus-like particles (VLPs)⁴ of MVMp. Structurally, the SA electron density is associated with the dimple-like depression located at the icosahedral two-fold axis in the MVM capsid (see Figure 3.1, p. 13). The binding pocket exposes highly positive charges which interact with SA moieties on the cell surface [280]. Interestingly, the localization of the SA binding domain in MVM is proximal to the CPV and FPV determinants of SA binding to erythrocytes [5, 26, 420, 455]. Significantly, the amino acids determining *in vitro* tropism (317 and 321) and *in vivo* pathogenicity (325, 362, and 368) for MVM invariably localize in close vicinity of the SA binding pocket (see Chapter 6, pp. 27 - 29) [247].

The identification of virus receptors and the characterization of virus-receptor interactions are of great relevance for understanding virus evolution, host tropism, and pathogenesis. A profound knowledge of the first steps of viral infections on the host cell surface is essential for the development of antiviral therapies and for the construction of gene therapy vectors with determined targeting.

Table 7.1.: Parvoviruses and their receptors

Virus	Receptor	Coreceptor	Host	Reference
AAV1	α 2-3 and α 2-6 N-linked SA	-	Human	[498]
AAV2	HSPG	Integrin $\alpha_5\beta_1$, $\alpha_V\beta_5$, FGFR1, HGFR, LamR	Human	[8, 15, 235, 376, 437, 438]
AAV3	HSPG	HGFR, LamR, FGFR1	Human	[8, 46, 269]
AAV4	α 2-3 O-linked SA	-	NHP	[231]
AAV5	α 2-3 and α 2-6 N-linked SA	PDGFR	Human	[150, 231, 409, 474]
AAV6	α 2-3 and α 2-6 N-linked SA, HSPG	EGFR	Human	[485, 497, 498]
AAV8	-	LamR	NHP	[8]
AAV9	Galactose	LamR	Human	[8, 38, 417]
Bovine	Gangliosides, chitotriose	-	Bovine	[151, 401]
AAV				
AMDV	AMDV-binding protein	-	Mink	[170]
BPV1	SA	Glycophorin A	Bovine	[45, 450]

⁴ VLPs are non-infectious particles which do not contain any viral genetic material. The expression of parvoviral structural proteins results in a spontaneous self-assembly of VLPs. Since VLPs mimic the organization and conformation of viral surface epitopes, they can elicit strong B cell and T cell immune responses. Therefore, they provide a useful tool for the development of vaccines.

7. The Parvovirus Life Cycle

Table 7.1 continued

Virus	Receptor	Coreceptor	Host	Reference
B19V	Erythrocyte P antigen	Integrin $\alpha_5\beta_1$, ku80	Human	[69, 236, 323, 479, 480]
MVM	SA	-	Rodent	[111, 233, 329]
CPV/FPV	SA	TfR	Cat, dog	[221, 358]
PPV	SA	-	Swine	[57]

This Table was adapted from reference [193]

7.2. Receptor-Mediated Endocytosis

All known parvoviruses enter the host cell by receptor-mediated endocytosis, using a wide variety of partially known glycosylated receptor molecules, exposed on the cell surface [199] (see Table 7.1, p. 33). The endocytic route is advantageous for karyophilic viruses. On the one hand, endosomes provide a rapid and efficient transport towards the nuclear periphery. On the other hand, the exposure to low pH enables the capsid to undergo conformational changes which are required for further stages of infection (see Section 7.3, p. 35), such as endosomal escape, uncoating, and nuclear localization. Recent research has demonstrated that, in addition to the classical clathrin-mediated endocytosis [57, 158, 357], several alternative endocytic routes can be used by parvoviruses. For example, AAV2 utilizes clathrin-independent carriers (CLICs) [337], AAV5 uses caveolae-dependent endocytosis [25], and PPV utilizes macropinocytosis [57] as additional endocytic pathways. Most recently, Garcin and Panté showed that MVM enters its host cell by at least three potential endocytic routes. Inhibition of various endocytic pathways with specific drugs in combination with EM, immunofluorescence microscopy (IF), and fluorescence-activated cell sorting, identified clathrin-, caveolin-, and CLIC-mediated endocytosis for MVM. However, the latter endocytic uptake mechanism was restricted to transformed cells only, but did not occur in murine A9 fibroblasts. This observation was confirmed in further experiments which demonstrated that dynasore, an inhibitor of dynamins, completely blocked MVMp uptake in A9 mouse fibroblasts, whereas its inhibitory effect was incomplete in transformed cells. These results indicate that both clathrin- and caveolin-mediated MVMp endocytosis is dependent on dynamin in murine A9 fibroblasts, but transformed cells allow for the dynamin-independent CLIC-mediated uptake of MVMp [175]. Although parvoviruses share some general features in receptor binding and in their routes of cellular entry, each appears to display their own unique mechanistic details.

7.3. Endosomal Trafficking and Capsid Rearrangements

Endosomal trafficking of parvovirus virions is thought to be a slow and rate-limiting process in viral infection [159, 195, 197, 293]. The delayed progression to infection allows parvoviruses the opportunity to undergo important structural transitions and prolonged processing within endosomes. For instance, AAVs escape from early endosomes but only reach the nucleus after 40 min to 2 hours post-infection (hpi) [30, 501]. MVM is exceptionally well characterized with respect to endosomal trafficking in spite of the rapid dynamics and complexity of viral movement within and between endosomal compartments. It has been reported to traffic even slower through the endocytic pathway and only reaches the cell nucleus after 8 hpi when DNA replication was detected [388].

Several lines of evidence confirm that endosomal processing of incoming parvovirus particles is essential. First, virions with or without exposed N-VP2 termini failed to confer a nuclear localization phenotype to AAV2 when directly injected into the cytoplasm to bypass the endocytic pathway [149, 426]. Similarly, low pH pre-treated CPV capsids were unable to accumulate in the nucleus following injection into the cytoplasm [469]. Also, for MVM all structural rearrangements were equally impaired by lysosomotropic drugs, thereby preventing infection [293, 388]. These drugs, such as bafilomycin A₁ or the weak base chloroquine diphosphate, raise the endosomal pH by inhibiting the vacuolar-type H⁺-adenosine triphosphatase (ATPase) [63, 208, 217] or by accumulation inside acidic compartments [145, 341, 370], respectively. Finally, endosomal acidification has been demonstrated to be essential for the infection of AAV [30, 49, 156, 195], CPV [31, 357, 469], and MVM [293, 388].

Already 30 min after endocytosis, three considerable structural rearrangements of the MVM capsid occurred simultaneously. Specifically, the capsid transitions include the cleavage of the exposed N-VP2 termini, the externalization of originally sequestered N-VP1 termini, and the release of the full-length viral DNA genome without the loss of capsid integrity [293]. The conformational changes of parvovirus capsids, which are induced by endosomal trafficking *in vivo*, can be partially mimicked *in vitro*. Treatment of CPV particles under acidic conditions mimicking endosomal pH induced VP1u exposure [435]. However, in the case of MVM full capsids (FC), prior cleavage of N-VP2 termini to VP3 is a prerequisite for VP1u externalization under such conditions [131, 166]. Contrarily, the N-VP2 termini remained buried in the interior of EC and thus they were not accessible to proteolytic digestion [293]. Surprisingly, EC exposed the N-VP1 termini with similar kinetics to FC, indicating that at least for EC, neither the genomic DNA nor the cleavage of N-VP2 is involved in the extrusion of N-VP1 [131, 293]. Harsh conditions, such as exposure to heat or urea, trigger VP1u externalization in AAV [254], CPV [471, 478], and MVM particles [131, 134]. Characterization of the biochemical and structural capsid dynamics was enabled by artificial *in vitro* treatments although they cannot directly reproduce physiological conditions [131, 134, 254, 471]. The differences observed in the *in vitro* and *in vivo* studies imply

7. The Parvovirus Life Cycle

that a combination of several factors, such as receptor binding, low endosomal pH, or interactions with unknown host factors play a role in these structural transitions of parvoviruses.

The study of the infectious pathway of parvoviruses is impeded by the fact that the bulk of incoming particles are retained within lysosomal compartments and only a minority escapes the endocytic route (see Section 7.4, p. 36). Moreover, the lack of dynamic information in fixed cell samples has complicated the examination of virus trafficking through the highly dynamic and overlapping vesicular endocytic pathway. However, emerging advances in time-lapse microscopy make live-cell imaging an important complementary method to study the complex nature of endosomal trafficking in the future.

7.4. Endosomal Escape

The high particle to infection (P/I) ratio⁵ of most parvoviruses (100:1 to >1 000:1) [354, 440, 463] indicates that most of the incoming viruses fail to enter the nucleus. Indeed, a substantial portion of the incoming MVM virions was demonstrated to follow a non-infectious pathway ending up in lysosomal compartments where they co-localized with co-endocytosed dextrans which had a MW of 10 kDa and were used as lysosomal markers. Hence, the endosomal escape represents the major barrier for the subsequent steps of MVM infection. However, the inability to escape from the endocytic route was not due to a failure in endosomal processing of MVM since all virions retained in lysosomal compartments underwent the required structural transitions. MVM VLPs or EC that accumulated in lysosomes remained intact up to 50 hpi but the exposed, capsid-tethered viral DNA of FC was degraded 21 hpi, most probably, by the lysosomal endonuclease DNase II activity [293].

Unlike enveloped viruses, non-enveloped viruses are unable to deliver their genomes into the host cell by fusion with the cellular plasma or endosomal membrane [201]. They must employ alternative strategies to breach their host cell's delimiting membrane. Although MVM has not yet been directly demonstrated to permeabilize endosomal membranes, there is evidence that parvoviruses have the capability to disrupt membranes. Labeled dextrans with a MW of 3 kDa were progressively liberated into the cytosol 8–20 h after co-endocytosis with CPV virions. However, despite the apparent change in the permeability of endosomal membranes, there is no complete disintegration of endosomal vesicles since larger dextrans with a MW of 10 kDa, as well as α -sarcin, were mainly retained in vesicles at the same time post-infection [357, 435].

Several arguments speak in favor of the N-VP1 terminal PLA₂ activity (see Section 4.4.1, p. 19) mediating endosomal escape of parvoviruses. Firstly, N-VP1 becomes exposed in early

⁵ The P/I ratio is the number of virus particles per plaque-forming unit (PFU).

7.5. Cytosolic Trafficking and Interactions with the Proteasome

endocytic vesicles [131, 167, 183, 293, 429, 435, 508]. Secondly, VP1 has been demonstrated to be essential for productive infection of parvoviruses in a step prior to the initiation of DNA replication [30, 31, 156, 195, 357, 388, 461, 469]. Lastly, pre-incubation of N-VP1-exposing CPV virions with PLA₂ inhibitors, such as quinacrine and manoalide, significantly reduced or completely abolished infectivity, respectively [435]. For MVM [167] and AAV2 [429], complementation assays between wild-type and mutant particles have been used to demonstrate that the lipolytic PLA₂ function is mediating phospholipid bilayer penetration. Accordingly, mutants with amino acid substitutions within their catalytic dyad (see Section 4.4.1, p. 19) were constructed. Their enzymatic activity was severely impaired and viral infectivity was completely abrogated. Polyethyleneimine-induced endosomal rupture or co-infection with wild-type or mutant virions could partially rescue the mutant phenotype. Similarly, co-infection with endosomolytically active adenoviral variants resulted in a partial complementation of the mutant phenotype. Contrarily, endosomolytically inactive adenoviral variants, as well as wild-type EC carrying sequestered VP1u sequences, were unable to restore infectivity of the PLA₂-negative mutants. Thus, the capsid-tethered PLA₂ motif seems to be either directly or indirectly required for successful penetration of the endosomal membranes.

Information about the site of endosomal escape for MVM is still lacking. Previous *in vitro* experiments showed that the optimal pH for the parvoviral PLA₂ enzymatic activity ranges between pH 6 to 7, but drastically decreases at a pH below 5 [79]. Correspondingly, the acidic, lysosomal environment would not provide optimal conditions for PLA₂-mediated escape from the degradative pathway. Therefore, it is tempting to speculate that only a few viruses manage to escape the endocytic route from a pre-lysosomal compartment in the absence of vesicle disintegration. This hypothesis is supported by the fact that MVM externalizes N-VP1 already within the first minutes of infection, thus exposing the functional PLA₂ enzymatic activity on its surface. Additionally, brefeldin A, a fungal antibiotic that blocks the transition between early and late endosomes [271], has been demonstrated to abrogate MVM infection [388]. In summary, these results collectively suggest that the minority of virions that enter the cytosol escape from an intermediate pre-lysosomal vesicle, namely late endosomes [293].

7.5. Cytosolic Trafficking and Interactions with the Proteasome

Free diffusion of macromolecular complexes, such as viruses, is strictly limited in the lattice-like mesh of actin microfilaments, intermediate filaments, and microtubules present in the cytoplasm [285, 411]. Karyophilic viruses require active transport through the cytoplasm in order to reach the perinuclear area. CPV has been demonstrated to depend on active, dynein-mediated retrograde transport along the microtubules. Nocodazole (ND), a highly specific antimicrotubular drug promoting tubulin depolymerization in mammalian cells, prevented nuclear translocation of CPV.

7. The Parvovirus Life Cycle

Similarly, an antibody against the intermediate chain of the motor protein dynein also reduced the nuclear accumulation of CPV capsids. EM based studies and co-immunoprecipitations (IPs) of CPV with the intermediate chain of dynein reinforced a dynein-mediated transport of CPV along the microtubules toward the nucleus [434, 436, 472]. For MVM similar observations were reported. Intracellular transport requires a functional cytoskeleton and particularly depends on both microfilaments and microtubules. Both compounds cytochalasin D (CD), a drug inhibiting actin filament function, and ND had a moderate decreasing effect on nuclear viral DNA amplification [388].

Parvoviruses likely undergo further processing in the cytoplasm because microinjection of virions with or without externalized N-termini did not confer a nuclear translocation phenotype [357, 426, 435, 436]. For AAV2 and AAV5 it has been demonstrated that phosphorylation of surface exposed tyrosine residues followed by ubiquitination targets viral capsids for proteasomal degradation [504, 512, 513]. Correspondingly, co-administration of proteasome inhibitors, such as e.g. the tripeptidyl aldehyde MG-132, enhances AAV2 and AAV5 transduction efficiency. In contrast, proteasome inhibition was detrimental to infection for the autonomous parvoviruses PPV, CPV, and MVM. In particular, the chymotrypsin-like activity of the proteasome appeared to be essential for infection. While PPV capsid proteins were ubiquitinated early during the course of infection, no particle ubiquitinylated or degradation was observed for CPV and MVM [57, 387, 388].

7.6. Nuclear Targeting

In addition to the plasma membrane, the nuclear envelope constitutes a second barrier to karyophilic viruses. They need to enter the host's nucleus in order to profit from the replication and transcription machinery for their own multiplication. In fact, viral structural components enter the nucleus at two stages of their life cycle. At the start of infection the incoming virion delivers its genome and late in infection viral subunits accumulate in the nucleus for self-assembly leading to the generation of virus progeny. Small molecules freely diffuse through the nuclear pore complex (NPC). In contrast, nuclear import of larger macromolecules, between 9 and 39 nm in diameter [353], is highly selective and depends on energy and temperature [468]. Nuclear translocation across the NPC is mediated through import signals exposed on the cargo molecules in conjunction with soluble transport receptors [164, 171, 364].

7.6.1. Nuclear Translocation of the Incoming Virion

Interestingly, the functional diameter of the NPC central channel which has been reported to be 23–39 nm [160, 353] is in the range of the diameter of the parvovirus capsids [443]. Therefore, incoming parvoviruses could physically traverse the NPC fully intact unlike influenza- or retroviruses

which partially or completely uncoat their capsids [62, 73, 234, 343, 486]. In the absence of nuclear membrane disintegration, the transport of viral particles must proceed across the NPC [142, 393, 431], as it is the case for cellular proteins. However, there is other evidence that MVM enters the host's nucleus in a NPC-independent way (see step 5b in Figure 7.1, p. 31) [102]. When microinjected into the cytoplasm of *Xenopus oocytes*, MVM has been shown to cause damage to the nuclear envelope in a time- and concentration-dependent manner [101]. It has been proposed that MVM hijacks a cellular pathway to disrupt the nuclear envelope of the host cell. The exact mechanism remains elusive but appears to involve the re-localization of caspase-3 from the cytoplasm to the nucleus without its activation above basal levels in MVM infected cells. In the nucleus, caspase-3 was demonstrated to cleave lamin B2, resulting in a sustained disruption of the nuclear lamina structure and progression of nuclear envelope rupture. MVM-mediated, non-apoptotic caspase-3 activity induces nuclear entry of MVM capsids and possibly the nuclear targeting of further accessory proteins required for replication. Inhibition of caspase-3 during MVM infection resulted in a significant reduction of nuclear entry of MVM capsids and delayed expression of early viral gene products. These results support the possibility of a caspase-facilitated disruption of the nuclear envelope [103].

Several observations are in line with the nuclear translocation of MVM as an intact particle. CPV particles microinjected into the cytoplasm slowly entered the nucleus, possibly crossed the NPC, and were detected by antibodies against intact capsids, indicating that nuclear entry occurs without extensive uncoating [434, 472]. Other reports describe alternative NPC-independent nuclear import mechanisms for intact AAV particles when co-infected with adenoviruses [196, 501]. However, nuclear translocation of intact AAV particles was inefficient [30, 290, 410] or even not detected [426] in the absence of the helper virus, suggesting viral uncoating before or during nuclear entry.

Despite the fact that the NLM domain (see Section 4.4.3, p. 21) is disposed of the inner surface of the capsid [4], the structural rearrangements of MVM during the early endosomal trafficking (see Section 7.3, p. 35) allow the externalization of the VP1u sequence. In this way, the basic NLS sequences (see Section 4.4.2, p. 20) become exposed on the capsid surface. The exposed BC sequences may direct the incoming particle toward the nucleus. Accordingly, deletions of BC1 to BC4 sequences within VP1u completely abrogated MVM infectivity [278]. Similarly, cytoplasmic microinjection of VP1u-specific antibodies was able to neutralize CPV infection [471]. However, nuclear translocation of MVM as a stable disassembly intermediate remains possible since the generation of BC1-4 mutant virions required nuclear localization competent, NLM-harboring VP subunits. Therefore, the NLM within the common part of VP1 and VP2 may act together with the BC sequences in the process of nuclear localization since MVM particles composed of only VP2 subunits are insufficient for MVM infection [278, 461].

7. The Parvovirus Life Cycle

7.6.2. Nuclear Translocation of the Structural Proteins

Although sharing a common C-terminal sequence, with VP1 extending along additional 142 amino acids at its N-terminus, the structural proteins of MVM (see Section 4.3, p.18) translocate to the nucleus using different mechanisms. Deletions in any part of the VP2 sequence prevented the major VP from nuclear import, indicating that nuclear translocation is mediated by the conformational NLM (see Section 4.4.3, p. 21) requiring the correct cytoplasmic folding of the whole polypeptide. In contrast, in spite of harboring the same deletions within the common amino acid sequence to VP2, VP1 was not retained in the cytoplasm [277]. VP1 was actively imported using its NLS (see Section 4.4.2, p. 20), located within the VP1u region [278]. The NLS comprised of BCs shows high homology to conventional NLS of many karyophilic polypeptides (see Figure 4.3, p. 20) [174, 229].

Lombardo *et al.* demonstrated that VP1 was able to co-operatively interact with NLM incompetent VP2 subunits, resulting in a predominant accumulation of VP2 in the nucleus in approximately 40 % of the transfected cells. Such coupling of capsid proteins and co-operative nuclear import has also been shown for AAV2 [392]. The efficient nuclear import of NLM-deficient VP2 is surprising because MVM VP1 and VP2 subunits are expressed in a 1:5 stoichiometry. Correspondingly, there is evidence that each VP1 subunit interacts with two VP2 subunits to form a trimer which represents the stable precursor in the MVM assembly pathway [277]. Large insertion loops between the β G and β H strands (see Figure 4.1, p. 17) of threefold symmetry-related subunits extensively interact with each other [495, 502] to form the threefold spikes of parvoviral virions [4, 457]. This observation reinforces the hypothesis of a stable VP trimer as assembly precursor [277]. Indeed, covalent crosslinking of assembly intermediates revealed two types of oligomeric assembly units. The larger species, a heterotrimer, contains one VP1 and two VP2 subunits whereas the smaller homotrimer consist of only VP2 subunits [384]. Moreover, the stable trimeric assembly intermediates have been directly demonstrated by the use of atomic force microscopy [81].

Nuclear translocation of the viral structural proteins depends on the cell cycle. In human and mouse fibroblasts synchronized at G₀, G₁, and G₁/S transition, VPs accumulated in the cytoplasm. Upon arrest release, VPs translocated to the nucleus contemporaneously when the cell entered S phase. In the nucleus they immediately assembled into capsids (see Section 7.10, p. 48) [182].

The NLS and NLM may be involved as major regulatory elements at several levels of MVM morphogenesis because they maintain the stoichiometry between the VP subunits in the host's nucleus. Moreover, nuclear translocation capacity is only conferred to a specific subviral assembly intermediate, namely the VP trimer, thus organizing capsid assembly in the nucleus. Finally, correct folding of the polypeptide chains is a prerequisite for efficient nuclear translocation. Misfolded proteins are excluded from nuclear entry, hence preventing from detrimental interference with MVM capsid assembly in the nuclei [277].

7.7. Non-Structural Proteins

The strong dependence of parvoviruses upon host cell “factories” is due to their restricted complexity and strictly limited coding capacity. Parvoviruses do not encode for their own DNA synthesis machinery like large DNA viruses, such as poxviruses, but instead they interfere with the host cell physiology at several distinct stages. Only a few pleiotropic, multifunctional NS proteins suffice to orchestrate the host’s DNA replication, protein synthesis, and transport systems for their own benefit. By this mean parvoviruses ensure the efficient production of all the required viral components necessary for the morphogenesis of progeny virions. Moreover, eventual antiviral responses of the host cell are efficiently evaded. During the course of parvovirus infection, this overwhelming adaptation of the host cell environment is mediated by only five tightly regulated NS proteins. Regulation of the NS proteins involves post-translational modifications (PTMs), re-organization of their cellular compartmental distribution, and interactions with specific cellular partner proteins. Such changes ultimately lead to the formation of novel protein complexes with distinct functions and activities [330].

7.7.1. Non-Structural Protein 1

NS1 (83 kDa) is a multifunctional, regulatory, nuclear phosphoprotein that consists of several distinct domains. These include ATPase [492], endonuclease [91, 113, 340, 490], and 3’ to 5’ helicase [225] activities, as well as sequence-specific DNA recognition motifs [129, 132, 321], oligomerization domains [375], and an NLS [338]. The functional domains of NS1 act in concert or alone to control and orchestrate a variety of activities essential for viral genome amplification [116, 135, 136], transcriptional regulation [154, 198, 282], interactions with the host cell environment, and mediation of cytotoxicity [65, 78, 263, 273]. NS1 is required in stoichiometric amounts in order to ensure such a fine-tuned control of the virus life cycle. The steady-state level of the major regulatory protein NS1 is controlled by alternative splicing events (see Section 7.9, p. 45) and by its relatively long half-life (> 6 h) [114, 311], thus ensuring a progressive accumulation of NS1 throughout the course of infection. Moreover, specific activities of each individual functional domain can be regulated by PTMs, particularly phosphorylations at serine and threonine residues [110, 316], which are even temporally regulated.

An example for the functional interplay between different NS1 domains is represented by adenosine triphosphate (ATP) binding to the nucleoside triphosphate binding domain which promotes oligomerization of NS1 proteins [338], thus enhancing its site-specific binding to the consensus duplex DNA recognition motif (ACCA)₂₋₃ (see Figure 5.1 C and D, p. 26) [129] and contributing to its cytotoxic potential [105, 264, 273]. In contrast, hydrolysis of bound ATP releases energy [492] which is essential for duplex DNA unwinding activity [96, 223, 340, 492] during replication (see Section 7.8, p. 43 and Figure 7.2 (step iii-iv), p. 43). Thereby, NS1

7. The Parvovirus Life Cycle

liberates separated ssDNA strands of the duplex replication origin, which subsequently allow an NS1-mediated introduction of a site and strand specific nick at the consensus nick site via an energy-neutral *trans*-esterification reaction (see Section 5.1.1, p. 24) [67, 339, 425].

7.7.2. Non-Structural Protein 2

Three forms of the small MVM NS2 proteins (25 kDa) are generated during a productive infection. Each protein harbors a slightly different C-terminal peptide (see Section 7.9, p. 45). Only a little amount of mutant dsDNA RF and no accumulation of progeny unit-length ssDNA genomes were detected following infection or transfection of restrictive murine cells with NS2-null mutants [82]. However, the restricted replication of MVM genomes was less evident in transformed permissive human cells [326]. Therefore, NS2 was demonstrated to have a critical role in MVM replication, depending on the infected cell type. NS2 lacks any enzyme activities but it mediates regulatory functions through multiple interactions with cellular partner proteins in restrictive murine cells. Such cellular interaction partners include the nuclear export factor chromosome region maintenance 1 (Crm1) as well as 14-3-3 protein family members [56, 68, 342]. Since Crm1 functions as a nuclear export receptor and 14-3-3 proteins directly or indirectly regulate cellular protein kinases and phosphatases (reviewed in references [7] and [75]), NS2 is most likely involved in the modulation of cellular signaling of the host cell. Therefore, NS2 plays a central role in the control of nuclear export and progeny virion egress (see Sections 7.12 and 7.13, pp. 50 - 52). Similar to NS1, NS2 can be phosphorylated at multiple residues. Phosphorylation and dephosphorylation influences the subcellular distribution of both viral NS proteins [114] and their ability to interact with cellular partner proteins [56]. Several functions have been attributed to NS2, such as capsid assembly (see Section 7.10, p. 48) [130], genome replication (see Section 7.8, p. 43), mRNA translation, virus production (see Sections 7.10 and 7.11, pp. 48 - 50) [326, 327], and nuclear export of progeny virions (see Section 7.12, p. 50) [56, 161, 312, 342]. Interference with these NS2-mediated functions will cause changes in viral tropism, pathogenesis (see Chapter 6, pp. 27 - 29), and NS1-mediated cytotoxicity (see Section 7.7.1, p. 41) [65, 71, 104, 141, 264].

7.7.3. Small Alternatively Translated Protein

The SAT protein is encoded within the capsid gene and is conserved across all members of the genus *Protoparvovirus*. As for the capsid proteins (see Section 4.3, p. 18), expression of the SAT protein occurs late in infection from the same mRNA as VP2 (see Section 7.9, p. 45). Currently, its role during viral infection remains elusive. SAT has been shown to localize to the endoplasmic reticulum (ER) and to affect virus spreading in cell culture by an unknown mechanism [507]. It has been suggested to prevent major histocompatibility complex type I processing [314, 356] and/or cause ER stress-induced cell lysis, which is in line with other ER-targeted viral proteins [148, 274, 433, 439].

7.8. Replication

The coding capacity of MVM genomic DNA is strictly limited due to the small capsid size of an approximate maximum external radius of 140 Å [275]. Consequently, viral genes do not code for their own DNA- and RNA polymerases and relevant accessory proteins. In order to efficiently initiate replication, MVM must recruit and assemble crucial cellular host factors at one of its active origins of replication. Thus, viral proliferation depends heavily on ancillary cellular factors that are essentially involved in viral genome replication and transcription. These factors are transiently supplied by proliferating host cells during the S-phase in the nucleus [111, 147, 386, 427, 440, 444, 449]. In contrast to other host cell dependent, small DNA viruses, such as simian vacuolating virus 40 (SV40) [181, 204], MVM does not have the capability to stimulate resting cells and to initiate its DNA replication. Infection of resting host cells results in an initial latent period until infected cells enter S-phase in order to amplify their DNA [33, 98, 440]. For these reasons, MVM, and parvoviruses in general, show a pronounced predilection for rapidly dividing cell populations [111].

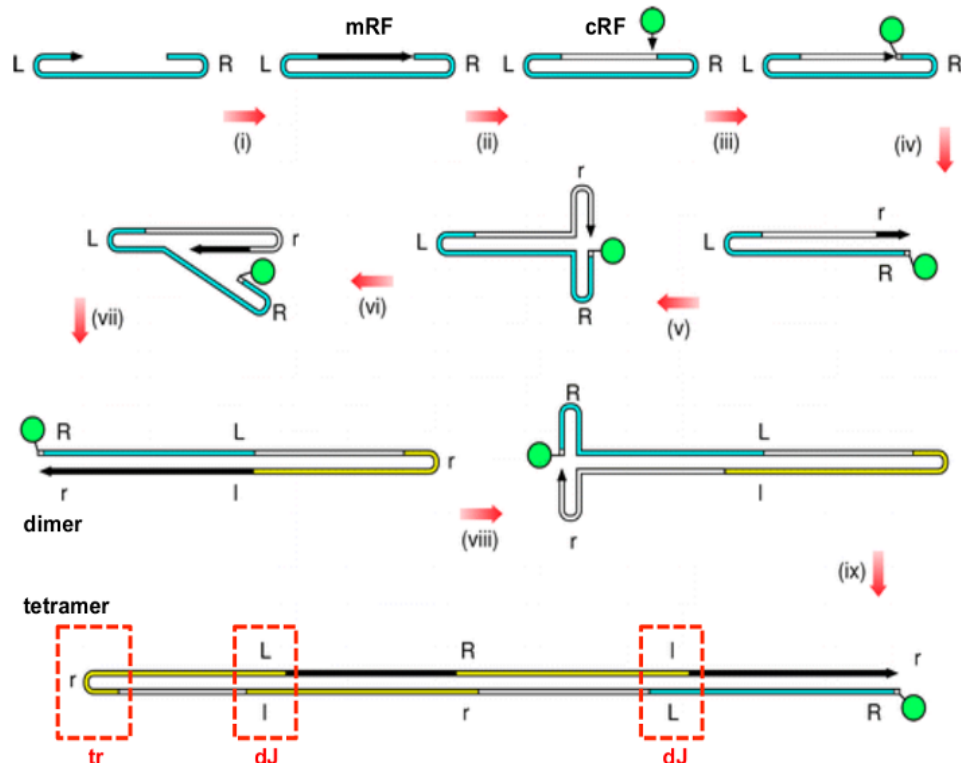


Figure 7.2.: Modified rolling hairpin model for MVM DNA replication. The sequence of the parvoviral genome is illustrated by a continuous line, colored blue for the parental genome, yellow for progeny genomes, and black for newly synthesized DNA, the 3' end of which is capped by an arrowhead. The green sphere represents NS1, which nicks the covalently closed monomer (cRF) and remains attached to its 5' end. The letters L and R depict the palindromic sequences at each terminus, with their inverted complements represented by l and r, respectively. Red dashed boxes depict the turnaround (tr) form of the right-end and the dimer junction (dJ) form of the left-end palindrome [120].

7. The Parvovirus Life Cycle

Parvoviruses are unique among all known viruses in having a DNA genome that is both linear and single-stranded. Thus, it is not surprising that they evolutionary adapted their own exclusive replication strategy. Their method to amplify the ssDNA genome resembles an ancient mechanism, called rolling circle replication. This is utilized by many other small, circular prokaryotic and viral replicons [222, 249, 259, 306, 346] but in parvoviruses it is modified and adapted for the replication of a linear chromosome. The parvoviral replication strategy, termed rolling hairpin replication (RHR), proceeds by a single-strand displacement mechanism. Thus, there is no lagging-strand synthesis and the integrity of the terminal hairpin sequences is maintained [445]. The unidirectional progression of the replication fork results in the synthesis of a single, continuous DNA strand. In addition, MVM replication forks are aphidicolin-sensitive and require the proliferating cell nuclear antigen (PCNA). These findings suggest a DNA polymerase δ -mediated DNA replication [33, 91, 336]. Initiation of parvovirus replication induces the reorganization of the host cell nucleus, leading to formation of distinct nuclear foci, referred to as autonomous parvovirus-associated replication bodies [34, 140, 505]. These bodies were shown to be active sites of viral replication and to accumulate essential cellular replication proteins, such as cyclin A, DNA polymerases α and δ , PCNA, and replication protein A [33].

In the initial stage of the RHR, complementary strand synthesis starts from the left-end snap-back telomere, which serves as a primer for the generation of double-stranded monomeric replicative form (mRF) DNA (see step (i) in Figure 7.2, p. 43). Subsequently, the growing complementary strand is ligated to the flipped-back right-end telomere by a host ligase, generating a covalently continuous closed replicative form DNA (cRF) species (see step (ii) in Figure 7.2, p. 43) [133, 276]. This monomer-length turnaround intermediate functions as a transcription template for NS1 (see Section 7.7.1, p. 41) expression. NS1 is essential for all further stages of the RHR pathway because the cellular replication machinery is unable to melt, copy, and re-orient the left-end telomere [22]. Specifically, NS1 nicks the right-end telomere (*OriR*) of the cRF intermediate [490], assisted by a host DNA-bending protein from the high-mobility group 1/2 family (see step (iii) in Figure 7.2, p. 43) [119]. The resulting, liberated, 3' nt at the nick site serves as a platform for the assembly of a new replication fork. NS1 remains covalently attached to the 5' end of the mRF DNA, where it also functions as the 3' to 5' replicative helicase [91, 112, 189]. The next step (see step (iv) in Figure 7.2, p. 43), called “hairpin transfer”, involves reopening and copying of the right-end hairpin sequence in order to generate a right-end extended duplex molecule, replacing the original sequence of the right-end telomere (R) with its inverted complement (r). The two previous steps (iii and iv) of the RHR are commonly referred to as “terminal resolution” [118]. In a NS1 dependent reaction, the extended duplex RF is melted and refolded into two hairpins, creating a “rabbit-ear” structure (see step (v) in Figure 7.2, p. 43) [283, 491]. In this way, the path of the replication fork is reversed effectively, redirecting it back along the internal coding sequences (see step (vi) in Figure 7.2, p. 43). Finally, this results

in the generation of dimeric RF and higher-order concatemeric molecules (see steps (vii-ix) in Figure 7.2, p. 43), in such a way that the viral coding sequence is replicated twice as frequently as the telomeres. Viral genomes are fused through a single palindromic junction, in either a left-end:left-end or right-end:right-end orientation. In a last step, individual, unit-length, ssDNA genomes are excised and displaced from the concatemeric RF intermediates. Initially, they feed back as new templates into the replicative pool to promote exponential DNA amplification but later they are consumed by encapsidation [122, 125].

7.9. Transcription and RNA Processing

Parvoviruses use a wide variety of alternative RNA processing strategies in order to exploit the strictly limited coding capacity of their small genomes. Alternative splicing of messenger RNA precursors (pre-mRNA) provides a powerful mechanism to generate structurally related but distinct proteins from a single gene, hence contributing to a complex but efficient and compact genome organization [304, 424]. The complex nature of MVM RNA processing of primary transcripts is summarized and simplified in Figure 7.3, p.47. The genome of MVM is transcribed in overlapping transcription units from two promoters located at m. u. 4 and 38, termed P4 and P38, respectively (see Figure 7.3 A, p. 47) [368]. Products of these promoters are three major transcript classes, R1 (4.8 kb) and R2 (3.3 kb), generated from P4, as well as R3 (2.8 kb), generated from P38 [257]. All MVM mRNAs are polyadenylated at a single polyadenylation site at the far right-hand end of the genome (see Figure 7.3 B, p. 47) [17, 97]. On the one hand, transcripts R1 and R2 encode the viral NS proteins NS1 and NS2, respectively, utilizing the ORF in the left half of the genome [109]. On the other hand, the R3 transcripts encode the overlapping viral capsid proteins VP1 and VP2, utilizing the ORF in the right half of the genome. Additionally, the non-structural SAT protein (see Section 7.7.3, p. 42) lies embedded within the capsid genes and likewise, is expressed from the P38 promoter [507]. Transcription from the viral early and late promoters is accomplished by the host RNA polymerase II [107, 368] and accompanied by various cellular transcription factors [6, 165, 178, 191, 369].

All MVM pre-mRNAs contain an overlapping set of downstream small introns in the center of the genome (m. u. 44-46) that is alternatively spliced using two donor sites (D1 and D2) and two acceptor sites (A1 and A2) [99, 114, 228, 318]. In addition to the small downstream intron, P4-generated transcripts also have a large upstream intron, located between m. u. 10 and 39. Intron splicing events are represented by the thin-lined carets in Figure 7.3 B, p. 47. Excision of the large intron is required to produce the R2 transcripts which encode the three NS2 protein isoforms [137, 228, 368]. Splicing at this site is critical in determining the steady state levels of NS1 and NS2 (see Section 7.7, p. 41) [114, 403]. Since R1 and R2 transcripts have similar stabilities [403], and are transported equally to the cytoplasm [328], the ratio of accumulated levels of R1

7. The Parvovirus Life Cycle

transcripts relative to R2 directly depends upon the percentage of P4-generated R2 transcripts which lack the large intron. In this way, MVM manages to maintain the optimal balance between the crucial roles which NS1 and NS2 play in viral replication and cytotoxicity [111]. On the contrary, alternative splicing of the small downstream intron from P4-generated pre-mRNAs leads to the production of three isoforms of NS2 [99, 114, 318] of the one part and the two structural capsid proteins, derived from P38-generated R3 transcripts, of the other part. The joining of donor D1 to acceptor A1 [major, M (\sim 70 %)] produces an mRNA which encodes the major capsid protein VP2, or a mRNA encoding NS2^P from R3 or R2 transcripts, respectively. Alternatively, joining of D2 to A2 [minor, m (\sim 25 %)] generates an mRNA encoding the minor capsid protein VP1, or an mRNA that encodes NS2^Y from R3 or R2 transcripts, respectively. Finally, a rare splicing pattern that joins D1 to A2 [rare, r (\sim 5 %)] is required for the production of NS2^L encoding mRNAs from R2 transcripts [17, 228, 257, 318]. The fourth splicing pattern that joins D2 to A1 is not detected *in vivo* [318], presumably because the distance between this sites (60 nucleotides) is too short to enable successful excision of introns in mammalian cells [348]. To date, only a few examples of small overlapping introns with two donors and two acceptors have been described in literature [187, 292, 304]. For MVM, the small central intron, which is excised efficiently from all classes of MVM pre-mRNA transcripts, appears to be the entry of the spliceosome. In addition, it dictates the relative amounts of VP1 and VP2 or of the three isoforms of NS2 produced during infection. Splicing of the large upstream intron occurs subsequent to small intron recognition and splicing. This second processing step is slowed to make sure that the spliced RNA can leave the nucleus to encode NS1. This delay is most likely ensured by the large non-consensus donors and acceptors of the splice site of the large intron [379]. However, the determinants governing the alternative excision of the large and small intron from MVM pre-mRNAs are poorly understood [180, 205, 206, 509–511]. Nonetheless, it is known that wild-type patterns of alternative splicing of MVM pre-mRNAs are achieved exclusively by cellular splicing factors without the involvement of auxiliary viral proteins [328]. Moreover, it has been shown that polyadenylation of MVM RNAs precedes splicing of the small intron since unspliced polyadenylated molecules can be detected in the nucleus. In contrast, no detectable accumulation of unspliced MVM RNAs were observed in the cytoplasm of infected cells [98]. This does not apply for the large intron which is only spliced in a proportion of the pre-mRNAs prior to its export from the nucleus. Once in the cytoplasm, R1 transcripts are prevented from further splicing to R2 transcripts. The mechanisms that regulate the export of R1 versus its nuclear retention and further splicing to R2 remain elusive [379]. All aforementioned splicing patterns are exemplified in Figure 7.3 B, p. 47.

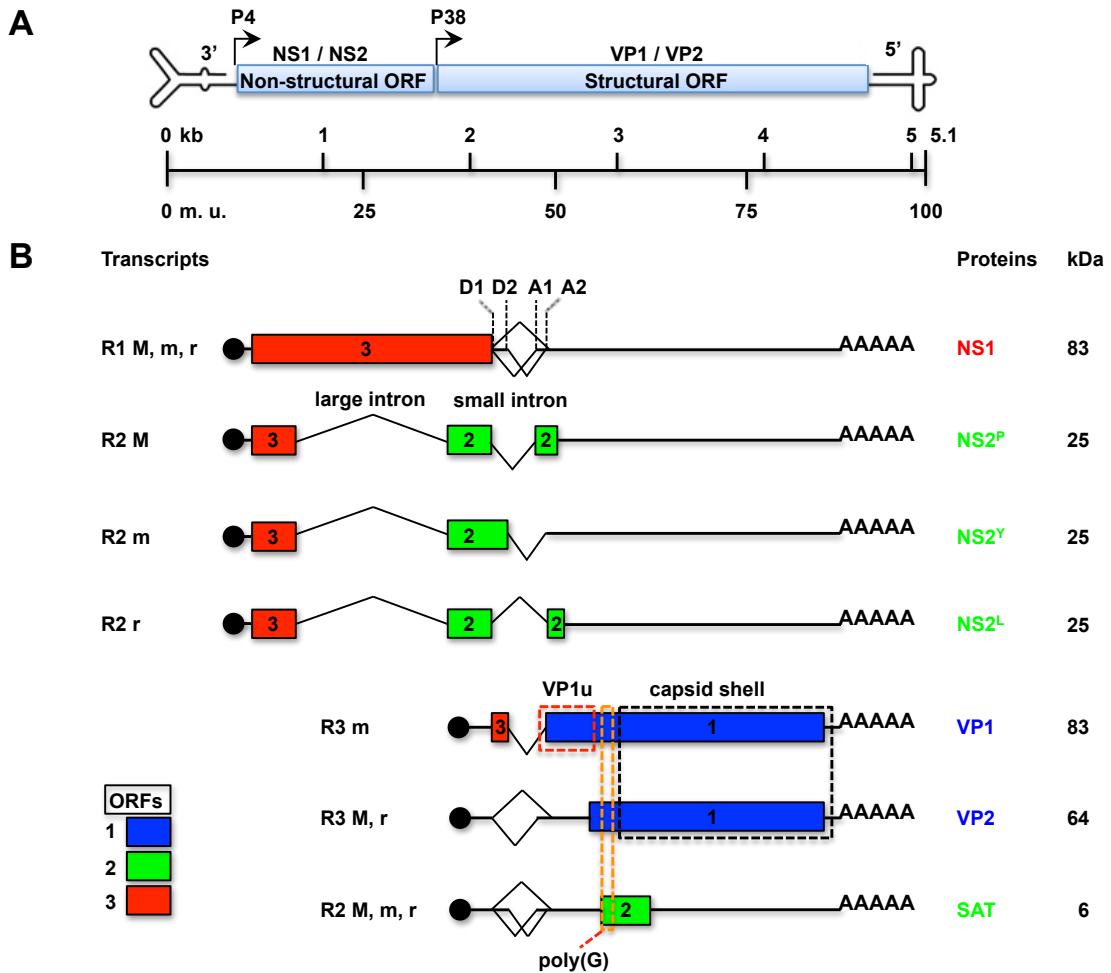


Figure 7.3.: Transcription map of MVM. (A) The single-stranded, negative-sense DNA genome of MVM is illustrated by a single line terminating in dissimilar hairpin telomeres. The two major ORFs are boxed in light blue and the proteins which they encode are indicated above. The two viral promoters, P4 and P38 are shown by rightward arrows. Below, arbitrary m. u. are diagrammed relative to the 5.1 kb genome. **(B)** The three major cytoplasmic transcript classes R1, R2, and R3 are displayed. A black sphere indicates the capped 5' ends and (AAAAA) denotes their polyadenylated tails near the far right-hand end of the genome. ORFs encoding the viral proteins, named on the right, are displayed in different coloring according to their reading phase. Their spliced-out large or small introns are indicated by thin-lined caretts. The small intron is excised from each transcript class by the alternative use of three different splicing patterns, denoted M (major), m (minor), and r (rare). Splice donor and acceptor sites for splicing of the small intron are denoted D1, D2 and A1, A2, respectively. On the one hand, alternative splicing of the small intron generates the R3 transcripts encoding VP1 and VP2, the two structural capsid proteins, and the R2 transcripts encoding three C-terminally distinct isoforms of NS2, referred to as NS2^P, NS2^Y, and NS2^L. On the other hand, excision of the large intron is critical in determining the steady state levels of NS1 and NS2 transcripts. The N-terminal protein sequence boxed in red represents VP1u which harbors the PLA₂ motif that is involved in entry functions. Sequences boxed in black, comprising the C-terminal region common to all VP polypeptides, assemble to form the capsid shell. Poly(G), boxed in orange, identifies a short glycine-rich region present in all VPs that can be modeled into X-ray density occupying the fivefold pores in virions. This Figure was adapted from reference [127]

7. The Parvovirus Life Cycle

Although viral proteins are not participating in the regulation of alternative splicing, they are indispensable for controlling transcription, along with relevant cellular transcription factors and viral *cis*-acting sequences. Interestingly, there is a chronological order to the production of MVM RNA transcripts. It was demonstrated that R1 and R2, the P4-generated pre-mRNAs, precede the P38-generated R3 transcripts during synchronous infection [98]. This temporal phasing is the result of NS1-dependent up-regulation of transcription from the P38 promoter [154, 382]. The acidic C-terminal domain of NS1 acts as a classical transcriptional activator that can potentiate P38 transcription approximately 100-fold [263]. In this way, the NS proteins, particularly NS1 that is essential for MVM DNA replication (see Section 7.8, p. 43) are available prior to the structural capsid proteins in order to initiate early events in parvoviral infection and to stimulate the transcription of the VP and SAT genes under the control of the late P38 promoter. An example for viral *cis*-acting sequences that regulate infection can be found in the left-end hairpin sequence, where both transcription and replication factors compete for specific recognition elements distal to the bubble sequence. Binding of cAMP-responsive element (CRE) to this sequence has been shown to contribute to maintaining basal levels of P4 activity and also to the up-regulation of P4 activity in transformed cells [172, 366]. CRE binding overlaps with the distal of the two 5'-ACGT-3' half sites needed to bind PIF (see Figure 5.1 C, p. 26) which is essential for stabilizing NS1 binding to the active left-end origin (*OriLTC*) for replication initiation (see Section 5, p. 23) [91]. In this way, replication and transcription are in competition with each other co-ordinate viral infection.

7.10. Assembly

The assembly of MVM capsids occurs in the nucleus and involves cytoplasmic trimerization of viral structural proteins and subsequent nuclear translocation of those trimers (see Section 7.6.2, p. 40) [384]. The formation of trimers results from extensive intertwining of the VP polypeptides through extended surface loops which form tight, convoluted intratrimer interactions (see Figure 4.1, p. 17) [275, 365]. These trimers are incompetent for capsid assembly in the cytoplasm. In order to confer nuclear assembly, the trimeric precursors undergo a global conformational rearrangement on top of the 3-fold spike at the center of each trimer [237, 279, 384]. Nuclear association of trimeric assembly intermediates is mainly mediated by quasi-linear, hydrophobic interactions between trimeric subunits. Polar interactions only marginally contribute to capsid assembly and stability [381].

Currently, it remains uncertain whether auxiliary nuclear factors are required for the final steps of parvovirus assembly and maturation. There is evidence that the formation of MVM capsids requires both nuclear factors and the major capsid protein VP2. Expressed capsid proteins that were incompetent for nuclear localization, as well as singly expressed nuclear transport competent VP1 proteins in the absence of VP2 proteins, were not able to assemble [215, 277, 278]. In the

case of B19V it was demonstrated that VP1 deletion mutants formed morphologically normal capsids but only a limited extension of VP1 was tolerated. Further lengthening of VP1 versions resulted in less efficient assembly and any assembled particles showed dysmorphic appearance [494]. Truncations beyond 30 amino acids at the N-terminus of VP2 prevented assembly because they affected the β A-strand of the conserved β -barrel motif which constitutes the core of the capsid shell (see Figure 4.1, p. 17) [238].

Nuclear assembly occurs regardless whether the host cell is in S-phase. Inhibition of DNA synthesis resulted in a reduction of mature virions. Nonetheless, EC accumulated in the nucleus of infected cells [246, 383]. The viral NS2 protein was reported to play a host-range specific role in MVM capsid assembly. On the one hand, MVM expressing truncated forms of NS2 was able to give rise to progeny virus in transformed human cells, albeit with reduced efficiency. On the other hand, they were unable to assemble in their restrictive murine host cells in spite of properly expressing NS1 and the structural proteins in early stages post-infection. The involvement of NS2 in virus assembly remains elusive but is likely to be indirect, since an appropriate cellular environment can complement the defect [130].

A better understanding of the mechanisms underlying capsid assembly and disassembly will be fundamental to the development of antiviral drugs. Virus propagation may be prevented by interference with capsid assembly or by promoting or inhibiting capsid disassembly [373, 514]. Further applications include the use of self-assembling viral nanoparticles for biomedical and nanotechnological applications [157, 299].

7.11. DNA Packaging

Commonly, viruses use two alternative strategies to package their genomes into the capsids. On the one hand, viruses containing circular dsDNA genomes assemble their protein shell around the genome, driven by interactions between protein capsid subunits and nucleic acids and assisted by auxiliary scaffolding proteins [44, 48, 345]. Moreover, several ssDNA or ssRNA viruses, such as tobacco mosaic virus, F1, and M13 bacteriophage follow the same assembly pathway via association of structural proteins around the genome [242]. On the other hand, viruses with double-stranded linear genomes translocate their genetic material into pre-assembled EC. This process is ATP-dependent and involves auxiliary non-structural packaging enzymes [47]. The presence of a large excess of EC in parvovirus stocks and the fact that recombinant expression of their structural proteins is sufficient for capsid formation [392] implies that the viral DNA is not required for capsid assembly. Thus, parvoviruses use the latter mechanism for genome translocation into their pre-formed capsids which accumulate in the cell nucleus (see Section 7.10, p. 48). Significantly, the encapsidation process has been visualized by EM in an *in vitro* assembly and packaging reaction of LuIII parvovirus [322].

7. The Parvovirus Life Cycle

In the case of MVM, partially or fully packaged capsids were demonstrated to interact with NS1. The NS protein was covalently attached to the 5' termini of unit-length ssDNA genomes. These structures may represent intermediates of the packaging process and NS1, particularly its 3' to 5' helicase activity (see Section 7.7.1, p.41) may support genome translocation into the pre-assembled capsid [113]. Similar observations were reported for AAV2 capsids which were shown to interact with the homologous *rep* proteins [372, 493]. DNase protection studies in AAV [242] and binding experiments between DNA and capsids of autonomous parvoviruses [310, 489] suggest a 3' to 5' packaging direction for parvoviruses. According to the directionality of the encapsidation process, the 3' to 5' processivity of the virus-encoded helicase, rather than the strand displacement 5' to 3' RHR synthesis, seem to drive the translocation of the genome into pre-formed capsids [242].

Initiation of the encapsidation process involves viral *cis*-acting elements. The ITRs of AAV contain a packaging signal which is both required and sufficient for genome encapsidation [398]. So far, a direct, specific interaction of AAV ITRs with capsids has not been demonstrated [475, 476]. In contrast, specific binding of the 3' terminal repeat of MVM to VP1 [488] and to particles composed only of VP2 [489] have been reported. However, interaction with VP1 is not essential for genome translocation since VP1 is dispensable for MVM assembly and packaging [461].

Cross-packaging of LuIII-derived vector genomes into capsids of MVM reinforced the observation that strand selection for packaging occurs due to varying efficiency of excision from replicated genomes of one strand polarity *versus* the other rather than differences in packaging preference [123]. This phenomenon is further elucidated in Section 5.1.1, p. 24.

7.12. Nuclear Export

Besides having the possibility to passively egress the host cell by NS1-induced cellular lysis, the latest data of several research groups propose an active, pre-lytic egress for MVM (see Section 7.13, p. 52) [28, 29, 298]. In order to actively egress the host cell, progeny particles of karyophilic viruses need to cross considerable cellular barriers. Apart from the plasma membrane, the nuclear envelope constitutes a second barrier to MVM. Although the mechanism for nuclear export and subsequent release of MVM virions remains unknown, several important viral and cellular effectors involved in the egress of parvoviruses have been identified and characterized.

MVM is supposed to be exported from the host's nucleus by a Crm1 dependent mechanism. A stable interaction between NS2 and Crm1 has been documented [56, 342]. Classical nuclear export signals (NES) exhibit low affinity for Crm1 in order to prevent the formation of the Crm1/cargo complex in the cytoplasm where RanGTP is absent [325]. Surprisingly, the NES of NS2 belongs to the supraphysiological NES which tightly bind to Crm1 regardless of the presence of RanGTP. Therefore, NS2 competitively inhibits Crm1 function by sequestering endogenous nuclear export receptors. MVM mutant genomic clones generating NS2 proteins harboring either regular

7.12. Nuclear Export

NES, or substitutions which abrogated Crm1 interaction were shown to be compromised in viral nuclear export and productive infection [162]. As expected, NS2-Crm1-mutants showed nuclear accumulation of export deficient NS2 in transfected cells. Surprisingly, the nuclear retention of mutant NS2 proteins came along with a substantial accumulation of progeny virions in the nucleus of infected cells, suggesting a NS2-dependent export of progeny virions [161]. Additionally, an indirect involvement of NS2 in viral egress was demonstrated using the closely related H1-PV. For this virus, an in-frame deletion of 38 amino acids within the common coding sequence of NS1 and NS2 was demonstrated to beneficially influence infectivity *in vitro*, indicated by a lower particle-to-infectivity (P/I) ratio and a larger plaque phenotype. The increase in infectivity which resulted from an accelerated egress of the mutant progeny virions, positively affected tumor growth suppression *in vivo* [484]. However, approaches to demonstrate a direct interaction between NS2 and the viral capsid and/or individual structural proteins *in vitro* have not yet been successful despite extensive attempts. Such interactions might be very weak and highly dynamic, thus it is difficult to demonstrate them.

The differences in nuclear export observed during productive MVM infection in either permissive human cells or restrictive murine cells may be due to cell-type-specific use of alternative strategies for nuclear export. They became particularly apparent when the different cell types were treated with the anti-fungal antibiotic leptomycin B (LMB) to inhibit Crm1-dependent nuclear export [255]. LMB treatment of susceptible murine cells resulted in a significant but not complete inhibition of nuclear export of MVM progeny virions. In contrast, even high doses of LMB did not inhibit nuclear export of MVM in transformed human cells, indicating that Crm1 is not required for the nuclear export of MVM in these cells [298]. The observed differences may result from a cell-type dependent phosphorylation status of MVM. Generally, MVM capsids derived from permissive human cells displayed prominent phosphorylation compared to the decent phosphorylation status of capsids isolated from restrictive murine fibroblasts [297]. Significantly, the three distal serine residues at position 2, 6, and 10 of the unordered N-VP2 terminus showed high phosphorylation levels in permissive cells. Site-directed mutagenesis studies discovered an important role of these phosphorylations in the Crm1-independent nuclear export of MVM in permissive human cells. When the N-terminal phosphorylations were diminished, progeny virions were predominantly retained in the nucleus and the corresponding mutants displayed a small plaque phenotype, indicating the importance of those phosphorylations in viral spread [298].

7. The Parvovirus Life Cycle

7.13. Egress

MVM transport from the nucleus to the cell periphery is associated with the degradation of actin fibers and the formation of “actin-patches”. These alterations to the filamentous network were attributed to a virus-induced imbalance between the actin polymerization factor neural Wiskott-Aldrich syndrome protein and gelsolin, a member of the actin-severing protein family [333]. Indeed, the MVM titer in the culture medium following MVM infection drastically declined when gelsolin function was diminished. During MVM infection, gelsolin activity is regulated by the CKII α /NS1 complex which was demonstrated to be capable of phosphorylating gelsolin. Consequentially, inhibition of CKII α correlated with prolonged persistence of actin fibers and delayed formation of the characteristic “actin patches” [28, 331]. A great deal of experimental data would point to an active, vesicle-associated, gelsolin-dependent export of MVM. Progeny virions were shown to co-localize with exocytic, endosomal, and lysosomal markers in immunofluorescent experiments [28, 152]. Cell fractionation experiments confirmed this observation by demonstrating a co-migration of viral particles with cytosolic vesicles rather than free, vesicle-independent localization in the soluble cytosolic fraction. Furthermore, dynamin was found to accumulate in the perinuclear region where it co-localized with *de novo* synthesized MVM capsids. A co-operative cross-talk between actin- and microtubule dependent transport [371, 422, 430] might be involved in MVM transport from the nucleus to the cell periphery, resulting in the destruction of actin filaments and the stabilization of microtubules [28].

The secretory pathway has been proposed as the route for active egress of MVM. Progeny virions would become engulfed by COPII-vesicle formation in the perinuclear ER where they accumulated with dynamin. Accordingly, a dramatic retention of virions in the perinuclear area and inhibition of virion release into the medium was observed in cells lacking functional effectors of the secretory pathway [29]. However, no significant co-localization between MVM progeny virions and representative markers of the recycling pathway or the Trans Golgi Network (TGN) were evident [29]. Radixin and moesin were shown to play a role in virus maturation and spreading capacity, as judged by their impact on MVM plaque morphology [332]. Indeed, dominant negative mutants failed in wrapping progeny virions into transport vesicles, resulting in a marked reduction of egressed virions in the culture medium. As a consequence, corresponding markers for alternative export routes, e.g. direct transport from the TGN to the PM or through recycling endosomes, exhibited increased co-localization with progeny virions. Finally, active egress promotes cellular lysis as demonstrated by the prolonged viability of cells wherein vesicular transport was either inhibited or by-passed the Golgi apparatus. In addition, the involvement of progeny particles in cytolysis was demonstrated by the prolonged survival of murine cells transduced with a viral vector deficient for the production of progeny virion particles [29].

8. Aim of the Thesis and Experimental Strategy

8.1. Goals

Viral egress affects the transmission and proliferation of virus progeny through the host's tissue. For enveloped viruses, the late maturation steps and final egress via budding through the plasma membrane are well characterized. However, the current knowledge about late maturation, nuclear export, and egress of non-enveloped viruses remains largely unknown.

The present thesis aims for a better understanding of the critical maturation steps leading to nuclear export and egress of a non-enveloped virus. The following issues are the main subject of this study:

1. Confirmation of the existence of an active process of nuclear export and egress of virions prior to passive release through cell lysis.
2. Characterization of the critical capsid maturation steps that trigger active pre-lytic egress.

8.2. Experimental Strategy

Three main experimental procedures were used:

1. Fast protein liquid chromatography (FPLC) was used in order to separate, concentrate, and purify different intracellular virus populations representing distinct maturation intermediates of the parvovirus life cycle. Minute virus of mice (MVM) served as a model parvovirus to study late maturation steps, nuclear export, and egress of non-enveloped viruses. All experiments were performed using a restrictive murine cell line and/or a transformed human cell line.
2. Standard biochemical and molecular biological methods were performed to investigate the structural and functional characteristics of the isolated virus populations.
3. Site-directed mutagenesis on an infectious clone of MVM was applied to study the role of different capsid regions in active egress.

Part II

Methods

9. Standard Laboratory Protocols

9.1. Cell Cultures

A9 ouab^rl1 cells, a derivative from the original HGPRT⁻ L-cell line A9 represent a clone resistant to 10⁻³ M ouabain after nitrosoguanidine mutagenesis [272, 442]. NB324K cells are a clone of SV40-transformed human newborn kidney cells [416]. The SV40 large T antigen was detected by immunofluorescent staining with monoclonal antibodies (mAb) [200]. However, NB324K cells do not produce infectious SV40 spontaneously. Both cell lines, A9 mouse fibroblasts and NB324K cells, were routinely propagated under a minimal number of passages in Dulbecco's Modified Eagle Medium (DMEM) (see Table 12.10, p. 143) supplemented with 5 % of heat inactivated fetal calf serum (FCS) at 37 °C in 5 % CO₂ atmosphere.

9.1.1. Freezing and Thawing of Cells

Before use, the A9 mouse fibroblasts or NB324K cells were thawed at 37 °C and cultured in 5 mL of pre-warmed DMEM (see Table 12.10, p. 143) supplemented with 5 % FCS. The medium was replaced every 3 to 4 days. In order to freeze the cells for long storage in liquid nitrogen they were passed the day before in DMEM containing 10 % FCS, to ensure exponential growth. Subsequently, 7.5 % DMSO was added and the cells were frozen slowly at -70 °C over night before transfer to liquid nitrogen.

9.2. Virus Stocks

Stocks of MVM prototype (MVMp) without detectable levels of VP3 were propagated on A9 mouse fibroblast monolayers. As soon as the cytopathic effect was complete (7-8 days post-infection), the supernatant (SN) was collected and pre-cleared from cell debris by low-speed centrifugation. Thereby, intracellular VP3 rich capsids were discarded. In order to remove low-molecular contaminants, virus containing SN was pelleted through 20 % sucrose cushion in PBS by ultra-centrifugation. Virus titers were determined by quantitative PCR (qPCR) (see Section 9.5, p.60) as DNA-packaged particles per microliter.

9. Standard Laboratory Protocols

9.2.1. Separation of Empty and Full Capsids

Sucrose purified capsids were prepared as previously described in Section 9.2, p. 57. The virus pellet was resuspended in 10 mL PBS. Caesium chloride was added to a density of 1.38 g/mL adjusted by refractometry ($\eta=1.371$) at 4 °C. The gradient was centrifuged to equilibrium for 24 h at 41 000 rpm and 4 °C in a Beckman SW-41 Ti swinging bucket rotor. Gradients were fractionated and tested for intact capsids by dot blot analysis using B7 mAb (see Table 12.8, p. 142). CsCl was depleted from the corresponding fractions by size-exclusion chromatography through PD-10 desalting columns (GE Healthcare) and the capsids were concentrated in Amicon® centrifugal filter devices (Merck Millipore) when required.

9.3. Freezing Bacteria Stocks in Glycerol

Bacteria were frozen in dry ice. A volume of 700 μ L of the bacteria culture that was grown over night in LB-medium (see Table 12.10, p. 143) was mixed with 300 μ L of 50 % glycerol in a cryotube. In order to mix well the glycerol the cryotube was vortexed intensively. Following snap-freeze in dry ice the bacteria were stored at -70 °C.

9.4. Fast Protein Liquid Chromatography

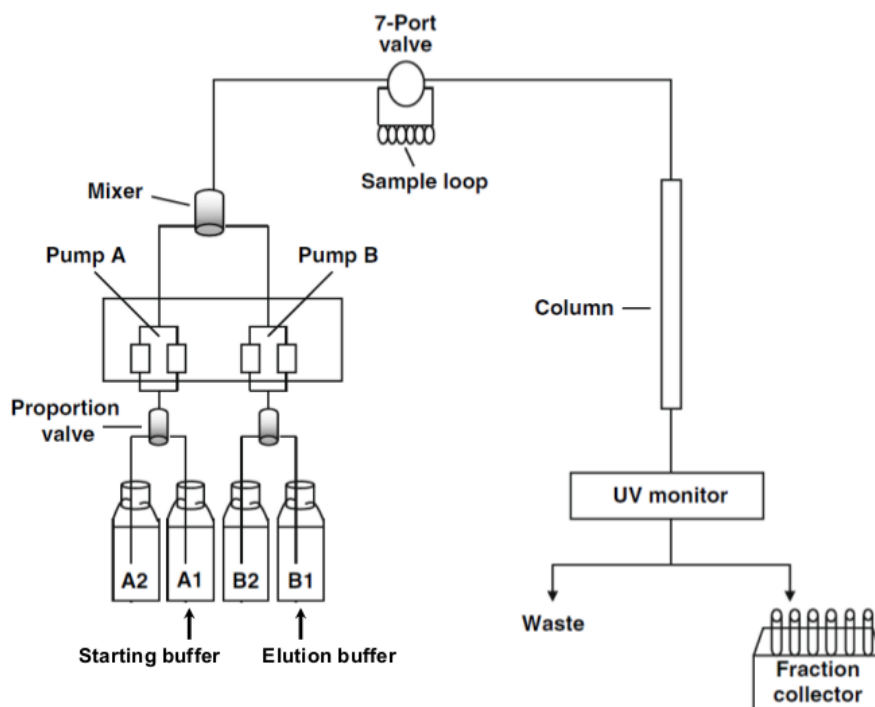


Figure 9.1.: Schematic outline of the ÄKTApurifier 10/100 UPC-900 chromatography system. This figure was adapted from reference [291].

9.4.1. Anion-Exchange Chromatography

A Mono QTM HR 5/5 (Pharmacia) column (5 x 50 mm) was used to analyse virus samples. The Mono Q column was connected to the ÄKTApurifier 10/100 UPC-900 chromatography system (GE Healthcare) that was operated by the unicorn 5.11 control software (GE Healthcare). The Mono QTM column was equilibrated with five column volumes (CV) starting buffer (see Table 12.3, p. 139). Samples (1 mL) containing at least 10¹⁰ DNA-containing virus particles in sample buffer (see Table 12.3, p. 139) were applied to the Mono QTM column through a 2 mL injection loop. Following sample application the loop and the column were rinsed with six CV starting buffer. In order to elute the bound proteins, a linear salt gradient (0-2 M NaCl) was applied by gradually increasing the concentration of the elution buffer (see Table 12.3, p. 139). The total elution volume of 24 CV was split into fractions of 185 µL which were collected in 96-well plates. The flow rate was kept constant at 1.5 mL/min and the salt concentration was monitored by measuring its electrical conductivity. Viral genomes in each fraction were quantified by qPCR (see Section 9.5, p. 60).

Increased back-pressure, color change at the top of the column, decreased sample recoveries, or loss of resolution indicate that the column matrix requires regeneration. In order to circumvent such problems, the column was washed every tenth run. To elute contaminants that stick tightly to the column the following harsh washing steps, summarized in Table 9.1, were applied to the reversed (bottom to top) Mono QTM column.

Table 9.1.: Steps 1-4 were performed to wash the Mono QTM HR 5/5 AEX column. The column was rinsed with 2 CV water in between each purification step.

Step	Reagent	Concentration	Volume
1	NaCl	2 M	500 µL
2	NaOH	2 M	500 µL
3	Acetic acid	75 %	500 µL
4	Starting buffer (see Table 12.3, p. 139)	-	10 mL

All runs were performed at 6 °C. Buffers were filtered and degassed before application to the Mono QTM column.

9.5. Quantitative PCR

Amplification of MVM DNA and real-time detection of PCR products were performed by using CFX96 technology (BioRad) with iTaq™ Universal SYBR® Green Supermix (see Table 12.6, p. 141). PCR was carried out by using the hot-start iTaq™ DNA polymerase (BioRad) following the manufacturer's guidelines. Viral DNA was isolated using the DNeasy blood and tissue kit (see Table 12.6, p. 141). Elution of the purified vDNA was carried out using 100 μ L elution buffer. As templates 2 μ L of the isolated viral DNA were used for the PCR reaction as outlined in Table 9.2.

Table 9.2.: Master mix for quantitative PCR. In order to minimize pipetting errors a master mix was prepared. Following preparation the master mix was distributed across the 96 well plates. The master mix contains all the ingredients which are required for the DNA amplification except the initial DNA template that differs among the samples.

Component	Amount	Final concentration
dH ₂ O, PCR grade	6 μ L	-
Forward primer (CR3), 10 pM	1 μ L	0.5 pM
Reverse primer (CR4), 10 pM	1 μ L	0.5 pM
2x IQ™ SYBR® Green Supermix	10 μ L	1 \times
Total volume	18 μL	

To ensure accurate quantification, the 96-well plates containing master mix and template DNA were shortly spun and transferred into the BioRad CFX96 unit. The PCR program used for quantification of viral DNA is detailed in Table 9.3.

Table 9.3.: PCR conditions for the amplification and real-time detection of MVM DNA.

Cycles	Step	Temperature	Time
1x	Initial denaturation	95 °C	300 s
40x	Denaturation	95 °C	15 s
	Annealing	61 °C	15 s
	Extension	72 °C	15 s
1x	Final denaturation	95 °C	60 s
1x	Melting curve	65 °C up to 95 °C	0.1 °C/s

To provide standards for sample quantification, serially diluted plasmids containing the entire MVM genomic DNA were used. For cell number variations that may exist between the samples, the number of applied cells per PCR reaction needed to be quantified for normalization as well. For this purpose quantification of cellular β -actin gene was performed. After normalization, direct comparison of the results is possible. β -actin quantification was carried out with the same PCR conditions outlined in Table 9.3, p. 60 with the annealing temperature ($60\text{ }^{\circ}\text{C}$) as the only exception.

In Table 9.4 all primers are listed which were used for MVM genome or β -actin gene quantification.

Table 9.4.: Different primers that were used for qPCR.

Primer	Sequence
CR3	5'-GACGCACAGAAAGAGAGTAACCAA-3'
CR4	5'-CCAACCATCTGCTCCAGTAAACAT-3'
Mouse β -actin forward	5'-TGGCACCAACACCTTCTACAATGA-3'
Mouse β -actin reverse	5'-CCGCTCGTTGCCAATAGTGA-3'
Human β -actin forward	5'-TGCTGTCCCTGTATGCCTCTG-3'
Human β -actin reverse	5'-AATGCCTGGGTACATGGTGGT-3'

9.6. Virus Infection

A9 or NB324K cells (10^5 for qPCR, IF, and Western blotting (WB) or 3×10^6 for AEX) were infected with MVM (5 000 DNA-containing particles per cell, corresponding to approximately 10 PFU/cell [440]) for 1 h at $4\text{ }^{\circ}\text{C}$ for binding. Unbound virus was removed by washings and the cells were incubated at $37\text{ }^{\circ}\text{C}$ to initiate infection. At progressive times post-internalization total cellular DNA was extracted for qPCR analysis (see Section 9.5, p. 60) or cells were fractionated (see Section 9.8, p. 62) and subjected to AEX (see Section 9.4.1, p. 59).

9. Standard Laboratory Protocols

9.7. Transfection

NB324K cells at a confluence of 70 % were trypsinized and resuspended in 10 mL of DMEM (see Table 12.10, p. 143) supplemented with 10 % FCS. A total amount of 10^6 cells were used for transfection with the AMAXATM nucleofectorTM II device following the manufacturer's instructions. Transfection was carried out with 5 μ g of the infectious clone of MVM (see Section 12.1, p. 131, [309]) using the V-001 program. As a transfection reagent, AMAXA[®] Cell Line Nucleofector[®] Kit V (see Table 12.6, p. 141) was used. Following transfection the weakened cells were maintained in 1.5 mL of pre-warmed culture medium and after 6 h, the culture medium was replaced with an equal amount of pre-warmed culture medium. The cells were further incubated for the required times.

9.8. Cell Fractionation

9.8.1. Nuclei Isolation

Isolation of A9 and NB324K nuclei was performed by using the Nuclei EZ Prep Nuclei Isolation Kit (see Table 12.6, p. 141) following the manufacturer's instructions. In order to obtain highly pure nuclear fractions, the isolated nuclei were pelleted through a sucrose gradient by low speed centrifugation at 500 g for 10 min. Extracted nuclei were lysed in nuclei lysis buffer (see Table 12.2, p. 138) at 4 °C for 30 min. Following vortexing thoroughly the nuclear lysate was passed through a 27 G needle 10 times. Debris was removed by centrifugation at 10 000 rpm for 10 min at 4 °C.

9.8.2. Extraction of the Cytoplasm

Cytoplasmic fractions were extracted in cell lysis buffer (see Table 12.2, p. 138) at 4 °C for 30 min. Following vortexing thoroughly, intact nuclei and cell debris was removed by centrifugation at 10 000 rpm for 10 min at 4 °C.

9.9. Immunoprecipitation

In vitro treated viruses or viruses from cell extracts were transferred to LoBind tubes that were pre-blocked with PBS containing 1 % bovine serum albumin (PBSA 1 %). The volume was adjusted to 200 μ L with PBSA 1 %. The antibody was added in excess and incubated with the viral capsids for 1 h at 4 °C on a rotary shaker. Subsequently, 20 μ L protein G-agarose beads were added. Following overnight incubation at 4 °C and centrifugation at 2 500 rpm for 5 min the supernatant was discarded. The beads were washed 4 times with PBSA 1 %. To remove the BSA an additional wash step was carried out with PBS. Finally, the beads were frozen at -20 °C until further use or immediately processed.

9.10. Dot Blot

Viruses (10^8 in 2 μL) were spotted on a nitrocellulose membrane. The membrane was blocked for 20 min with TBST containing 5 % milk. The primary antibody was diluted in TBST supplemented with 1 % milk and incubated for 30 min at room temperature. Unbound antibody was removed by washing the membrane 3 times for 5 min with TBST containing 1 % milk. The horseradish peroxidase (HRP)-coupled secondary antibody was diluted 1:20 000 in TBST supplemented with 1 % milk and added to the membrane for 30 min. Excess secondary antibody was removed by the same procedure as aforementioned for the primary antibody. The membrane was developed by exposure to photo films.

9.11. SDS-PAGE and Western Blotting

Immunoprecipitated capsids were dissolved in 20 μL 1× protein loading buffer (see Table 12.5, p. 140) containing 2 % SDS and 10 % glycerol. The samples were boiled at 96 °C for 8 min. Viral proteins were separated through a NuPAGE® 10 % Bis-Tris Gel (Invitrogen). The XCell Sure Lock™ Electrophoresis Cell (Invitrogen) was used to separate the proteins. The gel was first run at 30 V for 10 min to stack the proteins. In this way, sharper bands could be achieved. Separation of the different proteins was accomplished at 200 V. Following separation, the proteins were blotted on a methanol activated, porous, 0.2 μm polyvinylidene fluoride (PVDF) Immobilon® Transfer Membrane (EMD Millipore). Blotting was carried out at 30 V for 1 h 10 min using XCell II™ Blot Module (Invitrogen). The membrane was blocked in TBS-T buffer (see Table 12.5, p. 140) supplemented with 5 % milk overnight at 4 °C. Subsequently, the membrane was probed with a polyclonal rabbit antibody against linear MVM-VP epitopes (see Table 12.8, p. 142) that was diluted 1:2 000 in 3 mL TBS-T containing 1 % milk. The first antibody was incubated for 1 h at room temperature. The PVDF membrane was washed in TBS-T for a total 90 min with many buffer replacements. Subsequently, the horseradish peroxidise conjugated secondary antibody (goat α -rabbit-HRP, (see Table 12.9, p. 143) was added for 1 h at room temperature. This secondary goat anti-rabbit antibody was diluted 1:20 000 in TBS-T supplemented with 1 % milk. To deplete remaining antibodies, the membrane was washed in the same way as described above except for a final wash step with TBS (see Table 12.5, p. 140). VP1, VP2, and possibly VP3 were visualized by a chemiluminescence system (SuperSignal® West Femto Maximum Sensitivity Substrate, see Table 12.6, p. 141) following the manufacturer's instructions. After this treatment, the PVDF membrane was exposed to a film (Amersham Hyperfilm™ ECL, see Table 12.6, p. 141). Finally, the film was developed using Anatomix Developer Replenisher Solution and Fixer and Replenisher Solution (see Table 12.6, p. 141).

9. Standard Laboratory Protocols

9.12. Enzymatic Reactions

All enzymatic reactions were performed with 10^8 virus particles in a reaction volume of 50 μL . Viruses were incubated in PBS for 1.5 h at 37 °C with 0.5 mg/mL chymotrypsin (see Table 12.7, p. 142). The reaction was blocked by adding 100 μM chymostatin (see Table 12.1, p. 135).

Phosphatase lambda treatment (2000 Units, see Table 12.7, p. 142) was performed in 50 mM Tris-HCl, 100 mM NaCl, 2 mM MnCl₂, 5 mM DTT, pH 7.8 for 3 h at 37 °C in PBSA 1 % pre-blocked Protein LoBind eppendorf tubes. Phosphatase lambda was inactivated by supplementing the enzymatic reaction with 1 mM Na₃VO₄ and 1 mM NaF.

Free DNA was digested using 50 Units DNase I (see Table 12.7, p. 142) in 1× incubation buffer according to the manufacturer's protocol. DNase I was inhibited by incubation at 75 °C for 15 min.

Negative controls were incubated in the same buffers for the same time.

Part III

Results

10. Manuscript

**Late maturation steps in the nucleus preceding
pre-lytic active egress of progeny parvovirus.**

Raphael Wolfisberg, Christoph Kempf and Carlos Ros

1

2

3 **Late maturation steps in the nucleus preceding pre-lytic active egress of**

4 **progeny parvovirus**

5

6 Raphael Wolfisberg¹, Christoph Kempf^{1,2} and Carlos Ros^{1,2*}

7

8 ¹Department of Chemistry and Biochemistry, University of Bern, Freiestrasse 3,

9 3012 Bern, ²CSL Behring AG, Wankdorfstrasse 10, 3000 Bern 22, Switzerland

10

11

12 Running title: Late maturation preceding active egress of MVM

13 Word count for the abstract:

14 Word count for the text:

15

16

17

18

19

20 *Corresponding author: Department of Chemistry and Biochemistry, University of

21 Bern, Freiestrasse 3, 3012 Bern. Phone: +41 31 6314349. Fax: +41 31 6314887.

22 E-mail: carlos.ros@ibc.unibe.ch

23 **Abstract**

24 Although not well understood, growing evidence indicates that the non-enveloped
25 parvovirus minute virus of mice (MVM) may actively egress from the nucleus before
26 passive release through cell lysis. We have dissected the late maturation steps of the
27 intranuclear progeny with the aim to confirm the existence of an active pre-lytic
28 egress and to identify critical capsid rearrangements required to initiate the process.
29 By performing anion-exchange chromatography (AEX), intranuclear progeny particles
30 were separated by their net surface charges. Apart from empty capsids (EC), two
31 distinct progenies of full capsids (FC) arose in the nuclei of infected cells. The earliest
32 population of FC to appear was infectious but, similar to EC, could not be actively
33 exported from the nucleus. A further maturation of this early population, involving N-
34 VP2 exposure and phosphorylations of surface residues, gave rise to a second late
35 population with nuclear egress potential. While the capsid surface phosphorylations
36 were strictly associated to nuclear export capacity, mutational analysis revealed that
37 the phosphoserine-rich N-VP2 was dispensable. A reverse situation was observed for
38 the incoming particles, which were dephosphorylated in the endosomes acquiring the
39 AEX profile of the early nuclear progeny without nuclear export potential. Our results
40 confirm the existence of an active pre-lytic egress and reveal a phosphorylation-
41 dephosphorylation cycle associated to nuclear import and export potential required
42 for the replication of the karyophilic parvovirus.

43

44

45

46

47 **Importance**

48 In general, the process of egress of enveloped viruses is active and involves host cell
49 membranes, however, release of non-enveloped viruses seems to rely more on cell
50 lysis. At least for some non-enveloped viruses an active process before passive re-
51 lease by cell lysis has been described, although the mechanisms involved remain
52 poorly understood. By using the non-enveloped model parvovirus minute virus of
53 mice, we could confirm the existence of an active process of egress and further char-
54 acterize the capsid maturation steps involved. Following DNA packaging in the nu-
55 cleus, capsids required further modifications involving surface phosphorylations to
56 acquire export potential. Those surface phosphorylations were removed from the en-
57 tering capsids. This tightly controlled phosphorylation-dephosphorylation cycle allows
58 MVM to alternate its nuclear import and export potential required to complete the in-
59 fection.

60

61

62

63

64

65

66

67

68

69

70 **Introduction**

71 The egress of enveloped viruses is well characterized and involves budding through
72 host cell membranes (28, 58). The release of non-enveloped viruses is less well un-
73 derstood. In general, release of non-enveloped viruses is associated with cellular ly-
74 sis, thus considered a passive process (10, 29, 53). However, there is accumulating
75 data that an active egress precedes virus-induced cell lysis and subsequent passive
76 release. For instance, bluetongue virus has been demonstrated to usurp the ESCRT
77 machinery for egress by means of its L-domains (32, 59). Similarly, Hepatitis A virus
78 release involves ESCRT-associated proteins (15). Furthermore, drug-induced stimu-
79 lation of the autophagy pathway increased non-lytic spread of poliovirus and progeny
80 virions were shown to accumulate unilaterally on the apical surface of polarized and
81 productively infected epithelial cells (3, 54). Equally, simian vacuolating virus 40 and
82 simian rotavirus were almost exclusively recovered from the apical culture fluid of
83 polarized epithelial cells prior to cell lysis. Electron microscopy studies and specific
84 inhibition of vesicular transport pathways indicate a vesicle-associated release of
85 progeny virions (7, 17).

86 An active process of egress has also been suggested for parvoviruses (PV), a
87 group of small, non-enveloped viruses (1, 2, 27). Autonomous rodent PVs, including
88 minute virus of mice (MVM), display a T=1 icosahedral capsid containing a single-
89 stranded DNA genome of about 5 kb (9). Due to their simplicity, PVs strongly depend
90 on their host cell. Following entry, they are imported into the nucleus to profit from the
91 replication machinery of the host for their own replication. Subsequently, assembly
92 and genome packaging occur in the nucleus and give rise to the infectious progeny.
93 Productive PV infection causes dramatic morphological and physiological changes of

94 their host cells, culminating in cell death (5, 16) and passive release of progeny viruses.
95 PV cytotoxicity is mainly mediated by the large non-structural protein NS1.

96 Besides passive egress by cell lysis, the existence of an active, pre-lytic
97 egress for MVM has been suggested (1, 2, 27). Several important viral and cellular
98 factors involved in PV egress have been identified. The highly stable interaction of
99 the viral non-structural protein NS2 with Crm1 was suggested to play a role in egress
100 (4, 39). Classical nuclear export signals (NES) exhibit low affinity for Crm1 to prevent
101 the formation of stable Crm1/cargo complexes in the cytoplasm where RanGTP is
102 absent (34). Surprisingly, the NES of NS2 belongs to the supraphysiological NES
103 which tightly bind to Crm1 regardless of the presence of RanGTP. Therefore, NS2
104 competitively inhibits Crm1 function by sequestering endogenous nuclear export re-
105 ceptors (12). MVM mutants with disable Crm1 interaction were compromised in viral
106 nuclear export and productive infection. (11, 31). The exact role of NS2 in virus
107 egress was not elucidated and attempts to demonstrate an interaction of NS2 with
108 viral capsid proteins were not successful. Since NS2 has multiple functions, abroga-
109 tion of the tight NS2-Crm1 interaction might interfere with early functions during a
110 productive infection which may indirectly affect progeny maturation and their export
111 from the nucleus.

112 In human transformed cells, NS2 was dispensable for infection (35) and progeny
113 export was not affected by treatment with the antifungal antibiotic leptomycin B, a
114 drug which inhibits Crm1-dependent nuclear export. For these cells an alternative
115 export mechanism was proposed involving the unordered N-terminus of VP2 (N-VP2)
116 (27). Site-directed mutagenesis of the three distal serine residues at position 2, 6,
117 and 10 of N-VP2 revealed an important role of these phosphorylations in the Crm1-
118 independent nuclear export of MVM in permissive human transformed cells. When

119 the N-terminal phosphorylations were mutated, progeny virions showed an increased
120 nuclear retention and displayed a small plaque phenotype, indicating the importance
121 of those phosphorylations in viral spread (27).

122 Following nuclear export, it has been suggested that MVM is released actively
123 through a vesicle-associated, gelsolin-dependent mechanism, involving major rear-
124 rangements of the cytoskeleton. Progeny virions were shown to co-localize with exo-
125 cytic, endosomal, and lysosomal markers in immunofluorescent experiments. Cell
126 fractionation experiments confirmed this observation by demonstrating a co-migration
127 of viral particles with cytosolic vesicles (1). A co-operative cross-talk between actin
128 and microtubule-dependent transport might be involved in MVM transport from the
129 nucleus to the cell periphery (40, 46, 48).

130 The secretory pathway has been proposed as such a vesicle-dependent route
131 for active egress of MVM. Progeny virions would become engulfed by COPII-vesicle
132 formation in the perinuclear ER where they accumulated with dynamin. Accordingly,
133 a dramatic retention of virions in the perinuclear area and inhibition of virion release
134 into the medium was observed in cells lacking functional effectors of the secretory
135 pathway (2). In addition, members of the ERM family, such as radixin and moesin,
136 were shown to play a role in virus maturation and spreading capacity, as judged by
137 their impact on MVM plaque morphology (37). Consequentially, dominant negative
138 radixin or moesin mutants failed in wrapping progeny virions into transport vesicles,
139 resulting in a marked reduction of egressed virions in the medium. Finally, active
140 egress promotes cellular lysis as demonstrated by the prolonged viability of cells in
141 which vesicular transport was either inhibited or by-passing the Golgi apparatus. Be-
142 sides, the involvement of progeny particles in cytolysis was demonstrated by the pro-

143 longed survival of murine cells transduced with a viral vector deficient for the produc-
144 tion of progeny virion particles (2).

145 Documentation of active egress by non-enveloped viruses requires accurate
146 demonstration that no cell lysis occurred during the experiment. However, it is chal-
147 lenging to exclude the possibility that lysis of a few cells may passively release prog-
148 eny virions, which could additionally contribute to uncontrolled second rounds of in-
149 fection. Parvoviruses, particularly MVM, are highly robust and can persist as intact
150 particles in the lysosomes of infected cells (25). Since the entry and the proposed
151 egress route partially overlap in the dynamic endosomal pathway , the discrimination
152 between incoming and progeny virions represents a major challenge.

153 The present investigation aims to confirm the existence of an active egress for
154 MVM and to characterize the final capsid maturation steps leading to nuclear export
155 and egress of MVM. Using anion-exchange chromatography (AEX) in combination
156 with cell fractionation and quantitative PCR (qPCR) we demonstrate that two distinct
157 populations of DNA containing progeny particles co-exist in the nucleus of infected
158 murine cells. *De novo* synthesized capsids undergo a maturation step in the nucleus
159 that involves surface phosphorylation(s) and exposure of N-VP2. Only mature virions
160 were able to exit the nuclei and egress from the cells prior to cell lysis, confirming an
161 active egress of parvovirus MVM.

162 In tissue culture, passive egress considerably contributes to viral spread. However,
163 its importance in animal infection might be largely limited by clearance of virus-
164 infected cells by components of the immune system.

165

166

167 **Materials and Methods**

168 **Cells and viruses.** A9 mouse fibroblasts (51) and NB324K cells (45), were
169 routinely propagated under a minimal number of passages in DMEM supplemented
170 with 5 % FCS at 37 °C in 5 % CO₂ atmosphere. Stocks of MVM were propagated on
171 A9 cells. As soon as the cytopathic effect was complete, the supernatant was collect-
172 ed, pre-cleared from cell debris by low-speed centrifugation and the virus was pellet-
173 ed through 20 % sucrose cushion. The virus pellet was washed and resuspended in
174 PBS. Titers were determined by qPCR as DNA-containing particles per microliter.
175 DNA-containing (full capsids; FC) and empty capsids (EC) were separated by CsCl
176 gradient as previously described (42). CsCl was removed by size-exclusion chroma-
177 tography through PD-10 desalting columns (GE Healthcare, Chalfont St Giles, UK)
178 and when required, the capsids were concentrated in Amicon® centrifugal filter de-
179 vices (Merck Millipore, Billerica, MA).

180 **Antibodies, chemicals and enzymes.** Rabbit anti-VPs (polyclonal against
181 MVM structural proteins), rabbit anti-N-VP2 (polyclonal against the N-terminus of
182 VP2), and mouse anti-capsid (monoclonal against intact capsids; clone B7) antibod-
183 ies have been previously described (23, 27). Fluorescent-labeled secondary antibod-
184 ies were purchased from Santa Cruz Biotechnology (Santa Cruz, CA) and horserad-
185 ish peroxidase-conjugated antibodies were purchased from DakoCytomation
186 (Glostrup, DK). Bafilomycin A₁ (BafA1), chymotrypsin, and chymostatin were ob-
187 tained from Sigma-Aldrich (St. Louis, MO) and reconstituted in ethanol at 0.1 mg/mL
188 or in DMSO at 10 mM, respectively. To avoid enzymatic digestion or dephosphoryla-
189 tion during the processing of cell extracts, the lysis buffer was supplemented with
190 protease inhibitors (Roche, Basel, CH); 1 mM sodium orthovanadate (Na₃VO₄), and 1
191 mM sodium fluoride (NaF) (Sigma-Aldrich).

192 **Virus infection.** A9 or NB324K cells (8×10^3 for qPCR or 3×10^6 for AEX)
193 were infected with MVM (5000 DNA-containing particles per cell, corresponding to
194 approximately 10 PFU/cell (50)) for 1 h at 4 °C for binding. Unbound virus was re-
195 moved by washings and the cells were incubated at 37 °C to initiate infection. At pro-
196 gressive times post-internalization total cellular DNA was extracted for qPCR analysis
197 or cells were fractionated and subjected to AEX.

198 **Cell fractionation.** A9 and NB324K cytoplasmic fractions were extracted in 50
199 mM Tris-HCl, 150 mM NaCl, 5 mM EDTA, 1 % NP-40, 1 mM Na₃VO₄, 1 mM NaF,
200 protease inhibitor cocktail (Roche), pH 7.2 at 4 °C for 30 min. Following vortexing,
201 intact nuclei and cell debris were removed by high-speed centrifugation at 4 °C. Iso-
202 lation of nuclei was performed by using the Nuclei EZ Prep Nuclei Isolation Kit (Sig-
203 ma-Aldrich) following the manufacturer's instructions. In order to obtain highly pure
204 nuclear fractions, the isolated nuclei were further processed by centrifugation at 500
205 × g for 10 min through a sucrose gradient. The integrity of the isolated nuclei was
206 examined by light microscopy after trypan blue staining. The purity of the nuclei and
207 the absence of the outer nuclear membrane were evaluated with lamin A/C (inner
208 membrane) and serca 2 ATPase (outer membrane) antibodies. Purified nuclei were
209 lysed in 50 mM Tris-HCl, 150 mM NaCl, 5 mM EDTA, 1 % Triton X-100, 1 mM
210 Na₃VO₄, 1 mM NaF, protease inhibitor cocktail (Roche), pH 7.2 at 4 °C for 30 min.
211 Following vortexing, the nuclear lysate was passed 10 times through a 27 G needle
212 and nuclear debris was removed by high-speed centrifugation at 4 °C.

213 **Quantitative PCR (qPCR).** Template DNA was extracted by using the
214 DNeasy® Blood and Tissue Kit (Qiagen, Hilden, DE) following the manufacturer's
215 guidelines. Amplification and real-time detection of PCR products was performed by
216 using the CFX96™ Real-Time System with the iTaq™ Universal SYBR® Green Su-

217 permix (Biorad, Hercules, CA). Primers for MVM DNA amplification were: forward (5'-
218 GACGCACAGAAAGAGAGTAACCAA-3'; nucleotides 231 to 254) and reverse (5'-
219 CCAACCATCTGCTCCAGTAAACAT-3'; nucleotides 709 to 732). Specificity of the
220 amplification was determined by melting curve analysis. As external standard, an in-
221 fectious clone of MVM (30) was used in 10-fold serial dilutions.

222 **Anion-exchange chromatography (AEX).** The Mono Q HR 5/5 column (5 ×
223 50 mm; Pharmacia, Uppsala, SW) was connected to the ÄKTApurifier 10/100 UPC-
224 900 chromatography system operated by the UNICORN control software (GE
225 Healthcare). The Mono Q column was equilibrated with five column volumes (CV)
226 starting buffer (20 mM Tris-HCl, 1 mM EDTA, pH 7.2). Viruses (at least 10^8 virus par-
227 ticles) diluted in 1 mL starting buffer (10 mM Tris-HCl, 1 mM EDTA, pH 8) were ap-
228 plied to the Mono Q column through a 2 mL injection loop, rinsed with six CV of start-
229 ing buffer and eluted by a linear salt gradient (0-2 M NaCl) in 20 mM Tris-HCl, 1 mM
230 EDTA, pH 7.2. The flow rate was constantly kept at 1.5 mL/min and salt concentra-
231 tion was monitored by electrical conductivity. Viruses in each fraction (185 µl) were
232 quantified by qPCR.

233 **Immunofluorescence microscopy.** A9 cells (3×10^5) were seeded onto co-
234 verslips within 12-well plates. After 24 h, the cells were infected with 2'500 DNA-
235 containing particles per cell, corresponding to approximately 5 PFU/cell (41), for 1 h
236 at 4 °C. Subsequently, the cells were washed to remove unbound virus, and incubat-
237 ed at 37 °C. At different times, cells were washed and processed for immunofluores-
238 cence as previously described (21, 22) with fluorescent-conjugated secondary anti-
239 bodies. Cells were mounted with Mowiol (Calbiochem, Billerica, MA) containing 30
240 mg/ml of DABCO (Sigma-Aldrich, St. Louis, MO) as an anti-fading agent and exam-

241 ined by laser scanning microscopy (LSM 510 Meta; 100× magnification objective,
242 Carl Zeiss).

243 **Immunoprecipitation.** Viruses were incubated with specific antibodies in
244 LoBind eppendorf tubes pre-blocked with PBSA (PBS containing 1 % BSA) for 1 h at
245 4 °C. Subsequently, 20 µL protein G agarose beads were added and the samples
246 were further incubated overnight at 4 °C. The beads were washed with PBSA. To
247 remove residual BSA an additional washing step was carried out with PBS.

248 **Enzymatic reactions.** All enzymatic reactions were performed in a 50 µL re-
249 action volume. Viruses diluted in PBS (10^8 virus particles) were incubated for 1.5 h at
250 37°C with chymotrypsin (0.5 mg/mL) and the reaction was stopped by adding 100 µM
251 chymostatin. Lambda phosphatase treatment (40000 U/mL) was performed in 50 mM
252 Tris-HCl, 100 mM NaCl, 2 mM MnCl₂, 5 mM DTT, pH 7.8 for 3 h at 37 °C. Phospha-
253 tase was inactivated by adding 1 mM Na₃VO₄ and 1 mM NaF. Free DNA was digest-
254 ed using DNase I (50 U) at 37 °C for 1.5 h. DNase I was inhibited by incubation at 75
255 °C for 15 min.

256

257

258

259

260

261

262

263

264 **Results**

265 **Two distinct populations of progeny DNA-containing particles are detectable in**
266 **the nucleus of MVM infected cells.** Progeny viral particles released in the superna-
267 tant of infected cell cultures were collected 8 days post-infection (dpi), when cyto-
268 pathic effect was complete. Cell debris was excluded by centrifugation. The collected
269 viral capsids were analyzed by anion-exchange chromatography (AEX), which can
270 separate particles based on their net surface charges, followed by quantitative PCR
271 (qPCR). Two distinct virus populations of DNA-containing particles (full capsids; FC)
272 were separated and their relative amount quantified by qPCR (Fig. 1A). A second
273 AEX-qPCR analysis was performed in parallel, which included both medium and cell
274 lysate obtained by freeze and thaw cycles to release the remaining intracellular vi-
275 ruses. By including these additional intracellular viruses, the same two populations
276 were detected but their proportion was different. The more positively charged popula-
277 tion (referred to as FC progeny 1; FC-P₁) was predominantly associated with cells,
278 thus it increased when more intracellular viruses were included. In contrast, the more
279 negatively charged population (referred to as FC progeny 2; FC-P₂) was the predom-
280 inant population in the supernatant when most of the intracellular viruses were ex-
281 cluded.

282 In order to verify the integrity of the two DNA-containing viral populations, we
283 collected supernatant and intracellular viruses and subjected them to nucleolytic di-
284 gestion. As shown in Fig. 1B, both virus populations were resistant to nuclease diges-
285 tion and their AEX profile did not change, indicating that both particle types represent
286 assembled DNA-containing particles.

287 MVM capsid assembly occurs in the nucleus. It was therefore of interest to
288 verify the presence of both virus populations in the nucleus early at the onset of as-

289 semly and packaging. Viruses were collected from isolated nuclei of infected murine
290 fibroblasts early after infection and subjected to AEX-qPCR. As shown in Fig. 1C, by
291 18 hpi both DNA-containing viral populations co-existed in the cell nucleus in similar
292 amounts.

293 Besides DNA-containing capsids, MVM infection results in the accumulation of
294 empty capsids (EC), which represent assembled capsid precursors that have not yet
295 packaged viral genomes (33). To verify their AEX profile, EC precursors were purified
296 by CsCl, subjected to AEX and visualized by dot blot using an antibody against as-
297 sembled capsids (Mab B7) (23). As illustrated in Fig. 1D, EC had an AEX profile re-
298 sembling that of the FC-P₁ population. The fact that FC-P₁ particles are predomi-
299 nately cell-associated and have a similar AEX profile to that of the EC precursors would
300 suggest that they represent immature particles without egress potential, whereas FC-
301 P₂ would represent particles displaying a further maturation step enabling active re-
302 lease.

303 **FC-P₁ and FC-P₂ are infectious and differ in N-VP2 conformation.** In order
304 to further characterize the two FC populations, we separated them by AEX, pooled
305 the fractions corresponding to each population and performed a second AEX. In Fig.
306 2A the chromatograms of purified FC-P₁ and FC-P₂ are shown. The purified viral
307 populations were used to investigate their capacity to initiate the infection in A9 cells.
308 As demonstrated in Fig. 2B, both virus populations were able to reach the nucleus
309 and their genomes were replicated without significant differences.

310 In MVM virions the N-terminal region of the VP2 (N-VP2) occupies an external
311 positon in the capsid, however, during entry N-VP2 is cleaved by endosomal prote-
312 ases to render a shorter protein named VP3 (52, 56). The function of N-VP2 cleav-
313 age is not fully understood, but it is required to allow the exposure of the N-terminal

region of VP1 (N-VP1) (8, 13), which harbors important functional motifs essential for the infection (55), particularly endosomal escape (14) and nuclear targeting (22). We analyzed the surface conformation of N-VP2 in the two populations of FC by immunoprecipitation with a specific antibody raised against this region (27). As demonstrated in Fig. 2C, N-VP2 occupies a surface position in FC-P₂ but is predominantly sequestered in FC-P₁. Accordingly, FC-P₁ resembles to EC also in the sequestered N-VP2 conformation. In contrast to EC, exposure of FC-P₁ to temperature (50 °C) or to acidic conditions (pH 4.5) resulted in a significant externalization of N-VP2 (Fig. 2D). Chymotrypsin (CHT) has been previously demonstrated to mimic the *in vivo* cleavage of N-VP2. EC do not expose N-VP2 on the capsid surface and thus they cannot be cleaved. The AEX-purified capsid populations were subjected to proteolytic digestion by CHT under neutral and acidic conditions. As shown in Figure 2E, FC-P₂ particles were completely processed under all tested conditions. In contrast, the N-VP2 of FC-P₁ was only marginally accessible to CHT under neutral conditions and required acidification to improve the cleavage rate, confirming its predominant internal conformation. The substantial amount of VP2 that remained unprocessed originates from EC, which elute in the same AEX fractions as the FC-P₁.

When incubated with A9 cells, both virion progenies bound similarly to cells as shown by immunofluorescence. The N-VP2 from FC-P₂ was detectable on the surface of the cells and was fully processed by 4 hpi. As expected, the N-VP2 from FC-P₁ was not visible at binding but became exposed after internalization and a proportion remained detectable for several hpi (Fig. 2F), indicating a slower or less efficient VP2 to VP3 processing.

We next investigate whether the sequestered N-VP2 conformation in FC-P₁ is responsible for its distinct AEX profile. To this end, FC-P₁ virions were exposed to

acidic conditions to provoke the externalization of N-VP2 (as shown in Figure 2D) and analyzed by AEX-qPCR. The results showed that despite the externalization of N-VP2, the AEX profile remained unchanged. Accordingly, the distinct N-VP2 conformation is not responsible for the different AEX profile. The results also suggest that packaging does not directly result in N-VP2 externalization and further emphasize similarities between the FC-P₁ progeny virions and the EC precursors.

The surface phosphorylation status of the capsid is a key determinant of the different AEX profile. In order to further examine biochemical and structural differences between the two FC populations, both capsid species were isolated from the nuclei of infected A9 cells, treated with lambda phosphatase and subsequently analyzed by AEX-qPCR. When dephosphorylated by treatment with lambda phosphatase, FC-P₂ changed its AEX profile to that of FC-P₁, which remained unchanged (Fig. 3A). This result suggests that the differences between the two FC populations are due to a distinct surface phosphorylation status, other than the distal phosphoserines in N-VP2 (26). To confirm this, we used a MVM mutant, in which all distal serine residues on N-VP2 were substituted by glycine (referred to as 5SG). Similar to the wild-type (WT), the 5SG mutant generated also FC-P₁ and FC-P₂ particles (Fig. 3B) and pre-treatment with lambda phosphatase generated mostly FC-P₁ particles (Fig. 3C). These results confirm that additional phosphorylation(s), other than the distal phosphoserines in N-VP2, are present exclusively in the FC-P₂ population and are responsible for their specific AEX profile.

Only FC-P₂ has nuclear export potential and can actively egress from the infected host cell. The subcellular distribution of the two full capsid progenies was examined. A9 cells were infected with MVM and at progressive times pi, progeny viruses were collected from nuclear, cytoplasmic and supernatant fractions and sub-

364 jected to AEX-qPCR. While in the nucleus both FC populations accumulated with
365 similar kinetics, in the cytoplasm and in the supernatant, the accumulation of FC-P₂
366 preceded that of FC-P₁ (Fig. 4 A-C). The FC-P₂ egress started largely before the on-
367 set of cell lysis, which occurred from 30 hpi, as judged from the trypan blue exclusion
368 assay (Fig. 4E) and resulted in the appearance of FC-P₁ in the cytoplasmic and su-
369 pernatant fractions. The compartment-dependent segregation of the two full capsid
370 progenies at increasing times pi reveals the existence of an active mechanism of nu-
371 clear export and egress involving exclusively FC-P₂ particles and preceding the pas-
372 sive release of FC-P₁ and EC through late virus-induced cell lysis.

373 **FC-P₁ is the precursor of FC-P₂.** During infection in the presence of neuram-
374 inidase and anti-capsid antibody to prevent reinfections, FC-P₁ was the first popula-
375 tion to appear in the nucleus of murine A9 and human transformed NB324K cells.
376 While in NB324K cells FC-P₁ disappeared progressively to give rise to FC-P₂, in A9
377 cells this transfer was less efficient, leading to the accumulation of both populations
378 (Fig. 4A and Fig. 5A). In order to further confirm FC-P₁ as precursor of FC-P₂,
379 NB324K cells were transfected in the presence of neuraminidase and anti-capsid
380 antibody. FC-P₁ and FC-P₂ progeny virions were quantitatively analyzed by AEX-
381 qPCR at 24 and 48 hpt when no significant *de novo* production or degradation of viral
382 progeny particles was observed (Fig. 5B). As shown in Fig. 5C, FC-P₁ was the pre-
383 dominant virus population 24 hpt, representing approximately two third of the total
384 progeny virions. However, 48 hpt the total amount of FC-P₁ virions significantly de-
385 clined representing only one third of the whole virus progeny and giving rise to a sig-
386 nificant increase in the amount of FC-P₂ DNA-containing particles. Collectively, these
387 results indicate that FC-P₁ particles are the precursors of FC-P₂ virions. The matura-

388 tion of FC-P₁ into FC-P₂, which involves surface phosphorylations, would be more
389 efficient in the human transformed cells than in the A9 murine fibroblasts.

390 **The phosphoserine-rich N-VP2 is dispensable for active egress.** In sharp
391 contrast to FC-P₁ and empty particles, FC-P₂ capsids are exported from the nucleus
392 and subsequently released from the host cell prior to cell lysis. Distinct from EC or
393 from FC-P₁, N-VP2 of FC-P₂ is external and the capsids have additional capsid sur-
394 face phosphorylations. These features represent a late maturation step and might
395 confer the nuclear export potential to FC-P₂. N-VP2 is heavily phosphorylated at ser-
396 ine residues, which have been previously suggested to assist nuclear export in a cell-
397 specific manner. Mutants lacking N-VP2 distal phosphoserines were deficient in nu-
398 clear export and egress in NB324K cells, but not in A9 murine cells (27). We used a
399 mutant in which the four distal serine phosphorylations on the N-VP2 terminus and an
400 additional serine in the poly-glycine region, were substituted by glycine (referred to as
401 5SG). Additionally, we used a MVM mutant containing a bulky phenylalanine residue
402 at position 33 within the flexible poly-glycine stretch (referred to as G33F) (Fig. 6A).
403 Due to this substitution the mutant progeny particles were unable to externalize N-
404 VP2 following DNA packaging. Accordingly, transfection with this mutant generated
405 DNA-containing particles that were not infectious due to failure to expose and pro-
406 cess N-VP2 and to externalize VP1u during entry (6). Upon transfection, DNA-
407 containing progeny particles of 5SG and G33F progressively accumulated in the cell
408 culture medium to similar quantities and kinetics as the WT virions (Fig. 6B). AEX
409 analysis revealed that the G33F, as well as the 5SG progeny, consisted of both FC-
410 P₁ and FC-P₂ particles (data not shown), further substantiating that N-VP2 and/or its
411 distal phosphorylations are not responsible for the two distinct AEX profiles of FC-P₁
412 and FC-P₂. Transfection results in an increased cell lysis due to cell damage and

413 therefore, it is expected to increase passive release. To examine whether the ob-
414 served extracellular accumulation of G33F, 5SG, and WT progeny particles resulted
415 mostly from active egress, we analyzed the intra- and extracellular FC-P₁/FC-P₂ rati-
416 os 24 hpt. At this time, the FC-P₁ population exceeded that of FC-P₂ in the nucleus,
417 however, in the extracellular milieu the ratio was inverted (Fig. 5C and 6C). The in-
418 verted ratios can only be explained by the existence of an active egress of FC-P₂ par-
419 ticles, despite the presence of an increased passive release due to transfection-
420 mediated cell damage. These results emphasize that N-VP2 sequences and its distal
421 phosphorylations do not play a direct role in the nuclear export and egress of MVM.

422 **The nuclear FC-P₂ particles represent the ultimate maturation step of**
423 **MVM in terms of egress potential and infectivity.** We next examined whether the
424 nuclear FC-P₂ population represents the final maturation step in MVM morphogene-
425 sis or whether further maturation steps occur during the process of egress required
426 for infectivity. To this end, nuclear and extracellular FC-P₂ particles were purified by
427 AEX and their infectivity quantitatively compared. Apart from having the same AEX
428 profile, both particles were equally infectious (Fig. 7A). Therefore, virus egress does
429 not involve further maturation steps of the progeny required for infection.

430 **During entry, FC-P₂ particles are dephosphorylated acquiring the AEX**
431 **profile of FC-P₁.** In the nucleus, FC-P₁ particles mature through surface phosphor-
432 ylations to generate FC-P₂, which are particles with nuclear export potential. During
433 entry a reverse situation was observed, FC-P₂ particles were processed to generate
434 FC-P₁-like particles (Fig. 8). The N-VP2 of incoming FC-P₂ became cleaved by endo-
435 somal proteases (Fig. 2F). However, as previously shown in Figure 2G and 3B, the
436 presence or absence of N-VP2 with its distal phosphoserines has no influence in the
437 AEX profile. As already demonstrated *in vitro* (Fig. 3A), the different AEX profiles re-

438 sults from the presence of capsid surface phosphorylations. Accordingly, these criti-
439 cal surface phosphorylations are removed from the incoming FC-P₂ early during entry
440 by endosomal acid phosphatases. In order to confirm the involvement of acid phos-
441 phatases in the processing of incoming particles, bafilomycin A1 (BafA1), which rais-
442 es the endosomal pH and inhibits acid phosphatases, was applied to A9 cells. As
443 shown in Fig. 8, BafA1 totally abrogated the dephosphorylation of the incoming FC-
444 P₂ population.

445

446

447

448

449

450

451

452

453

454

455

456

457

458

459 **Discussion**

460 The active egress of enveloped viruses is well documented and involves budding
461 through host cell membranes. The egress of non-enveloped viruses is generally
462 thought to be the result of a lytic burst occurring at the end of the infection. However,
463 there is growing evidence that it may not be a mere consequence of the passive virus
464 release induced by cell lysis but involves a pre-lytic active transport of the progeny
465 virions (2, 3, 7, 15). The proof of an active pre-lytic egress for non-enveloped viruses
466 is challenging since the lysis of a few cells can passively release mature virions com-
467 plicating the discrimination between active and passive release. Therefore, it is not
468 sufficient to detect progeny virions in the culture media prior to significant cell lysis. In
469 addition, the identification of an active mechanism is necessary. By using anion-
470 exchange chromatography (AEX) and cell fractionation, we confirmed the existence
471 of an active egress for the model parvovirus minute virus of mice (MVM) prior to pas-
472 sive release by cell lysis. Additionally, we identified late capsid maturation steps oc-
473 curring in the cell nucleus preceding nuclear export.

474 The current model of MVM morphogenesis and egress suggests that EC pre-
475 cursors are first assembled in the nucleus and subsequently filled with the viral ssD-
476 NA to generate FC progeny (19). As a consequence of packaging, the phosphoser-
477 ine-rich N-VP2 becomes exposed outside of the shell through the fivefold axis of
478 symmetry (9, 52). The exposed N-VP2 has been suggested to mediate the export of
479 the FC progeny out of the nucleus (27), followed by virus egress, which was pro-
480 posed to occur by vesicular transport through the endoplasmic reticulum and Golgi
481 (2).

482 By using AEX, proteins can be separated based on their net surface charges.
483 We performed AEX to separate and characterize parvovirus progeny particles dis-

484 playing different protein surface configurations. Apart from EC precursors, the AEX
485 profile of intranuclear MVM progeny revealed not one but two well-defined DNA-
486 containing progeny populations, here named FC-P₁ and FC-P₂. FC-P₁ progeny
487 shares many characteristics with the EC precursors. They appeared early, had a sim-
488 ilar surface phosphorylation pattern, N-VP2 was essentially inaccessible and the par-
489 ticles were unable to be exported from the nucleus. FC-P₂ virions appeared later,
490 featured additional surface phosphorylations, N-VP2 was exposed and they showed
491 nuclear export potential. FC-P₁ would represent a previously unrecognized stage in
492 the MVM morphogenesis, intermediate between EC precursors and the late FC-P₂
493 virions. The nuclear export competent FC-P₂ virions represent the fully mature infec-
494 tious progeny. The infectivity and AEX profile of the FC-P₂ progeny isolated from the
495 nucleus (pre-egress) or actively released from the cells (post-egress) was the same
496 (Fig. 1 and 7). Hence, during active egress no further maturation steps were required
497 to acquire full infectivity.

498 The internal conformation of N-VP2 in FC-P₁ indicates that, in contrast to the
499 general assumption, DNA packaging alone is not sufficient to trigger the externaliza-
500 tion of N-VP2. Interestingly, the distinct N-VP2 conformation between the two FC
501 populations was not responsible for their different AEX profile. Heat treatment or in-
502 cubation at low pH externalized the N-VP2 termini of FC-P₁ but did not change its
503 AEX profile.

504 The N-VP2 termini, particularly their distal serine phosphorylations, have been
505 previously suggested to play a crucial role in the nuclear export of *de novo* synthe-
506 sized virion progeny (27). This data is in line with our findings which demonstrate that
507 following packaging, FC-P₁ particles with internal N-VP2 did not have nuclear export
508 capacity. In order to challenge a possible involvement of N-VP2 and its prominent

509 distal phosphorylations in the export of the late progeny FC-P₂ population, we used
510 two mutants. The first mutant, referred to as 5SG, lacks the five most distal serine
511 phosphorylations within the N-VP2 termini. The second mutant, referred to as G33F,
512 is unable to externalize the N-VP2 sequence on the surface of the capsid due to the
513 insertion of a bulky phenylalanine residue at position 33 of its poly-glycine stretch
514 within the VP2 protein sequence (Fig. 6A). Confirming our previous observations,
515 removal of the distal serine phosphorylations of N-VP2 or prevention of its externali-
516 zation had no influence in the different AEX profiles, which was exclusively defined
517 by additional surface phosphorylations (Fig. 3B and 3C). Following transfection in
518 NB324K cells, both mutants were able to generate the early FC-P₁ and the late FC-
519 P₂ progeny populations in the nucleus and accumulated in the culture media with
520 similar kinetics and quantities as observed for the WT (Fig. 3B, 6B and 6C). These
521 results confirm that the N-VP2 termini and their distal serine phosphorylations are not
522 key players in virus egress. Parvoviruses display a high mutation rate comparable to
523 RNA viruses (43, 44). Accordingly, genetic substitutions that interfere with crucial
524 stages of the viral life cycle result in reversions after only a few rounds of infection.
525 The distal S/G substitutions in N-VP2 were highly stable and no genetic reversions
526 were observed following several passages (data not shown). In agreement with our
527 findings, a deletion of seven amino acids within the sequence of N-VP2 with the in-
528 tention to disturb its function did not affect egress of progeny particles. However, this
529 truncation caused a retarded entry, leading to a delayed progeny egress. Additional-
530 ly, this mutant showed a lower cytotoxic effect (56). MVM infection is reported to in-
531 duce dramatic changes to the cytoskeleton of the host cell resulting in cell rounding
532 and detachment, culminating in lysis and passive progeny virus release (36). In infec-
533 tion experiments, the 5SG mutant showed also an inefficient nuclear entry, resulting
534 in a delayed egress (data not shown). The retardation of nuclear entry was accom-

535 panied by significantly reduced morphological alterations to the cytoskeleton of in-
536 fected murine cells. Dissimilar to wt infections, A9 cells infected with 5SG virions re-
537 mained intact and displayed the characteristic fibroblastic phenotype as late as 40
538 hpi.

539 Apart from the N-VP2 conformation, the surface phosphorylation pattern is the
540 second prominent difference between FC-P₁ and FC-P₂ (Fig. 3). Therefore, it is
541 tempting to speculate that the acquirement of these additional surface phosphoryla-
542 tion(s) confers nuclear export potential to the late progeny population. There are al-
543 ternative nuclear export routes that function in higher eukaryotes independently of
544 the Crm1/exportin1 pathway involving the prototypic leucine-rich NES (20, 49); re-
545 viewed in reference (24). These export mechanisms are predominantly regulated by
546 protein phosphorylation (18, 38). Accordingly, the additional capsid surface phos-
547 phorylations in FC-P₂ may explain their nuclear export potential. In line with this no-
548 tion, these surface phosphorylations were efficiently removed by acidic endosomal
549 phosphatases during entry of incoming virions, resulting in a complete reversion to
550 FC-P₁ particles (Fig. 8). Together with N-VP2 cleavage and N-VP1 externalization,
551 the dephosphorylation of surface residues would represent a novel processing step
552 during parvovirus cell entry which could be critical to stabilize incoming virions inside
553 the nucleus of infected cells. In line with this concept, it has been previously shown
554 that the endocytic route is required for nuclear targeting of CPV and AAV. Particles
555 microinjected into the cytoplasm to bypass the endocytic route failed to target the
556 nucleus, even when pretreated under acidic conditions (47, 57).

557 Heat or acidic treatment did not change the AEX profile of either progeny pop-
558 ulation, even though causing major structural transitions. Therefore, the phosphoryla-
559 tion of FC-P₁ to generate FC-P₂ particles should be mediated by resident nuclear

560 kinase(s) rather than by structural rearrangements exposing phosphorylated resi-
561 dues. The efficiency to achieve this late phosphorylation step was cell type depend-
562 ent, being more efficient in the human transformed NB324K than in the murine A9
563 cells. The more efficient phosphorylation in is in agreement with previous studies re-
564 porting lower overall capsid phosphorylation levels in murine A9 cells compared to
565 the transformed human cells (26).

566 The requirement of NS2 in progeny egress has already been demonstrated to
567 be indispensable for murine A9 cells but it is not a prerequisite in transformed
568 NB324K cells. NS2 harbors a supraphysiological NES and tightly interacts with Crm1.
569 Prevention of the NS2-Crm1 interaction has previously been demonstrated to impede
570 nuclear export of progeny virions in restrictive mouse fibroblasts (11, 31). These re-
571 sults explain the previously observed cell type specific inhibition of nuclear export by
572 leptomycin B (LMB) (27). However, NS2-Crm1 interaction is not required for the late
573 nuclear maturation of the virion progeny. A mutant containing amino acid substitu-
574 tions within the consensus NES sequence produced WT levels of FC-P₂ progeny but
575 nuclear export of the fully mature progeny was blocked (data not shown). Despite
576 extensive attempts, demonstration of a direct or indirect interaction between N-VP2
577 or other capsid regions and Crm1 failed. Therefore, the dependence of progeny
578 egress on the Crm1 export pathway may rather be indirect via the supraphysiological
579 interaction between NS2 and Crm1 (12).

580 In this study, the identified spatially and temporally controlled changes in cap-
581 sid surface phosphorylation would provide nuclear import and export potential re-
582 quired to complete the infectious cycle of the karyophilic virus. Further studies are
583 required to identify the corresponding phosphorylations on the capsid surface and to
584 demonstrate their specific role in the active egress of the non-enveloped parvovirus.

585 **Acknowledgements**

586 The authors thank J. M. Almendral for kindly providing infectious clones and antibod-
587 ies against MVM. We acknowledge A. Stocker and W. Aeschimann for competent
588 support and excellent technical assistance with the ÄKTA chromatography system.

589

590

591

592

593

594

595

596

597

598

599

600

601

602

603

604

605

606

607 **Legends for figures**

608 **Figure 1: Isolation of two distinct populations of *de novo* DNA-containing parti-**
609 **cles.** (A) Viruses (10^{10} DNA-containing particles) were collected 8 dpi from the cul-
610 ture media of infected A9 monolayers (SN). The media was enriched with additional
611 intracellular particles by repeated freeze and thaw cycles (SN + cells). Anion-
612 exchange chromatography (AEX) was performed and fractions were collected. DNA-
613 containing particles in each fraction were quantified by qPCR. (B) Prior to AEX-
614 qPCR, viruses collected from the culture media were treated with 50 U DNase I. (C)
615 A9 cells (3×10^6) were infected at a MOI of 5'000 DNA-containing particles per cell
616 for 1 h at 4 °C, followed by washing to remove unbound virus. The cells were further
617 incubated at 37 °C for 18 h. Nuclei were purified and the nuclear progeny was sub-
618 jected to AEX-qPCR analysis. To avoid re-infections, neuraminidase and α-capsid
619 mAb were added to the cells. (D) EC isolated from infected A9 cells were subjected
620 to AEX followed by dot blot using the α-capsid mAb for detection.

621

622 **Figure 2: FC-P₁ and FC-P₂ are infectious but differ in their N-VP2 conformation.**
623 (A) Fractions enriched in FC-P₁ or FC-P₂ virions (fractions 10-12 and 14-17, respec-
624 tively, see Fig. 1A) were pooled, dialyzed in TE-buffer pH 8, and re-subjected to AEX.
625 (B) A9 cells (8×10^3) were infected with purified FC-P₁ or FC-P₂ particles at a MOI of
626 2500 DNA-containing particles per cell for 1 h at 4 °C, followed by washing to remove
627 unbound virus. The cells were further incubated at 37 °C for 40 min or 22 h. Total
628 DNA was extracted and quantified as described in Materials and Methods. (C) Im-
629 munoprecipitation of 10^8 FC-P₁ or FC-P₂ particles with a B7 α-capsid mAb (total) or a
630 rabbit α-N-VP2 pAb. Specificity of the antibodies was confirmed using unspecific rab-
631 bit IgG. (D) FC-P₁ particles (10^8) were incubated at 50 °C or at pH 4.5. Immunopre-

632 cipitation was performed as explained above. (E) Purified FC-P₁ or FC-P₂ particles
633 (10^8) were incubated at pH 7, 6, or 5 and subjected to CHT treatment (+) or not (-).
634 Proteolytic N-VP2 processing was analyzed by 10 % SDS-PAGE followed by West-
635 ern blotting analysis. (F) A9 cells (3×10^5) were infected with purified FC-P₁ or FC-P₂
636 virions as indicated above. At different intervals pi the proteolytic processing of N-
637 VP2 was examined by immunofluorescence with B7 α -capsid mAb (green) and α -N-
638 VP2 pAb (red). (G) Purified FC-P₁ particles (10^{10}) were treated at pH 7 or pH 4.5 fol-
639 lowed by dilution in TE-buffer pH 8 and AEX-qPCR analysis.

640

641 **Figure 3: The surface phosphorylation status determines the AEX profiles of**
642 **FC-P₁ and FC-P₂.** (A) Nuclear virus progeny (10^{10} DNA-containing particles) was
643 treated with lambda phosphatase (40000 U/mL) for 3 h at 37 °C prior to AEX-qPCR
644 analysis. (B) A9 cells (3×10^6) were infected with 5SG mutant viruses as previously
645 described. Nuclear progeny virions (10^{10} DNA-containing particles) were analyzed by
646 AEX-qPCR analysis. (C) An identical amount of nuclear 5SG progeny virions was
647 treated with lambda phosphatase as outlined above and subjected to AEX-qPCR
648 analysis.

649

650 **Figure 4: FC-P₂ progeny actively egress from the infected host cell.** A9 cells ($3 \times$
651 10^6) were infected with 5000 DNA-containing particles per cell at 4 °C. Following
652 washing to remove unbound viruses the cells were incubated at 37 °C in the pres-
653 ence of neuraminidase and B7 for the indicated times. Cells were fractionated as ex-
654 plained in Materials and Methods and subjected to AEX-qPCR analysis. Relative
655 amounts of FC-P₁ and FC-P₂ virions were calculated and plotted. (A) Progeny in the
656 nuclei of infected A9 cells. (B) Progeny in the cytoplasm of infected A9 cells. (C)

657 Progeny in the culture media of infected A9 cells. (D) Phase contrast pictures of the
658 infected cells were taken using a Zeiss Axiovert 35 microscope with a 20 \times magnifica-
659 tion objective. Cell viability was accessed via trypan blue exclusion using the TC10TM
660 automated cell counter (BioRad). The average of three independent measurements
661 is indicated.

662

663 **Figure 5: Dynamics of FC-P₁ and FC-P₂ in infection and transfection.** (A) A9 and
664 NB324K cells (3×10^6) were infected with 5000 DNA-containing particles per cell at 4
665 °C. Following washing to remove unbound viruses the cells were incubated at 37 °C
666 in the presence of neuraminidase and B7 mAb for the indicated times. Nuclei isola-
667 tion and AEX-qPCR analysis were performed as specified in Materials and Methods.
668 (B) NB cells (10^6) were transfected in the presence of neuraminidase and B7 mAb.
669 Intracellular virus was immunoprecipitated with B7 mAb and quantified at the indicat-
670 ed time points post-transfection. (C) NB cells were transfected as explained above.
671 AEX-qPCR analysis was performed at the indicated time-points.

672

673 **Figure 6: The phosphoserine-rich N-VP2 is dispensable for active egress.** (A)
674 Schematic representation illustrating the introduced mutations used for the transfec-
675 tion experiments. (B) NB cells (10^6) were transfected with the WT infectious clone or
676 the indicated mutants in the presence of neuraminidase and B7 mAb. The virus
677 progeny in the media was treated with DNase I and quantified. (C) AEX-qPCR analy-
678 sis of intracellular and released virions was performed 24 hpt and the FC-P₁ to FC-P₂
679 ratio was calculated.

680

681 **Figure 7: Nuclear FC-P₂ virions do not require further maturation to acquire**
682 **infectivity.** FC-P₂ particles were purified by AEX from the nuclei of infected A9 cells
683 and from the culture media. A9 cells (8×10^3) were infected at 4 °C for 1 h. Following
684 removal of the unbound virus the cells were incubated at 37 °C for the indicated
685 times. Intracellular DNA was extracted and viral genome copies were quantified.

686

687 **Figure 8: During entry, acidic phosphatases remove the surface phosphoryla-**
688 **tions associated to nuclear export potential.** A9 mouse fibroblasts (3×10^6) were
689 infected with purified FC-P₂ (5000 particles per cell) at 4 °C. Following removal of
690 unbound viruses, cells were incubated at 37 °C for the indicated times and subjected
691 to AEX-qPCR. In order to inhibit acidic phosphatases, 150 nM BafA1 was added 15
692 min prior to virus internalization at 37 °C.

693

694

695

696

697

698

699

700

701

702

703

704 **References**

- 705 1. **Bar, S., L. Daeffler, J. Rommelaere, and J. P. F. Nuesch.** 2008. Vesicular egress of non-
706 enveloped lytic parvoviruses depends on gelsolin functioning. *Plos Pathogens* **4**.
- 707
- 708 2. **Bar, S., J. Rommelaere, and J. P. F. Nuesch.** 2013. Vesicular Transport of Progeny Parvovirus
709 Particles through ER and Golgi Regulates Maturation and Cytolysis. *Plos Pathogens* **9**.
- 710
- 711 3. **Bird, S. W., N. D. Maynard, M. W. Covert, and K. Kirkegaard.** 2014. Nonlytic viral spread
712 enhanced by autophagy components. *Proc Natl Acad Sci U S A* **111**:13081-6.
- 713
- 714 4. **Bodendorf, U., C. Cziepluch, J. C. Jauniaux, J. Rommelaere, and N. Salome.** 1999. Nuclear
715 export factor CRM1 interacts with nonstructural proteins NS2 from parvovirus minute virus
716 of mice. *J Virol* **73**:7769-79.
- 717
- 718 5. **Caillet-Fauquet, P., M. Perros, A. Brandenburger, P. Spegelaere, and J. Rommelaere.** 1990.
719 Programmed killing of human cells by means of an inducible clone of parvoviral genes
720 encoding non-structural proteins. *EMBO J* **9**:2989-95.
- 721
- 722 6. **Castellanos, M., R. Perez, A. Rodriguez-Huete, E. Grueso, J. M. Almendral, and M. G.
723 Mateu.** 2013. A slender tract of glycine residues is required for translocation of the VP2
724 protein N-terminal domain through the parvovirus MVM capsid channel to initiate infection.
725 *Biochemical Journal* **455**:87-94.
- 726
- 727 7. **Clayson, E. T., L. V. Brando, and R. W. Compans.** 1989. Release of simian virus 40 virions
728 from epithelial cells is polarized and occurs without cell lysis. *J Virol* **63**:2278-88.
- 729 8. **Cotmore, S. F., A. M. D'Abromo, C. M. Ticknor, and P. Tattersall.** 1999. Controlled
730 conformational transitions in the MVM virion expose the VP1 N-terminus and viral genome
731 without particle disassembly. *Virology* **254**:169-181.
- 732
- 733 9. **Cotmore, S. F., and P. Tattersall.** 1987. The Autonomously Replicating Parvoviruses of
734 Vertebrates. *Adv Virus Res* **33**:91-174.
- 735
- 736 10. **Daeffler, L., R. Horlein, J. Rommelaere, and J. P. F. Nuesch.** 2003. Modulation of minute
737 virus of mice cytotoxic activities through site-directed mutagenesis within the NS coding
738 region. *J Virol* **77**:12466-12478.
- 739
- 740 11. **Eichwald, V., L. Daeffler, M. Klein, J. Rommelaere, and N. Salome.** 2002. The NS2 proteins of
741 parvovirus minute virus of mice are required for efficient nuclear egress of progeny virions in
742 mouse cells. *J Virol* **76**:10307-10319.
- 743
- 744 12. **Engelsma, D., N. Valle, A. Fish, N. Salome, J. M. Almendral, and M. Fornerod.** 2008. A
745 supraphysiological nuclear export signal is required for parvovirus nuclear export. *Molecular
746 Biology of the Cell* **19**:2544-2552.
- 747
- 748 13. **Farr, G. A., S. F. Cotmore, and P. Tattersall.** 2006. VP2 cleavage and the leucine ring at the
749 base of the fivefold cylinder control pH-dependent externalization of both the VP1 N terminus
750 and the genome of minute virus of mice. *J Virol* **80**:161-171.
- 751
- 752 14. **Farr, G. A., L. G. Zhang, and P. Tattersall.** 2005. Parvoviral virions deploy a capsid-tethered
753 lipolytic enzyme to breach the endosomal membrane during cell entry. *Proc Natl Acad Sci U S
754 A* **102**:17148-17153.

- 755 15. **Feng, Z., L. Hensley, K. L. McKnight, F. Hu, V. Madden, L. Ping, S. H. Jeong, C. Walker, R. E.**
756 **Lanford, and S. M. Lemon.** 2013. A pathogenic picornavirus acquires an envelope by
757 hijacking cellular membranes. *Nature* **496**:367-71.
- 758
- 759 16. **Herrero, Y. C. M., J. J. Cornelis, C. Herold-Mende, J. Rommelaere, J. R. Schlehofer, and K.**
760 **Geletneky.** 2004. Parvovirus H-1 infection of human glioma cells leads to complete viral
761 replication and efficient cell killing. *Int J Cancer* **109**:76-84.
- 762
- 763 17. **Jourdan, N., M. Maurice, D. Delautier, A. M. Quero, A. L. Servin, and G. Trugnan.** 1997.
764 Rotavirus is released from the apical surface of cultured human intestinal cells through
765 nonconventional vesicular transport that bypasses the Golgi apparatus. *J Virol* **71**:8268-8278.
- 766
- 767 18. **Kaffman, A., N. M. Rank, E. M. O'Neill, L. S. Huang, and E. K. O'Shea.** 1998. The receptor
768 Msn5 exports the phosphorylated transcription factor Pho4 out of the nucleus. *Nature*
769 **396**:482-486.
- 770
- 771 19. **King, J. A., R. Dubielzig, D. Grimm, and J. A. Kleinschmidt.** 2001. DNA helicase-mediated
772 packaging of adeno-associated virus type 2 genomes into preformed capsids. *Embo Journal*
773 **20**:3282-3291.
- 774
- 775 20. **Kutay, U., F. R. Bischoff, S. Kostka, R. Kraft, and D. Gorlich.** 1997. Export of importin alpha
776 from the nucleus is mediated by a specific nuclear transport factor. *Cell* **90**:1061-1071.
- 777
- 778 21. **Lombardo, E., J. C. Ramirez, M. Agbandje-McKenna, and J. M. Almendral.** 2000. A beta-
779 stranded motif drives capsid protein oligomers of the parvovirus minute virus of mice into
780 the nucleus for viral assembly. *J Virol* **74**:3804-3814.
- 781
- 782 22. **Lombardo, E., J. C. Ramirez, J. Garcia, and J. M. Almendral.** 2002. Complementary roles of
783 multiple nuclear targeting signals in the capsid proteins of the parvovirus minute virus of
784 mice during assembly and onset of infection. *J Virol* **76**:7049-7059.
- 785
- 786 23. **Lopez-Bueno, A., M. G. Mateu, and J. M. Almendral.** 2003. High mutant frequency in
787 populations of a DNA virus allows evasion from antibody therapy in an immunodeficient
788 host. *J Virol* **77**:2701-2708.
- 789
- 790 24. **Macara, I. G.** 2001. Transport into and out of the nucleus. *Microbiology and Molecular*
791 *Biology Reviews* **65**:570-+.
- 792
- 793 25. **Mani, B., C. Baltzer, N. Valle, J. M. Almendral, C. Kempf, and C. Ros.** 2006. Low pH-
794 dependent endosomal processing of the incoming parvovirus minute virus of mice virion
795 leads to externalization of the VP1 N-terminal sequence (N-VP1), N-VP2 cleavage, and
796 uncoating of the full-length genome. *J Virol* **80**:1015-24.
- 797
- 798 26. **Maroto, B., J. C. Ramirez, and J. M. Almendral.** 2000. Phosphorylation status of the
799 parvovirus minute virus of mice particle: mapping and biological relevance of the major
800 phosphorylation sites. *J Virol* **74**:10892-902.
- 801
- 802 27. **Maroto, B., N. Valle, R. Saffrich, and J. M. Almendral.** 2004. Nuclear export of the
803 nonenveloped parvovirus virion is directed by an unordered protein signal exposed on the
804 capsid surface. *J Virol* **78**:10685-10694.
- 805

- 806 28. **Martin-Serrano, J., and S. J. Neil.** 2011. Host factors involved in retroviral budding and
807 release. *Nat Rev Microbiol* **9**:519-31.
- 808
- 809 29. **Maul, G. G.** 1976. Fibrils attached to the nuclear pore prevent egress of SV40 particles from
810 the infected nucleus. *J Cell Biol* **70**:714-9.
- 811
- 812 30. **Merchlinsky, M. J., P. J. Tattersall, J. J. Leary, S. F. Cotmore, E. M. Gardiner, and D. C. Ward.**
813 1983. Construction of an Infectious Molecular Clone of the Autonomous Parvovirus Minute
814 Virus of Mice. *J Virol* **47**:227-232.
- 815
- 816 31. **Miller, C. L., and D. J. Pintel.** 2002. Interaction between parvovirus NS2 protein and nuclear
817 export factor Crm1 is important for viral egress from the nucleus of murine cells. *J Virol*
818 **76**:3257-3266.
- 819
- 820 32. **Mohl, B. P., and P. Roy.** 2014. Bluetongue virus capsid assembly and maturation. *Viruses*
821 **6**:3250-70.
- 822
- 823 33. **Muller, D. E., and G. Siegl.** 1983. Maturation of Parvovirus Luiii in a Subcellular System .2.
824 Isolation and Characterization of Nucleoprotein Intermediates. *Journal of General Virology*
825 **64**:1055-1067.
- 826
- 827 34. **Nachury, M. V., and K. Weis.** 1999. The direction of transport through the nuclear pore can
828 be inverted. *Proc Natl Acad Sci U S A* **96**:9622-9627.
- 829
- 830 35. **Naeger, L. K., J. Cater, and D. J. Pintel.** 1990. The Small Nonstructural Protein (Ns2) of the
831 Parvovirus Minute Virus of Mice Is Required for Efficient DNA-Replication and Infectious
832 Virus Production in a Cell-Type-Specific Manner. *J Virol* **64**:6166-6175.
- 833
- 834 36. **Nuesch, E. R., S. Lachmann, and J. Rommelaere.** 2005. Selective alterations of the host cell
835 architecture upon infection with parvovirus minute virus of mice. *Virology* **331**:159-174.
- 836
- 837 37. **Nuesch, J. P., S. Bar, S. Lachmann, and J. Rommelaere.** 2009. Ezrin-radixin-moesin family
838 proteins are involved in parvovirus replication and spreading. *J Virol* **83**:5854-63.
- 839
- 840 38. **Ohno, M., A. Segref, A. Bach, M. Wilm, and I. W. Mattaj.** 2000. PHAX, a mediator of U
841 snRNA nuclear export whose activity is regulated by phosphorylation. *Cell* **101**:187-198.
- 842
- 843 39. **Ohshima, T., T. Nakajima, T. Oishi, N. Imamoto, Y. Yoneda, A. Fukamizu, and K. Yagami.**
844 1999. CRM1 mediates nuclear export of nonstructural protein 2 from parvovirus minute virus
845 of mice. *Biochem Biophys Res Commun* **264**:144-50.
- 846
- 847 40. **Praefcke, G. J., and H. T. McMahon.** 2004. The dynamin superfamily: universal membrane
848 tubulation and fission molecules? *Nat Rev Mol Cell Biol* **5**:133-47.
- 849
- 850 41. **Rubio, M. P., A. Lopez-Bueno, and J. M. Almendral.** 2005. Virulent variants emerging in mice
851 infected with the apathogenic prototype strain of the parvovirus minute virus of mice exhibit
852 a capsid with low avidity for a primary receptor. *J Virol* **79**:11280-11290.
- 853
- 854 42. **Segovia, J. C., A. Real, J. A. Bueren, and J. M. Almendral.** 1991. Invitro Myelosuppressive
855 Effects of the Parvovirus Minute Virus of Mice (Mvmi) on Hematopoietic Stem and
856 Committed Progenitor Cells. *Blood* **77**:980-988.
- 857

- 858 43. **Shackelton, L. A., and E. C. Holmes.** 2006. Phylogenetic evidence for the rapid evolution of
859 human B19 erythrovirus. *J Virol* **80**:3666-3669.
- 860
- 861 44. **Shackelton, L. A., C. R. Parrish, U. Truyen, and E. C. Holmes.** 2005. High rate of viral
862 evolution associated with the emergence of carnivore parvovirus. *Proc Natl Acad Sci U S A*
863 **102**:379-384.
- 864
- 865 45. **Shein, H. M., and J. F. Enders.** 1962. Multiplication and Cytopathogenicity of Simian
866 Vacuolating Virus 40 in Cultures of Human Tissues. *Proceedings of the Society for*
867 *Experimental Biology and Medicine* **109**:495-&.
- 868
- 869 46. **Slepchenko, B. M., I. Semenova, I. Zaliapin, and V. Rodionov.** 2007. Switching of membrane
870 organelles between cytoskeletal transport systems is determined by regulation of the
871 microtubule-based transport. *J Cell Biol* **179**:635-41.
- 872
- 873 47. **Sonntag, F., S. Bleker, B. Leuchs, R. Fischer, and J. A. Kleinschmidt.** 2006. Adeno-associated
874 virus type 2 capsids with externalized VP1/VP2 trafficking domains are generated prior to
875 passage through the cytoplasm and are maintained until uncoating occurs in the nucleus. *J*
876 *Virol* **80**:11040-11054.
- 877
- 878 48. **Stamnes, M.** 2002. Regulating the actin cytoskeleton during vesicular transport. *Curr Opin*
879 *Cell Biol* **14**:428-33.
- 880
- 881 49. **Stuven, T., E. Hartmann, and D. Gorlich.** 2003. Exportin 6: a novel nuclear export receptor
882 that is specific for profilin center dot actin complexes. *Embo Journal* **22**:5928-5940.
- 883
- 884 50. **Tattersa.P.** 1972. Replication of Parvovirus Mvm .1. Dependence of Virus Multiplication and
885 Plaque-Formation on Cell-Growth. *J Virol* **10**:586-&.
- 886
- 887 51. **Tattersall, P., and J. Bratton.** 1983. Reciprocal Productive and Restrictive Virus-Cell
888 Interactions of Immunosuppressive and Prototype Strains of Minute Virus of Mice. *J Virol*
889 **46**:944-955.
- 890
- 891 52. **Tattersall, P., A. J. Shatkin, and D. C. Ward.** 1977. Sequence Homology between Structural
892 Polypeptides of Minute Virus of Mice. *Journal of Molecular Biology* **111**:375-394.
- 893
- 894 53. **Tucker, S. P., and R. W. Compans.** 1993. Virus infection of polarized epithelial cells. *Adv Virus*
895 *Res* **42**:187-247.
- 896
- 897 54. **Tucker, S. P., C. L. Thornton, E. Wimmer, and R. W. Compans.** 1993. Vectorial release of
898 poliovirus from polarized human intestinal epithelial cells. *J Virol* **67**:4274-82.
- 899
- 900 55. **Tullis, G. E., L. R. Burger, and D. J. Pintel.** 1993. The Minor Capsid Protein Vp1 of the
901 Autonomous Parvovirus Minute Virus of Mice Is Dispensable for Encapsidation of Progeny
902 Single-Stranded-DNA but Is Required for Infectivity. *J Virol* **67**:131-141.
- 903
- 904 56. **Tullis, G. E., L. R. Burger, and D. J. Pintel.** 1992. The Trypsin-Sensitive RVER Domain in the
905 Capsid Proteins of Minute Virus of Mice Is Required for Efficient Cell Binding and Viral-
906 Infection but Not for Proteolytic Processing Invivo. *Virology* **191**:846-857.
- 907
- 908 57. **VihinenRanta, M., A. Kalela, P. Makinen, L. Kakkola, V. Marjomaki, and M. Vuento.** 1998.
909 Intracellular route of canine parvovirus entry. *J Virol* **72**:802-806.

- 910
- 911 58. **Votteler, J., and W. I. Sundquist.** 2013. Virus Budding and the ESCRT Pathway. *Cell Host &*
912 *Microbe* **14**:232-241.
- 913
- 914 59. **Wirblich, C., B. Bhattacharya, and P. Roy.** 2005. Nonstructural protein 3 of bluetongue virus
915 assists virus release by recruiting ESCRT-I protein Tsg101. *J Virol* **80**:460-73.
- 916
- 917

Fig. 1

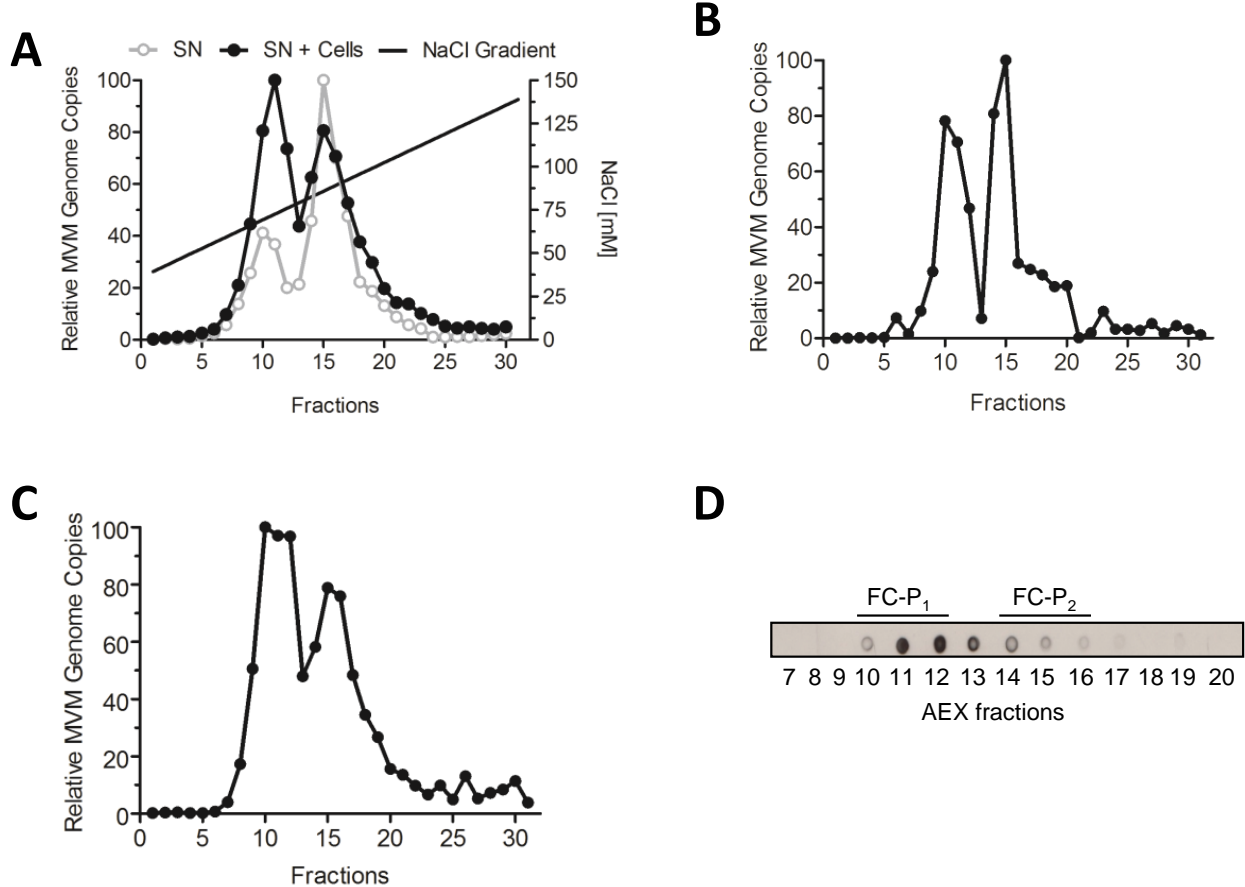


Fig. 2

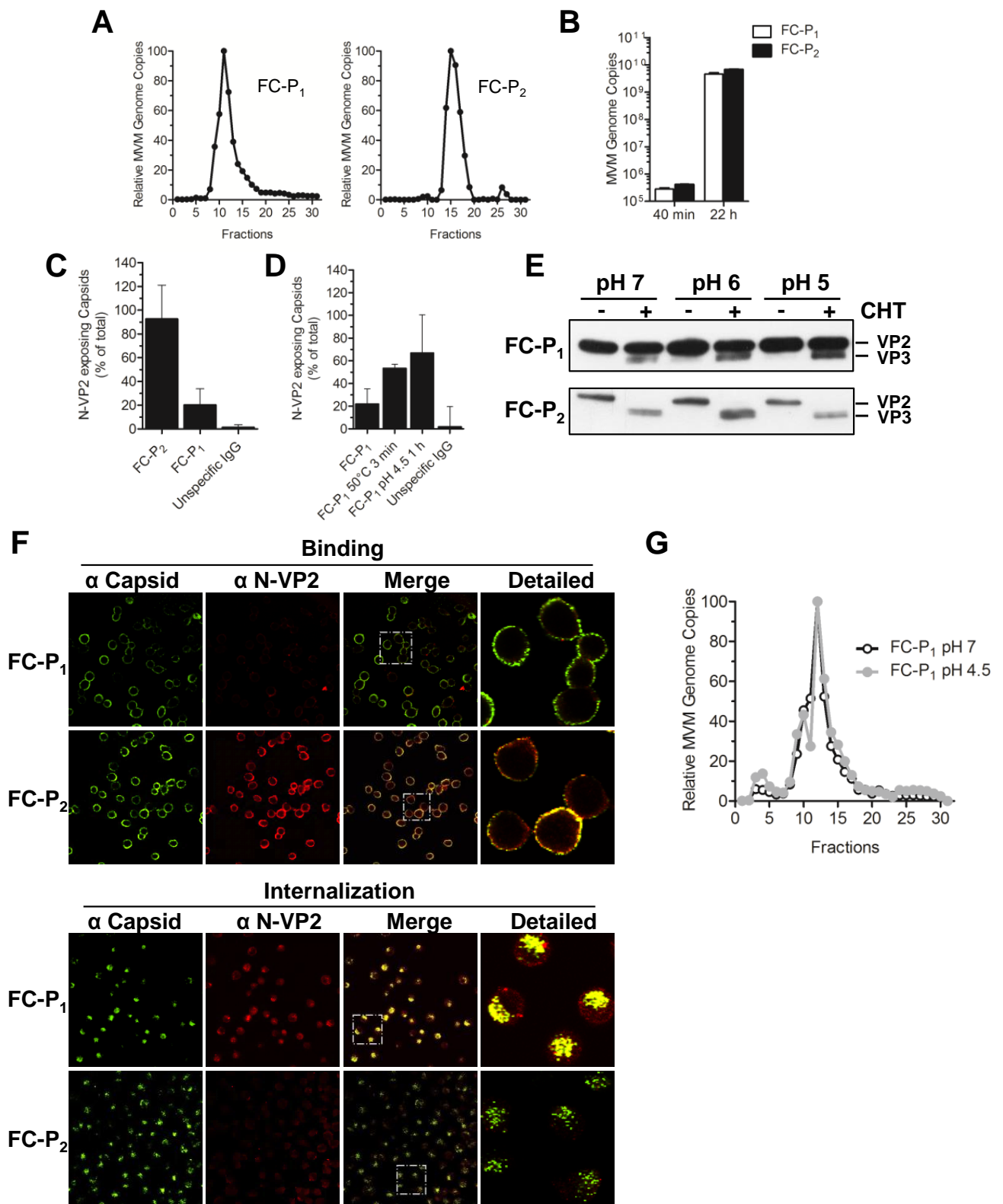


Fig. 3

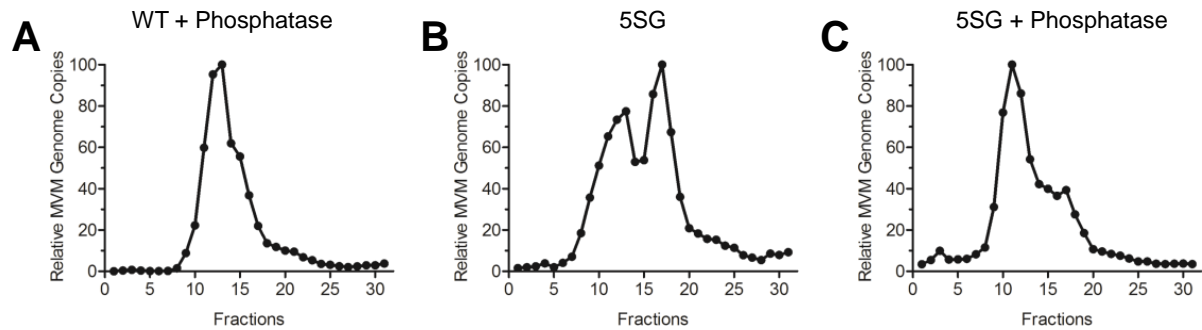


Fig. 4

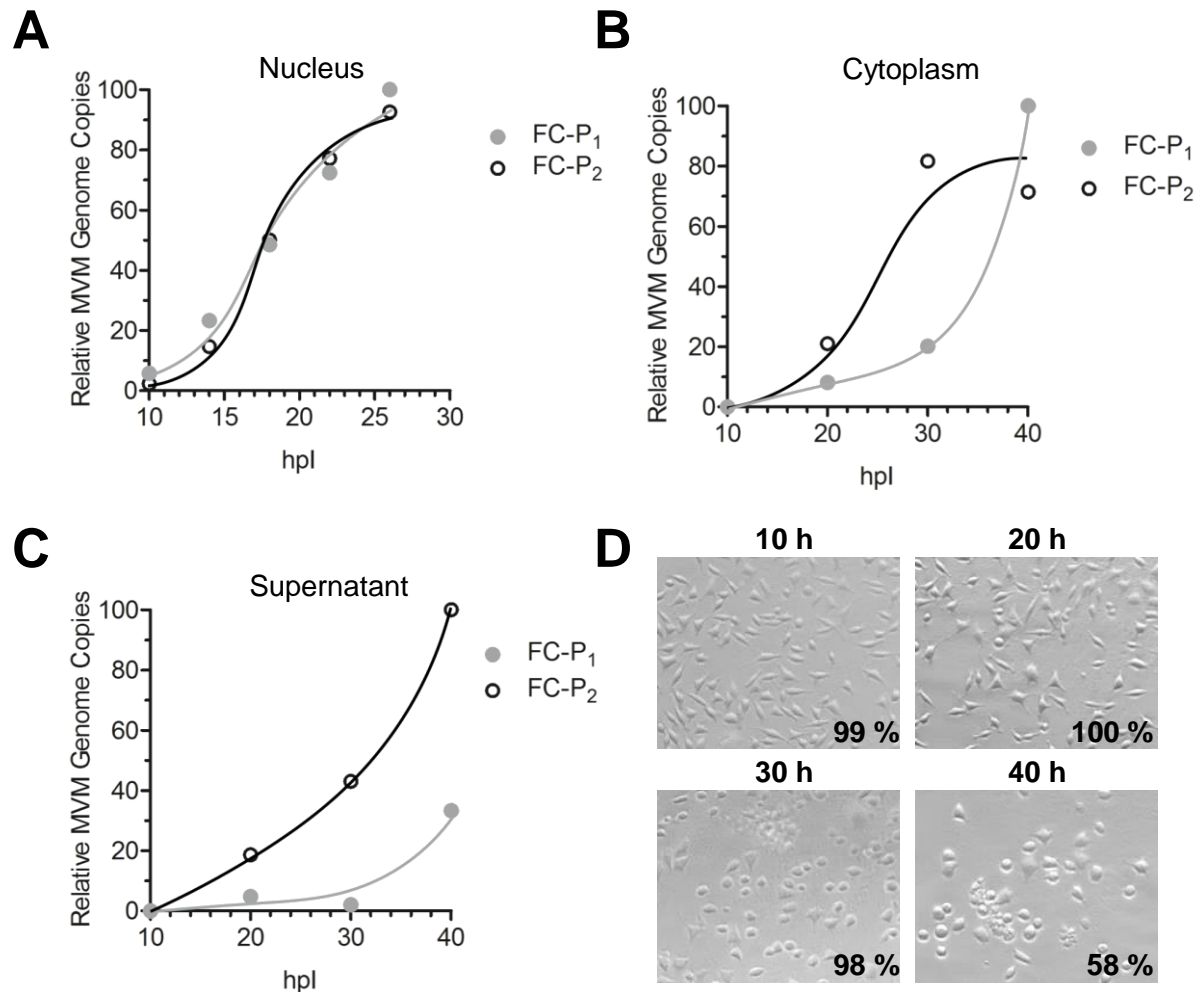


Fig. 5

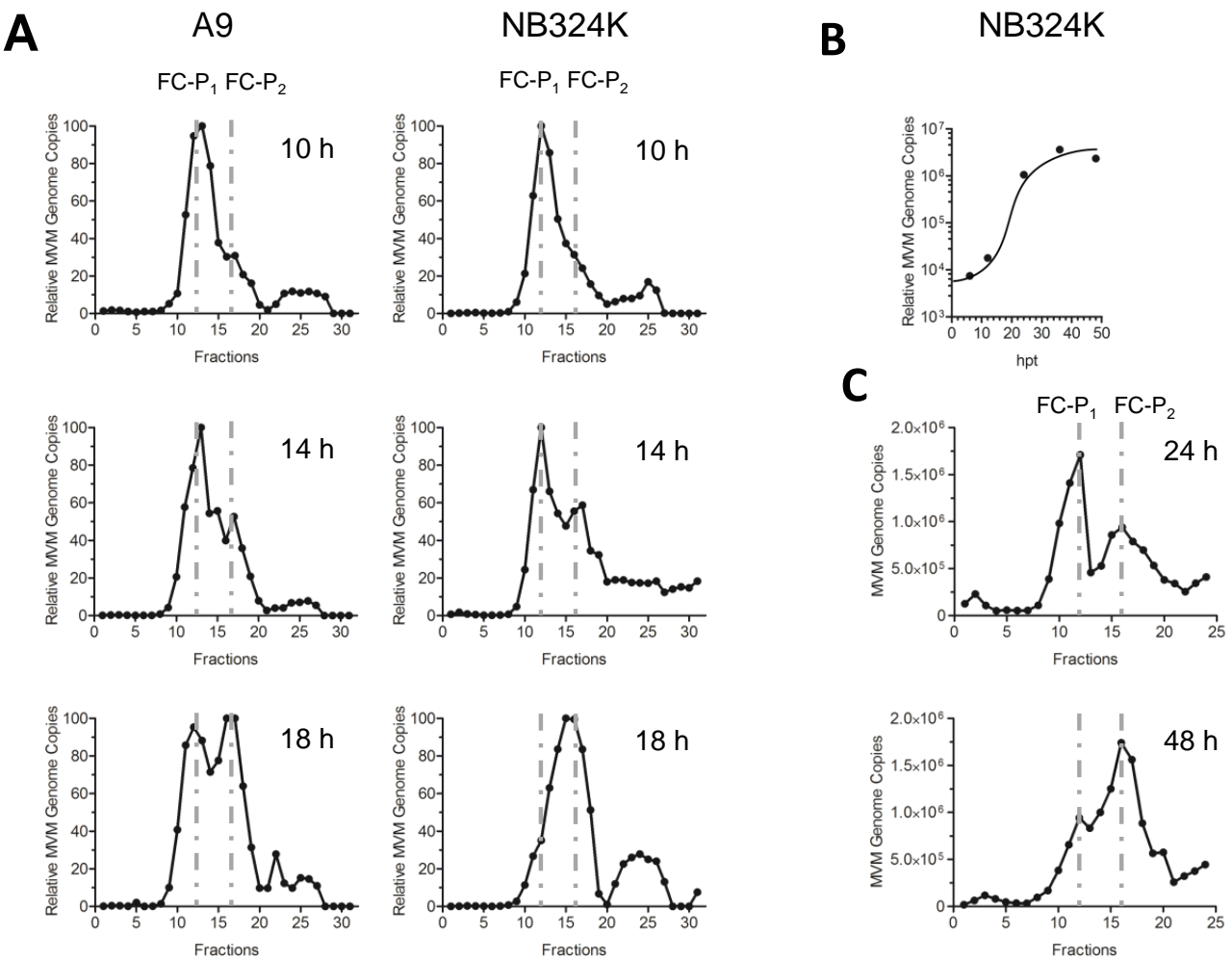
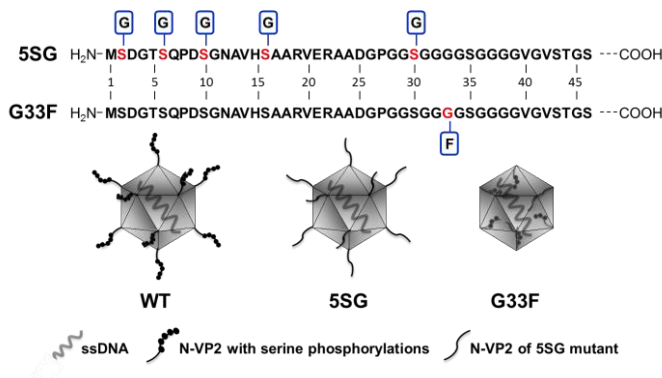
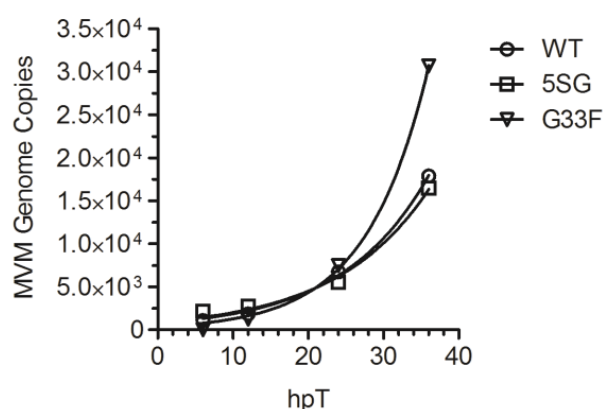


Fig. 6

A



B



C

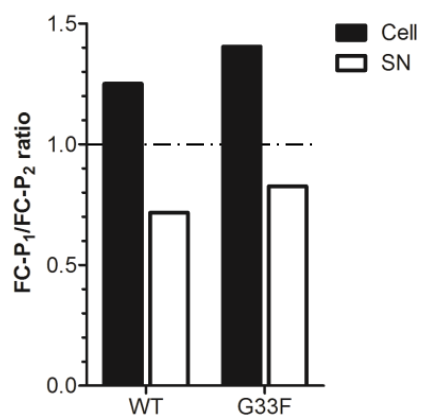


Fig. 7

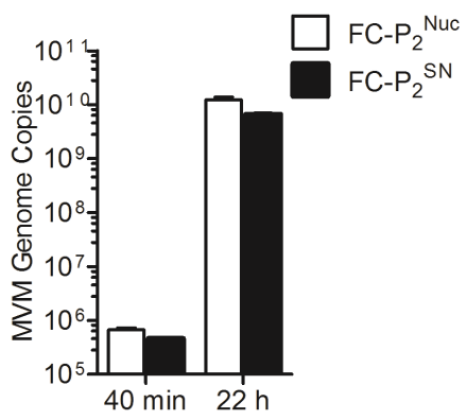
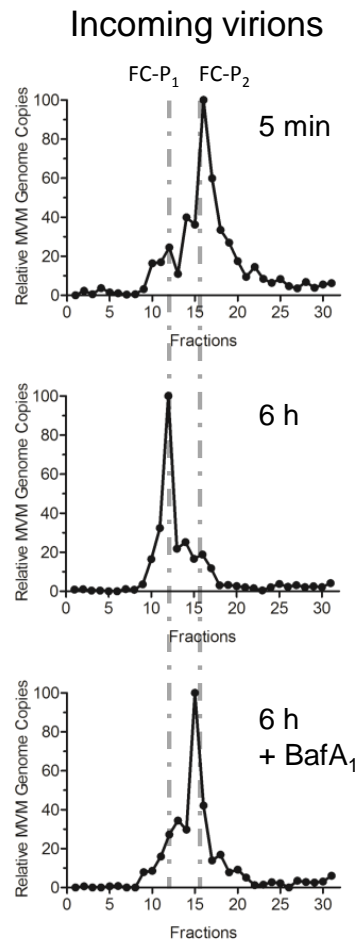


Fig. 8



11. Supplementary Data

11.1. The Phosphoserine-Rich N-VP2 of MVM Facilitates Nuclear Targeting and Assists in Cytolysis

In order to investigate a possible involvement of the distal serine phosphorylations within N-VP2 in MVM egress, we generated a mutant, referred to as 5SG, having all the distal serine residues substituted by glycine. In Figure S1, p. 112 several aspects of the infection with 5SG, such as nuclear targeting, nuclear export, and cytotoxicity are shown.

We analyzed the capacity of 5SG to enter the cells and target the nucleus. To this end, the accumulation of viral DNA in the nucleus at increasing times pi was quantitatively determined by qPCR. 5SG was approximately 5× less efficient in replicating viral DNA in the nucleus, indicating that fewer virions reached the nucleus, thus delivering less DNA templates to initiate viral replication. Indeed, the amount of viral DNA in the nuclei of 5SG infected cells was similar to the quantities that were obtained when the cells were infected with 5× less WT virions (see Figure S1 A, p. 112).

Nuclear export of 5SG progeny was not significantly affected. Virions were efficiently exported from the nucleus even though showing a slight delay in cytoplasmic accumulation (see Figure S1 B, p. 112). This delay is caused by defects in early steps of infection prior to the initiation of DNA replication, such as binding, endosomal escape, viral uptake, or nuclear targeting. Genetic removal of the distal phosphorylations of N-VP2 might hamper an efficient *in vivo* cleavage of VP2 to generate VP3, thus affecting endosomal processing and escape. Hence, fewer incoming virions reach the nuclei where they initiate the replication of the viral DNA. However, since only a lower amount of viral DNA serves as a template for replication, the amplification of the viral genome is delayed. Collectively, the delayed nuclear DNA accumulation and progeny morphogenesis directly affect the kinetics of egress, explaining the slight lag in progeny accumulation in the cytoplasm seen in Figure S1 B, p. 112.

As early as 20 hpi, the WT virus caused a pronounced reorganization of the cytoskeleton resulting in cell rounding. At later times (40 hpi), increasing amounts of cells appeared rounded and detached, eventually resulting in cell death (see Figure S1 C, 1st row, p. 112). In contrast, 5SG virions were significantly less cytotoxic. Even as late as 40 hpi most of the infected cells still exhibited the typical fibroblastic phenotype and only a few cells became rounded. No signs of

11. Supplementary Data

apoptosis and cytolysis were observed (see Figure S1 C, 2nd row, p. 112).

Productive MVM infection produces a strong cytopathic effect in the host cell, ultimately causing cellular lysis. Such dramatic changes in the cytoskeleton filaments involve gelsolin-mediated degradation of actin fibers resulting in the generation of characteristic “actin-patches” [28]. While the actin filaments become destabilized, the microtubule network is maintained during the course of infection [333]. The latter observation together with the previously reported capsid-dynamin co-localization [28] would be in agreement with a microtubule dependent egress of MVM. The modest delay in nuclear targeting and the fewer amount of progeny DNA accumulated in the nucleus by the 5SG mutant (see Figure S1 A, p. 112) cannot explain the considerable delay of the

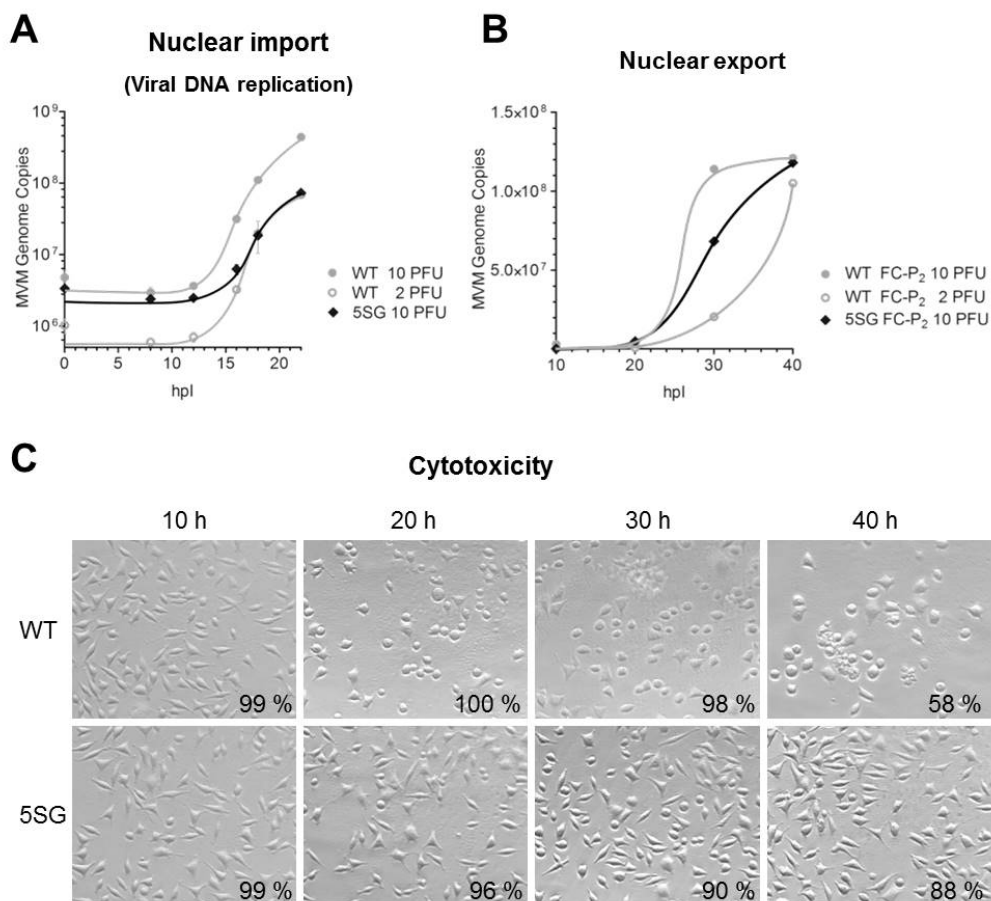


Figure S1.: Nuclear import, export, and cytotoxicity during an infection with 5SG virions. (A) A9 cells (8×10^3) were infected with the indicated PFU of WT or 5SG virus. Following binding at 4 °C unbound viruses were removed. Viral DNA was extracted and quantified at the specified times post-infection. (B) A9 cells (3×10^6) were infected using the indicated viruses and PFU. Binding was performed at 4 °C. Unbound virus was removed prior to incubation at 37 °C for the indicated times. Cytosolic fractions were isolated and applied for AEX-qPCR. Exported FC-P₂ virions were quantified using qPCR. All infections were performed in the presence of α -capsid mAb (B7) and neuraminidase in order to prevent re-infections. (C) A9 cells were infected with WT or 5SG MVM using 10 PFU per cell. Following binding at 4 °C unbound virus was removed by washings. Cells were incubated at 37 °C for the specified times. Phase contrast pictures of the infected cells were taken using a 20× magnification objective built in a Zeiss Axiovert 35 microscope. Cell viability was accessed via trypan blue exclusion using the TC10™ automated cell counter (BioRad). The average of three independent measurements is indicated.

11.1. The Phosphoserine-Rich N-VP2 of MVM Facilitates Nuclear Targeting and Assists in Cytolysis

cytopathic effect of more than 20 h. N-VP2 is removed by proteolytic digestion during endosomal uptake. Hence, it is not involved in important signaling for viral DNA replication. Additionally, it has been demonstrated that there are no significant differences in the cytoplasmic accumulation of WT and 5SG progeny virions (see Figure S1 B, p. 112). Therefore, the phosphorylations on N-VP2, which represent the only difference between the WT and 5SG progeny, are likely involved in late events mediating the rearrangement of the cytoskeleton during egress. 5SG seems to be defective for severing the actin filaments resulting in prolonged maintenance of the cytoskeleton and cell integrity.

Similar observations have been reported by Tullis *et al.* [460] by using a MVM mutant harboring a deletion in N-VP2 without altering the phosphorylated residues. The 7 amino acid deletion mutant lacking the trypsin-sensitive residues 17-23 within N-VP2 was slightly defective for binding and approximately 10× deficient, compared to the WT, in initiating a productive infection. However, *in vivo* processing of N-VP2 was still achieved. Because this mutation affects both structural proteins VP1 and VP2, it is difficult to distinguish their relative contribution to the mutant phenotype. However, the binding defect is more likely a VP2 effect since virions lacking VP1 are not defective in binding to susceptible cells [461]. In addition to its defect in cell binding, the mutant produced approximately 10× less viral DNA in the nuclei of infected cells, suggesting that fewer mutant virions, on the average, reached the nucleus where they can initiate DNA replication. Nonetheless, those that managed to reach the nucleus, replicated normally. Similar to 5SG, this mutant was delayed in egress from the cells late in asynchronous infections. However, mutant progeny virions efficiently egress early in the infection, as well as in highly synchronized infections. Therefore, this effect might be a nonspecific defect in some aspect of cytolysis rather than a defect in an active egress mechanism [460]. A less efficient cytolysis would hamper the passive release and spread of intracellular progeny virions, thus preventing their contribution in a next round of infection.

Summary: Collectively, these results strongly suggest an involvement of the phosphoserine-rich N-VP2 late in infection. N-VP2 appears to be involved in cytoskeleton reorganization and cytolysis facilitating passive release of progeny virions but it does not actively participate in the transport mechanism underlying active egress. During entry, its proteolytic removal is required. Mutations affecting the tightly controlled processing of N-VP2 during virus entry have important implications in the efficiency of endosomal escape and nuclear targeting.

11. Supplementary Data

11.2. NS2-Crm1 Interaction is Required for Nuclear Export but Not for the Late Nuclear Maturation

Interestingly, a substantial retention of progeny virions in the nucleus of infected cells was observed for NS2 mutants defective for the interaction with Crm1 (see Section 7.12, p. 50) [161, 312]. Since FC-P₁ virions are nuclear export deficient, it is tempting to speculate that NS2 might assist the nuclear maturation of FC-P₁ to generate FC-P₂. This maturation includes the externalization of N-VP2 and phosphorylation of readily accessible residues on the capsid surface (see Manuscript, pp. 67 - 111). A putative direct or indirect involvement of NS2 in the final nuclear maturation of MVM progeny virions would be cell type specific because the nuclear export of the progeny in human transformed cells has been demonstrated to be NS2 and/or Crm1 independent [298, 326]. Moreover, it has been previously shown that human transformed cells are capable of phosphorylating the viral capsids more efficiently compared to restrictive mouse fibroblasts [297]. In line with this concept, late nuclear maturation of NS2-Crm⁻ mutants might be less impaired in transformed cells due to their elevated basal kinase activity. To test this hypothesis we produced NS2-Crm1⁻ mutants using transfection in NB324K cells. The generated progeny was used to infect A9 mouse fibroblasts in order to analyze the late nuclear maturation steps for the NS2-Crm1⁻ mutant.

As shown in Figure S2 A p. 115, NB324K cells were able to produce fully mature FC-P₂ MVM NES-22 [161] progeny virions. Similar quantities were obtained as for transfections with the WT infectious clone pIC-MVMP (see Section 12.1, p. 131). The NS2-Crm1 interaction is not required for the late nuclear maturation in the nuclei of mouse fibroblasts as demonstrated in Figure S2 B, p. 115. Both DNA containing particles, FC-P₁ and FC-P₂, appeared in the nucleus of murine cells infected with the NES-22 mutant. However, at 26 hpi the mutant showed a dissimilar AEX profile to that of the WT. Instead of the typically balanced ratio between FC-P₁ and FC-P₂ observed for the WT, NES-22 FC-P₂ was the predominant population 26 hpi. This data reinforces previous reports suggesting a nuclear retention of NES-22 progeny virions [161, 312].

Summary: Collectively, these results indicate that the late nuclear progeny maturation does not require the interaction of NS2 with Crm1. However, we confirm previous data suggesting a nuclear retention of progeny virions for the NES-22 mutant in murine fibroblasts. Our result shows that the NES of NS2 is involved in the export of the fully mature FC-P₂ virion progeny and not in late nuclear maturation events. Currently, it is unknown whether NS2 directly interacts with the capsid to export it from the nucleus. Extensive attempts to demonstrate such an interaction failed. Hence, the multi-functional NS2 protein might indirectly assist the nuclear export of the virion progeny by orchestrating cellular pathways which do not affect progeny maturation in the nucleus of mouse fibroblasts. The requirement of NS2 for progeny egress is cell type specific since NS2 null mutants grow to wild-type levels in human NB324K cells. Moreover, the requirement of

11.2. NS2-Crm1 Interaction is Required for Nuclear Export but Not for the Late Nuclear Maturation

the Crm1 pathway in nuclear export of progeny virions is restricted to murine fibroblasts since MVM progeny virions egress from human transformed cells even following LMB treatment.

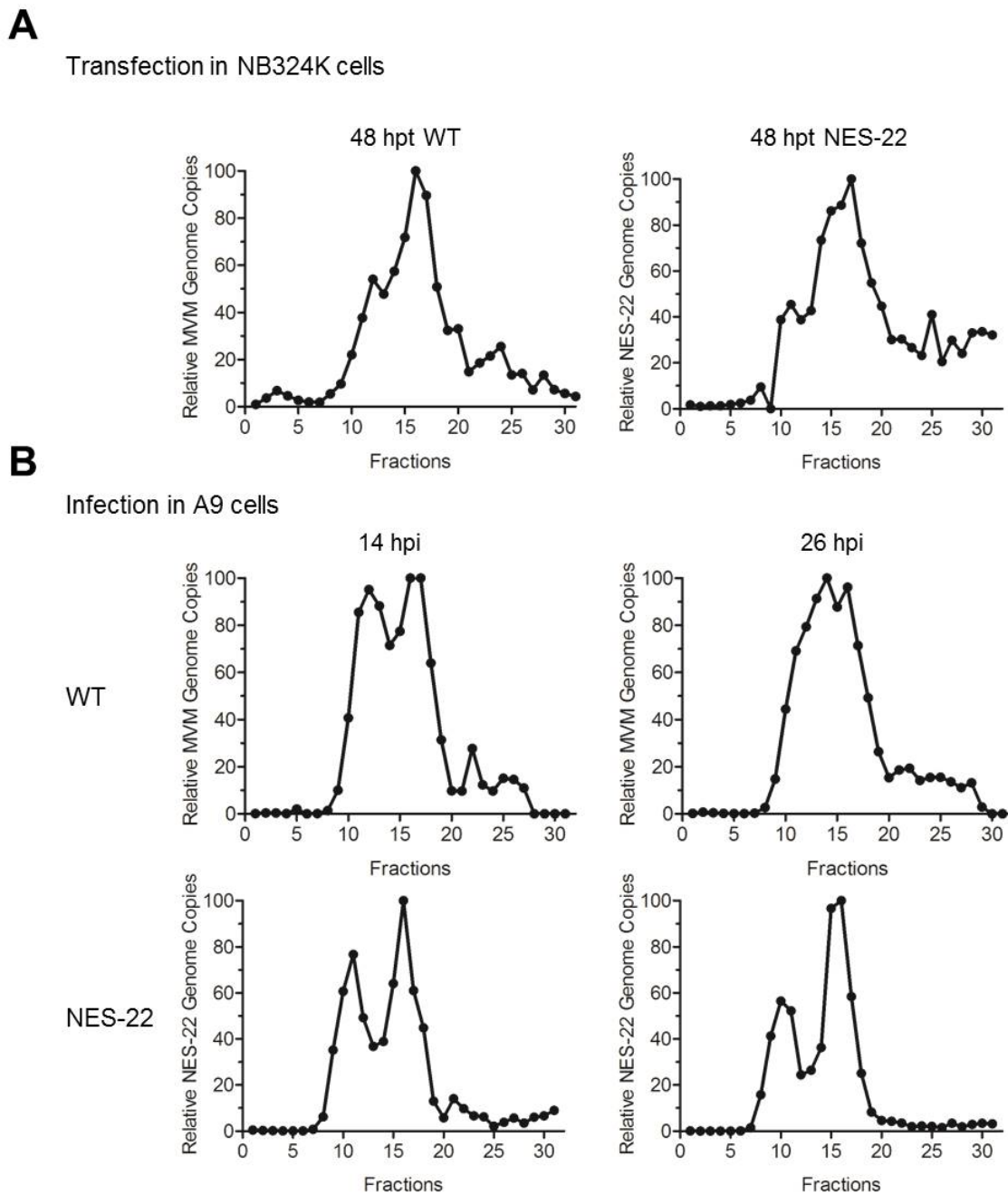


Figure S2.: The NES-22 substitution within the NS2 protein does not prevent the late nuclear maturation steps but NS2-Crm1-interaction is required for nuclear export of MVM progeny virions. (A) NB324K cells (10^6) were transfected with $5 \mu\text{g}$ pIC-MVMP-NES-22 and further incubated for 48 h. Total cell extracts were isolated and applied to AEX. Viral DNA in each fraction was quantified by qPCR. (B) Mutant MVM NES-22 progeny was collected 3 dpi from culture media and cellular extracts of transfected NB324K cells and used to infect 3×10^6 A9 mouse fibroblasts. At the specified times pi the nuclei of infected cells were extracted and nuclear extracts were applied to AEX. Viral DNA in each fraction was quantified by qPCR.

11. Supplementary Data

11.3. The Role of Empty Capsids During the Infection

Empty capsids (EC) represent more than half of the virus progeny. They are not infectious but might interfere with a productive infection. Therefore, it is of interest to characterize their role during the course of infection. DNA packaging and the late capsid surface phosphorylations are a prerequisite for the externalization of N-VP2. EC lack both a viral genome and the late phosphorylations, thus having their N-VP2 termini buried in the interior of the capsid. Hence, EC represent a useful tool to study the role of N-VP2 during early steps in infection, such as binding and endosomal uptake.

11.3.1. Isolation and Characterization of Empty Capsids

In addition to the previously characterized FC populations (FC-P₁ and FC-P₂), infected cells produce a considerable amount of EC. Due to the lack of DNA, EC band at lower density compared to FC following differential centrifugation in CsCl. While FC entered the gradient to a density of 1.46 gcm⁻³, EC banded at 1.32 gcm⁻³, as determined by refractometry (see Figure S3 A, p. 117). A quantitative PCR analysis of the corresponding fractions confirmed that viral DNA containing particles were depleted from EC to almost a thousand times (see Figure S3 B, p. 117). First of all, we verified their N-VP2 conformation. In Figure S3 C and D, p. 117 it is shown that N-VP2 of EC is not accessible to specific antibodies and proteolytic digestion by α -chymotrypsin (CHT), respectively.

11.3.2. Empty Capsids Specifically Bind to Sialic Acid

Figure S4 A and B, p. 117 demonstrates that both EC and FC restrictively bind to sialic acid (SA) moieties on the surface of murine A9 cells. Binding of both capsid species can be efficiently prevented by pre-treatment of A9 cells using neuraminidase (Neur, see Table 12.7, p. 142) at doses higher than 50 U/mL. Neuraminidase specifically hydrolyzes glycosidic linkages of neuraminic acids. These results confirm that both capsid species bind to the same class of receptor molecules on the surface of susceptible murine cells. Therefore, EC could have the potential to compete with FC for SA moieties on the cell surface and disturb early steps of the infection.

11.3. The Role of Empty Capsids During the Infection

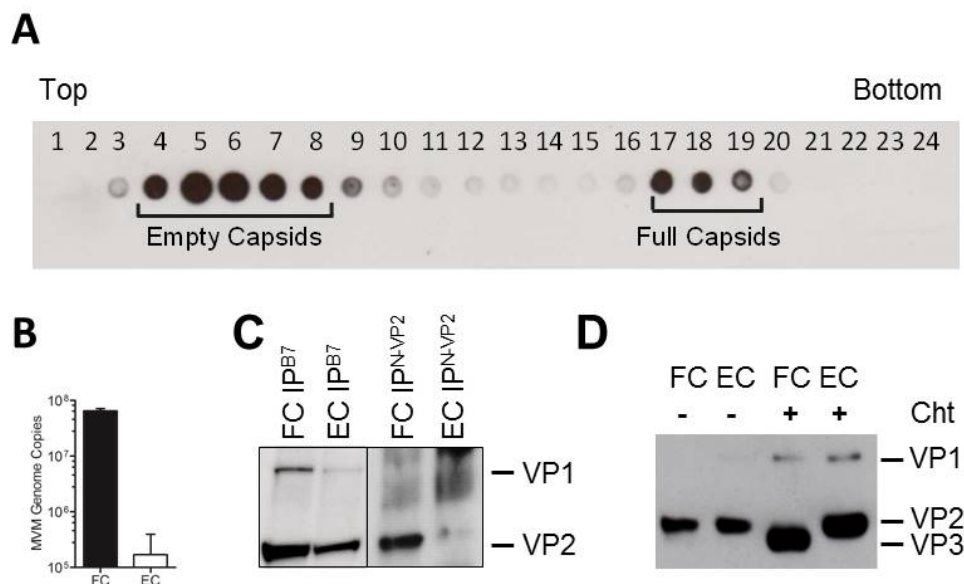


Figure S3.: Purification and analysis of FC and EC. **(A)** FC and EC were separated by differential centrifugation through a CsCl gradient as described in Section 9.2.1, p. 58. Fractions (500 μ L each) are labeled from top to bottom of the gradient. 2 μ L of each fraction were spotted on a nitrocellulose membrane and probed with an α -capsid mAB (B7). A HRP-coupled secondary antibody was used and the membrane was developed by exposure to a photo film. **(B)** EC and FC fractions were pooled. qPCR analysis was performed to quantify DNA-containing particles. **(C)** N-VP2 accessibility of EC and FC was tested by IP using an antibody raised against the N-VP2 region. The total amount of applied viral particles was verified using an α -capsid antibody (B7 mAb). **(D)** EC and FC (10^8 particles each) were treated with 0.5 mg/mL chymotrypsin (CHT) or not. Proteolytic N-VP2 processing was analyzed by 10 % SDS-PAGE. After transfer to a polyvinylidene difluoride membrane, the blot was probed with a rabbit α -VP pAb, followed by a HRP conjugated secondary antibody. The membrane was developed by exposure to a photo film.

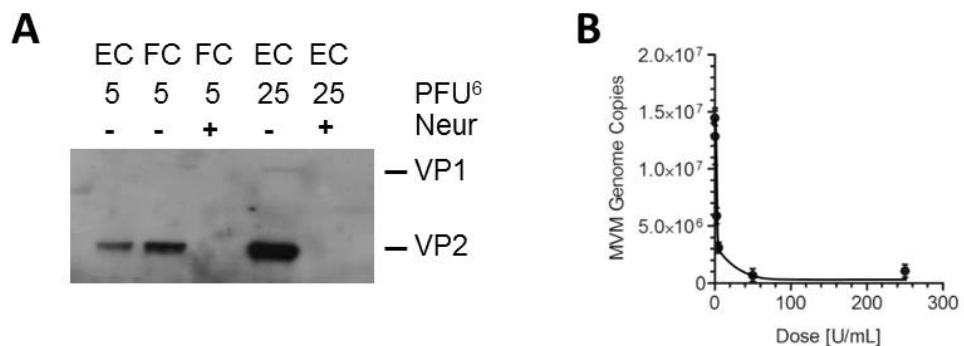


Figure S4.: Specific binding of FC and EC to SA. **(A)** Following treatment with 50 U/mL neuraminidase (Neur) or not, A9 cells were infected at 4 °C using the indicated PFU of FC or EC⁶. Following washings to remove unbound viruses the cells were lysed in protein loading buffer and proteins were separated by 10 % SDS-PAGE. Membranes were probed as outlined above. **(F)** Estimation of the effective dose of Neur in order to completely deplete MVM binding on A9 fibroblasts. Following neuraminidase treatment using the indicated doses, virus (5 PFU) was bound to 3×10^5 cells for 1 h at 4 °C. Unbound virus was removed by washings, DNA was extracted and viral DNA was quantified by qPCR.

⁶ EC do not contain DNA and thus, they are not infectious. As a consequence, no PFUs can be calculated for EC. FC were quantified by qPCR analysis and used as “external standards” for dot blot analyses. EC were quantified by spot densitometry by comparison to serial dilutions of quantified FC.

11. Supplementary Data

11.3.3. Preferential Binding of Full Capsids to Murine Fibroblasts

In order to characterize the binding specificity of FC and EC, both capsid types were allowed to bind discretely to susceptible, restrictive murine fibroblasts. It was important to minimize uptake of virus into cells to exclusively study virus-receptor interactions. Viral entry can be prevented at reduced temperatures. At 4 °C, active cell-mediated uptake through endocytosis is prohibited, thus bound viral particles remain attached to their receptor molecules on the cell surface but do not internalize [270]. The differences for N-VP2 accessibility can be used to distinguish EC and FC in IF experiments. Staining of FC results in co-localization of α -capsid and α -N-VP2 antibodies whereas EC are detected by α -capsid antibodies only (see Figure S5 A, upper rows, p. 119). When FC and EC were bound to cells at equal stoichiometry, FC had a higher binding affinity for SA. Even under non-saturated conditions, EC were detected rarely when applied as mixed populations (see Figure S5 A, 3rd row, p. 119). Only when an equal amount of EC was added prior to the FC a slight increase in bound EC was observed (see Figure S5 A, lowest row, p. 119). Quantification of co-localization by scatter plot analysis in representative IF pictures revealed that binding of FC was not disturbed in the presence of EC (see Figure S5 B, p. 119).

11.3.4. Full Capsids have Better Binding Capacity to Sialic Acids than Empty Capsids

A critical criteria for studying the attachment of a virus to its surface receptor represents the binding specificity of such an interaction. In general, specific attachment is limited to the number of available receptor molecules, thus it saturates as the amount of input virus increases. For A9 cells it has been reported that they offer 5×10^5 specific binding sites per cell [270]. In Figure S6 A, p. 121 it is shown that saturation could be achieved at PFUs higher than 20, corresponding to approximately 10^4 viruses per cell. In addition, specific binding can be competed by adding an excess of particles competing for the same receptor. Linser *et al.* demonstrated that preliminary bound radio-labeled capsids were displaced by subsequently adding an excess of unlabeled particles. However, large quantities of unlabeled particles were required in order to demonstrate competition. Only by exceeding the amount of initially bound virus particles by 20-40 \times , competition was observed under saturating conditions. Due to the large amount of viral particles required, they were not able to demonstrate complete competition [270]. Even though working under similar conditions, we were not able to demonstrate competition between FC and EC, FC and proteolytically cleaved FC (FC^{CHT}), and FC^{CHT} and EC (see Figure S6 B, C, and D, respectively, p. 121). This indicates that still higher PFUs would have been required to demonstrate competition. However, it might be more difficult to compete for binding with EC or FC^{CHT} since N-VP2 might stabilize the primary attachment to the cell surface. The most clear evidence for this assumption is given by the fact that EC only modestly bind to the cell surface when applied together with FC, as observed in IF experiments (see Figure S5 A, lower rows,

11.3. The Role of Empty Capsids During the Infection

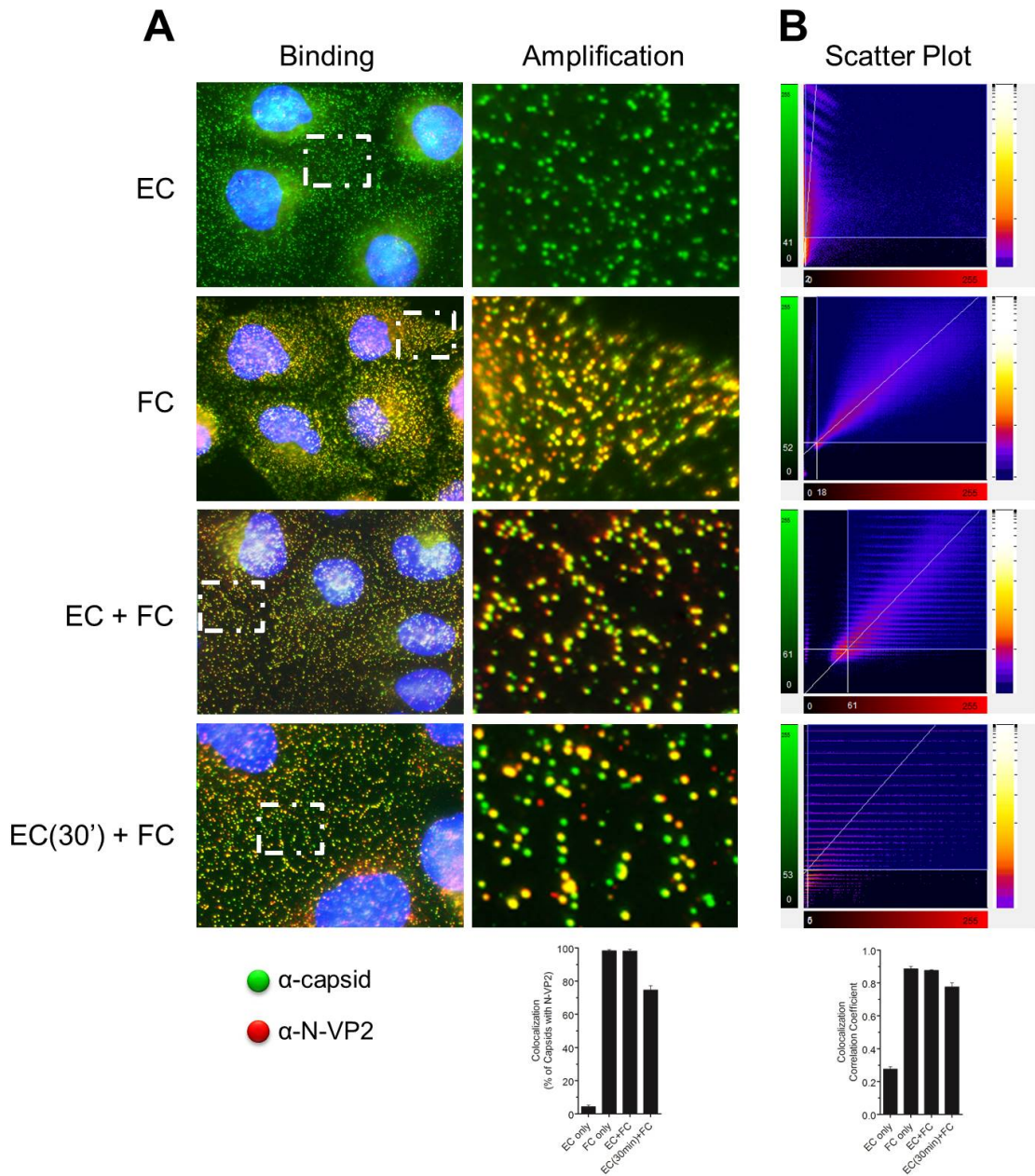


Figure S5.: FC bind more efficiently to SA than EC. (A) A9 cells (3×10^5) were grown on cover slips and infected independently or combined with FC and EC (5 PFU per cell) at 4 °C. In the 4th row EC were incubated with the cells 30 min prior to the addition of FC. Following removal of unbound viruses the cells were fixed and stained for IF using an antibody (mAb B7) raised against assembled capsids (green) and an antibody recognizing N-VP2 (red). Percentage of capsids showing N-VP2 signal was calculated for the indicated areas of interest. (B) Scatter plot analysis showing the indicated areas of interest was used to calculate the corresponding correlation coefficient as a measurement for the degree of co-localization.

11. Supplementary Data

p. 119). EC might not only compete for primary receptor attachment but also for intracellular interactions required for uncoating and trafficking. Therefore, we studied the potential of EC to interfere with the progression of a natural infection. As shown in Figure S6, p. 121, even a large excess of EC does not interfere with the infection process.

Collectively, we conclude that EC do not interfere with a productive infection, even though representing a large population in a normal infection. In order to disturb binding to cells, an overwhelming excess of EC which is not found in nature would be required. N-VP2 might be involved in the stabilization of primary attachment of MVM to susceptible cells as judged by IF analyses (see Figure S5 A, 3rd row, p. 119). However, besides N-VP2 exposure, the packaged ssDNA genome and the surface phosphorylations represent further known differences between EC and FC which might directly or indirectly influence receptor binding. In summary, N-VP2 might have minor importance during early steps in infection except for its own proteolytic digestion which is important to allow N-VP1 externalization. However, N-VP2 appears to mediate the rearrangement of the cytoskeleton late in infection (see Section 11.1, p. 111), thus being a key player in cytolysis and viral release.

Summary: Both FC and EC specifically bind to SA moieties coupled to an unknown receptor(s) on susceptible cells. Hence, they are both sensitive to neuraminidase. The overwhelming amount of receptor molecules on the cell surface complicates working under saturated conditions. Under non-saturated conditions EC bound significantly less efficient than FC and they were not able to compete with FC even when added at an excess of up to 40×. However, although N-VP2 represents the major structural difference between FC and EC, it is not directly involved in stabilizing the binding of MVM since its proteolytic removal did not decrease the binding efficiency.

11.4. Anion-Exchange Chromatography as a Novel Tool to Study the Surface of Small Non-Enveloped Viruses

As previously mentioned, parvoviruses undergo many interactions with their respective host cell due to their strong host cell dependence. Such interactions may preferentially occur on the very surface of incoming or progeny particles because it is readily accessible to the host's enzymes. Therefore, their net surface electrostatics can change as a consequence of host cell induced modifications on the capsid surface. As demonstrated in the present thesis, intranuclear virion populations representing different maturation stages of MVM were successfully separated by AEX based on different surface charges, in this case as a result of distinct surface phosphorylations. Fast protein liquid chromatography (FPLC, see Section 9.4, p. 58) is a high performance chromatography method that combines several advantages. First, the small-diameter stationary phase enables high resolution and fast flow rates. Secondly, samples can be diluted in bio-compatible aqueous buffer systems and large sample volumes can be injected to the system. Thirdly, separation is highly

11.4. AEX as a Novel Tool to Study the Surface Conformation of Small Non-Enveloped Viruses

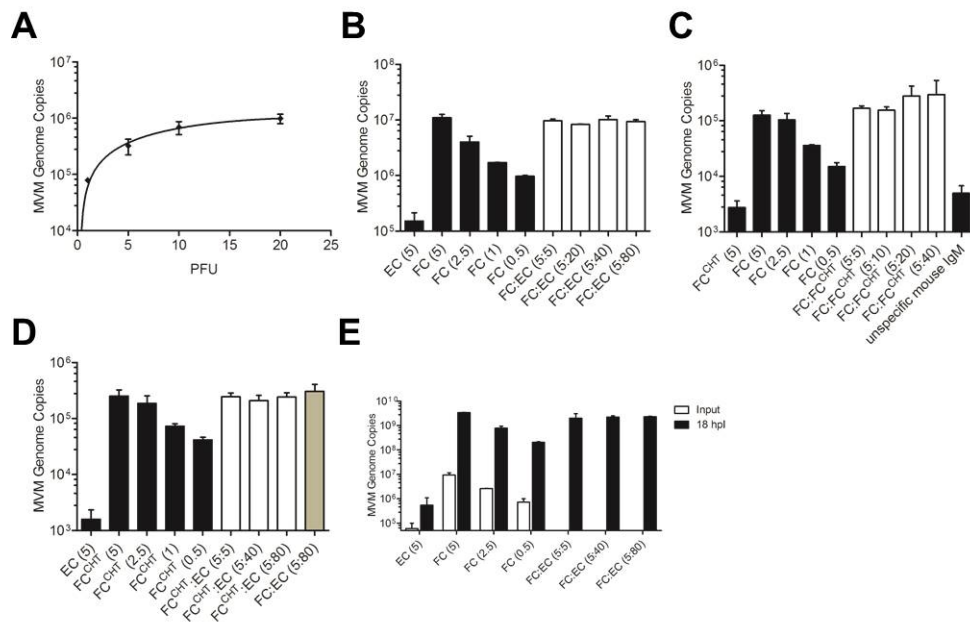


Figure S6.: N-VP2 exposure alone is not sufficient for the better binding to SA moieties. (A) A9 cells (3×10^5) were incubated with MVM at increasing PFU. Following binding at 4°C unbound virus was removed and total amount of bound virus was quantified. (B) EC or FC were bound to A9 cells at the PFUs indicated in brackets (black bars). In order to compete the bound FC (5 PFU) increasing amounts of EC were added (5-80 PFU, white bars). (C) FC^{CHT} or FC were bound to A9 cells at the PFUs indicated in brackets (black bars). In order to compete the bound FC (5 PFU) increasing amounts of FC^{CHT} were added (5-40 PFU, white bars). Cells were washed and lysed in cell lysis buffer (see Table 12.2, p. 138). FC were quantified following IP using α -N-VP2 Ab (see Table 12.8, p. 142) (D) EC or FC^{CHT} were bound to A9 cells at the PFUs indicated in brackets (black bars). In order to compete the bound FC^{CHT} (5 PFU) increasing amounts of EC were added (5-80 PFU, white bars). Grey bar: As a negative control experiment, FC (5 PFU) were simultaneously incubated with an excess of EC (80 PFU). (E) A9 cells (8×10^3) were infected at the PFUs indicated in brackets. Increasing amount of EC were added to FC. Inputs are represented by white bars.

11. Supplementary Data

reproducible due to a high level of automation including gradient program control and fraction collection. Finally, a full range of chromatography modes, such as ion exchange, chromatofocusing, gel filtration, hydrophobic interaction, and reverse phase can be provided [291].

We tried to apply AEX on other parvoviruses than MVM, such as B19V and CPV. B19V is a widespread human pathogen which can cause severe disease in human beings. It belongs to the genus *Erythroparvovirus* (see Section 2.1.6, p. 9) and thus, it is highly erythrotropic. B19V efficiently replicates in rapidly dividing erythroid progenitor cells, such as erythroblasts and megakaryocytes present in the bone marrow [207]. Only fully mature virions migrate to the blood plasma of infected individuals where they can persist at high titers (see Figure S7 A, p. 123). CPV emerged in the mid-1970s as a new pathogen of dogs. Equally to MVM, it belongs to the genus *Protoparvovirus* (see Section 2.1.7, p. 10) and replicates in tissues containing rapidly proliferating cells, including the bone marrow, lymph nodes, and the spleen [211]. Stocks of CPV were generated in canine A72 cell culture. The cells were productively infected and virus progeny was isolated by lysis of infected cell cultures. By doing so, pre-mature and mature virus progeny were not physically separated (see Figure S7 B, p. 123).

The AEX profiles of B19V derived from plasma samples and CPV derived from cell culture were analyzed. As expected, there was one sharp peak in the case of B19V. Since only the fully mature virions can migrate from the bone marrow to the blood plasma, they eluted as a single homogeneous population from the AEX column (see Figure S7 C, p. 123). Similar to MVM, two populations were detectable in the case of CPV (see Figure S7 F, p. 123). Binding interaction is known to rearrange the VP1u conformation of B19V. Upon receptor attachment, B19V exposes its VP1u on the surface of the capsid [55]. Since such a rearrangement of the capsid surface influences the surface electrostatics, the profile of bound B19V was found to be distinct from the one of the stock virus (see Figure S7 D, p. 123). The situation became even more complex when intracellular virus was analyzed. B19V undergoes complex phosphorylation and partially uncoats during entry (Ruprecht, N. *et al.*, manuscript in preparation). The formerly homogeneous stock virus displayed a highly complex AEX profile consisting of several peaks (see Figure S7 E, p. 123). In order to analyze such a complex profile, cell fractionation prior to AEX analysis should be required. Another possibility would be to infect the cells in the presence of chemical compounds which interfere with certain maturation steps preventing such a complex AEX profile.

Summary: AEX represents a powerful tool to physically separate intracellular virus populations and to gain insights into progeny virus maturation. Coupled to cell fractionation and/or pharmacological interference it can provide valuable information on the role of a particular cellular pathway in the infection. Isolated virus sub-populations can be further characterized by standard biochemical and molecular biological methods.

11.4. AEX as a Novel Tool to Study the Surface Conformation of Small Non-Enveloped Viruses

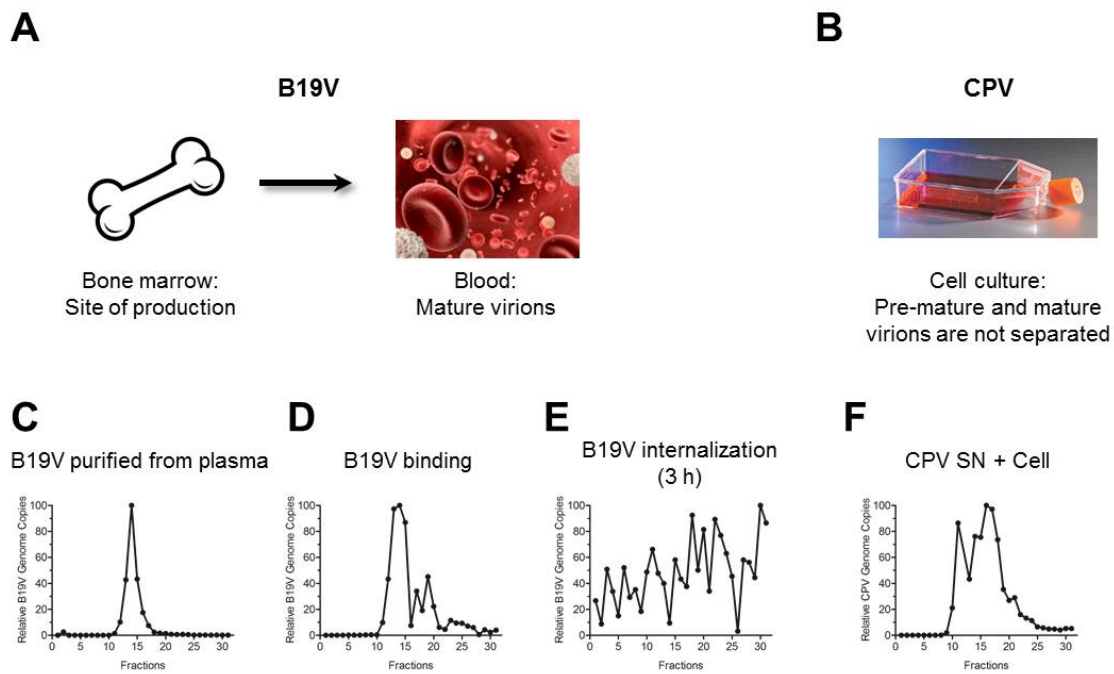


Figure S7.: AEX can be applied to study other parvoviruses. (A) B19V is produced in the bone marrow of infected individuals. Only mature particles accumulate in the blood plasma where they productively infect erythroid progenitor cells. (B) CPV was produced in tissue cell culture. Pre-mature and mature particles were not efficiently separated. (C) AEX profile of B19V derived from blood plasma. (D) AEX profile of B19V following binding to UT-7/EPO-S1 cells at 4 °C for 1h. (E) AEX profile of B19V internalized in UT-7/EPO-S1 cells for 3 h at 37 °C. (F) AEX profile of CPV produced in canine A72 cells. Virus was recovered from infected cells by repeated freeze and thaw cycles to lyse the cells.

Part IV

Conclusion

Conclusion

The release of non-enveloped viruses has been for a long time considered a passive process associated with cellular lysis. Recently, growing evidence suggests an active mechanism for the egress of non-enveloped progeny virions, thus challenging this basic principle in virology. However, the mechanism involved remains elusive. The current knowledge concerning nuclear maturation, export, and egress of non-enveloped viruses is limited. The main aim of this thesis was to confirm the existence of an active mechanism of egress and to identify the late nuclear maturation steps of minute virus of mice (MVM) leading to nuclear export of the virion progeny.

Anion-exchange chromatography (AEX) was performed to separate intracellular virus populations displaying different protein surface configurations. Apart from empty capsids (EC), two well defined DNA-containing populations were separated based on their net surface charges. The full capsid (FC) populations, referred to as FC-P₁ and FC-P₂, differed in the conformation of their N-termini of the viral capsid protein VP2 (N-VP2), as well as in their surface phosphorylation status. Nuclear export and active egress prior to cytolysis was observed only for the late FC-P₂ population. The segregation of the two FC populations confirms an active mechanism of egress. While N-VP2 was not involved in the active nuclear export of MVM, the surface phosphorylations were strictly associated with nuclear export.

During their life cycle, karyophilic viruses need to master a bidirectional nuclear transport. Early in infection, the virus is imported into the nucleus where it hijacks the replication machinery of the host cell. Following assembly and DNA-packaging, progeny virions are exported from the nucleus. In order to achieve this paradoxical situation, the virus needs to rearrange its capsid surface to acquire nuclear import or export potential. Our findings revealed spatially and temporally controlled modifications of capsid surface phosphorylations (see Figure 11.8, p. 128) as a pivotal mechanism mediating nuclear import and export of a karyophilic virus.

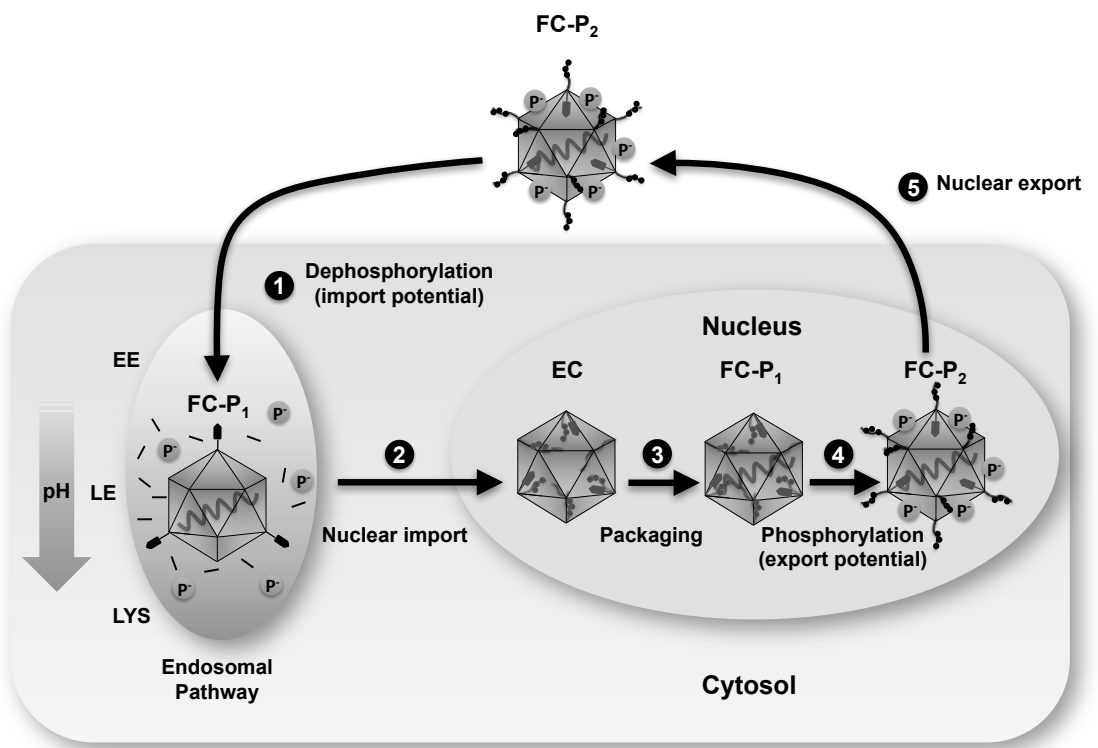


Figure 11.8.: Model of nuclear import and export of MVM. Surface phosphorylations play a pivotal role in determining nuclear import/export of MVM. ① During entry, the surface phosphorylations of export competent FC-P₂ virions are removed by acidic phosphatases, adopting the FC-P₁ phosphorylation pattern. ② Infectious incoming virions escape the endosomal pathway and are imported into the nucleus. ③ Following self-assembly of the structural proteins, the empty capsids (EC) are filled with a ssDNA genome, leading to the generation of FC-P₁ virions. ④ FC-P₁ particles are phosphorylated by a nuclear kinase, resulting in the accumulation of FC-P₂ virion progeny. ⑤ FC-P₂ virions are exported from the nucleus of infected cells and egress the host cell. The most important capsid elements involved in the viral life cycle are explained below the representation.

Part V

Appendix

12. Materials

12.1. Infectious Clone of MVMp (pIC_MVMp)

12.1.1. Plasmid Map of pIC_MVMp

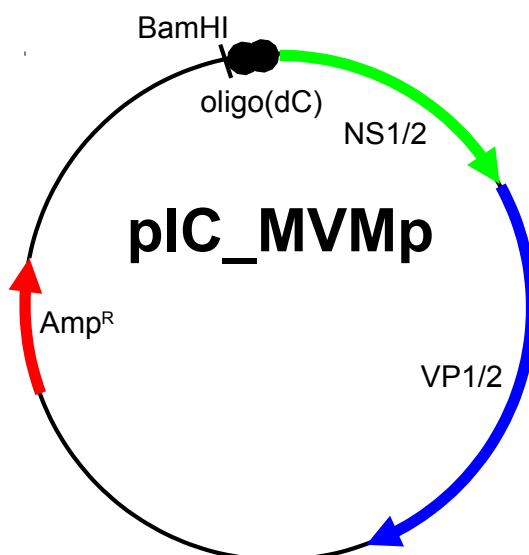


Figure 12.1.: Plasmid map of the infectious clone of MVMp (pIC_MVMp). Colored arrows indicate the genes in either the MVM genome or the pBR322 cloning vector. The circles at the left-hand end of the MVM genome represent the oligo(dC) linker sequence which was originally used for cloning [309].

12. Materials

12.1.2. Complete Sequence of pIC_MVMp

The complete nucleotide sequence of the infectious clone of MVM (pIC_MVMp) is shown below. Sequences in black correspond to the backbone of the pBR322 cloning vector. The sequence colored red corresponds to the viral negative (-) strand in 3' to 5' direction which is predominantly packaged into MVM capsids.

```
1 AAGAACTTCT GCTTTCCCGG AGCACTATGC GGATAAAAAT ATCCAATTAC AGTACTATTA TTACCAAAGA
 71 ATCTGCAGTC CACCGTAAAA AGCCCCTTA CACGCGCCTT GGGGATAAAC AAATAAAAAG ATTTATGTAA
141 GTTTATACAT AGGCGAGTAC TCTGTTATTG GGACTATTAA CGAAGTTATT ATAACCTTTT CCTTCTCATA
211 CTCATAAGTT GTAAAGGCAC AGCGGAAATA AGGGAAAAAA CGCGTAAAAA CGGAAGGACA AAAACGAGTG
281 GGTCTTTGCG ACCACTTTCA TTTTCTACGA CTTCAGTCA ACCCACGTGC TCACCCAATG TAGCTTGACC
351 TAGAGTTGTC GCCATTCTAG GAACTCTCAA AAGCGGGGCT TCTTGCAAAA GGTTACTACT CGTAAAATT
421 TCAAGACGAT ACACCGCGCC ATAATAGGGC ACAACTGCGG CCCGTTCTCG TTGAGCCAGC GGCGTATGTG
491 ATAAGAGTCT TACTGAACCA ACTCATGAGT GGTAGTGTCTTTCTAGA ATGCCTACCG TACTGTCATT
561 CTCTTAATAC GTCACGACGG TATTGGTACT CACTATTGTG ACGCCGGTTG AATGAAGACT GTTGCTAGCC
631 TCCTGGCTTC CTCGATTGGC GAAAAAACGT GTTGTACCCC CTAGTACATT GAGCGGAAC AGCAACCCCTT
701 GGCCTCGACT TACTTCGGTA TGTTTGCTG CTCGCACTGT GGTGCTACGG ACGTCGTTAC CGTTGTTGCA
771 ACGCGTTTGA TAATTGACCG CTTGATGAAT GAGATCGAAG GGCGGTTGTT AATTATCTGA CCTACCTCCG
841 CCTATTTCAA CGTCCTGGT AAGACCGGAG CGGGGAAGGC CGACCGACCA AATAACGACT ATTTAGACCT
911 CGGCCACTCG CACCCAGAGC GCCATAGTAA CGTCGTGACC CCGGTCTACC ATTGGGAGG GCATAGCATC
981 AATAGATGTG CTGCCCTCA GTCCGTTGAT ACCTACTTGC TTTATCTGTCTAGC ACTGACTCT ATCCACGGAG
1051 TGACTAATTG GTAACCATTG ACAGTCTGGT TCAAATGAGT ATATATGAAA TCTAACTAAA TTTTGAAGTA
1121 AAAATTAAT TTTCTAGAT CCACCTCTAG GAAAAACTAT TAGAGTACTG GTTTTAGGGA ATTGCACTCA
1191 AAAGCAAGGT GACTCGCAGT CTGGGGCATC TTTCTAGTT TCCTAGAAGA ACTCTAGGAA AAAAGACGCG
1261 GCATTAGACG ACGAACGTTT GTTTTTTGG TGCGATGGT CGCCACCAAA CAAACGGCCT AGTTCTCGAT
1331 GGTTGAGAAA AAGGCTTCCA TTGACCGAAG TCGTCTCGCG TCTATGGTT ATGACAGGAA GATCACATCG
1401 GCATCAATCC GGTGGTGAAG TTCTTGAGAC ATCGTGGCGG ATGTATGGAG CGAGACGATT AGGACAATGG
1471 TCACCGACGA CGGTACCGC TATTCAAGCAC AGAATGGCCC AACCTGAGTT CTGCTATCAA TGGCTTATTC
1541 CGCGTCGCCA GCCCCACTTG CCCCCCAAGC ACGTGTGTCG GGTGAAACCT CGCTTGCTGG ATGTGGCTTG
1611 ACTCTATGGA TGTCGCACTC GATACTTTT CGCGGTGCGA AGGGCTTCCC TCTTCCGCC TGTCCATAGG
1681 CCATTGCGCG TCCCAGCCTT GTCCCTCTCGC GTGCTCCCTC GAAGGTCCCC CTTTGGGAC CATAGAAATA
1751 TCAGGACAGC CCAAAGCGGT GGAGACTGAA CTCGCAGCTA AAAACACTAC GAGCAGTCCC CCCGCCTCGG
1821 ATACCTTTT GCGGTGCGT CGCGGAAAAA ATGCCAAGGA CGGGAAAACG ACCGGAAAAC GAGTGTACAA
1891 GAAAGGACGC AATAGGGGAC TAAGACACCT ATTGGCATAA TGGCGAAAC TCACTCGACT ATGGCGAGCG
1961 GCGTCGGCTT GCTGGCTCGC GTCGCTCACTCGT CACTCGCTCC TTGCGCTTCT CGCGGACTAC GCCATAAAAG
2031 AGGAATGCGT AGACACGCCA TAAAGTGTGG CGTATACCAAC GTGAGAGTCA TGTTAGACGA GACTACGGCG
2101 TATCAATTG GTCATATGTG AGGGATAGC GATGCACTGA CCCAGTACCG ACGCGGGCT GTGGCGGTT
2171 GTGGGCGACT GCGCGGGACT GCCCCAACAG ACGAGGGCCG TAGGCGAATG TCTGTTGAC ACTGGCAGAG
2241 GCCCTCGACG TACACAGTCT CCAAAAGTGG CAGTAGTGGC TTTGCGCGCT CCGTCGACGC CATTTCGAGT
2311 AGTCGCACCA GCACCTCGCT AAGTGTCTAC AGACGGACAA GTAGGCGCAG GTCGAGCAAC TCAAAGAGGT
2381 CTTCGCAATT ACAGACCGAA GACTATTGCG CCCGGTACAA TTCCCGCCAA AAAAGGACAA ACCAGTGAAC
2451 TACGGAGGCA CATTCCCCCT TAAAGACAAG TACCCCCATT ACTATGGCTA CTTTGCTCTC TCCTACGGAGT
2521 GCTATGCCCA ATGACTACTA CTTGTACGGG CCAATGACCT TGCAACACTC CCATTGTTG ACCGCCATAC
2591 CTACGCCGCC CTGGTCTCTT TTTAGTGTGAGT CCCAGTTACG GTGCGAAGC AATTATGTCT ACATCCACAA
```

12.1. Infectious Clone of MVMP (*pIC_MVMP*)

2661 GGTGTCCCAT CGGTCGTCGT AGGACGCTAC GTCTAGGCCT TGTATTACCA CGTCCCGCGA CTGAAGGCC
2731 AAAGGTCTGA AATGCTTTGT GCCTTTGGCT TCTGGTAAGT ACAACAACGA GTCCACGCGTC TGCAAAACGT
2801 CGTCGTCAGC GAAGTGCAAG CGAGCGCATA GCCACTAAGT AAGACGATTG GTCATTCCGT TGGGGCGGTC
2871 GGATCGGGCCC AGGAGTTGCT GTCTCGTGC TAGTACGCGT GGGCACCGGT CCTGGGTTGC GACGGGCTCT
2941 ACGCGGGCGA CGCCGACGAC CTCTACCGCC TCGCCTACCT ATACAAGACG GTTCCAACC AAACCGTAA
3011 GTGTCAAGAG GCGTTCTTAA CTAACCGAGG TTAAGAACCT CACCACTTAG GCAATCGCTC CACGGCGGCC
3081 GAAGGTAAGT CCAGCTCCAC CGGGCCGAGG TACGTGGCGC TCGCTTGCCT CCCTCCGTCT GTTCCATATC
3151 CCGCCGCGGA TGTTAGGTAC GGTTGGGCAA GGTACACGAG CGGCTCCGCC GTATTAGCG GCACGTGCTAG
3221 TCGCCAGGTC ACTAGCTTCA ATCCGACCAT TCTCGCGCT CGCTAGGAAC TTGACAGGG ACTACCAGCA
3291 GTAGATGGAC GGACCTGTG TACCGGACGT TGCGCCCGTA GGGCTACCGC GGCCTTCGCT CTTCTTAGTA
3361 TTACCCCTTC CGGTAGGTG GAGCGCAGCG CTTGCGGTG TTCTGCATCG GGTCGCGCAG CGGGCGGTAC
3431 GGCGCTATT ACCGGACGAA GAGCGGCTTT GCAAACACC ACCCTGGTCA CTGCTTCCGA ACTCGCTCCC
3501 GCACGTTCTA AGGCTTATGG CGTCGCTGT CGCGCTAGTA GCAGCGCGAG GTGCTTTCG CCAGGAGCGG
3571 CTTTACTGG GTCTCGCGAC GGCGTGGAC AGGATGCTCA ACGTACTATT TCTTCTGTCA GTATTACCGC
3641 CGCTGCTATC AGTACGGGGC GCGGGTGGCC TTCTCGACT GACCCAACCTT CCGAGAGTTG CCGTAGGCCAG
3711 CTGCGAGAGG GAATACGCTG AGGACGTAAT CCTTCGTCGG GTCATCATCC AACTCCGGCA ACTCGTGGCG
3781 GCGGCGTTCC TTACACGTA CGTCTCTCTA CGCGGGTTG TCAGGGGGCC GGTGCCCCGG ACGGTGGTAT
3851 GGGTGCAGGCT TTGTTCGCGA GTACTCGGCG TTCACCGCTC GGGCTAGAAAG GGGTAGCCAC TACAGCCGCT
3921 ATATCCGCGG TCGTTGGCGT GGACACCGCG GCACTACCG CCGGTGCTAC GCAGGGCGCA TCTCCTAGGC
3991 CCCCCCCCCC CCC~~AAAATCT~~ TGACTGGTTG GTACAAGTGC ATTCACTGCA CTACTCGCG CGACCGCGC
4061 GACGGAAGGCC GTCAGTGTGC AGTGAATGCA AAGTGTACCA ACCAGTCAAG ATTTTTACTA TTGCGCAAGT
4131 CCCTCAAATT TGGTCCGCG CTTTCTCTT ACCCGCACCA AATTTCATAT ATTCTGTGAT GACTTCAGTC
4201 AATGAATAGA AAAGAAAGTA AGACACTCAG CTCTGCGTGT CTTTCTCTA TTGGTTGATT GGTACCGACC
4271 TTTACGAATG AGACTACTTC AAAACCCCTCG TTGGTTGACC AATTTCCTT TTTCATTGGT CCTTCACAAG
4341 AGTAAACAAA AATTTTACT TTTACAAGTT GACTTACCTT TTCTATAGCC TACCTTATCA ATGTTTTTC
4411 TCGACGTCT CCTGCTCGAC TTAGAAATG TTGCTCTCG CTTTGTGATGA ACCCTGGTT CGCTCCTGTA
4481 CCTTACCCCTT TGGTGCACC TACTTTACTG GTTTTCTGTT CATAAGTAAA AACTAAGAAA CCAATTTTT
4551 ACAAAATAAC TTCACGAATT GTGTTCTTA TATAAAGGAC CACTACAATT AACCAAACAC GTTGTACTTA
4621 CCCCCTTCTT GGTCCGACC GTGACGGTAC ATGATTAACC TCCTTCTCG AAATCAGTTC GAGTTCCCTT
4691 TACCACTCT TCCGTTGATT TACAAATGAC CTCGTCTACC AACCAATTGTC GGACATTACA CGTTGATTGT
4761 GGTCGACTTT CTTAATTGTA TTCTCTTCTG CGTCTCTGT TACTCACCCA ATGAGATGAA TGAATATTG
4831 TATTGTTTG GTTTTCTG ATATGGTTCA CACAAGAAAA ACCTTTGTAC TAACGAATGA TAAAAAATTG
4901 ATTTTCTTT TATTGCGAT CAGGTGGTTC TCTGCCTCCG ATAAAAGAAA TCGTCACTGA AACCGACCTT
4971 TTGATTGAAA AATTTCCTTC CGCTCGCGGT AGATCACTCG TTTGATATGT GACTACTGTA CGCCGGCTT
5041 TGCAACTTT GGTGTCATTG GTGACGGTC CTTGATTG CGCCGTCTTA AGTTGATTT TTTCTTCAAA
5111 GATAATTGTTG ATGTGAATT CTCGACCGACG TATTTCCTCA TTGGAGTGGT CTCTGACCT ACTACTACGT
5181 CGGTCTGTCA ATGTAACCTT ACTACCGAGT TGGTCCACCT CTTTGGACG ACTTTTATG CGATCTCTAA
5251 ACATGTGATT GAGACGGTC TTGGTTTG CGTAAACTGA ATTTAAATCT TTTGACTT TGGTCGTTG
5321 ATTGGTTGAA AAGTGACGGA CTGTGTTCTT GGACGTCTTA AAAACGAAAA GTACCGACCT TGATACAATT
5391 TCAAACGGTA CGATAAACGA CACAAAATTG GTCTGTTCTT CCGTTTCTT TATGACAAAA TAAAGTACCT
5461 GGTGGTCGTT GTCCGTTAG ATAATAACGT GTTCGGTATC GTGTCGTCA ACCGTTACAA CCAACGATAT
5531 TACGTGCGTT ACATTTGAAA GGTAATTAC TGACATGGTT GTTCTTGAA TAAACCCATC TTCTTCGACC
5601 ATTGAAACCT GTCGTTCTT TGGTCAAATT TCGGTAAACCG AGACCAGTT GATAACGTA ACTAGTTTT
5671 CCTTTCTCGT CGTTGTTCTA ACTTGGTTGT GGTCACTAGT ACTGGTGTGTT ACTCTTGAA TGTCACTAGT
5741 CTTATCCGAC GCTTCTTCTT GGTCTTGTGT GAGTTGGTTA GTCTCTGTCT TACGAATTGT AAGTAGATTG
5811 TGTATGGAAC GGACCACTGA AACCAAACCA ACTGTTTTA CTTACCGGGT ACTAAACACG AACCAACCAT

12. Materials

5881 TTCTTACCAA TGGTTAGATG GTACCGTCG ATGACACGAT TTACCCCGTT TCAAGGACTA ACCAGTCTTT
5951 TGACCCGCCT CGGTTTCCAC GGTTGAGGAT ATTTAAATGA TCCAAGCCGT GCGAGTGGTA AGTGCTGTGG
6021 CTTTCATGC GGAGAGTCGG TCTTGATACG TGATTGAGGT GAACGTAGCC TAGAGCTCCT GGACCGAAAT
6091 CTGGAACCT CGTGTGGTTT ATGAGGACAA CGCCCGTGAC GTCTTGGGT CTTGTGACCC CTTCGACCAA
6161 GGTTTCGGAC GGTTCTACCA GTTGAECTCGG GTTGAACCAG TCTCTAGCTC CTCTAAACT CTCGCACGAA
6231 GCCACGCCTT GGCAACTTCT TTCTGAAGTC GCTCGGCAC TTGAACCTGA TTCCATGCTA CCGGGAGGT
6301 CGATTTCTC GATTTCTCC ATTCCCAAAT TCCCTACCAA CCAACCACCC CATAATTACA AATTAAATGGA
6371 CAAAATGTCC GGACTTTAGT GAACCAAAT CCAACCCACG GAGGACCGAT GTTCATGGAC CCTGGTCCCT
6441 TGTCGGAACCT GGTTCTCTT GGTTGGTTAG GTAGACTGCG GCGACGGTTT CTCGTGCTGC TCCGGATACT
6511 AGTTATGTAG TTTAGACCTT TTTAGGAAT GGACATGAAG AGACGACGAC TAGTTGCGAA ATAATGGTT
6581 TGTTCCCTGC GGTTCTGAC CCCTCCGTT CAACCACTGA TGAAAAAAATC TTGGTTCCGG CGAAAACGTG
6651 GATTCGAACG ATGACTGAGA CTTGGACCTT GAAGACCACA TTCGTCTCGA CCATTCGCGT GATCTGGTGG
6721 ACGAATGTA AAATAATTGG TTCGGTCTCG ATTTTTTTT GAATGAAGAA GACGACGTG CGTTTCGTCA
6791 GTTTGGTACT CACTACCGTG GTCGGTTGGA CTGTCGCCCT TGCGACAGGT GAGTCGACGT TCTCAACTTG
6861 CTCGTCGACT GCCGGGACCT CCGAGACCCC CACCCCCGAG ACCGCCCCCA CCCAACACAA AAAGATGACC
6931 CAGAATACTA TTAGTTGCG TAATATCTAA GAACCCACTG CCGACCCATC TTTAATGACG TGATCGTTGA
7001 TCTGATCATG TAAATTGTA CGGATTAGT CTTTGATAA CGTCTTAGTC TCAAGTGTAA TGTGCTGT
7071 GTAGTCAGTT TCCGTTGTAC CGTTTCTAC TACGAGTACT CGTTTAAACC TGTGGTACCT CGAACCCACT
7141 ACGATTACGA ACCCCTAAA CCGAGGTCGG TTCACTGACC GTTATGTAAA CGTTGCGTA CTCGGTCGA
7211 TTGAACCATA GTGAACACTGT TCTTTATAAG TTACATCACG ACTTTTGACA ATGTCCTGTT CTGAATCCTC
7281 CAGTTCGATA TTTTTATATG TTGTTACTGG AATGTCGAAAC GTACTACCAA CGTCATCTGA GTTTGTTGTA
7351 AAACGGTATG TGTGGACGTC GTTGGAGTTA CCTTTGTGAA CCAAAGATGG GGACCTTGG TTGGTATCGT
7421 AGTGGTATGT CCATGATAAA AACGCAACTG TCTCTAGAAA GTCACTGGAT GCTTTAGTT CTTCCGTGTC
7491 AACTTGTATT ACACTACCCCT TGTGGTTTTC CTACTTAAG AGTTAAAAAA TGGTAACTCT TGTGTTGT
7561 TTAGTGTAAAC GAGTCTTGTCC CCTCGCTTAA ACGGTGTCCG TGAATGATGA AACTGTGTTT AGGTCAATT
7631 GAGTGTGTGT GCACCGTTTG GTTGGCAGTT GAACCTGTGAG GAGGTGACGA CAGTTGAAA GGACTTCGAC
7701 TGTGACTACG TCCATGTGAA TGACGAGTTC CCTCGTCTGT ACCTTGTGTT GTTTACCCCC AATTGACCCA
7771 CTCACTTCGT TAGTCTTGGT CTGGACGAGT TCATCCTAAA ACAGTTGGT TGTTACTGAA ACTTCGGTCG
7841 TCTCGACCTG GTAAACGACG GGGTTTCAA GGTGCTAT AATGAGTTC TCATCTGTT CTTCCGTTAC
7911 CGTCACAATC TATGTCAATA CCGTTTGTG TACCACTTTT AACCCGAAGT GTACCTGGTC GTGGTCTCGC
7981 GATGTGTACC CTACTTTGTT CGAAACCAAG TCCATCTCTG TGGTTTCTAC CAAAATAAGT TAGTCGTGGT
8051 GATCAACAAG GTGGTGGTGA TTTACCGTAA GAATGTTAC GTTGGGATA ACCCTGATTT TTACTGTAAG
8121 TAAAAAGTTT ACAAAAATTG TCGATACCAAG GTGATTGACG TAAAAGTGTG GGTCAGGAC ATATGGAGT
8191 TCCTGTTTAT ACCCTGTTTC TTGATCTAGA ACTTGTGTTT GGATCTGAAG TGTATTGACG AGGTAACCAA
8261 ACATTTTGT TACGTGGACC GTTACCAAC CAATCTAAC TCGTTGGGA TTGACTGGTT ATACTAGTT
8331 TGCCCTCGGTG TGAAAGATCT TAACAATGTA TACCATGTA AAAGACCTTT CCTTTGATT GGTACTCTCG
8401 TTTGAAATCT CGATTGTGGT GAACCTGGG TCACATGGTT CATTCAACGAC TTCTGTTACC GTTGAGTATG
8471 TACTCACATT GATTTACCGA TGTTGACGA TGACCTTGT ACGTCAGACA CGGCGAATAT TGTTCTGGAC
8541 AACGATCTT ATGAATGATT GATTGGTACG AAAAAGAAAG ACATGAAGTA TATAATAATT CTGATTATTT
8611 CTATGTTGTA TCTTTATATT ATAATGTATA TCTAAATTCT TTATCTTATT ATACCATGAA TCATTGACAA
8681 TTTTATTAT CTTGGAAACC TTATTGTTCT ATCAATCAAC CAATTACAAT CTATCTTATT CTTCTAGTAC
8751 ATATTACTTA TTTTCCACC TTCCACCAA CCATCCAATT ACAATCTATC TTATTCTCT AGTACATATT
8821 ACTTATTTTC CCACCTTCCC ACCAACCATC CATAAGGGAA TCTGAACCTAC AATTCCGGT TTTTTTATTA
8891 TTTGAAAAAA ATTTGAGTT GGTTCTGATG ACAGATAAGT CACTTGGTTG ACTTGGTAAT CATAATGATA
8961 CAAAATCCC ACCCTCCAGT TAGTTAGTCC TT

12.2. Chemicals and Compounds

Table 12.1.: List of chemicals and compounds

Chemical	Provider
Acetic Acid (Glacial)	Merck
Acetone	Merck
Agarose low EEO	Applichem
Ampicillin (Ready Made Solution, 100 g/mL, 0.2 μ M filtered)	Sigma-Aldrich
Bafilomycin A ₁	Sigma-Aldrich
Bovine Serum Albumin (BSA)	Sigma-Aldrich
Bromophenol Blue	Merck
Caesium Chloride (CsCl)	Sigma-Aldrich
Chymostatin	Sigma-Aldrich
Citric Acid	Sigma-Aldrich
Complete Mini Protease Inhibitor Cocktail Tablets	Roche
Complete Mini Protease Inhibitor Cocktail Tablets EDTA-free	Roche
1,4-diazabicyclo[2.2.2]octane (DABCO)	Sigma-Aldrich
4',6-diamidino-2-phenylindole (DAPI)	Invitrogen
Dimethyl Sulfoxide (DMSO)	Sigma-Aldrich
Dithiothreitol (DTT)	Sigma-Aldrich
1kb DNA Ladder	Invitrogen
Ethylenediaminetetraacetic Acid (EDTA)	Sigma-Aldrich
Ethanol (99.89 %)	Sigma-Aldrich
Ethanol (94 %) denat. with 2 % MEK	Grogg Chemie AG
Ethidium Bromide (10 mg/mL)	Invitrogen
EZMix™ N-Z-Amine® A (NZ Amine)	Sigma-Aldrich
Fetal Calf Serum (FCS)	Amimed
Glycerol (Anhydrous)	Sigma-Aldrich
Goat Serum	DAKO
G-Protein Agarose Beads	Santa Cruz Biotech
Hydrochloric Acid (HCl)	Sigma-Aldrich
Imidazole	Sigma-Aldrich
Iminodiacetic Acid	Sigma-Aldrich

12. Materials

Table 12.1 continued

Chemical	Provider
Isopropyl β -D-1-thiogalactopyranoside (IPTG)	Invitrogen
LB-Agar, Miller	Sigma-Aldrich
LB Broth Base	Invitrogen
L-Glutamine (200 mM)	Biochrom
Magnesium Chloride ($MgCl_2$)	Sigma-Aldrich
Magnesium Sulfate ($MgSO_4$)	Sigma-Aldrich
Manganese(II) chloride ($MnCl_2$)	Sigma-Aldrich
2-Mercaptoethanol	Sigma-Aldrich
Methanol HPLC grade	Fisher Chemical
Milk Powder (Adapta)	Coop
Mowiol	Calbiochem
Nitrocellulose Transfer Membranes 0.45 μ m	Millipore
2-(<i>N</i> -morpholino)ethanesulfonic acid (MES)	Sigma-Aldrich
3-(<i>N</i> -morpholino)propanesulfonic acid (MOPS)	Sigma-Aldrich
Nonidet P40 (NP-40)	Applichem
NuPage MOPS SDS-Running Buffer (20 \times)	Invitrogen
Nupage Transfer Buffer (20 \times)	Invitrogen
N-Z-Amine [®] A	Sigma-Aldrich
Penicillin/Streptomycin	Biochrom AG
Phosphate-Buffered-Saline (PBS)	Oxoid
Polybuffer [®] 74	Sigma-Aldrich
Precision Plus Protein Standards, Dual Color	BioRad
Sodium Acetate, anhydrous	Sigma-Aldrich
Sodium Citrate	Sigma-Aldrich
Sodium Chloride (NaCl)	Roth
Sodium dihydrogen phosphate Dihydrate ($NaH_2PO_4 \cdot 2H_2O$)	Sigma-Aldrich
Sodium dodecyl sulfate (SDS)	Sigma-Aldrich
di-Sodium hydrogen phosphate Dihydrate ($Na_2HPO_4 \cdot 2H_2O$)	Sigma-Aldrich
Sodium Fluoride (NaF)	Sigma-Aldrich
Sodium Hydroxide (NaOH)	Sigma-Aldrich
Sodium Orthovanadate (Na_3VO_4)	ICN Biomedicals Inc.

12.2. Chemicals and Compounds

Table 12.1 continued

Chemical	Provider
D(+)Sucrose	Sigma-Aldrich
Sulfuric Acid 95-98 %	Sigma-Aldrich
Tris(hydroxymethyl)aminoethane (Tris Buffer)	Sigma-Aldrich
Triton X-100	Siegfried
Tween 20	Applichem
Yeast Extract	Sigma-Aldrich

12. Materials

12.3. Buffers

12.3.1. General Buffers

Table 12.2.: Buffers used for cell lysis and standard incubations.

Buffer	Reagent	Concentration
Cell Lysis Buffer	Tris-HCl (pH 7.2)	50 mM
	NaCl	150 mM
	Nonidet P40 (NP-40)	1 % (v/v)
	EDTA	5 mM
	Sodium orthovanadate (Na_3VO_4)	1 mM
	Sodium fluoride (NaF)	1 mM
	Protease Inhibitor Cocktail	1 tablet per 10 mL
Nuclei Lysis Buffer	Tris-HCl (pH 7.2)	50 mM
	NaCl	150 mM
	Triton X-100	1 % (v/v)
	EDTA	5 mM
	Sodium orthovanadate (Na_3VO_4)	1 mM
	Sodium fluoride (NaF)	1 mM
	Protease Inhibitor Cocktail	1 tablet per 10 mL
Phosphate Buffered Saline (PBS Buffer)	PBS Tablets	1 tablet in 100 mL
		dH ₂ O
Phosphate Buffered Saline with Bovine Serum Albumin (PBSA Buffer)	PBS Buffer Bovine Serum Albumin (BSA)	1% (w/v) in PBS

12.3.2. Anion-Exchange Chromatography

Table 12.3.: Buffers used for anion-exchange chromatography.

Buffer	Reagent	Concentration
Sample Buffer	Tris-HCl (pH 8)	10 mM
	EDTA	1 mM
	Sodium orthovanadate (Na_3VO_4)	1 mM
	Sodium fluoride (NaF)	1 mM
Starting Buffer	Tris-HCl (pH 7.2)	20 mM
	EDTA	1 mM
Elution Buffer	Tris-HCl (pH 7.2)	20 mM
	EDTA	1 mM
	NaCl	2 M

12.3.3. Agarose Gel Electrophoresis

Table 12.4.: Buffers used for agarose gel electrophoresis.

Buffer	Reagent	Concentration
6× DNA Loading Buffer	D(+)Sucrose	40 % (w/v)
	Bromophenol blue	0.25 % (w/v)
10× Tris-Acetate-EDTA Buffer (TAE Buffer)	Tris base (pH 8.0)	400 mM
	Acetic acid (glacial)	11.5 % (v/v)
	EDTA	10 mM

12. Materials

12.3.4. Western Blot

Table 12.5.: Buffers used for Western blotting analysis.

Buffer	Reagent	Concentration
1× NuPage MOPS Buffer	20× buffer was diluted to 1× with dH ₂ O and used for SDS page.	
1× NuPage Transfer Buffer	20× buffer was diluted to 1× with 20 % methanol. This Buffer was used to transfer the separated proteins to the nitrocellulose membrane.	
2× Protein Loading Buffer (PLB) (non-reducing, [258])	Tris-HCl (pH 6.8) Sodium dodecyl sulfate (SDS) Glycerol Bromophenol blue	120 mM 4 % (w/v) 20 % (v/v) 0.02 % (w/v)
10× Tris-Buffered Saline (TBS Buffer)	Tris-HCl (pH 7.3) NaCl	0.2 M 1.5 M
1× Tris-Buffered Saline with Tween 20 (TBST Buffer)	10× TBS Tween 20	10 % (v/v) 0.05 % (v/v)

12.4. Kits

Table 12.6.: Ready-to-use kits.

Ready-to-use Reaction System (Kit)	Provider
Amaxa™ Cell Line Nucleofector™ Kit R	Lonza Group AG
Amaxa™ Cell Line Nucleofector™ Kit V	Lonza Group AG
Amersham Hyperfilm™ ECL	GE Healthcare
Carestream® Kodak® autoradiography GBX developer/replenisher	Sigma-Aldrich
Carestream® Kodak® autoradiography GBX fixer/replenisher	Sigma-Aldrich
DNeasy Blood and Tissue Kit	Qiagen
Dynabeads® mRNA DIRECT™ Kit	Invitrogen
iTaq™ Universal SYBR® Green Supermix	BioRad
Nuclei EZ Prep Kit	Sigma-Aldrich
pBluescript II KS(+) Phagemid Kit	Agilent Technologies
QIAEX II® Gel Extraction Kit	Qiagen
QIAGEN Plasmid Midi Kit	Qiagen
QIAprep® Spin Miniprep Kit	Qiagen
QIAquick® PCR Purification Kit	Qiagen
QuikChange® Site-Directed Mutagenesis Kit	Agilent Technologies
SuperSignal® West Femto Maximum Sensitivity Substrate	Thermo Scientific
XL-10 Ultracompetent Cells	Agilent Technologies

12. Materials

12.5. Enzymes

Table 12.7.: The listed enzymes were used for *in vitro* treatments or passing tissue culture cells.

Enzyme	Concentration	Provider
α -Chymotrypsin	10 mg/mL	Sigma-Aldrich
DNase I, RNase free	10 000 U/mL	Roche
Neuraminidase	50 000 U/mL	New England Biolabs
λ -Phosphatase	400 000 U/mL	Merck
Trypsin/EDTA solution	0.25 % / 0.02 % (w/v)	Biochrom AG

12.6. Antibodies

12.6.1. Primary Antibodies

Table 12.8.: The primary antibodies were used for immunolabeling, immunoprecipitation, and Western blotting analysis.

Name	Specificity	Host	Clonality	Dilution	Provider
α -VP (Jimmy)	Linear epitopes on VP1 and VP2 of MVM.	Rabbit	Polyclonal	IF: 1/800 WB: 1/2 000	J. M. Almendral [298]
α -Caps (B7)	Conformational surface epitope on intact capsids of MVM.	Mouse	Monoclonal	IF: 1/100	J. M. Almendral [279]
N-VP2	N-terminal part of VP2.	Rabbit	Polyclonal	IF: 1/200 WB: 1/1 000	J. M. Almendral [298]

12.6.2. Secondary Antibodies

Table 12.9.: The secondary antibodies were used for immunofluorescence assays and Western blotting analysis.

Name	Target species	Host	Conjugate	Dilution	Provider
Goat α -mouse IgG	Mouse	Goat	Alexa Fluor® 488	IF: 1/500	Life Technologies
Goat α -mouse IgG	Mouse	Goat	Alexa Fluor® 594	IF: 1/500	Life Technologies
Goat α -mouse Ig	Mouse	Goat	Horseradish peroxidase (HRP)	WB: 1/20 000	Dako
Goat α -rabbit Ig	Rabbit	Goat	Horseradish peroxidase (HRP)	WB: 1/20 000	Dako
Goat α -rabbit IgG	Rabbit	Goat	Alexa Fluor® 488	IF: 1/500	Life Technologies
Goat α -rabbit IgG	Rabbit	Goat	Alexa Fluor® 594	IF: 1/500	Life Technologies

All secondary antibodies listed in this table are polyclonal.

12.7. Media

Table 12.10.: The denoted media were used for the cultivation of A9 and NB324K cells, as well as XL1-blue and XL10-gold bacteria.

Name	Provider
Dulbecco's Modified Eagle Medium (DMEM)	Gibco
Lysogeny Broth Agar (LB Agar)	Sigma-Aldrich
Lysogeny Broth Medium (LB Medium)	Sigma-Aldrich
SOC Medium	Sigma-Aldrich

Bibliography

- [1] Adeyemi, R. O., Landry, S., Davis, M. E., Weitzman, M. D., and Pintel, D. J. Parvovirus minute virus of mice induces a DNA damage response that facilitates viral replication. *PLoS Pathog.*, 6(10):e1001141, 2010.
- [2] Adlhoch, C., Kaiser, M., Ellerbrok, H., and Pauli, G. High prevalence of porcine Herpesvirus in German wild boar populations. *Virol. J.*, 7:171, 2010.
- [3] Agbandje-McKenna, M. and Chapman, M. S. Correlating structure with function in the viral capsid. In Kerr, J. R., Bloom, M. E., Cotmore, S. F., Linden, R. M., and Parrish, C. R., eds., *Parvoviruses*, pp. 125–139. Hodder Arnold, London, UK, 2006.
- [4] Agbandje-McKenna, M., Llamas-Saiz, A. L., Wang, F., Tattersall, P., and Rossmann, M. G. Functional implications of the structure of the murine parvovirus, minute virus of mice. *Structure*, 6(11):1369–1381, Nov 1998.
- [5] Agbandje, M., McKenna, R., Rossmann, M. G., Strassheim, M. L., and Parrish, C. R. Structure determination of feline panleukopenia virus empty particles. *Proteins*, 16(2):155–171, Jun 1993.
- [6] Ahn, J. K., Gavin, B. J., Kumar, G., and Ward, D. C. Transcriptional analysis of minute virus of mice P4 promoter mutants. *J. Virol.*, 63(12):5425–5439, Dec 1989.
- [7] Aitken, A. 14-3-3 proteins on the MAP. *Trends Biochem. Sci.*, 20(3):95–97, Mar 1995.
- [8] Akache, B., Grimm, D., Pandey, K., Yant, S. R., Xu, H., and Kay, M. A. The 37/67-kilodalton laminin receptor is a receptor for adeno-associated virus serotypes 8, 2, 3, and 9. *J. Virol.*, 80(19):9831–9836, Oct 2006.
- [9] Alexandersen, S., Bloom, M. E., and Perryman, S. Detailed transcription map of Aleutian mink disease parvovirus. *J. Virol.*, 62(10):3684–3694, Oct 1988.
- [10] Allander, T., Emerson, S. U., Engle, R. E., Purcell, R. H., and Bukh, J. A virus discovery method incorporating DNase treatment and its application to the identification of two bovine parvovirus species. *Proc. Natl. Acad. Sci. U.S.A.*, 98(20):11609–11614, Sep 2001.
- [11] Allander, T., Tammi, M. T., Eriksson, M., Bjerkner, A., Tiveljung-Lindell, A., and Andersson, B. Cloning of a human parvovirus by molecular screening of respiratory tract samples. *Proc. Natl. Acad. Sci. U.S.A.*, 102(36):12891–12896, Sep 2005.
- [12] Allaume, X., El-Andaloussi, N., Leuchs, B., Bonifati, S., Kulkarni, A., Marttila, T., Kaufmann, J. K., Nettelbeck, D. M., Kleinschmidt, J., Rommelaere, J., and Marchini, A. Retargeting of rat parvovirus H-1PV to cancer cells through genetic engineering of the viral capsid. *J. Virol.*, 86(7):3452–3465, Apr 2012.
- [13] Angata, T. and Varki, A. Chemical diversity in the sialic acids and related α -keto acids: an evolutionary perspective. *Chem. Rev.*, 102(2):439–469, Feb 2002.
- [14] Antonietti, J. P., Sahli, R., Beard, P., and Hirt, B. Characterization of the cell type-specific determinant in the genome of minute virus of mice. *J. Virol.*, 62(2), Feb 1988.
- [15] Asokan, A., Hamra, J. B., Govindasamy, L., Agbandje-McKenna, M., and Samulski, R. J. Adeno-associated virus type 2 contains an integrin $\alpha 5\beta 1$ binding domain essential for viral cell entry. *J. Virol.*, 80(18):8961–8969, Sep 2006.
- [16] Astell, C. R., Chow, M. B., and Ward, D. C. Sequence analysis of the termini of virion and replicative forms of minute virus of mice DNA suggests a modified rolling hairpin model for autonomous parvovirus DNA replication. *J. Virol.*, 54(1):171–177, Apr 1985.
- [17] Astell, C. R., Gardiner, E. M., and Tattersall, P. DNA sequence of the lymphotropic variant of minute virus of mice, MVM(i), and comparison with the DNA

Bibliography

- sequence of the fibrotropic prototype strain. *J. Virol.*, 57(2):656–669, Feb 1986.
- [18] **Astell, C. R., Smith, M., Chow, M. B., and Ward, D. C.** Structure of the 3' hairpin termini of four rodent parvovirus genomes: nucleotide sequence homology at origins of DNA replication. *Cell*, 17(3):691–703, Jul 1979.
- [19] **Astell, C. R., Thomson, M., Chow, M. B., and Ward, D. C.** Structure and replication of minute virus of mice DNA. *Cold Spring Harb. Symp. Quant. Biol.*, 47 Pt 2:751–762, 1983.
- [20] **Astell, C. R., Thomson, M., Merchlinsky, M., and Ward, D. C.** The complete DNA sequence of minute virus of mice, an autonomous parvovirus. *Nucleic Acids Res.*, 11(4):999–1018, Feb 1983.
- [21] **Atchison, R. W.** The role of herpesviruses in adenovirus-associated virus replication *in vitro*. *Virology*, 42(1):155–162, Sep 1970.
- [22] **Baldauf, A. Q., Willwand, K., Mumtsidu, E., Nüesch, J. P., and Rommelaere, J.** Specific initiation of replication at the right-end telomere of the closed species of minute virus of mice replicative-form DNA. *J. Virol.*, 71(2):971–980, Feb 1997.
- [23] **Ball-Goodrich, L. J. and Tattersall, P.** Two amino acid substitutions within the capsid are coordinately required for acquisition of fibrotropism by the lymphotropic strain of minute virus of mice. *J. Virol.*, 66(6):3415–3423, Jun 1992.
- [24] **Ball-Goodrich, L. J., Moir, R. D., and Tattersall, P.** Parvoviral target cell specificity: acquisition of fibrotropism by a mutant of the lymphotropic strain of minute virus of mice involves multiple amino acid substitutions within the capsid. *Virology*, 184(1):175–186, Sep 1991.
- [25] **Bantel-Schaal, U., Braspenning-Wesch, I., and Kartenbeck, J.** Adeno-associated virus type 5 exploits two different entry pathways in human embryo fibroblasts. *J. Gen. Virol.*, 90(Pt 2):317–322, Feb 2009.
- [26] **Barbis, D. P., Chang, S. F., and Parrish, C. R.** Mutations adjacent to the dimple of the canine parvovirus capsid structure affect sialic acid binding. *Virology*, 191(1):301–308, Nov 1992.
- [27] **Barnes, H. J., Guy, J. S., and Vaillancourt, J. P.** Poult enteritis complex. *Rev. - Off. Int. Epizoot.*, 19(2):565–588, Aug 2000.
- [28] **Bar, S., Daeffler, L., Rommelaere, J., and Nüesch, J. P.** Vesicular egress of non-enveloped lytic parvoviruses depends on gelsolin functioning. *PLoS Pathog.*, 4(8):e1000126, 2008.
- [29] **Bar, S., Rommelaere, J., and Nüesch, J. P.** Vesicular transport of progeny parvovirus particles through ER and Golgi regulates maturation and cytolysis. *PLoS Pathog.*, 9(9):e1003605, Sep 2013.
- [30] **Bartlett, J. S., Wilcher, R., and Samulski, R. J.** Infectious entry pathway of adeno-associated virus and adeno-associated virus vectors. *J. Virol.*, 74(6):2777–2785, Mar 2000.
- [31] **Basak, S. and Turner, H.** Infectious entry pathway for canine parvovirus. *Virology*, 186(2):368–376, Feb 1992.
- [32] **Basak, S., Turner, H., and Parr, S.** Identification of a 40- to 42-kDa attachment polypeptide for canine parvovirus in A72 cells. *Virology*, 205(1):7–16, Nov 1994.
- [33] **Bashir, T., Horlein, R., Rommelaere, J., and Willwand, K.** Cyclin A activates the DNA polymerase δ-dependent elongation machinery *in vitro*: A parvovirus DNA replication model. *Proc. Natl. Acad. Sci. U.S.A.*, 97(10):5522–5527, May 2000.
- [34] **Bashir, T., Rommelaere, J., and Cziepluch, C.** *In vivo* accumulation of cyclin A and cellular replication factors in autonomous parvovirus minute virus of mice-associated replication bodies. *J. Virol.*, 75(9):4394–4398, May 2001.
- [35] **Bastien, N., Chui, N., Robinson, J. L., Lee, B. E., Dust, K., Hart, L., and Li, Y.** Detection of human bocavirus in Canadian children in a 1-year study. *J. Clin. Microbiol.*, 45(2):610–613, Feb 2007.
- [36] **Bates, R. C., Snyder, C. E., Banerjee, P. T., and Mitra, S.** Autonomous parvovirus LuIII encapsidates equal amounts of plus and minus DNA strands. *J. Virol.*, 49(2):319–324, Feb 1984.
- [37] **Bayburt, T. and Gelb, M. H.** Interfacial catalysis by human 85 kDa cytosolic phospholipase A₂ on anionic vesicles in the scooting mode. *Biochemistry*, 36(11):3216–3231, Mar 1997.
- [38] **Bell, C. L., Vandenberghe, L. H., Bell, P., Limberis, M. P., Gao, G. P., Van Vliet, K., Agbandje-McKenna, M., and Wilson, J. M.** The AAV9 receptor and its modification to improve *in vivo* lung gene transfer in mice. *J. Clin. Invest.*, 121(6):2427–2435, Jun 2011.

- [39] **Belyi, V. A., Levine, A. J., and Skalka, A. M.** Sequences from ancestral single-stranded DNA viruses in vertebrate genomes: the parvoviridae and circoviridae are more than 40 to 50 million years old. *J. Virol.*, 84(23):12458–12462, Dec 2010.
- [40] **Bergeron, J., Hebert, B., and Tijssen, P.** Genome organization of the Kresse strain of porcine parvovirus: identification of the allotropic determinant and comparison with those of NADL-2 and field isolates. *J. Virol.*, 70(4):2508–2515, Apr 1996.
- [41] **Berns, K. I. and Adler, S.** Separation of two types of adeno-associated virus particles containing complementary polynucleotide chains. *J. Virol.*, 9(2):394–396, Feb 1972.
- [42] **Berns, K. I. and Rose, J. A.** Evidence for a single-stranded adenovirus-associated virus genome: isolation and separation of complementary single strands. *J. Virol.*, 5(6):693–699, Jun 1970.
- [43] **DeLano, W. L.** *The PyMOL Molecular Graphic System*. DeLano Scientific, San Carlos, CA, 2002.
- [44] **Bina, M., Ng, S. C., and Blasquez, V.** Simian virus 40 chromatin interaction with the capsid proteins. *J. Biomol. Struct. Dyn.*, 1(3):689–704, Dec 1983.
- [45] **Blackburn, S. D., Cline, S. E., Hemming, J. P., and Johnson, F. B.** Attachment of bovine parvovirus to O-linked alpha 2,3 neuraminic acid on glycophorin A. *Arch. Virol.*, 150(7):1477–1484, Jul 2005.
- [46] **Blackburn, S. D., Steadman, R. A., and Johnson, F. B.** Attachment of adeno-associated virus type 3H to fibroblast growth factor receptor 1. *Arch. Virol.*, 151(3):617–623, Mar 2006.
- [47] **Black, L. W.** DNA packaging in dsDNA bacteriophages. *Annu. Rev. Microbiol.*, 43:267–292, 1989.
- [48] **Blasquez, V., Beecher, S., and Bina, M.** Simian virus 40 morphogenetic pathway. An analysis of assembly-defective tsB201 DNA protein complexes. *J. Biol. Chem.*, 258(13):8477–8484, Jul 1983.
- [49] **Bleker, S., Sonntag, F., and Kleinschmidt, J. A.** Mutational analysis of narrow pores at the fivefold symmetry axes of adeno-associated virus type 2 capsids reveals a dual role in genome packaging and activation of phospholipase A2 activity. *J. Virol.*, 79(4):2528–2540, Feb 2005.
- [50] **Blomstrom, A. L., Stahl, K., Masembe, C., Okoth, E., Okurut, A. R., Atmnedi, P., Kemp, S., Bishop, R., Belak, S., and Berg, M.** Viral metagenomic analysis of bushpigs (*Potamochoerus larvatus*) in Uganda identifies novel variants of Porcine parvovirus 4 and Torque teno sus virus 1 and 2. *J. Virol.*, 9:192, 2012.
- [51] **Bloom, M. E., Berry, B. D., Wei, W., Perryman, S., and Wolfenbarger, J. B.** Characterization of chimeric full-length molecular clones of Aleutian mink disease parvovirus (ADV): identification of a determinant governing replication of ADV in cell culture. *J. Virol.*, 67(10):5976–5988, Oct 1993.
- [52] **Bloom, M. E., Martin, D. A., Oie, K. L., Huh-tanen, M. E., Costello, F., Wolfenbarger, J. B., Hayes, S. F., and Agbandje-McKenna, M.** Expression of Aleutian mink disease parvovirus capsid proteins in defined segments: localization of immunoreactive sites and neutralizing epitopes to specific regions. *J. Virol.*, 71(1):705–714, Jan 1997.
- [53] **Bloom, M. E., Race, R. E., and Wolfenbarger, J. B.** Characterization of Aleutian disease virus as a parvovirus. *J. Virol.*, 35(3):836–843, Sep 1980.
- [54] **Blumel, J., Schmidt, I., Willkommen, H., and Lower, J.** Inactivation of parvovirus B19 during pasteurization of human serum albumin. *Transfusion*, 42(8):1011–1018, Aug 2002.
- [55] **Bönsch, C., Zuercher, C., Lieby, P., Kempf, C., and Ros, C.** The globoside receptor triggers structural changes in the B19 virus capsid that facilitate virus internalization. *J. Virol.*, 84(22):11737–11746, Nov 2010.
- [56] **Bodendorf, U., Cziepluch, C., Jauniaux, J. C., Rommelaere, J., and Salome, N.** Nuclear export factor CRM1 interacts with nonstructural proteins NS2 from parvovirus minute virus of mice. *J. Virol.*, 73(9):7769–7779, Sep 1999.
- [57] **Boisvert, M., Fernandes, S., and Tijssen, P.** Multiple pathways involved in porcine parvovirus cellular entry and trafficking toward the nucleus. *J. Virol.*, 84(15):7782–7792, Aug 2010.
- [58] **Bonnard, G. D., Manders, E. K., Campbell, D. A., Herberman, R. B., and Collins, M. J.** Immunosuppressive activity of a subline of the mouse EL-4 lymphoma. Evidence for minute virus of mice causing the inhibition. *J. Exp. Med.*, 143(1):187–205, Jan 1976.
- [59] **Boschetti, N., Wyss, K., Mischler, A., Hostettler, T., and Kempf, C.** Stability of minute virus of mice against temperature and sodium hydroxide. *Biologicals*, 31(3):181–185, Sep 2003.

Bibliography

- [60] Bosma, G. C., Custer, R. P., and Bosma, M. J. A severe combined immunodeficiency mutation in the mouse. *Nature*, 301(5900):527–530, Feb 1983.
- [61] Bourguignon, G. J., Tattersall, P. J., and Ward, D. C. DNA of minute virus of mice: self-priming, non-permuted, single-stranded genome with a 5'-terminal hairpin duplex. *J. Virol.*, 20(1):290–306, Oct 1976.
- [62] Bouyac-Bertoia, M., Dvorin, J. D., Fouchier, R. A., Jenkins, Y., Meyer, B. E., Wu, L. I., Emerman, M., and Malim, M. H. HIV-1 infection requires a functional integrase NLS. *Mol. Cell*, 7(5):1025–1035, May 2001.
- [63] Bowman, E. J., Siebers, A., and Altendorf, K. Baflomycins: a class of inhibitors of membrane ATPases from microorganisms, animal cells, and plant cells. *Proc. Natl. Acad. Sci. U.S.A.*, 85(21):7972–7976, Nov 1988.
- [64] Brailovsky, C. Research on the rat K virus (Parvovirus ratti). I. A method of titration by plaques and its application to the study of the multiplication cycle of the virus. *Ann Inst Pasteur (Paris)*, 110(1):49–59, Jan 1966.
- [65] Brandenburger, A., Legendre, D., Avalosse, B., and Rommelaere, J. NS-1 and NS-2 proteins may act synergistically in the cytopathogenicity of parvovirus MVMP. *Virology*, 174(2):576–584, Feb 1990.
- [66] Brauniger, S., Fischer, I., and Peters, J. The temperature stability of bovine parvovirus. *Zentralbl Hyg Umweltmed*, 196(3):270–278, Oct 1994.
- [67] Brister, J. R. and Muzyczka, N. Rep-mediated nicking of the adeno-associated virus origin requires two biochemical activities, DNA helicase activity and transesterification. *J. Virol.*, 73(11):9325–9336, Nov 1999.
- [68] Brockhaus, K., Plaza, S., Pintel, D. J., Rommelaere, J., and Salome, N. Nonstructural proteins NS2 of minute virus of mice associate *in vivo* with 14-3-3 protein family members. *J. Virol.*, 70(11):7527–7534, Nov 1996.
- [69] Brown, K. E., Anderson, S. M., and Young, N. S. Erythrocyte P antigen: cellular receptor for B19 parvovirus. *Science*, 262(5130):114–117, Oct 1993.
- [70] Brownstein, D. G., Smith, A. L., Jacoby, R. O., Johnson, E. A., Hansen, G., and Tattersall, P. Pathogenesis of infection with a virulent allotropic variant of minute virus of mice and regulation by host genotype. *Lab. Invest.*, 65(3):357–364, Sep 1991.
- [71] Brownstein, D. G., Smith, A. L., Johnson, E. A., Pintel, D. J., Naeger, L. K., and Tattersall, P. The pathogenesis of infection with minute virus of mice depends on expression of the small nonstructural protein NS2 and on the genotype of the allotropic determinants VP1 and VP2. *J. Virol.*, 66(5):3118–3124, May 1992.
- [72] Bruemmer, A., Scholari, F., Lopez-Ferber, M., Conway, J. F., and Hewat, E. A. Structure of an insect parvovirus (*Junonia coenia* Densovirus) determined by cryo-electron microscopy. *J. Mol. Biol.*, 347(4):791–801, Apr 2005.
- [73] Bui, M., Whittaker, G., and Helenius, A. Effect of M1 protein and low pH on nuclear transport of influenza virus ribonucleoproteins. *J. Virol.*, 70(12):8391–8401, Dec 1996.
- [74] Buller, R. M., Janik, J. E., Sebring, E. D., and Rose, J. A. Herpes simplex virus types 1 and 2 completely help adenovirus-associated virus replication. *J. Virol.*, 40(1):241–247, Oct 1981.
- [75] Burbelo, P. D. and Hall, A. 14-3-3 proteins. Hot numbers in signal transduction. *Curr. Biol.*, 5(2):95–96, Feb 1995.
- [76] Burnett, E. and Tattersall, P. Reverse genetic system for the analysis of parvovirus telomeres reveals interactions between transcription factor binding sites in the hairpin stem. *J. Virol.*, 77(16):8650–8660, Aug 2003.
- [77] Burnett, E., Cotmore, S. F., and Tattersall, P. Segregation of a single outboard left-end origin is essential for the viability of parvovirus minute virus of mice. *J. Virol.*, 80(21):10879–10883, Nov 2006.
- [78] Caillet-Fauquet, P., Perros, M., Brandenburger, A., Spegelaere, P., and Rommelaere, J. Programmed killing of human cells by means of an inducible clone of parvoviral genes encoding non-structural proteins. *EMBO J.*, 9(9):2989–2995, Sep 1990.
- [79] Canaan, S., Zadot, Z., Ghomashchi, F., Bollinger, J., Sadilek, M., Moreau, M. E., Tijssen, P., and Gelb, M. H. Interfacial enzymology of parvovirus phospholipases A₂. *J. Biol. Chem.*, 279(15):14502–14508, Apr 2004.
- [80] Carreira, A., Menendez, M., Reguera, J., Almendral, J. M., and Mateu, M. G. *In vitro* disassembly of a parvovirus capsid and effect on capsid stability of heterologous peptide insertions in surface loops. *J. Biol. Chem.*, 279(8):6517–6525, Feb 2004.

- [81] Castellanos, M., Perez, R., Carrillo, P. J., de Pablo, P. J., and Mateu, M. G. Mechanical disassembly of single virus particles reveals kinetic intermediates predicted by theory. *Biophys. J.*, 102(11):2615–2624, Jun 2012.
- [82] Cater, J. E. and Pintel, D. J. The small non-structural protein NS2 of the autonomous parvovirus minute virus of mice is required for virus growth in murine cells. *J. Gen. Virol.*, 73 (Pt 7):1839–1843, Jul 1992.
- [83] Chang, S. F., Sgro, J. Y., and Parrish, C. R. Multiple amino acids in the capsid structure of canine parvovirus coordinately determine the canine host range and specific antigenic and hemagglutination properties. *J. Virol.*, 66(12):6858–6867, Dec 1992.
- [84] Chapman, M. S. and Agbandje-McKenna, M. Atomic structure of viral particles. In Kerr, J. R., Bloom, M. E., Cotmore, S. F., Linden, R. M., and Parrish, C. R., eds., *Parvoviruses*, pp. 107–124. Hodder Arnold, London, UK, 2006.
- [85] Chapman, M. S. and Rossmann, M. G. Structure, sequence, and function correlations among parvoviruses. *Virology*, 194(2):491–508, Jun 1993.
- [86] Chapman, M. S. and Rossmann, M. G. Single-stranded DNA-protein interactions in canine parvovirus. *Structure*, 3(2):151–162, Feb 1995.
- [87] Cheng, W. X., Li, J. S., Huang, C. P., Yao, D. P., Liu, N., Cui, S. X., Jin, Y., and Duan, Z. J. Identification and nearly full-length genome characterization of novel porcine bocaviruses. *PLoS ONE*, 5(10):e13583, 2010.
- [88] Chen, K. C., Shull, B. C., Moses, E. A., Lederman, M., Stout, E. R., and Bates, R. C. Complete nucleotide sequence and genome organization of bovine parvovirus. *J. Virol.*, 60(3):1085–1097, Dec 1986.
- [89] Chen, S., Kapturczak, M., Loiler, S. A., Zolotukhin, S., Glushakova, O. Y., Madsen, K. M., Samulski, R. J., Hauswirth, W. W., Campbell-Thompson, M., Berns, K. I., Flotte, T. R., Atkinson, M. A., Tisher, C. C., and Agarwal, A. Efficient transduction of vascular endothelial cells with recombinant adeno-associated virus serotype 1 and 5 vectors. *Hum. Gene Ther.*, 16(2):235–247, Feb 2005.
- [90] Cheung, A. K., Wu, G., Wang, D., Bayles, D. O., Lager, K. M., and Vincent, A. L. Identification and molecular cloning of a novel porcine parvovirus. *Arch. Virol.*, 155(5):801–806, May 2010.
- [91] Christensen, J. and Tattersall, P. Parvovirus initiator protein NS1 and RPA coordinate replication fork progression in a reconstituted DNA replication system. *J. Virol.*, 76(13):6518–6531, Jul 2002.
- [92] Christensen, J., Cotmore, S. F., and Tattersall, P. A novel cellular site-specific DNA-binding protein cooperates with the viral NS1 polypeptide to initiate parvovirus DNA replication. *J. Virol.*, 71(2):1405–1416, Feb 1997.
- [93] Christensen, J., Cotmore, S. F., and Tattersall, P. Parvovirus initiation factor PIF: a novel human DNA-binding factor which coordinately recognizes two ACGT motifs. *J. Virol.*, 71(8):5733–5741, Aug 1997.
- [94] Christensen, J., Cotmore, S. F., and Tattersall, P. Two new members of the emerging KDWK family of combinatorial transcription modulators bind as a heterodimer to flexibly spaced PuCCPy half-sites. *Mol. Cell. Biol.*, 19(11):7741–7750, Nov 1999.
- [95] Christensen, J., Cotmore, S. F., and Tattersall, P. Minute virus of mice initiator protein NS1 and a host KDWK family transcription factor must form a precise ternary complex with origin DNA for nicking to occur. *J. Virol.*, 75(15):7009–7017, Aug 2001.
- [96] Christensen, J., Pedersen, M., Aasted, B., and Andersen, S. Purification and characterization of the major nonstructural protein (NS-1) of Aleutian mink disease parvovirus. *J. Virol.*, 69(3):1802–1809, Mar 1995.
- [97] Clemens, K. E. and Pintel, D. Minute virus of mice (MVM) mRNAs predominantly polyadenylate at a single site. *Virology*, 160(2):511–514, Oct 1987.
- [98] Clemens, K. E. and Pintel, D. J. The two transcription units of the autonomous parvovirus minute virus of mice are transcribed in a temporal order. *J. Virol.*, 62(4):1448–1451, Apr 1988.
- [99] Clemens, K. E., Cerutis, D. R., Burger, L. R., Yang, C. Q., and Pintel, D. J. Cloning of minute virus of mice cDNAs and preliminary analysis of individual viral proteins expressed in murine cells. *J. Virol.*, 64(8):3967–3973, Aug 1990.
- [100] Clinton, G. M. and Hayashi, M. The parvovirus MVM: a comparison of heavy and light particle infectivity and their density conversion *in vitro*. *Virology*, 74(1):57–63, Oct 1976.
- [101] Cohen, S. and Pante, N. Pushing the envelope: microinjection of Minute virus of mice into *Xenopus*

Bibliography

- oocytes causes damage to the nuclear envelope. *J. Gen. Virol.*, 86(Pt 12):3243–3252, Dec 2005.
- [102] **Cohen, S., Behzad, A. R., Carroll, J. B., and Pante, N.** Parvoviral nuclear import: bypassing the host nuclear-transport machinery. *J. Gen. Virol.*, 87 (Pt 11):3209–3213, Nov 2006.
- [103] **Cohen, S., Marr, A. K., Garcin, P., and Pante, N.** Nuclear envelope disruption involving host caspases plays a role in the parvovirus replication cycle. *J. Virol.*, 85(10):4863–4874, May 2011.
- [104] **Colomar, M. C., Hirt, B., and Beard, P.** Two segments in the genome of the immunosuppressive minute virus of mice determine the host-cell specificity, control viral DNA replication and affect viral RNA metabolism. *J. Gen. Virol.*, 79 (Pt 3):581–586, Mar 1998.
- [105] **Corbau, R., Duverger, V., Rommelaere, J., and Nuesch, J. P.** Regulation of MVM NS1 by protein kinase C: impact of mutagenesis at consensus phosphorylation sites on replicative functions and cytopathic effects. *Virology*, 278(1):151–167, Dec 2000.
- [106] **Cossens, N., Faust, E. A., and Zannis-Hadjopoulos, M.** DNA polymerase δ-dependent formation of a hairpin structure at the 5' terminal palindrome of the minute virus of mice genome. *Virology*, 216(1):258–264, Feb 1996.
- [107] **Cotmore, S. F.** Gene expression in the autonomous parvoviruses. In Tijssen, P., ed., *Handbook of parvoviruses*, vol. 1, pp. 141–154. CRC Press, Inc., Boca Raton, FL, 1990.
- [108] **Cotmore, S. F., Agbandje-McKenna, M., Chiorini, J. A., Mukha, D. V., Pintel, D. J., Qiu, J., Soderlund-Venermo, M., Tattersall, P., Tijssen, P., Gatherer, D., and Davison, A. J.** The family Parvoviridae. *Arch. Virol.*, 159(5):1239–1247, May 2014.
- [109] **Cotmore, S. F. and Tattersall, P.** Organization of nonstructural genes of the autonomous parvovirus minute virus of mice. *J. Virol.*, 58(3):724–732, Jun 1986.
- [110] **Cotmore, S. F. and Tattersall, P.** The NS-1 polypeptide of the autonomous parvovirus MVM is a nuclear phosphoprotein. *Virus Res.*, 4(3):243–250, May 1986.
- [111] **Cotmore, S. F. and Tattersall, P.** The autonomously replicating parvoviruses of vertebrates. *Adv. Virus Res.*, 33:91–174, 1987.
- [112] **Cotmore, S. F. and Tattersall, P.** The NS-1 polypeptide of minute virus of mice is covalently attached to the 5' termini of duplex replicative-form DNA and progeny single strands. *J. Virol.*, 62(3):851–860, Mar 1988.
- [113] **Cotmore, S. F. and Tattersall, P.** A genome-linked copy of the NS-1 polypeptide is located on the outside of infectious parvovirus particles. *J. Virol.*, 63(9):3902–3911, Sep 1989.
- [114] **Cotmore, S. F. and Tattersall, P.** Alternate splicing in a parvoviral nonstructural gene links a common amino-terminal sequence to downstream domains which confer radically different localization and turnover characteristics. *Virology*, 177(2):477–487, Aug 1990.
- [115] **Cotmore, S. F. and Tattersall, P.** *In vivo* resolution of circular plasmids containing concatemer junction fragments from minute virus of mice DNA and their subsequent replication as linear molecules. *J. Virol.*, 66(1):420–431, Jan 1992.
- [116] **Cotmore, S. F. and Tattersall, P.** An asymmetric nucleotide in the parvoviral 3' hairpin directs segregation of a single active origin of DNA replication. *EMBO J.*, 13(17):4145–4152, Sep 1994.
- [117] **Cotmore, S. F. and Tattersall, P.** DNA replication in the autonomous parvoviruses. *Semin. Virol.*, 6: 271–281, 1995.
- [118] **Cotmore, S. F. and Tattersall, P.** Parvovirus DNA replication. In DePamphilis, M. L., ed., *DNA replication in eukaryotic cells*, pp. 799–813. Cold Spring Harbor Laboratory Press, Cold Spring Harbor, NY, 1996.
- [119] **Cotmore, S. F. and Tattersall, P.** High-mobility group 1/2 proteins are essential for initiating rolling-circle-type DNA replication at a parvovirus hairpin origin. *J. Virol.*, 72(11):8477–8484, Nov 1998.
- [120] **Cotmore, S. F. and Tattersall, P.** Parvoviruses. *eLS.*, Jul 2003. John Wiley and Sons Ltd, Chichester, UK.
- [121] **Cotmore, S. F. and Tattersall, P.** Resolution of parvovirus dimer junctions proceeds through a novel heterocruciform intermediate. *J. Virol.*, 77(11):6245–6254, Jun 2003.
- [122] **Cotmore, S. F. and Tattersall, P.** Genome packaging sense is controlled by the efficiency of the nick site in the right-end replication origin of parvoviruses minute virus of mice and LuIII. *J. Virol.*, 79(4):2287–2300, Feb 2005.

- [123] **Cotmore, S. F. and Tattersall, P.** Encapsidation of minute virus of mice DNA: aspects of the translocation mechanism revealed by the structure of partially packaged genomes. *Virology*, 336(1):100–112, May 2005.
- [124] **Cotmore, S. F. and Tattersall, P.** A rolling-hairpin strategy: basic mechanisms of DNA replication in the parvoviruses. In Kerr, J. R., Bloom, M. E., Cotmore, S. F., Linden, R. M., and Parrish, C. R., eds., *Parvoviruses*, pp. 171–188. Hodder Arnold, London, UK, 2006.
- [125] **Cotmore, S. F. and Tattersall, P.** Parvoviruses. In DePamphilis, M. L., ed., *DNA Replication and Human Disease*, pp. 593–608. Cold Spring Harbor Laboratory Press, Cold Spring Harbor, NY, 2006.
- [126] **Cotmore, S. F. and Tattersall, P.** Structure and organization of the viral genome. In Kerr, J. R., Bloom, M. E., Cotmore, S. F., Linden, R. M., and Parrish, C. R., eds., *Parvoviruses*, pp. 73–90. Hodder Arnold, London, UK, 2006.
- [127] **Cotmore, S. F. and Tattersall, P.** Parvoviruses: Small Does Not Mean Simple. *Annual Review of Virology*, 1:515–537, Jul 2014.
- [128] **Cotmore, S. F., Christensen, J., and Tattersall, P.** Two widely spaced initiator binding sites create an HMG1-dependent parvovirus rolling-hairpin replication origin. *J. Virol.*, 74(3):1332–1341, Feb 2000.
- [129] **Cotmore, S. F., Christensen, J., Nüesch, J. P., and Tattersall, P.** The NS1 polypeptide of the murine parvovirus minute virus of mice binds to DNA sequences containing the motif [ACCA]₂₋₃. *J. Virol.*, 69(3):1652–1660, Mar 1995.
- [130] **Cotmore, S. F., D'Abromo, A. M., Carbonell, L. F., Bratton, J., and Tattersall, P.** The NS2 polypeptide of parvovirus MVM is required for capsid assembly in murine cells. *Virology*, 231(2):267–280, May 1997.
- [131] **Cotmore, S. F., D'abromo, A. M., Ticknor, C. M., and Tattersall, P.** Controlled conformational transitions in the MVM virion expose the VP1 N-terminus and viral genome without particle disassembly. *Virology*, 254(1):169–181, Feb 1999.
- [132] **Cotmore, S. F., Gottlieb, R. L., and Tattersall, P.** Replication initiator protein NS1 of the parvovirus minute virus of mice binds to modular divergent sites distributed throughout duplex viral DNA. *J. Virol.*, 81(23):13015–13027, Dec 2007.
- [133] **Cotmore, S. F., Gunther, M., and Tattersall, P.** Evidence for a ligation step in the DNA replication of the autonomous parvovirus minute virus of mice. *J. Virol.*, 63(2):1002–1006, Feb 1989.
- [134] **Cotmore, S. F., Hafenstein, S., and Tattersall, P.** Depletion of virion-associated divalent cations induces parvovirus minute virus of mice to eject its genome in a 3'-to-5' direction from an otherwise intact viral particle. *J. Virol.*, 84(4):1945–1956, Feb 2010.
- [135] **Cotmore, S. F., Nüesch, J. P., and Tattersall, P.** *In vitro* excision and replication of 5' telomeres of minute virus of mice DNA from cloned palindromic concatemer junctions. *Virology*, 190(1):365–377, Sep 1992.
- [136] **Cotmore, S. F., Nuesch, J. P., and Tattersall, P.** Asymmetric resolution of a parvovirus palindrome *in vitro*. *J. Virol.*, 67(3):1579–1589, Mar 1993.
- [137] **Cotmore, S. F., Sturzenbecker, L. J., and Tattersall, P.** The autonomous parvovirus MVM encodes two nonstructural proteins in addition to its capsid polypeptides. *Virology*, 129(2):333–343, Sep 1983.
- [138] **Crawford, L. V.** A minute virus of mice. *Virology*, 29(4):605–612, Aug 1966.
- [139] **Crawford, L. V., Follett, E. A., Burdon, M. G., and McGeoch, D. J.** The DNA of a minute virus of mice. *J. Gen. Virol.*, 4(1):37–46, Jan 1969.
- [140] **Cziepluch, C., Lampel, S., Grewenig, A., Grund, C., Licher, P., and Rommelaere, J. H.** H-1 parvovirus-associated replication bodies: a distinct virus-induced nuclear structure. *J. Virol.*, 74(10):4807–4815, May 2000.
- [141] **D'Abromo, A. M., Ali, A. A., Wang, F., Cotmore, S. F., and Tattersall, P.** Host range mutants of Minute Virus of Mice with a single VP2 amino acid change require additional silent mutations that regulate NS2 accumulation. *Virology*, 340(1):143–154, Sep 2005.
- [142] **Daigle, N., Beaudouin, J., Hartnell, L., Imreh, G., Hallberg, E., Lippincott-Schwartz, J., and Ellenberg, J.** Nuclear pore complexes form immobile networks and have a very low turnover in live mammalian cells. *J. Cell Biol.*, 154(1):71–84, Jul 2001.
- [143] **Daya, S. and Berns, K. I.** Gene therapy using adeno-associated virus vectors. *Clin. Microbiol. Rev.*, 21(4): 583–593, Oct 2008.
- [144] **Day, J. M. and Zsak, L.** Determination and analysis of the full-length chicken parvovirus genome. *Virology*, 399(1):59–64, Mar 2010.

Bibliography

- [145] de Duve, C., de Barsy, T., Poole, B., Trouet, A., Tulkens, P., and Van Hoof, F. Commentary. Lysosomotropic agents. *Biochem. Pharmacol.*, 23(18):2495–2531, Sep 1974.
- [146] Deiss, V., Tratschin, J. D., Weitz, M., and Siegl, G. Cloning of the human parvovirus B19 genome and structural analysis of its palindromic termini. *Virology*, 175(1):247–254, Mar 1990.
- [147] Deleu, L., Fuks, F., Spitkovsky, D., Horlein, R., Faisst, S., and Rommelaere, J. Opposite transcriptional effects of cyclic AMP-responsive elements in confluent or p27KIP-overexpressing cells versus serum-starved or growing cells. *Mol. Cell. Biol.*, 18(1):409–419, Jan 1998.
- [148] Dimcheff, D. E., Askovic, S., Baker, A. H., Johnson-Fowler, C., and Portis, J. L. Endoplasmic reticulum stress is a determinant of retrovirus-induced spongiform neurodegeneration. *J. Virol.*, 77(23):12617–12629, Dec 2003.
- [149] Ding, W., Zhang, L., Yan, Z., and Engelhardt, J. F. Intracellular trafficking of adeno-associated viral vectors. *Gene Ther.*, 12(11):873–880, Jun 2005.
- [150] Di Pasquale, G., Davidson, B. L., Stein, C. S., Martins, I., Scudiero, D., Monks, A., and Chiorini, J. A. Identification of PDGFR as a receptor for AAV-5 transduction. *Nat. Med.*, 9(10):1306–1312, Oct 2003.
- [151] Di Pasquale, G., Kaludov, N., Agbandje-McKenna, M., and Chiorini, J. A. BAAV transcytosis requires an interaction with β -1-4 linked-glucosamine and gp96. *PLoS ONE*, 5(3):e9336, 2010.
- [152] Di Piazza, M., Mader, C., Geletneky, K., Herrero Y Calle, M., Weber, E., Schlehofer, J., Deleu, L., and Rommelaere, J. Cytosolic activation of cathepsins mediates parvovirus H-1-induced killing of cisplatin and TRAIL-resistant glioma cells. *J. Virol.*, 81(8):4186–4198, Apr 2007.
- [153] Doerig, C., Beard, P., and Hirt, B. A transcriptional promoter of the human parvovirus B19 active *in vitro* and *in vivo*. *Virology*, 157(2):539–542, Apr 1987.
- [154] Doerig, C., Hirt, B., Beard, P., and Antonietti, J. P. Minute virus of mice non-structural protein NS-1 is necessary and sufficient for *trans*-activation of the viral P39 promoter. *J. Gen. Virol.*, 69 (Pt 10):2563–2573, Oct 1988.
- [155] Dorsch, S., Liebisch, G., Kaufmann, B., von Landenberg, P., Hoffmann, J. H., Drobnik, W., and Modrow, S. The VP1 unique region of parvovirus B19 and its constituent phospholipase A₂-like activity. *J. Virol.*, 76(4):2014–2018, Feb 2002.
- [156] Douar, A. M., Poulard, K., Stockholm, D., and Danos, O. Intracellular trafficking of adeno-associated virus vectors: routing to the late endosomal compartment and proteasome degradation. *J. Virol.*, 75(4):1824–1833, Feb 2001.
- [157] Douglas, T. and Young, M. Viruses: making friends with old foes. *Science*, 312(5775):873–875, May 2006.
- [158] Duan, D., Li, Q., Kao, A. W., Yue, Y., Pessin, J. E., and Engelhardt, J. F. Dynamin is required for recombinant adeno-associated virus type 2 infection. *J. Virol.*, 73(12):10371–10376, Dec 1999.
- [159] Duan, D., Yue, Y., Yan, Z., Yang, J., and Engelhardt, J. F. Endosomal processing limits gene transfer to polarized airway epithelia by adeno-associated virus. *J. Clin. Invest.*, 105(11):1573–1587, Jun 2000.
- [160] Dworetzky, S. I., and Feldherr, C. M. Translocation of RNA-coated gold particles through the nuclear pores of oocytes. *J. Cell Biol.*, 106(3):575–584, Mar 1988.
- [161] Eichwald, V., Daeffler, L., Klein, M., Rommelaere, J., and Salome, N. The NS2 proteins of parvovirus minute virus of mice are required for efficient nuclear egress of progeny virions in mouse cells. *J. Virol.*, 76(20):10307–10319, Oct 2002.
- [162] Engelsma, D., Valle, N., Fish, A., Salome, N., Almendral, J. M., and Fornerod, M. A supraphysiological nuclear export signal is required for parvovirus nuclear export. *Mol. Biol. Cell*, 19(6):2544–2552, Jun 2008.
- [163] Engers, H. D., Louis, J. A., Zubler, R. H., and Hirt, B. Inhibition of T cell-mediated functions by MVM(i), a parvovirus closely related to minute virus of mice. *J. Immunol.*, 127(6):2280–2285, Dec 1981.
- [164] Fahrenkrog, B. and Aeby, U. The nuclear pore complex: nucleocytoplasmic transport and beyond. *Nat. Rev. Mol. Cell Biol.*, 4(10):757–766, Oct 2003.
- [165] Faisst, S., Perros, M., Deleu, L., Spruyt, N., and Rommelaere, J. Mapping of upstream regulatory elements in the P4 promoter of parvovirus minute virus of mice. *Virology*, 202(1):466–470, Jul 1994.

- [166] **Farr, G. A., Cotmore, S. F., and Tattersall, P.** VP2 cleavage and the leucine ring at the base of the fivefold cylinder control pH-dependent externalization of both the VP1 N terminus and the genome of minute virus of mice. *J. Virol.*, 80(1):161–171, Jan 2006.
- [167] **Farr, G. A., Zhang, L. G., and Tattersall, P.** Parvoviral virions deploy a capsid-tethered lipolytic enzyme to breach the endosomal membrane during cell entry. *Proc. Natl. Acad. Sci. U.S.A.*, 102(47):17148–17153, Nov 2005.
- [168] **Fields, B. N. and Greene, M. I.** Genetic and molecular mechanisms of viral pathogenesis: implications for prevention and treatment. *Nature*, 300(5887):19–23, Nov 1982.
- [169] **Fortune, J. M., Pavlov, Y. I., Welch, C. M., Johansson, E., Burgers, P. M., and Kunkel, T. A.** *Saccharomyces cerevisiae* DNA polymerase δ: high fidelity for base substitutions but lower fidelity for single- and multi-base deletions. *J. Biol. Chem.*, 280(33):29980–29987, Aug 2005.
- [170] **Fox, J. M. and Bloom, M. E.** Identification of a cell surface protein from Crandell feline kidney cells that specifically binds Aleutian mink disease parvovirus. *J. Virol.*, 73(5):3835–3842, May 1999.
- [171] **Fried, H. and Kutay, U.** Nucleocytoplasmic transport: taking an inventory. *Cell. Mol. Life Sci.*, 60(8):1659–1688, Aug 2003.
- [172] **Fuks, F., Deleu, L., Dinsart, C., Rommelaere, J., and Faisst, S.** *ras* oncogene-dependent activation of the P4 promoter of minute virus of mice through a proximal P4 element interacting with the Ets family of transcription factors. *J. Virol.*, 70(3):1331–1339, Mar 1996.
- [173] **Gao, G., Alvira, M. R., Somanathan, S., Lu, Y., Vandenberghe, L. H., Rux, J. J., Calcedo, R., Sanmiguel, J., Abbas, Z., and Wilson, J. M.** Adeno-associated viruses undergo substantial evolution in primates during natural infections. *Proc. Natl. Acad. Sci. U.S.A.*, 100(10):6081–6086, May 2003.
- [174] **Garcia-Bustos, J., Heitman, J., and Hall, M. N.** Nuclear protein localization. *Biochim. Biophys. Acta*, 1071(1):83–101, Mar 1991.
- [175] **Garcin, P. O. and Panté, N.** The minute virus of mice exploits different endocytic pathways for cellular uptake. *Virology*, 482:157–166, Apr 2015.
- [176] **Gardiner, E. M. and Tattersall, P.** Evidence that developmentally regulated control of gene expression by a parvoviral allotropic determinant is particle mediated. *J. Virol.*, 62(5):1713–1722, May 1988.
- [177] **Gardiner, E. M. and Tattersall, P.** Mapping of the fibrotropic and lymphotropic host range determinants of the parvovirus minute virus of mice. *J. Virol.*, 62(8):2605–2613, Aug 1988.
- [178] **Gavin, B. J. and Ward, D. C.** Positive and negative regulation of the minute virus of mice P38 promoter. *J. Virol.*, 64(5):2057–2063, May 1990.
- [179] **Gelb, M. H., Jain, M. K., Hanel, A. M., and Berg, O. G.** Interfacial enzymology of glycerolipid hydrolases: lessons from secreted phospholipases A₂. *Annu. Rev. Biochem.*, 64:653–688, 1995.
- [180] **Gersappe, A. and Pintel, D. J.** CA- and purine-rich elements form a novel bipartite exon enhancer which governs inclusion of the minute virus of mice NS2-specific exon in both singly and doubly spliced mRNAs. *Mol. Cell. Biol.*, 19(1):364–375, Jan 1999.
- [181] **Gershon, D., Sachs, L., and Winocour, E.** The induction of cellular DNA synthesis by simian virus 40 in contact-inhibited and in X-irradiated cells. *Proc. Natl. Acad. Sci. U.S.A.*, 56(3):918–925, Sep 1966.
- [182] **Gil-Ranedo, J., Hernando, E., Riobos, L., Dominguez, C., Kann, M., and Almendral, J. M.** The Mammalian Cell Cycle Regulates Parvovirus Nuclear Capsid Assembly. *PLoS Pathog.*, 11(6):e1004920, Jun 2015.
- [183] **Girod, A., Wobus, C. E., Zadori, Z., Ried, M., Leike, K., Tijssen, P., Kleinschmidt, J. A., and Hallek, M.** The VP1 capsid protein of adeno-associated virus type 2 is carrying a phospholipase A₂ domain required for virus infectivity. *J. Gen. Virol.*, 83 (Pt 5):973–978, May 2002.
- [184] **Goodwin, M. A., Davis, J. F., McNulty, M. S., Brown, J., and Player, E. C.** Enteritis (so-called runting stunting syndrome) in Georgia broiler chicks. *Avian Dis.*, 37(2):451–458, 1993.
- [185] **Gottschalck, E., Alexandersen, S., Cohn, A., Poulsen, L. A., Bloom, M. E., and Aasted, B.** Nucleotide sequence analysis of Aleutian mink disease parvovirus shows that multiple virus types are present in infected mink. *J. Virol.*, 65(8):4378–4386, Aug 1991.
- [186] **Govindasamy, L., Hueffer, K., Parrish, C. R., and Agbandje-McKenna, M.** Structures of host

Bibliography

- range-controlling regions of the capsids of canine and feline parvoviruses and mutants. *J. Virol.*, 77(22):12211–12221, Nov 2003.
- [187] **Green, M. R.** Biochemical mechanisms of constitutive and regulated pre-mRNA splicing. *Annu. Rev. Cell Biol.*, 7:559–599, 1991.
- [188] **Green, M. R. and Roeder, R. G.** Definition of a novel promoter for the major adenovirus-associated virus mRNA. *Cell*, 22(1 Pt 1):231–242, Nov 1980.
- [189] **Gunther, M. and Tattersall, P.** The terminal protein of minute virus of mice is an 83 kilodalton polypeptide linked to specific forms of double-stranded and single-stranded viral DNA. *FEBS Lett.*, 242(1):22–26, Dec 1988.
- [190] **Gurda, B. L., Parent, K. N., Bladek, H., Sinkovits, R. S., DiMatta, M. A., Rence, C., Castro, A., McKenna, R., Olson, N., Brown, K., Baker, T. S., and Agbandje-McKenna, M.** Human bocavirus capsid structure: insights into the structural repertoire of the parvoviridae. *J. Virol.*, 84(12):5880–5889, Jun 2010.
- [191] **Gu, Z., Plaza, S., Perros, M., Cziepluch, C., Rommelaere, J., and Cornelis, J. J.** NF-Y controls transcription of the minute virus of mice P4 promoter through interaction with an unusual binding site. *J. Virol.*, 69(1):239–246, Jan 1995.
- [192] **Hafenstein, S. and Fane, B. A.** ϕ X174 genome-capsid interactions influence the biophysical properties of the virion: evidence for a scaffolding-like function for the genome during the final stages of morphogenesis. *J. Virol.*, 76(11):5350–5356, Jun 2002.
- [193] **Halder, S., Ng, R. and Agbandje-McKenna, M.** Parvoviruses: structure and infection. *Future Virol.*, 7(3):253–278, Mar 2012.
- [194] **Hallauer, C., Siegl, G., and Kronauer, G.** Parvoviruses as contaminants of permanent human cell lines. 3. Biological properties of the isolated viruses. *Arch Gesamte Virusforsch.*, 38(4):366–382, 1972.
- [195] **Hansen, J., Qing, K., and Srivastava, A.** Adeno-associated virus type 2-mediated gene transfer: altered endocytic processing enhances transduction efficiency in murine fibroblasts. *J. Virol.*, 75(9):4080–4090, May 2001.
- [196] **Hansen, J., Qing, K., and Srivastava, A.** Infection of purified nuclei by adeno-associated virus 2. *Mol. Ther.*, 4(4):289–296, Oct 2001.
- [197] **Hansen, J., Qing, K., Kwon, H. J., Mah, C., and Srivastava, A.** Impaired intracellular trafficking of adeno-associated virus type 2 vectors limits efficient transduction of murine fibroblasts. *J. Virol.*, 74(2):992–996, Jan 2000.
- [198] **Hanson, N. D. and Rhode, S. L.** Parvovirus NS1 stimulates P4 expression by interaction with the terminal repeats and through DNA amplification. *J. Virol.*, 65(8):4325–4333, Aug 1991.
- [199] **Harbison, C. E., Chiorini, J. A., and Parrish, C. R.** The parvovirus capsid odyssey: from the cell surface to the nucleus. *Trends Microbiol.*, 16(5):208–214, May 2008.
- [200] **Harlow, E., Crawford, L. V., Pim, D. C., and Williamson, N. M.** Monoclonal antibodies specific for simian virus 40 tumor antigens. *J. Virol.*, 39(3):861–869, Sep 1981.
- [201] **Harrison, S. C.** Viral membrane fusion. *Nat. Struct. Mol. Biol.*, 15(7):690–698, Jul 2008.
- [202] **Harrison, S. C., Skehel, J. J., and Wiley, D. C.** Virus structure. In Fields, B. N., Knipe, D. M., Howley, P. M., Chanock, R. M., Melnick, J. L., Monath, T. P., Roizman, B., and Straus, S. E., eds., *Fundamental Virology*, pp. 59–99. Lippincott-Raven Press, Philadelphia, PA, 1996.
- [203] **Harris, R. E., Coleman, P. H., and Morahan, P. S.** Stability of minute virus of mice to chemical and physical agents. *Appl Microbiol.*, 28(3):351–354, Sep 1974.
- [204] **Hatanaka, M. and Dulbecco, R.** Induction of DNA synthesis by SV40. *Proc. Natl. Acad. Sci. U.S.A.*, 56(2):736–740, Aug 1966.
- [205] **Haut, D. D. and Pintel, D. J.** Intron definition is required for excision of the minute virus of mice small intron and definition of the upstream exon. *J. Virol.*, 72(3):1834–1843, Mar 1998.
- [206] **Haut, D. D. and Pintel, D. J.** Inclusion of the NS2-specific exon in minute virus of mice mRNA is facilitated by an intronic splicing enhancer that affects definition of the downstream small intron. *Virology*, 258(1):84–94, May 1999.
- [207] **Heegaard, E. D. and Brown, K. E.** Human parvovirus B19. *Clin. Microbiol. Rev.*, 15(3):485–505, Jul 2002.

- [208] Hensens, O. D., Monaghan, R. L., Huang, L., and Albers-Schonberg, G. Structure of the sodium and potassium ion activated adenosine triphosphatase inhibitor L-681,110. *J. Am. Soc.*, 105(11):3672–3679, 1983.
- [209] Hernando, E., Llamas-Saiz, A. L., Foces-Foces, C., McKenna, R., Portman, I., Agbandje-McKenna, M., and Almendral, J. M. Biochemical and physical characterization of parvovirus minute virus of mice virus-like particles. *Virology*, 267(2):299–309, Feb 2000.
- [210] Hirt, B. Molecular biology of autonomous parvoviruses. *Contrib Microbiol*, 4:163–177, 2000.
- [211] Hoelzer, K. and Parrish, C. R. The emergence of parvoviruses of carnivores. *Vet. Res.*, 41(6):39, 2010.
- [212] Hoggan, M. D., Blacklow, N. R., and Rowe, W. P. Studies of small DNA viruses found in various adenovirus preparations: physical, biological, and immunological characteristics. *Proc. Natl. Acad. Sci. U.S.A.*, 55(6):1467–1474, Jun 1966.
- [213] Hoggan, M. D., Maramorosch, K., and Kurstak, E. *Small DNA viruses*. Academic Press, New York, NY, 1971.
- [214] Holland, J. J. Receptor affinities as major determinants of enterovirus tissue tropisms in humans. *Virology*, 15:312–326, Nov 1961.
- [215] Hoque, M., Ishizu, K., Matsumoto, A., Han, S. I., Arisaka, F., Takayama, M., Suzuki, K., Kato, K., Kanda, T., Watanabe, H., and Handa, H. Nuclear transport of the major capsid protein is essential for adeno-associated virus capsid formation. *J. Virol.*, 73(9):7912–7915, Sep 1999.
- [216] Horiuchi, M., Ishiguro, N., Goto, H., and Shinnagawa, M. Characterization of the stage(s) in the virus replication cycle at which the host-cell specificity of the feline parvovirus subgroup is regulated in canine cells. *Virology*, 189(2):600–608, Aug 1992.
- [217] Huang, L., Albers-Schonberg, G., Monaghan, R. L., Jakubas, K., Pong, S. S., Hensens, O. D., Burg, R. W., Ostlind, D. A., Conroy, J., and Stapley, E. O. Discovery, production and purification of the Na^+ , K^+ activated ATPase inhibitor, L-681,110 from the fermentation broth of *Streptomyces* sp. MA-5038. *J. Antibiot.*, 37(9):970–975, Sep 1984.
- [218] Huang, L., Zhai, S. L., Cheung, A. K., Zhang, H. B., Long, J. X., and Yuan, S. S. Detection of a novel porcine parvovirus, PPV4, in Chinese swine herds. *Virol. J.*, 7:333, 2010.
- [219] Hueffer, K. and Parrish, C. R. Parvovirus host range, cell tropism and evolution. *Curr. Opin. Microbiol.*, 6(4):392–398, Aug 2003.
- [220] Hueffer, K., Govindasamy, L., Agbandje-McKenna, M., and Parrish, C. R. Combinations of two capsid regions controlling canine host range determine canine transferrin receptor binding by canine and feline parvoviruses. *J. Virol.*, 77(18):10099–10105, Sep 2003.
- [221] Hueffer, K., Parker, J. S., Weichert, W. S., Geisel, R. E., Sgro, J. Y., and Parrish, C. R. The natural host range shift and subsequent evolution of canine parvovirus resulted from virus-specific binding to the canine transferrin receptor. *J. Virol.*, 77(3):1718–1726, Feb 2003.
- [222] Ilyina, T. V. and Koonin, E. V. Conserved sequence motifs in the initiator proteins for rolling circle DNA replication encoded by diverse replicons from eubacteria, eucaryotes and archaebacteria. *Nucleic Acids Res.*, 20(13):3279–3285, Jul 1992.
- [223] Im, D. S. and Muzychka, N. The AAV origin binding protein Rep68 is an ATP-dependent site-specific endonuclease with DNA helicase activity. *Cell*, 61(3):447–457, May 1990.
- [224] Itah, R., Tal, J., and Davis, C. Host cell specificity of minute virus of mice in the developing mouse embryo. *J. Virol.*, 78(17):9474–9486, Sep 2004.
- [225] Jindal, H. K., Yong, C. B., Wilson, G. M., Tam, P., and Astell, C. R. Mutations in the NTP-binding motif of minute virus of mice (MVM) NS-1 protein uncouple ATPase and DNA helicase functions. *J. Biol. Chem.*, 269(5):3283–3289, Feb 1994.
- [226] Johnson, F. B., Fenn, L. B., Owens, T. J., Faucheu, L. J., and Blackburn, S. D. Attachment of bovine parvovirus to sialic acids on bovine cell membranes. *J. Gen. Virol.*, 85(Pt 8):2199–2207, Aug 2004.
- [227] Jones, M. S., Kapoor, A., Lukashov, V. V., Simmonds, P., Hecht, F., and Delwart, E. New DNA viruses identified in patients with acute viral infection syndrome. *J. Virol.*, 79(13):8230–8236, Jul 2005.
- [228] Jongeneel, C. V., Sahli, R., McMaster, G. K., and Hirt, B. A precise map of splice junctions in the mRNAs of minute virus of mice, an autonomous parvovirus. *J. Virol.*, 59(3):564–573, Sep 1986.

Bibliography

- [229] Kalderon, D., Richardson, W. D., Markham, A. F., and Smith, A. E. Sequence requirements for nuclear location of simian virus 40 large-T antigen. *Nature*, 311(5981):33–38, 1984.
- [230] Kalderon, D., Roberts, B. L., Richardson, W. D., and Smith, A. E. A short amino acid sequence able to specify nuclear location. *Cell*, 39(3 Pt 2):499–509, Dec 1984.
- [231] Kaludov, N., Brown, K. E., Walters, R. W., Zabner, J., and Chiorini, J. A. Adeno-associated virus serotype 4 (AAV4) and AAV5 both require sialic acid binding for hemagglutination and efficient transduction but differ in sialic acid linkage specificity. *J. Virol.*, 75(15):6884–6893, Aug 2001.
- [232] Kamerling, J. P. and Gerwig, G. J. Structural analysis of naturally occurring sialic acids. *Methods Mol. Biol.*, 347:69–91, 2006.
- [233] Kannagi, R. Molecular mechanism for cancer-associated induction of sialyl Lewis X and sialyl Lewis A expression-The Warburg effect revisited. *Glycoconj. J.*, 20(5):353–364, 2004.
- [234] Kasamatsu, H. and Nakanishi, A. How do animal DNA viruses get to the nucleus? *Annu. Rev. Microbiol.*, 52:627–686, 1998.
- [235] Kashiwakura, Y., Tamayose, K., Iwabuchi, K., Hirai, Y., Shimada, T., Matsumoto, K., Nakamura, T., Watanabe, M., Oshimi, K., and Daida, H. Hepatocyte growth factor receptor is a coreceptor for adeno-associated virus type 2 infection. *J. Virol.*, 79(1):609–614, Jan 2005.
- [236] Kaufmann, B., Baxa, U., Chipman, P. R., Rossman, M. G., Modrow, S., and Seckler, R. Parvovirus B19 does not bind to membrane-associated globoside *in vitro*. *Virology*, 332(1):189–198, Feb 2005.
- [237] Kaufmann, B., Lopez-Bueno, A., Mateu, M. G., Chipman, P. R., Nelson, C. D., Parrish, C. R., Almendral, J. M., and Rossmann, M. G. Minute virus of mice, a parvovirus, in complex with the Fab fragment of a neutralizing monoclonal antibody. *J. Virol.*, 81(18):9851–9858, Sep 2007.
- [238] Kawase, M., Momoeda, M., Young, N. S., and Kajigaya, S. Modest truncation of the major capsid protein abrogates B19 parvovirus capsid formation. *J. Virol.*, 69(10):6567–6571, Oct 1995.
- [239] Kilham, L. and Olivier, L. J. A latent virus of rats isolated in tissue culture. *Virology*, 7(4):428–437, Apr 1959.
- [240] Kimsey, P. B., Engers, H. D., Hirt, B., and Jongeneel, C. V. Pathogenicity of fibroblast- and lymphocyte-specific variants of minute virus of mice. *J. Virol.*, 59(1):8–13, Jul 1986.
- [241] King, A. M. Q., Adams, M. J., Carstens, E. B., and Lefkowitz, E. J. *Virus taxonomy: Ninth report of the International Committee on Taxonomy of Viruses*. Elsevier Academic Press, San Diego, CA, 2012.
- [242] King, J. A., Dubielzig, R., Grimm, D., and Kleinschmidt, J. A. DNA helicase-mediated packaging of adeno-associated virus type 2 genomes into preformed capsids. *EMBO J.*, 20(12):3282–3291, Jun 2001.
- [243] Kisary, J. Experimental infection of chicken embryos and day-old chickens with parvovirus of chicken origin. *Avian Pathol.*, 14(1):1–7, Jan 1985.
- [244] Kisary, J., Avalosse, B., Miller-Faures, A., and Rommelaere, J. The genome structure of a new chicken virus identifies it as a parvovirus. *J. Gen. Virol.*, 66 (Pt 10):2259–2263, Oct 1985.
- [245] Kisary, J., Nagy, B., and Bitay, Z. Presence of parvoviruses in the intestine of chickens showing stunting syndrome. *Avian Pathol.*, 13(2):339–343, Apr 1984.
- [246] Kleinschmidt, J. A. and King, J. A. Molecular interactions involved in assembling the viral particle and packaging the genome. In Kerr, J. R., Bloom, M. E., Cotmore, S. F., Linden, R. M., and Parrish, C. R., eds., *Parvoviruses*, pp. 305–319. Hodder Arnold, London, UK, 2006.
- [247] Kontou, M., Govindasamy, L., Nam, H. J., Bryant, N., Llamas-Saiz, A. L., Foces-Foces, C., Hernando, E., Rubio, M. P., McKenna, R., Almendral, J. M., and Agbandje-McKenna, M. Structural determinants of tissue tropism and *in vivo* pathogenicity for the parvovirus minute virus of mice. *J. Virol.*, 79(17):10931–10943, Sep 2005.
- [248] Koo, B. S., Lee, H. R., Jeon, E. O., Han, M. S., Min, K. C., Lee, S. B., Bae, Y. J., Cho, S. H., Mo, J. S., Kwon, H. M., Sung, H. W., Kim, J. N., and Mo, I. P. Genetic characterization of three novel chicken parvovirus strains based on analysis of their coding sequences. *Avian Pathol.*, 44(1): 28–34, Feb 2015.
- [249] Koonin, E. V. and Ilyina, T. V. Computer-assisted dissection of rolling circle DNA replication. *BioSystems*, 30(1-3):241–268, 1993.

Bibliography

- [250] **Kotin, R. M., Linden, R. M., and Berns, K. I.** Characterization of a preferred site on human chromosome 19q for integration of adeno-associated virus DNA by non-homologous recombination. *EMBO J.*, 11(13): 5071–5078, Dec 1992.
- [251] **Kotin, R. M., Menninger, J. C., Ward, D. C., and Berns, K. I.** Mapping and direct visualization of a region-specific viral DNA integration site on chromosome 19q13-qter. *Genomics*, 10(3):831–834, Jul 1991.
- [252] **Kotin, R. M., Siniscalco, M., Samulski, R. J., Zhu, X. D., Hunter, L., Laughlin, C. A., McLaughlin, S., Muzyczka, N., Rocchi, M., and Berns, K. I.** Site-specific integration by adeno-associated virus. *Proc. Natl. Acad. Sci. U.S.A.*, 87(6): 2211–2215, Mar 1990.
- [253] **Kresse, J. I., Taylor, W. D., Stewart, W. W., and Eernisse, K. A.** Parvovirus infection in pigs with necrotic and vesicle-like lesions. *Vet. Microbiol.*, 10(6):525–531, Dec 1985.
- [254] **Kronenberg, S., Bottcher, B., von der Lieth, C. W., Bleker, S., and Kleinschmidt, J. A.** A conformational change in the adeno-associated virus type 2 capsid leads to the exposure of hidden VP1 N termini. *J. Virol.*, 79(9):5296–5303, May 2005.
- [255] **Kudo, N., Wolff, B., Sekimoto, T., Schreiner, E. P., Yoneda, Y., Yanagida, M., Horinouchi, S., and Yoshida, M.** Leptomycin B inhibition of signal-mediated nuclear export by direct binding to CRM1. *Exp. Cell Res.*, 242(2):540–547, Aug 1998.
- [256] **Kupfer, B., Vehreschild, J., Cornely, O., Kaiser, R., Plum, G., Viazov, S., Franzen, C., Tillmann, R. L., Simon, A., Muller, A., and Schildgen, O.** Severe pneumonia and human bocavirus in adult. *Emerging Infect. Dis.*, 12(10):1614–1616, Oct 2006.
- [257] **Labieniec-Pintel, L. and Pintel, D.** The minute virus of mice P39 transcription unit can encode both capsid proteins. *J. Virol.*, 57(3):1163–1167, Mar 1986.
- [258] **Laemmli, U. K.** Cleavage of structural proteins during the assembly of the head of bacteriophage T4. *Nature*, 227(5259):680–685, Aug 1970.
- [259] **Laufs, J., Jupin, I., David, C., Schumacher, S., Heyraud-Nitschke, F., and Gronenborn, B.** Geminiivirus replication: genetic and biochemical characterization of Rep protein function, a review. *Biochimie*, 77(10):765–773, 1995.
- [260] **Lau, S. K., Woo, P. C., Tse, H., Fu, C. T., Au, W. K., Chen, X. C., Tsoi, H. W., Tsang, T. H., Chan, J. S., Tsang, D. N., Li, K. S., Tse, C. W., Ng, T. K., Tsang, O. T., Zheng, B. J., Tam, S., Chan, K. H., Zhou, B., and Yuen, K. Y.** Identification of novel porcine and bovine parvoviruses closely related to human parvovirus 4. *J. Gen. Virol.*, 89(Pt 8):1840–1848, Aug 2008.
- [261] **Lavoie, M., Sharp, C. P., Pepin, J., Pennington, C., Fouopouapouognigni, Y., Pybus, O. G., Njouom, R., and Simmonds, P.** Human parvovirus 4 infection, Cameroon. *Emerging Infect. Dis.*, 18(4): 680–683, Apr 2012.
- [262] **Lederman, M., Patton, J. T., Stout, E. R., and Bates, R. C.** Virally coded noncapsid protein associated with bovine parvovirus infection. *J. Virol.*, 49(2): 315–318, Feb 1984.
- [263] **Legendre, D. and Rommelaere, J.** Terminal regions of the NS-1 protein of the parvovirus minute virus of mice are involved in cytotoxicity and promoter *trans* inhibition. *J. Virol.*, 66(10):5705–5713, Oct 1992.
- [264] **Legrand, C., Rommelaere, J., and Caillet-Fauquet, P.** MVM(p) NS-2 protein expression is required with NS-1 for maximal cytotoxicity in human transformed cells. *Virology*, 195(1):149–155, Jul 1993.
- [265] **Leisi, R., Ruprecht, N., Kempf, C., and Ros, C.** Parvovirus B19 uptake is a highly selective process controlled by VP1u, a novel determinant of viral tropism. *J. Virol.*, 87(24):13161–13167, Dec 2013.
- [266] **Li, B., Ma, J., Xiao, S., Wen, L., Ni, Y., Zhang, X., Fang, L., and He, K.** Genome sequence of a highly prevalent porcine partetravivirus in Mainland China. *J. Virol.*, 86(3):1899, Feb 2012.
- [267] **Li, L., Cotmore, S. F., and Tattersall, P.** Maintenance of the flip sequence orientation of the ears in the parvoviral left-end hairpin is a nonessential consequence of the critical asymmetry in the hairpin stem. *J. Virol.*, 86(22):12187–12197, Nov 2012.
- [268] **Li, L., Pesavento, P. A., Woods, L., Clifford, D. L., Luff, J., Wang, C., and Delwart, E.** Novel amdovirus in gray foxes. *Emerging Infect. Dis.*, 17(10): 1876–1878, Oct 2011.
- [269] **Ling, C., Lu, Y., Kalsi, J. K., Jayandharan, G. R., Li, B., Ma, W., Cheng, B., Gee, S. W., McGoogan, K. E., Govindasamy, L., Zhong, L., Agbandje-McKenna, M., and Srivastava, A.** Human hepatocyte growth factor receptor is a cellular

Bibliography

- coreceptor for adeno-associated virus serotype 3. *Hum. Gene Ther.*, 21(12):1741–1747, Dec 2010.
- [270] **Linser, P., Bruning, H., and Armentrout, R. W.** Specific binding sites for a parvovirus, minute virus of mice, on cultured mouse cells. *J. Virol.*, 24(1):211–221, Oct 1977.
- [271] **Lippincott-Schwartz, J., Yuan, L., Tipper, C., Amherdt, M., Orci, L., and Klausner, R. D.** Brefeldin A's effects on endosomes, lysosomes, and the TGN suggest a general mechanism for regulating organelle structure and membrane traffic. *Cell*, 67(3):601–616, Nov 1991.
- [272] **Littlefield, J. W.** Three degrees of guanylic acid-inosinic acid pyrophosphorylase deficiency in mouse fibroblasts. *Nature*, 203:1142–1144, Sep 1964.
- [273] **Li, X. and Rhode, S. L.** Mutation of lysine 405 to serine in the parvovirus H-1 NS1 abolishes its functions for viral DNA replication, late promoter *trans* activation, and cytotoxicity. *J. Virol.*, 64(10):4654–4660, Oct 1990.
- [274] **Li, X. D., Lankinen, H., Putkuri, N., Vapalahti, O., and Vaheri, A.** Tula hantavirus triggers pro-apoptotic signals of ER stress in Vero E6 cells. *Virology*, 333(1):180–189, Mar 2005.
- [275] **Llamas-Saiz, A. L., Agbandje-McKenna, M., Wikoff, W. R., Bratton, J., Tattersall, P., and Rossmann, M. G.** Structure determination of minute virus of mice. *Acta Crystallogr. D Biol. Crystallogr.*, 53(Pt 1):93–102, Jan 1997.
- [276] **Lochelt, M., Delius, H., and Kaaden, O. R.** A novel replicative form DNA of Aleutian disease virus: the covalently closed linear DNA of the parvoviruses. *J. Gen. Virol.*, 70 (Pt 5):1105–1116, May 1989.
- [277] **Lombardo, E., Ramirez, J. C., Agbandje-McKenna, M., and Almendral, J. M.** A β -stranded motif drives capsid protein oligomers of the parvovirus minute virus of mice into the nucleus for viral assembly. *J. Virol.*, 74(8):3804–3814, Apr 2000.
- [278] **Lombardo, E., Ramirez, J. C., Garcia, J., and Almendral, J. M.** Complementary roles of multiple nuclear targeting signals in the capsid proteins of the parvovirus minute virus of mice during assembly and onset of infection. *J. Virol.*, 76(14):7049–7059, Jul 2002.
- [279] **Lopez-Bueno, A., Mateu, M. G., and Almendral, J. M.** High mutant frequency in populations of a DNA virus allows evasion from antibody therapy in an immunodeficient host. *J. Virol.*, 77(4):2701–2708, Feb 2003.
- [280] **Lopez-Bueno, A., Rubio, M. P., Bryant, N., McKenna, R., Agbandje-McKenna, M., and Almendral, J. M.** Host-selected amino acid changes at the sialic acid binding pocket of the parvovirus capsid modulate cell binding affinity and determine virulence. *J. Virol.*, 80(3):1563–1573, Feb 2006.
- [281] **Lopez-Bueno, A., Segovia, J. C., Bueren, J. A., O'Sullivan, M. G., Wang, F., Tattersall, P., and Almendral, J. M.** Evolution to pathogenicity of the parvovirus minute virus of mice in immunodeficient mice involves genetic heterogeneity at the capsid domain that determines tropism. *J. Virol.*, 82(3):1195–1203, Feb 2008.
- [282] **Lorson, C., Pearson, J., Burger, L., and Pintel, D. J.** An Sp1-binding site and TATA element are sufficient to support full transactivation by proximally bound NS1 protein of minute virus of mice. *Virology*, 240(2):326–337, Jan 1998.
- [283] **Lou, H. J., Brister, J. R., Li, J. J., Chen, W., Muzyczka, N., and Tan, W.** Adeno-associated virus Rep78/Rep68 promotes localized melting of the rep binding element in the absence of adenosine triphosphate. *ChemBioChem*, 5(3):324–332, Mar 2004.
- [284] **Lou, S., Xu, B., Huang, Q., Zhi, N., Cheng, F., Wong, S., Brown, K., Delwart, E., Liu, Z., and Qiu, J.** Molecular characterization of the newly identified human parvovirus 4 in the family Parvoviridae. *Virology*, 422(1):59–69, Jan 2012.
- [285] **Luby-Phelps, K.** Cytoarchitecture and physical properties of cytoplasm: volume, viscosity, diffusion, intracellular surface area. *Int. Rev. Cytol.*, 192:189–221, 2000.
- [286] **Lukashov, V. V. and Goudsmit, J.** Evolutionary relationships among parvoviruses: virus-host coevolution among autonomous primate parvoviruses and links between adeno-associated and avian parvoviruses. *J. Virol.*, 75(6):2729–2740, Mar 2001.
- [287] **Luo, M., Tsao, J., Rossmann, M. G., Basak, S., and Compans, R. W.** Preliminary X-ray crystallographic analysis of canine parvovirus crystals. *J. Mol. Biol.*, 200(1):209–211, Mar 1988.
- [288] **Lusby, E., Fife, K. H., and Berns, K. I.** Nucleotide sequence of the inverted terminal repetition in adeno-associated virus DNA. *J. Virol.*, 34(2):402–409, May 1980.

- [289] **Lusby, E. W. and Berns, K. I.** Mapping of the 5' termini of two adeno-associated virus 2 RNAs in the left half of the genome. *J. Virol.*, 41(2):518–526, Feb 1982.
- [290] **Lux, K., Goerlitz, N., Schlemminger, S., Perabo, L., Goldnau, D., Endell, J., Leike, K., Kofler, D. M., Finke, S., Hallek, M., and Buning, H.** Green fluorescent protein-tagged adeno-associated virus particles allow the study of cytosolic and nuclear trafficking. *J. Virol.*, 79(18):11776–11787, Sep 2005.
- [291] **Madadlou, A., O'Sullivan, S., and Sheehan, D.** Fast protein liquid chromatography. *Methods Mol Biol.*, 681:439–447, 2011.
- [292] **Maniatis, T.** Mechanisms of alternative pre-mRNA splicing. *Science*, 251(4989):33–34, Jan 1991.
- [293] **Mani, B., Baltzer, C., Valle, N., Almendral, J. M., Kempf, C., and Ros, C.** Low pH-dependent endosomal processing of the incoming parvovirus minute virus of mice virion leads to externalization of the VP1 N-terminal sequence (N-VP1), N-VP2 cleavage, and uncoating of the full-length genome. *J. Virol.*, 80(2):1015–1024, Jan 2006.
- [294] **Mani, B., Gerber, M., Lieby, P., Boschetti, N., Kempf, C., and Ros, C.** Molecular mechanism underlying B19 virus inactivation and comparison to other parvoviruses. *Transfusion*, 47(10):1765–1774, Oct 2007.
- [295] **Manning, A., Russell, V., Eastick, K., Leadbetter, G. H., Hallam, N., Templeton, K., and Simmonds, P.** Epidemiological profile and clinical associations of human bocavirus and other human parvoviruses. *J. Infect. Dis.*, 194(9):1283–1290, Nov 2006.
- [296] **Manning, A., Willey, S. J., Bell, J. E., and Simmonds, P.** Comparison of tissue distribution, persistence, and molecular epidemiology of parvovirus B19 and novel human parvoviruses PARV4 and human bocavirus. *J. Infect. Dis.*, 195(9):1345–1352, May 2007.
- [297] **Maroto, B., Ramirez, J. C., and Almendral, J. M.** Phosphorylation status of the parvovirus minute virus of mice particle: mapping and biological relevance of the major phosphorylation sites. *J. Virol.*, 74(23):10892–10902, Dec 2000.
- [298] **Maroto, B., Valle, N., Saffrich, R., and Almendral, J. M.** Nuclear export of the nonenveloped parvovirus virion is directed by an unordered protein signal exposed on the capsid surface. *J. Virol.*, 78(19):10685–10694, Oct 2004.
- [299] **Mastrobattista, E., van der Aa, M. A., Hennink, W. E., and Crommelin, D. J.** Artificial viruses: a nanotechnological approach to gene delivery. *Nat Rev Drug Discov*, 5(2):115–121, Feb 2006.
- [300] **Mattaj, J. W. and Englmeier, L.** Nucleocytoplasmic transport: the soluble phase. *Annu. Rev. Biochem.*, 67:265–306, 1998.
- [301] **Ma, X., Endo, R., Ishiguro, N., Ebihara, T., Ishiko, H., Ariga, T., and Kikuta, H.** Detection of human bocavirus in Japanese children with lower respiratory tract infections. *J. Clin. Microbiol.*, 44(3):1132–1134, Mar 2006.
- [302] **Maxwell, I. H., Spitzer, A. L., Maxwell, F., and Pintel, D. J.** The capsid determinant of fibrotropism for the MVMP strain of minute virus of mice functions via VP2 and not VP1. *J. Virol.*, 69(9):5829–5832, Sep 1995.
- [303] **McKenna, R., Olson, N. H., Chipman, P. R., Baker, T. S., Booth, T. F., Christensen, J., Aasted, B., Fox, J. M., Bloom, M. E., Wolfenbarger, J. B., and Agbandje-McKenna, M.** Three-dimensional structure of Aleutian mink disease parvovirus: implications for disease pathogenicity. *J. Virol.*, 73(8):6882–6891, Aug 1999.
- [304] **McKeown, M.** Alternative mRNA splicing. *Annu. Rev. Cell Biol.*, 8:133–155, 1992.
- [305] **McMaster, G. K., Beard, P., Engers, H. D., and Hirt, B.** Characterization of an immunosuppressive parvovirus related to the minute virus of mice. *J. Virol.*, 38(1):317–326, Apr 1981.
- [306] **Meehan, B. M., Creelan, J. L., McNulty, M. S., and Todd, D.** Sequence of porcine circovirus DNA: affinities with plant circoviruses. *J. Gen. Virol.*, 78 (Pt 1):221–227, Jan 1997.
- [307] **Mengeling, W. L.** Prenatal infection following maternal exposure to porcine parvovirus on either the seventh or fourteenth day of gestation. *Can. J. Comp. Med.*, 43(1):106–109, Jan 1979.
- [308] **Mengeling, W. L. and Cutlip, R. C.** Reproductive disease experimentally induced by exposing pregnant gilts to porcine parvovirus. *Am. J. Vet. Res.*, 37(12):1393–1400, Dec 1976.
- [309] **Merchlinsky, M. J., Tattersall, P. J., Leary, J. J., Cotmore, S. F., Gardiner, E. M., and Ward, D. C.** Construction of an infectious molecular clone of the autonomous parvovirus minute virus of mice. *J. Virol.*, 47(1):227–232, Jul 1983.

Bibliography

- [310] Metcalf, J. B., Bates, R. C., and Lederman, M. Interaction of virally coded protein and a cell cycle-regulated cellular protein with the bovine parvovirus left terminus *ori*. *J. Virol.*, 64(11):5485–5490, Nov 1990.
- [311] Miller, C. L. and Pintel, D. J. The NS2 protein generated by the parvovirus minute virus of mice is degraded by the proteasome in a manner independent of ubiquitin chain elongation or activation. *Virology*, 285 (2):346–355, Jul 2001.
- [312] Miller, C. L. and Pintel, D. J. Interaction between parvovirus NS2 protein and nuclear export factor Crm1 is important for viral egress from the nucleus of murine cells. *J. Virol.*, 76(7):3257–3266, Apr 2002.
- [313] Migozzi, F. and High, K. A. Therapeutic *in vivo* gene transfer for genetic disease using AAV: progress and challenges. *Nat. Rev. Genet.*, 12(5):341–355, May 2011.
- [314] Misaghi, S., Sun, Z. Y., Stern, P., Gaudet, R., Wagner, G., and Ploegh, H. Structural and functional analysis of human cytomegalovirus US3 protein. *J. Virol.*, 78(1):413–423, Jan 2004.
- [315] Mizukami, H., Young, N. S., and Brown, K. E. Adeno-associated virus type 2 binds to a 150-kilodalton cell membrane glycoprotein. *Virology*, 217(1):124–130, Mar 1996.
- [316] Molitor, T. W., Joo, H. S., and Collett, M. S. Identification and characterization of a porcine parvovirus nonstructural polypeptide. *J. Virol.*, 55(3):554–559, Sep 1985.
- [317] Momoeda, M., Wong, S., Kawase, M., Young, N. S., and Kajigaya, S. A putative nucleoside triphosphate-binding domain in the nonstructural protein of B19 parvovirus is required for cytotoxicity. *J. Virol.*, 68(12):8443–8446, Dec 1994.
- [318] Morgan, W. R. and Ward, D. C. Three splicing patterns are used to excise the small intron common to all minute virus of mice RNAs. *J. Virol.*, 60(3):1170–1174, Dec 1986.
- [319] Morishima, T., McClintock, P. R., Aulakh, G. S., Billups, L. C., and Notkins, A. L. Genomic and receptor attachment differences between mengovirus and encephalomyocarditis virus. *Virology*, 122(2):461–465, Oct 1982.
- [320] Morishima, T., McClintock, P. R., Billups, L. C., and Notkins, A. L. Expression and modulation of virus receptors on lymphoid and myeloid cells: relationship to infectivity. *Virology*, 116(2):605–618, Jan 1982.
- [321] Mouw, M. and Pintel, D. J. Amino acids 16–275 of minute virus of mice NS1 include a domain that specifically binds (ACCA)_{2–3}-containing DNA. *Virology*, 251 (1):123–131, Nov 1998.
- [322] Muller, D. E. and Siegl, G. Maturation of parvovirus LuIII in a subcellular system. II. Isolation and characterization of nucleoprotein intermediates. *J. Gen. Virol.*, 64(Pt 5):1055–1067, May 1983.
- [323] Munakata, Y., Saito-Ito, T., Kumura-Ishii, K., Huang, J., Kodera, T., Ishii, T., Hirabayashi, Y., Koyanagi, Y., and Sasaki, T. Ku80 autoantigen as a cellular coreceptor for human parvovirus B19 infection. *Blood*, 106(10):3449–3456, Nov 2005.
- [324] Muzychka, N. and Berns, K. I. Parvoviridae: the viruses and their replication. In Knipe, D. M. and Howley, P. M., eds., *Fields virology*, pp. 2327–2359. Lippincott Williams and Wilkins, Philadelphia, PA, 4 edition, 2001.
- [325] Nachury, M. V. and Weis, K. The direction of transport through the nuclear pore can be inverted. *Proc. Natl. Acad. Sci. U.S.A.*, 96(17):9622–9627, Aug 1999.
- [326] Naeger, L. K., Cater, J., and Pintel, D. J. The small nonstructural protein (NS2) of the parvovirus minute virus of mice is required for efficient DNA replication and infectious virus production in a cell-type-specific manner. *J. Virol.*, 64(12):6166–6175, Dec 1990.
- [327] Naeger, L. K., Salome, N., and Pintel, D. J. NS2 is required for efficient translation of viral mRNA in minute virus of mice-infected murine cells. *J. Virol.*, 67(2):1034–1043, Feb 1993.
- [328] Naeger, L. K., Schoborg, R. V., Zhao, Q., Tullis, G. E., and Pintel, D. J. Nonsense mutations inhibit splicing of MVM RNA in *cis* when they interrupt the reading frame of either exon of the final spliced product. *Genes Dev.*, 6(6):1107–1119, Jun 1992.
- [329] Nam, H. J., Gurda-Whitaker, B., Gan, W. Y., Ilaria, S., McKenna, R., Mehta, P., Alvarez, R. A., and Agbandje-McKenna, M. Identification of the sialic acid structures recognized by minute virus of mice and the role of binding affinity in virulence adaptation. *J. Biol. Chem.*, 281(35):25670–25677, Sep 2006.

Bibliography

- [330] Nüesch, J. P. Regulation of non-structural protein functions by differential synthesis, modification and trafficking. In Kerr, J. R., Bloom, M. E., Cotmore, S. F., Linden, R. M., and Parrish, C. R., eds., *Parvoviruses*, pp. 275–289. Hodder Arnold, London, UK, 2006.
- [331] Nüesch, J. P. and Rommelaere, J. NS1 interaction with CKIIα: novel protein complex mediating parvovirus-induced cytotoxicity. *J. Virol.*, 80(10):4729–4739, May 2006.
- [332] Nüesch, J. P., Bar, S., Lachmann, S., and Rommelaere, J. Ezrin-radixin-moesin family proteins are involved in parvovirus replication and spreading. *J. Virol.*, 83(11):5854–5863, Jun 2009.
- [333] Nüesch, J. P., Lachmann, S., and Rommelaere, J. Selective alterations of the host cell architecture upon infection with parvovirus minute virus of mice. *Virology*, 331(1):159–174, Jan 2005.
- [334] Nigg, E. A. Nucleocytoplasmic transport: signals, mechanisms and regulation. *Nature*, 386(6627):779–787, Apr 1997.
- [335] Ni, J., Qiao, C., Han, X., Han, T., Kang, W., Zi, Z., Cao, Z., Zhai, X., and Cai, X. Identification and genomic characterization of a novel porcine parvovirus (PPV6) in china. *Virol. J.*, 11(1):203, Dec 2014.
- [336] Ni, T. H., McDonald, W. F., Zolotukhin, I., Melendy, T., Waga, S., Stillman, B., and Muzyczka, N. Cellular proteins required for adeno-associated virus DNA replication in the absence of adenovirus coinfection. *J. Virol.*, 72(4):2777–2787, Apr 1998.
- [337] Nonnenmacher, M. and Weber, T. Adeno-associated virus 2 infection requires endocytosis through the CLIC/GEEC pathway. *Cell Host Microbe*, 10(6):563–576, Dec 2011.
- [338] Nuesch, J. P. and Tattersall, P. Nuclear targeting of the parvoviral replicator molecule NS1: evidence for self-association prior to nuclear transport. *Virology*, 196(2):637–651, Oct 1993.
- [339] Nuesch, J. P., Christensen, J., and Rommelaere, J. Initiation of minute virus of mice DNA replication is regulated at the level of origin unwinding by atypical protein kinase C phosphorylation of NS1. *J. Virol.*, 75(13):5730–5739, Jul 2001.
- [340] Nuesch, J. P., Cotmore, S. F., and Tattersall, P. Sequence motifs in the replicator protein of parvovirus MVM essential for nicking and covalent attachment to the viral origin: identification of the linking tyrosine. *Virology*, 209(1):122–135, May 1995.
- [341] Ohkuma, S. and Poole, B. Fluorescence probe measurement of the intralysosomal pH in living cells and the perturbation of pH by various agents. *Proc. Natl. Acad. Sci. U.S.A.*, 75(7):3327–3331, Jul 1978.
- [342] Ohshima, T., Nakajima, T., Oishi, T., Imamoto, N., Yoneda, Y., Fukamizu, A., and Yagami, K. i. CRM1 mediates nuclear export of nonstructural protein 2 from parvovirus minute virus of mice. *Biochem. Biophys. Res. Commun.*, 264(1):144–150, Oct 1999.
- [343] Ojala, P. M., Sodeik, B., Ebersold, M. W., Kuttay, U., and Helenius, A. Herpes simplex virus type 1 entry into host cells: reconstitution of capsid binding and uncoating at the nuclear pore complex *in vitro*. *Mol. Cell. Biol.*, 20(13):4922–4931, Jul 2000.
- [344] Olofsson, S. and Bergstrom, T. Glycoconjugate glycans as viral receptors. *Ann. Med.*, 37(3):154–172, 2005.
- [345] Oppenheim, A., Sandalon, Z., Peleg, A., Shaul, O., Nicolis, S., and Ottolenghi, S. A *cis*-acting DNA signal for encapsidation of simian virus 40. *J. Virol.*, 66(9):5320–5328, Sep 1992.
- [346] Orozco, B. M., Miller, A. B., Settlage, S. B., and Hanley-Bowdoin, L. Functional domains of a geminivirus replication protein. *J. Biol. Chem.*, 272(15):9840–9846, Apr 1997.
- [347] Ozawa, K., Ayub, J., Hao, Y. S., Kurtzman, G., Shimada, T., and Young, N. Novel transcription map for the B19 (human) pathogenic parvovirus. *J. Virol.*, 61(8):2395–2406, Aug 1987.
- [348] Padgett, R. A., Grabowski, P. J., Konarska, M. M., Seiler, S., and Sharp, P. A. Splicing of messenger RNA precursors. *Annu. Rev. Biochem.*, 55:1119–1150, 1986.
- [349] Padron, E., Bowman, V., Kaludov, N., Govindasamy, L., Levy, H., Nick, P., McKenna, R., Muzyczka, N., Chiorini, J. A., Baker, T. S., and Agbandje-McKenna, M. Structure of adeno-associated virus type 4. *J. Virol.*, 79(8):5047–5058, Apr 2005.
- [350] Page, R. K., Fletcher, O. J., Rowland, G. N., Gaudry, D., and Villegas, P. Malabsorption syndrome in broiler chickens. *Avian Dis.*, 26(3):618–624, 1982.

Bibliography

- [351] Palermo, L. M., Hueffer, K., and Parrish, C. R. Residues in the apical domain of the feline and canine transferrin receptors control host-specific binding and cell infection of canine and feline parvoviruses. *J. Virol.*, 77(16):8915–8923, Aug 2003.
- [352] Panning, M., Kobbe, R., Vollbach, S., Drexler, J. F., Adjei, S., Adjei, O., Drosten, C., May, J., and Eis-Hubinger, A. M. Novel human parvovirus 4 genotype 3 in infants, Ghana. *Emerging Infect. Dis.*, 16(7):1143–1146, Jul 2010.
- [353] Panté, N. and Kann, M. Nuclear pore complex is able to transport macromolecules with diameters of about 39 nm. *Mol. Biol. Cell*, 13(2):425–434, Feb 2002.
- [354] Paradiso, P. R. Infectious process of the parvovirus H-1: correlation of protein content, particle density, and viral infectivity. *J. Virol.*, 39(3):800–807, Sep 1981.
- [355] Paradiso, P. R., Williams, K. R., and Costantino, R. L. Mapping of the amino terminus of the H-1 parvovirus major capsid protein. *J. Virol.*, 52(1):77–81, Oct 1984.
- [356] Park, B., Kim, Y., Shin, J., Lee, S., Cho, K., Fruh, K., Lee, S., and Ahn, K. Human cytomegalovirus inhibits tapasin-dependent peptide loading and optimization of the MHC class I peptide cargo for immune evasion. *Immunity*, 20(1):71–85, Jan 2004.
- [357] Parker, J. S. and Parrish, C. R. Cellular uptake and infection by canine parvovirus involves rapid dynamin-regulated clathrin-mediated endocytosis, followed by slower intracellular trafficking. *J. Virol.*, 74(4):1919–1930, Feb 2000.
- [358] Parker, J. S., Murphy, W. J., Wang, D., O'Brien, S. J., and Parrish, C. R. Canine and feline parvoviruses can use human or feline transferrin receptors to bind, enter, and infect cells. *J. Virol.*, 75(8):3896–3902, Apr 2001.
- [359] Park, G. S., Best, S. M., and Bloom, M. E. Two mink parvoviruses use different cellular receptors for entry into CRFK cells. *Virology*, 340(1):1–9, Sep 2005.
- [360] Parrish, C. R. and Carmichael, L. E. Characterization and recombination mapping of an antigenic and host range mutation of canine parvovirus. *Virology*, 148(1):121–132, Jan 1986.
- [361] Parrish, C. R., Aquadro, C. F., and Carmichael, L. E. Canine host range and a specific epitope map along with variant sequences in the capsid protein gene of canine parvovirus and related feline, mink, and raccoon parvoviruses. *Virology*, 166(2):293–307, Oct 1988.
- [362] Parrish, C. R., Aquadro, C. F., Strassheim, M. L., Evermann, J. F., Sgro, J. Y., and Mohammed, H. O. Rapid antigenic-type replacement and DNA sequence evolution of canine parvovirus. *J. Virol.*, 65(12):6544–6552, Dec 1991.
- [363] Pass, D. A., Robertson, M. D., and Wilcox, G. E. Runtling syndrome in broiler chickens in Australia. *Vet. Rec.*, 110(16):386–387, Apr 1982.
- [364] Pemberton, L. F. and Paschal, B. M. Mechanisms of receptor-mediated nuclear import and nuclear export. *Traffic*, 6(3):187–198, Mar 2005.
- [365] Perez, R., Castellanos, M., Rodriguez-Huete, A., and Mateu, M. G. Molecular determinants of self-association and rearrangement of a trimeric intermediate during the assembly of a parvovirus capsid. *J. Mol. Biol.*, 413(1):32–40, Oct 2011.
- [366] Perros, M., Deleu, L., Vanacker, J. M., Kherrouche, Z., Spruyt, N., Faisst, S., and Rommeelaere, J. Upstream CREs participate in the basal activity of minute virus of mice promoter P4 and in its stimulation in *ras*-transformed cells. *J. Virol.*, 69(9):5506–5515, Sep 1995.
- [367] Pettersen, E. F., Goddard, T. D., Huang, C. C., Couch, G. S., Greenblatt, D. M., Meng, E. C., and Ferrin, T. E. UCSF Chimera—a visualization system for exploratory research and analysis. *J. Comput. Chem.*, 25(13):1605–1612, Oct 2004.
- [368] Pintel, D., Dadachanji, D., Astell, C. R., and Ward, D. C. The genome of minute virus of mice, an autonomous parvovirus, encodes two overlapping transcription units. *Nucleic Acids Res.*, 11(4):1019–1038, Feb 1983.
- [369] Pitluk, Z. W. and Ward, D. C. Unusual Sp1-GC box interaction in a parvovirus promoter. *J. Virol.*, 65(12):6661–6670, Dec 1991.
- [370] Poole, B. and Ohkuma, S. Effect of weak bases on the intralysosomal pH in mouse peritoneal macrophages. *J. Cell Biol.*, 90(3):665–669, Sep 1981.
- [371] Praefcke, G. J. and McMahon, H. T. The dynamin superfamily: universal membrane tubulation and fission molecules? *Nat. Rev. Mol. Cell Biol.*, 5(2):133–147, Feb 2004.
- [372] Prasad, K. M. and Trempe, J. P. The adenovirus-associated virus Rep78 protein is covalently linked to viral DNA in a preformed virion. *Virology*, 214(2):360–370, Dec 1995.

- [373] Prevelige, P. E. New approaches for antiviral targeting of HIV assembly. *J. Mol. Biol.*, 410(4):634–640, Jul 2011.
- [374] Previsani, N., Fontana, S., Hirt, B., and Beard, P. Growth of the parvovirus minute virus of mice MVMp3 in EL4 lymphocytes is restricted after cell entry and before viral DNA amplification: cell-specific differences in virus uncoating *in vitro*. *J. Virol.*, 71(10):7769–7780, Oct 1997.
- [375] Pujol, A., Deleu, L., Nuesch, J. P., Cziepluch, C., Jauniaux, J. C., and Rommelaere, J. Inhibition of parvovirus minute virus of mice replication by a peptide involved in the oligomerization of nonstructural protein NS1. *J. Virol.*, 71(10):7393–7403, Oct 1997.
- [376] Qing, K., Mah, C., Hansen, J., Zhou, S., Dwarki, V., and Srivastava, A. Human fibroblast growth factor receptor 1 is a co-receptor for infection by adeno-associated virus 2. *Nat. Med.*, 5(1):71–77, Jan 1999.
- [377] Qiu, J., Cheng, F., Burger, L. R., and Pintel, D. The transcription profile of Aleutian mink disease virus in CRFK cells is generated by alternative processing of pre-mRNAs produced from a single promoter. *J. Virol.*, 80(2):654–662, Jan 2006.
- [378] Qiu, J., Cheng, F., Johnson, F. B., and Pintel, D. The transcription profile of the bocavirus bovine parvovirus is unlike those of previously characterized parvoviruses. *J. Virol.*, 81(21):12080–12085, Nov 2007.
- [379] Qui, J., Yoto, Y., Tullis, G., and Pintel, D. J. Parvovirus RNA processing strategies. In Kerr, J. R., Bloom, M. E., Cotmore, S. F., Linden, R. M., and Parish, C. R., eds., *Parvoviruses*, pp. 253–273. Hodder Arnold, London, UK, 2006.
- [380] Ramirez, J. C., Fairen, A., and Almendral, J. M. Parvovirus minute virus of mice strain i multiplication and pathogenesis in the newborn mouse brain are restricted to proliferative areas and to migratory cerebellar young neurons. *J. Virol.*, 70(11):8109–8116, Nov 1996.
- [381] Reguera, J., Carreira, A., Riolobos, L., Almendral, J. M., and Mateu, M. G. Role of interfacial amino acid residues in assembly, stability, and conformation of a spherical virus capsid. *Proc. Natl. Acad. Sci. U.S.A.*, 101(9):2724–2729, Mar 2004.
- [382] Rhode, S. L. *trans*-Activation of parvovirus P38 promoter by the 76K noncapsid protein. *J. Virol.*, 55(3): 886–889, Sep 1985.
- [383] Richards, R., Linser, P., and Armentrout, R. W. Kinetics of assembly of a parvovirus, minute virus of mice, in synchronized rat brain cells. *J. Virol.*, 22(3):778–793, Jun 1977.
- [384] Riolobos, L., Reguera, J., Mateu, M. G., and Almendral, J. M. Nuclear transport of trimeric assembly intermediates exerts a morphogenetic control on the icosahedral parvovirus capsid. *J. Mol. Biol.*, 357(3): 1026–1038, Mar 2006.
- [385] Robbins, J., Dilworth, S. M., Laskey, R. A., and Dingwall, C. Two interdependent basic domains in nucleoplasmin nuclear targeting sequence: identification of a class of bipartite nuclear targeting sequence. *Cell*, 64(3):615–623, Feb 1991.
- [386] Ron, D. and Tal, J. Spontaneous curing of a minute virus of mice carrier state by selection of cells with an intracellular block of viral replication. *J. Virol.*, 58(1): 26–30, Apr 1986.
- [387] Ros, C. and Kempf, C. The ubiquitin-proteasome machinery is essential for nuclear translocation of incoming minute virus of mice. *Virology*, 324(2):350–360, Jul 2004.
- [388] Ros, C., Burckhardt, C. J., and Kempf, C. Cytoplasmic trafficking of minute virus of mice: low-pH requirement, routing to late endosomes, and proteasome interaction. *J. Virol.*, 76(24):12634–12645, Dec 2002.
- [389] Rose, J. A., Berns, K. I., Hoggan, M. D., and Koczot, F. J. Evidence for a single-stranded adenovirus-associated virus genome: formation of a DNA density hybrid on release of viral DNA. *Proc. Natl. Acad. Sci. U.S.A.*, 64(3):863–869, Nov 1969.
- [390] Rossmann, M. G. and Johnson, J. E. Icosahedral RNA virus structure. *Annu. Rev. Biochem.*, 58: 533–573, 1989.
- [391] Rubio, M. P., Lopez-Bueno, A., and Almendral, J. M. Virulent variants emerging in mice infected with the apathogenic prototype strain of the parvovirus minute virus of mice exhibit a capsid with low avidity for a primary receptor. *J. Virol.*, 79(17):11280–11290, Sep 2005.
- [392] Ruffing, M., Zentgraf, H., and Kleinschmidt, J. A. Assembly of viruslike particles by recombinant structural proteins of adeno-associated virus type 2 in insect cells. *J. Virol.*, 66(12):6922–6930, Dec 1992.
- [393] Ryan, K. J. and Wente, S. R. The nuclear pore complex: a protein machine bridging the nucleus and

Bibliography

- cytoplasm. *Curr. Opin. Cell Biol.*, 12(3):361–371, Jun 2000.
- [394] **Sahli, R., McMaster, G. K., and Hirt, B.** DNA sequence comparison between two tissue-specific variants of the autonomous parvovirus, minute virus of mice. *Nucleic Acids Res.*, 13(10):3617–3633, May 1985.
- [395] **Saif, Y. M., Barnes, H. J., Glisson, J. R., Fadly, A. M., McDougald, L. R., and Swayne, D. E.** *Diseases of Poultry 11th edn.* Wiley-Blackwell, Hoboken, NJ, 2003. pp 1171-1180.
- [396] **Saknimit, M., Inatsuki, I., Sugiyama, Y., and Yagami, K.** Virucidal efficacy of physico-chemical treatments against coronaviruses and parvoviruses of laboratory animals. *Jikken Dobutsu*, 37(3):341–345, Jul 1988.
- [397] **Salzman, L. A. and Jori, L. A.** Characterization of the Kilham rat virus. *J. Virol.*, 5(2):114–122, Feb 1970.
- [398] **Samulski, R. J., Chang, L. S., and Shenk, T.** Helper-free stocks of recombinant adeno-associated viruses: normal integration does not require viral gene expression. *J. Virol.*, 63(9):3822–3828, Sep 1989.
- [399] **Samulski, R. J., Zhu, X., Xiao, X., Brook, J. D., Housman, D. E., Epstein, N., and Hunter, L. A.** Targeted integration of adeno-associated virus (AAV) into human chromosome 19. *EMBO J.*, 10(12):3941–3950, Dec 1991.
- [400] **Sauerbrei, A. and Wutzler, P.** Testing thermal resistance of viruses. *Arch. Virol.*, 154(1):115–119, 2009.
- [401] **Schmidt, M. and Chiorini, J. A.** Gangliosides are essential for bovine adeno-associated virus entry. *J. Virol.*, 80(11):5516–5522, Jun 2006.
- [402] **Schmitt, M. W., Matsumoto, Y., and Loeb, L. A.** High fidelity and lesion bypass capability of human DNA polymerase δ. *Biochimie*, 91(9):1163–1172, Sep 2009.
- [403] **Schoborg, R. V. and Pintel, D. J.** Accumulation of MVM gene products is differentially regulated by transcription initiation, RNA processing and protein stability. *Virology*, 181(1):22–34, Mar 1991.
- [404] **Schwartz, D., Green, B., Carmichael, L. E., and Parrish, C. R.** The canine minute virus (minute virus of canines) is a distinct parvovirus that is most similar to bovine parvovirus. *Virology*, 302(2):219–223, Oct 2002.
- [405] **Schwarz, T. F., Serke, S., Von Brunn, A., Hottentrager, B., Huhn, D., Deinhardt, F., and Roggendorf, M.** Heat stability of parvovirus B19: kinetics of inactivation. *Zentralbl. Bakteriol.*, 277(2):219–223, Jul 1992.
- [406] **Segovia, J. C., Bueren, J. A., and Almendral, J. M.** Myeloid depression follows infection of susceptible newborn mice with the parvovirus minute virus of mice (strain i). *J. Virol.*, 69(5):3229–3232, May 1995.
- [407] **Segovia, J. C., Gallego, J. M., Bueren, J. A., and Almendral, J. M.** Severe leukopenia and dysregulated erythropoiesis in SCID mice persistently infected with the parvovirus minute virus of mice. *J. Virol.*, 73(3):1774–1784, Mar 1999.
- [408] **Segovia, J. C., Guenechea, G., Gallego, J. M., Almendral, J. M., and Bueren, J. A.** Parvovirus infection suppresses long-term repopulating hematopoietic stem cells. *J. Virol.*, 77(15):8495–8503, Aug 2003.
- [409] **Seiler, M. P., Miller, A. D., Zabner, J., and Halbert, C. L.** Adeno-associated virus types 5 and 6 use distinct receptors for cell entry. *Hum. Gene Ther.*, 17(1):10–19, Jan 2006.
- [410] **Seisenberger, G., Ried, M. U., Endress, T., Buning, H., Hallek, M., and Brauchle, C.** Real-time single-molecule imaging of the infection pathway of an adeno-associated virus. *Science*, 294(5548):1929–1932, Nov 2001.
- [411] **Seksek, O., Biwersi, J., and Verkman, A. S.** Translational diffusion of macromolecule-sized solutes in cytoplasm and nucleus. *J. Cell Biol.*, 138(1):131–142, Jul 1997.
- [412] **Shackelton, L. A. and Holmes, E. C.** Phylogenetic evidence for the rapid evolution of human B19 erythrovirus. *J. Virol.*, 80(7):3666–3669, Apr 2006.
- [413] **Shackelton, L. A., Parrish, C. R., Truyen, U., and Holmes, E. C.** High rate of viral evolution associated with the emergence of carnivore parvovirus. *Proc. Natl. Acad. Sci. U.S.A.*, 102(2):379–384, Jan 2005.
- [414] **Sharp, C. P., Lail, A., Donfield, S., Gomperts, E. D., and Simmonds, P.** Virologic and clinical features of primary infection with human parvovirus 4 in subjects with hemophilia: frequent transmission by virally inactivated clotting factor concentrates. *Transfusion*, 52(7):1482–1489, Jul 2012.

- [415] Sharp, C. P., LeBreton, M., Kantola, K., Nana, A., Diffo, J. I. e. D., Djoko, C. F., Tamoufe, U., Kiyang, J. A., Babila, T. G., Ngole, E. M., Pybus, O. G., Delwart, E., Delaporte, E., Peeters, M., et al. Widespread infection with homologues of human parvoviruses B19, PARV4, and human bocavirus of chimpanzees and gorillas in the wild. *J. Virol.*, 84(19):10289–10296, Oct 2010.
- [416] Shein, H. M. and Enders, J. F. Multiplication and cytopathogenicity of Simian vacuolating virus 40 in cultures of human tissues. *Proc. Soc. Exp. Biol. Med.*, 109:495–500, Mar 1962.
- [417] Shen, S., Bryant, K. D., Brown, S. M., Randell, S. H., and Asokan, A. Terminal N-linked galactose is the primary receptor for adeno-associated virus 9. *J. Biol. Chem.*, 286(15):13532–13540, Apr 2011.
- [418] Simmons, R., Sharp, C., Levine, J., Bowness, P., Simmonds, P., Cox, A., and Klenerman, P. Evolution of CD8+ T cell responses after acute PARV4 infection. *J. Virol.*, 87(6):3087–3096, Mar 2013.
- [419] Simmons, R., Sharp, C., McClure, C. P., Rohrbach, J., Kovari, H., Frangou, E., Simmonds, P., Irving, W., Rauch, A., Bowness, P., Klenerman, P., Battegay, M., Bernasconi, E., Boni, J., Bucher, H. C., Burgisser, P., et al. Parvovirus 4 infection and clinical outcome in high-risk populations. *J. Infect. Dis.*, 205(12):1816–1820, Jun 2012.
- [420] Simpson, A. A., Chandrasekar, V., Hebert, B., Sullivan, G. M., Rossmann, M. G., and Parrish, C. R. Host range and variability of calcium binding by surface loops in the capsids of canine and feline parvoviruses. *J. Mol. Biol.*, 300(3):597–610, Jul 2000.
- [421] Simpson, A. A., Chipman, P. R., Baker, T. S., Tijssen, P., and Rossmann, M. G. The structure of an insect parvovirus (*Galleria mellonella* densovirus) at 3.7 Å resolution. *Structure*, 6(11):1355–1367, Nov 1998.
- [422] Slepchenko, B. M., Semenova, I., Zaliapin, I., and Rodionov, V. Switching of membrane organelles between cytoskeletal transport systems is determined by regulation of the microtubule-based transport. *J. Cell Biol.*, 179(4):635–641, Nov 2007.
- [423] Smith, A. L. and Tignor, G. H. Host cell receptors for two strains of Sindbis virus. *Arch. Virol.*, 66(1):11–26, 1980.
- [424] Smith, C. W., Patton, J. G., and Nadal-Ginard, B. Alternative splicing in the control of gene expression. *Annu. Rev. Genet.*, 23:527–577, 1989.
- [425] Snyder, R. O., Im, D. S., and Muzyczka, N. Evidence for covalent attachment of the adeno-associated virus (AAV) rep protein to the ends of the AAV genome. *J. Virol.*, 64(12):6204–6213, Dec 1990.
- [426] Sonntag, F., Bleker, S., Leuchs, B., Fischer, R., and Kleinschmidt, J. A. Adeno-associated virus type 2 capsids with externalized VP1/VP2 trafficking domains are generated prior to passage through the cytoplasm and are maintained until uncoating occurs in the nucleus. *J. Virol.*, 80(22):11040–11054, Nov 2006.
- [427] Spalholz, B. A. and Tattersall, P. Interaction of minute virus of mice with differentiated cells: strain-dependent target cell specificity is mediated by intracellular factors. *J. Virol.*, 46(3):937–943, Jun 1983.
- [428] Spalholz, B. A., Bratton, J., Ward, D. C., and Tattersall, P. *Tumor Viruses and Differentiation*. Academic Press, New York, NY, 1982.
- [429] Stahnke, S., Lux, K., Uhrig, S., Kreppel, F., Hosel, M., Coutelle, O., Ogris, M., Hallek, M., and Buning, H. Intrinsic phospholipase A₂ activity of adeno-associated virus is involved in endosomal escape of incoming particles. *Virology*, 409(1):77–83, Jan 2011.
- [430] Stamnes, M. Regulating the actin cytoskeleton during vesicular transport. *Curr. Opin. Cell Biol.*, 14(4):428–433, Aug 2002.
- [431] Stoffler, D., Fahrenkrog, B., and Aebi, U. The nuclear pore complex: from molecular architecture to functional dynamics. *Curr. Opin. Cell Biol.*, 11(3):391–401, Jun 1999.
- [432] Streck, A. F., Bonatto, S. L., Homeier, T., Souza, C. K., Goncalves, K. R., Gava, D., Canal, C. W., and Truyen, U. High rate of viral evolution in the capsid protein of porcine parvovirus. *J. Gen. Virol.*, 92(Pt 11):2628–2636, Nov 2011.
- [433] Su, H. L., Liao, C. L., and Lin, Y. L. Japanese encephalitis virus infection initiates endoplasmic reticulum stress and an unfolded protein response. *J. Virol.*, 76(9):4162–4171, May 2002.
- [434] Siikkanen, S., Aaltonen, T., Nevalainen, M., Valilehto, O., Lindholm, L., Vuento, M., and Vihinen-Ranta, M. Exploitation of microtubule cytoskeleton and dynein during parvoviral traffic toward the nucleus. *J. Virol.*, 77(19):10270–10279, Oct 2003.

Bibliography

- [435] Suikkanen, S., Antila, M., Jaatinen, A., Vihinen-Ranta, M., and Vuento, M. Release of canine parvovirus from endocytic vesicles. *Virology*, 316(2):267–280, Nov 2003.
- [436] Suikkanen, S., Saajarvi, K., Hirsimaki, J., Valilehto, O., Reunanan, H., Vihinen-Ranta, M., and Vuento, M. Role of recycling endosomes and lysosomes in dynein-dependent entry of canine parvovirus. *J. Virol.*, 76(9):4401–4411, May 2002.
- [437] Summerford, C. and Samulski, R. J. Membrane-associated heparan sulfate proteoglycan is a receptor for adeno-associated virus type 2 virions. *J. Virol.*, 72(2):1438–1445, Feb 1998.
- [438] Summerford, C., Bartlett, J. S., and Samulski, R. J. $\alpha_V\beta_5$ -integrin: a co-receptor for adeno-associated virus type 2 infection. *Nat. Med.*, 5(1):78–82, Jan 1999.
- [439] Tardif, K. D., Mori, K., Kaufman, R. J., and Siddiqui, A. Hepatitis C virus suppresses the IRE1-XBP1 pathway of the unfolded protein response. *J. Biol. Chem.*, 279(17):17158–17164, Apr 2004.
- [440] Tattersall, P. Replication of the parvovirus MVM. I. Dependence of virus multiplication and plaque formation on cell growth. *J. Virol.*, 10(4):586–590, Oct 1972.
- [441] Tattersall, P. The evolution of parvovirus taxonomy. In Kerr, J. R., Bloom, M. E., Cotmore, S. F., Linden, R. M., and Parrish, C. R., eds., *Parvoviruses*, p. 9. Hodder Arnold, London, UK, 2006.
- [442] Tattersall, P. and Bratton, J. Reciprocal productive and restrictive virus-cell interactions of immunosuppressive and prototype strains of minute virus of mice. *J. Virol.*, 46(3):944–955, Jun 1983.
- [443] Tattersall, P. and Cotmore, S. F. The nature of parvoviruses. In Pattison, J. R., ed., *Parvoviruses and Human Diseases*, pp. 5–41. CRC Press, Inc., Boca Raton, FL, 1988.
- [444] Tattersall, P. and Gardiner, E. M. Autonomous parvovirus-host-cell interactions. In Tijssen, P., ed., *Handbook of parvoviruses*, vol. 1, pp. 111–121. CRC Press, Inc., Boca Raton, FL, 1990.
- [445] Tattersall, P. and Ward, D. C. Rolling hairpin model for replication of parvovirus and linear chromosomal DNA. *Nature*, 263(5573):106–109, Sep 1976.
- [446] Tattersall, P. and Ward, D. C. The parvoviruses – an introduction. In Ward, D. C. and Tattersall, P., eds., *Replication of mammalian parvoviruses*, pp. 3–12. Cold Spring Harbor Laboratory Press, Cold Spring Harbor, NY, 1978.
- [447] Tattersall, P., Cawte, P. J., Shatkin, A. J., and Ward, D. C. Three structural polypeptides coded for by minute virus of mice, a parvovirus. *J. Virol.*, 20(1):273–289, Oct 1976.
- [448] Tattersall, P., Shatkin, A. J., and Ward, D. C. Sequence homology between the structural polypeptides of minute virus of mice. *J. Mol. Biol.*, 111(4):375–394, Apr 1977.
- [449] Tennant, R. W., Layman, K. R., and Hand, R. E. Effect of cell physiological state on infection by rat virus. *J. Virol.*, 4(6):872–878, Dec 1969.
- [450] Thacker, T. C. and Johnson, F. B. Binding of bovine parvovirus to erythrocyte membrane sialylglycoproteins. *J. Gen. Virol.*, 79 (Pt 9):2163–2169, Sep 1998.
- [451] Tijssen, P. *Handbook of parvoviruses*, vol. 1. CRC Press, Inc., Boca Raton, FL, 1990.
- [452] Tijssen, P. Molecular and structural basis of the evolution of parvovirus tropism. *Acta Vet. Hung.*, 47(3):379–394, 1999.
- [453] Tijssen, P., Szelei, J., and Zádori, Z. Phospholipase A₂ domains in structural proteins of parvoviruses. In Kerr, J. R., Bloom, M. E., Cotmore, S. F., Linden, R. M., and Parrish, C. R., eds., *Parvoviruses*, pp. 95–105. Hodder Arnold, London, UK, 2006.
- [454] Trampel, D. W., Kinden, D. A., Solorzano, R. F., and Stogsdill, P. L. Parvovirus-like enteropathy in Missouri turkeys. *Avian Dis.*, 27(1):49–54, 1983.
- [455] Tresnan, D. B., Southard, L., Weichert, W., Sgro, J. Y., and Parrish, C. R. Analysis of the cell and erythrocyte binding activities of the dimple and canyon regions of the canine parvovirus capsid. *Virology*, 211(1):123–132, Aug 1995.
- [456] Tryoen, U., Agbandje, M., and Parrish, C. R. Characterization of the feline host range and a specific epitope of feline panleukopenia virus. *Virology*, 200(2):494–503, May 1994.
- [457] Tsao, J., Chapman, M. S., Agbandje, M., Keller, W., Smith, K., Wu, H., Luo, M., Smith, T. J., Rossmann, M. G., and Compans, R. W. The three-dimensional structure of canine parvovirus and its functional implications. *Science*, 251(5000):1456–1464, Mar 1991.

Bibliography

- [458] Tsao, J., Chapman, M. S., Wu, H., Agbandje, M., Keller, W., and Rossmann, M. G. Structure determination of monoclinic canine parvovirus. *Acta Crystallogr., B*, 48 (Pt 1):75–88, Feb 1992.
- [459] Tse, H., Tsoi, H. W., Teng, J. L., Chen, X. C., Liu, H., Zhou, B., Zheng, B. J., Woo, P. C., Lau, S. K., and Yuen, K. Y. Discovery and genomic characterization of a novel ovine partetravirus and a new genotype of bovine partetravirus. *PLoS ONE*, 6 (9):e25619, 2011.
- [460] Tullis, G. E., Burger, L. R., and Pintel, D. J. The trypsin-sensitive RVER domain in the capsid proteins of minute virus of mice is required for efficient cell binding and viral infection but not for proteolytic processing *in vivo*. *Virology*, 191(2):846–857, Dec 1992.
- [461] Tullis, G. E., Burger, L. R., and Pintel, D. J. The minor capsid protein VP1 of the autonomous parvovirus minute virus of mice is dispensable for encapsidation of progeny single-stranded DNA but is required for infectivity. *J. Virol.*, 67(1):131–141, Jan 1993.
- [462] Valle, N., Riobos, L., and Almendral, J. M. Synthesis, post-translational modification and trafficking of the parvovirus structural polypeptides. In Kerr, J. R., Bloom, M. E., Cotmore, S. F., Linden, R. M., and Parrish, C. R., eds., *Parvoviruses*, pp. 291–304. Hodder Arnold, London, UK, 2006.
- [463] Vandenberghe, L. H., Xiao, R., Lock, M., Lin, J., Korn, M., and Wilson, J. M. Efficient serotype-dependent release of functional vector into the culture medium during adeno-associated virus manufacturing. *Hum. Gene Ther.*, 21(10):1251–1257, Oct 2010.
- [464] van Leengoed, L. A., Vos, J., Gruys, E., Rondhuis, P., and Brand, A. Porcine Parvovirus infection: review and diagnosis in a sow herd with reproductive failure. *Vet Q*, 5(3):131–141, Jul 1983.
- [465] Varki, N. M. and Varki, A. Diversity in cell surface sialic acid presentations: implications for biology and disease. *Lab. Invest.*, 87(9):851–857, Sep 2007.
- [466] Vasudevacharya, J. and Compans, R. W. The NS and capsid genes determine the host range of porcine parvovirus. *Virology*, 187(2):515–524, Apr 1992.
- [467] Vicente, D., Cilla, G., Montes, M., Perez-Yarza, E. G., and Perez-Trallero, E. Human bocavirus, a respiratory and enteric virus. *Emerging Infect. Dis.*, 13 (4):636–637, Apr 2007.
- [468] Vihinen-Ranta, M., Kakkola, L., Kalela, A., Vilja, P., and Vuento, M. Characterization of a nuclear localization signal of canine parvovirus capsid proteins. *Eur. J. Biochem.*, 250(2):389–394, Dec 1997.
- [469] Vihinen-Ranta, M., Kalela, A., Makinen, P., Kakkola, L., Marjomaki, V., and Vuento, M. Intracellular route of canine parvovirus entry. *J. Virol.*, 72(1):802–806, Jan 1998.
- [470] Vihinen-Ranta, M., Suikkanen, S., and Parrish, C. R. Pathways of cell infection by parvoviruses and adeno-associated viruses. *J. Virol.*, 78(13):6709–6714, Jul 2004.
- [471] Vihinen-Ranta, M., Wang, D., Weichert, W. S., and Parrish, C. R. The VP1 N-terminal sequence of canine parvovirus affects nuclear transport of capsids and efficient cell infection. *J. Virol.*, 76(4):1884–1891, Feb 2002.
- [472] Vihinen-Ranta, M., Yuan, W., and Parrish, C. R. Cytoplasmic trafficking of the canine parvovirus capsid and its role in infection and nuclear transport. *J. Virol.*, 74(10):4853–4859, May 2000.
- [473] Walker, S. L., Wonderling, R. S., and Owens, R. A. Mutational analysis of the adeno-associated virus type 2 Rep68 protein helicase motifs. *J. Virol.*, 71(9):6996–7004, Sep 1997.
- [474] Walters, R. W., Yi, S. M., Keshavjee, S., Brown, K. E., Welsh, M. J., Chiorini, J. A., and Zabner, J. Binding of adeno-associated virus type 5 to 2,3-linked sialic acid is required for gene transfer. *J. Biol. Chem.*, 276(23):20610–20616, Jun 2001.
- [475] Wang, X. S., Ponnazhagan, S., and Srivastava, A. Rescue and replication of adeno-associated virus type 2 as well as vector DNA sequences from recombinant plasmids containing deletions in the viral inverted terminal repeats: selective encapsidation of viral genomes in progeny virions. *J. Virol.*, 70(3):1668–1677, Mar 1996.
- [476] Wang, X. S., Qing, K., Ponnazhagan, S., and Srivastava, A. Adeno-associated virus type 2 DNA replication *in vivo*: mutation analyses of the D sequence in viral inverted terminal repeats. *J. Virol.*, 71 (4):3077–3082, Apr 1997.
- [477] Ward, D. C. and Tattersall, P. Minute virus of mice. In Foster, H. L., Small, J. D., and Fox, J. G., eds., *The mouse in biomedical research*, vol. 2, pp. 313–334. Academic Press, Inc., New York, NY, 1982.

Bibliography

- [478] Weichert, W. S., Parker, J. S., Wahid, A. T., Chang, S. F., Meier, E., and Parrish, C. R. Assessing for structural variation in the parvovirus capsid and its role in infection. *Virology*, 250(1):106–117, Oct 1998.
- [479] Weigel-Kelley, K. A., Yoder, M. C., and Srivastava, A. Recombinant human parvovirus B19 vectors: erythrocyte P antigen is necessary but not sufficient for successful transduction of human hematopoietic cells. *J. Virol.*, 75(9):4110–4116, May 2001.
- [480] Weigel-Kelley, K. A., Yoder, M. C., and Srivastava, A. $\alpha_5\beta_1$ -integrin as a cellular co-receptor for human parvovirus B19: requirement of functional activation of β_1 -integrin for viral entry. *Blood*, 102(12):3927–3933, Dec 2003.
- [481] Weiner, H. L., Ault, K. A., and Fields, B. N. Interaction of reovirus with cell surface receptors. I. Murine and human lymphocytes have a receptor for the hemagglutinin of reovirus type 3. *J. Immunol.*, 124(5):2143–2148, May 1980.
- [482] Weiner, H. L., Drayna, D., Averill, D. R., and Fields, B. N. Molecular basis of reovirus virulence: role of the S1 gene. *Proc. Natl. Acad. Sci. U.S.A.*, 74(12):5744–5748, Dec 1977.
- [483] Weis, K. Nucleocytoplasmic transport: cargo trafficking across the border. *Curr. Opin. Cell Biol.*, 14(3):328–335, Jun 2002.
- [484] Weiss, N., Stroh-Dege, A., Rommelaere, J., Dinsart, C., and Salome, N. An in-frame deletion in the NS protein-coding sequence of parvovirus H-1PV efficiently stimulates export and infectivity of progeny virions. *J. Virol.*, 86(14):7554–7564, Jul 2012.
- [485] Weller, M. L., Amornphimoltham, P., Schmidt, M., Wilson, P. A., Gutkind, J. S., and Chiorini, J. A. Epidermal growth factor receptor is a co-receptor for adeno-associated virus serotype 6. *Nat. Med.*, 16(6):662–664, Jun 2010.
- [486] Whittaker, G. R., Kann, M., and Helenius, A. Viral entry into the nucleus. *Annu. Rev. Cell Dev. Biol.*, 16:627–651, 2000.
- [487] Wichman, H. A., Badgett, M. R., Scott, L. A., Boulian, C. M., and Bull, J. J. Different trajectories of parallel evolution during viral adaptation. *Science*, 285(5426):422–424, Jul 1999.
- [488] Willwand, K. and Hirt, B. The minute virus of mice capsid specifically recognizes the 3' hairpin structure of the viral replicative-form DNA: mapping of the binding site by hydroxyl radical footprinting. *J. Virol.*, 65(9):4629–4635, Sep 1991.
- [489] Willwand, K. and Hirt, B. The major capsid protein VP2 of minute virus of mice (MVM) can form particles which bind to the 3'-terminal hairpin of MVM replicative-form DNA and package single-stranded viral progeny DNA. *J. Virol.*, 67(9):5660–5663, Sep 1993.
- [490] Willwand, K., Baldauf, A. Q., Deleu, L., Mumtisidu, E., Costello, E., Beard, P., and Rommelaere, J. The minute virus of mice (MVM) nonstructural protein NS1 induces nicking of MVM DNA at a unique site of the right-end telomere in both hairpin and duplex conformations *in vitro*. *J. Gen. Virol.*, 78 (Pt 10):2647–2655, Oct 1997.
- [491] Willwand, K., Moroianu, A., Horlein, R., Stremmel, W., and Rommelaere, J. Specific interaction of the nonstructural protein NS1 of minute virus of mice (MVM) with [ACCA]₂ motifs in the centre of the right-end MVM DNA palindrome induces hairpin-primed viral DNA replication. *J. Gen. Virol.*, 83(Pt 7):1659–1664, Jul 2002.
- [492] Wilson, G. M., Jindal, H. K., Yeung, D. E., Chen, W., and Astell, C. R. Expression of minute virus of mice major nonstructural protein in insect cells: purification and identification of ATPase and helicase activities. *Virology*, 185(1):90–98, Nov 1991.
- [493] Wistuba, A., Kern, A., Weger, S., Grimm, D., and Kleinschmidt, J. A. Subcellular compartmentalization of adeno-associated virus type 2 assembly. *J. Virol.*, 71(2):1341–1352, Feb 1997.
- [494] Wong, S., Momoeda, M., Field, A., Kajigaya, S., and Young, N. S. Formation of empty B19 parvovirus capsids by the truncated minor capsid protein. *J. Virol.*, 68(7):4690–4694, Jul 1994.
- [495] Wu, H. and Rossmann, M. G. The canine parvovirus empty capsid structure. *J. Mol. Biol.*, 233(2):231–244, Sep 1993.
- [496] Wu, H., Keller, W., and Rossmann, M. G. Determination and refinement of the canine parvovirus empty-capsid structure. *Acta Crystallogr. D Biol. Crystallogr.*, 49(Pt 6):572–579, Nov 1993.
- [497] Wu, Z., Asokan, A., Grieger, J. C., Govindasamy, L., Agbandje-McKenna, M., and Samulski, R. J. Single amino acid changes can influence titer, heparin binding, and tissue tropism in different adeno-associated virus serotypes. *J. Virol.*, 80(22):11393–11397, Nov 2006.

- [498] Wu, Z., Miller, E., Agbandje-McKenna, M., and Samulski, R. J. α 2,3 and α 2,6 N-linked sialic acids facilitate efficient binding and transduction by adeno-associated virus types 1 and 6. *J. Virol.*, 80(18): 9093–9103, Sep 2006.
- [499] Xiao, C. T., Gimenez-Lirola, L. G., Jiang, Y. H., Halbur, P. G., and Opriessnig, T. Characterization of a novel porcine parvovirus tentatively designated PPV5. *PLoS ONE*, 8(6):e65312, 2013.
- [500] Xiao, C. T., Halbur, P. G., and Opriessnig, T. Complete Genome Sequence of a Novel Porcine Parvovirus (PPV) Provisionally Designated PPV5. *Genome Announc*, 1(1), Jan 2013.
- [501] Xiao, W., Warrington, K. H., Hearing, P., Hughes, J., and Muzyczka, N. Adenovirus-facilitated nuclear translocation of adeno-associated virus type 2. *J. Virol.*, 76(22):11505–11517, Nov 2002.
- [502] Xie, Q. and Chapman, M. S. Canine parvovirus capsid structure, analyzed at 2.9 Å resolution. *J. Mol. Biol.*, 264(3):497–520, Dec 1996.
- [503] Xie, Q., Bu, W., Bhatia, S., Hare, J., Somasundaram, T., Azzi, A., and Chapman, M. S. The atomic structure of adeno-associated virus (AAV-2), a vector for human gene therapy. *Proc. Natl. Acad. Sci. U.S.A.*, 99(16):10405–10410, Aug 2002.
- [504] Yan, Z., Zak, R., Luxton, G. W., Ritchie, T. C., Bantel-Schaal, U., and Engelhardt, J. F. Ubiquitination of both adeno-associated virus type 2 and 5 capsid proteins affects the transduction efficiency of recombinant vectors. *J. Virol.*, 76(5):2043–2053, Mar 2002.
- [505] Young, P. J., Jensen, K. T., Burger, L. R., Pintel, D. J., and Lorson, C. L. Minute virus of mice NS1 interacts with the SMN protein, and they colocalize in novel nuclear bodies induced by parvovirus infection. *J. Virol.*, 76(8):3892–3904, Apr 2002.
- [506] Yu, X., Zhang, J., Hong, L., Wang, J., Yuan, Z., Zhang, X., and Ghildyal, R. High prevalence of human parvovirus 4 infection in HBV and HCV infected individuals in Shanghai. *PLoS ONE*, 7(1):e29474, 2012.
- [507] Zadori, Z., Szelei, J., and Tijssen, P. SAT: a late NS protein of porcine parvovirus. *J. Virol.*, 79(20): 13129–13138, Oct 2005.
- [508] Zadori, Z., Szelei, J., Lacoste, M. C., Li, Y., Gariepy, S., Raymond, P., Allaire, M., Nabi, I. R., and Tijssen, P. A viral phospholipase A₂ is required for parvovirus infectivity. *Dev. Cell*, 1(2):291–302, Aug 2001.
- [509] Zhao, Q., Gersappe, A., and Pintel, D. J. Efficient excision of the upstream large intron from P4-generated pre-mRNA of the parvovirus minute virus of mice requires at least one donor and the 3' splice site of the small downstream intron. *J. Virol.*, 69(10): 6170–6179, Oct 1995.
- [510] Zhao, Q., Mathur, S., Burger, L. R., and Pintel, D. J. Sequences within the parvovirus minute virus of mice NS2-specific exon are required for inclusion of this exon into spliced steady-state RNA. *J. Virol.*, 69(9):5864–5868, Sep 1995.
- [511] Zhao, Q., Schoborg, R. V., and Pintel, D. J. Alternative splicing of pre-mRNAs encoding the nonstructural proteins of minute virus of mice is facilitated by sequences within the downstream intron. *J. Virol.*, 68(5):2849–2859, May 1994.
- [512] Zhong, L., Li, B., Jayandharan, G., Mah, C. S., Govindasamy, L., Agbandje-McKenna, M., Herzog, R. W., Weigel-Van Aken, K. A., Hobbs, J. A., Zolotukhin, S., Muzyczka, N., and Srivastava, A. Tyrosine-phosphorylation of AAV2 vectors and its consequences on viral intracellular trafficking and transgene expression. *Virology*, 381(2):194–202, Nov 2008.
- [513] Zhong, L., Li, B., Mah, C. S., Govindasamy, L., Agbandje-McKenna, M., Cooper, M., Herzog, R. W., Zolotukhin, I., Warrington, K. H., Weigel-Van Aken, K. A., Hobbs, J. A., Zolotukhin, S., Muzyczka, N., and Srivastava, A. Next generation of adeno-associated virus 2 vectors: point mutations in tyrosines lead to high-efficiency transduction at lower doses. *Proc. Natl. Acad. Sci. U.S.A.*, 105(22):7827–7832, Jun 2008.
- [514] Zlotnick, A. and Mukhopadhyay, S. Virus assembly, allostery and antivirals. *Trends Microbiol.*, 19(1): 14–23, Jan 2011.
- [515] Zsak, L., Strother, K. O., and Kisary, J. Partial genome sequence analysis of parvoviruses associated with enteric disease in poultry. *Avian Pathol.*, 37(4):435–441, Aug 2008.

Declaration of consent

on the basis of Article 28 para. 2 of the RSL05 phil.-nat.

Name/First Name: Wolfisberg Raphael

Matriculation Number: 07-120-074

Study program: Freies Doktorat

Bachelor

Master

Dissertation

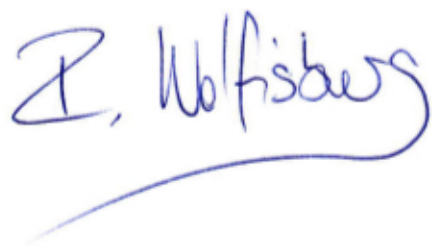
Title of the thesis: Characterization of the pre-lytic active egress of a non-enveloped virus.

Supervisor: Prof. Dr. Christoph Kempf and PD Dr. Carlos Ros

I declare herewith that this thesis is my own work and that I have not used any sources other than those stated. I have indicated the adoption of quotations as well as thoughts taken from other authors as such in the thesis. I am aware that the Senate pursuant to Article 36 para. 1 lit. r of the University Act of 5 September, 1996 is authorised to revoke the title awarded on the basis of this thesis. I allow herewith inspection in this thesis.

Bern, 01. 10. 2015

Place/Date

A handwritten signature in blue ink, appearing to read "R. Wolfisberg", is written over a blue curved line.

Signature

Curriculum Vitae

Personal Details

First Name	Raphael
Surname	Wolfisberg
Date of Birth	14. May 1988
Nationality	Swiss
E-mail	raphael.w@hotmail.com
Mobile	+41 (0) 79 837 19 62



Education

Mar. 2012 - present	PhD in the Department of Chemistry and Biochemistry (DCB) University of Bern, Switzerland Title of the PhD thesis: "Characterization of the pre-lytic active egress of a non-enveloped virus." Supervisors: PD Dr. Carlos Ros and Prof. Dr. Christoph Kempf
Oct. - Dec. 2013	Scientific exchange at Centro de Biología Molecular Severo Ochoa Universidad Autónoma de Madrid, Spain Collaboration with Prof. Dr. José María Almendral del Río
Sept. 2010 - Jan. 2012	Master of Science (MSc) in Chemistry and Molecular Science DCB, University of Bern, Switzerland Title of the master thesis: "Changing the surface of human parvovirus B19." Supervisors: PD Dr. Carlos Ros and Prof. Dr. Christoph Kempf
Sept. 2007 - Aug. 2010	Bachelor of Science (BSc) in Chemistry or Biochemistry DCB, University of Bern, Switzerland Title of the bachelor thesis: "Die Suche nach dem NMD Mechanismus in <i>Trypanosoma brucei</i> ." Supervisor: Prof. Dr. André Schneider

Teaching experience

Teaching of undergraduate students in biochemistry internships at the University of Bern.

Conferences

22.-26. June 2014 15th Biennial International Parvovirus Workshop Bordeaux, France

Publications

Peer-reviewed journal articles

Wolfisberg R, Ruprecht N, Kempf C, Ros C. Impaired genome encapsidation restricts the *in vitro* propagation of human parvovirus B19.

J Virol Methods. 2013 Oct;193(1):215-25.

Wolfisberg R, Kempf C, Ros C. Late maturation steps in the nucleus preceding pre-lytic active egress of a non-enveloped parvovirus.

Manuscript in preparation

Skills

Languages	German (Mother tongue), English (Advanced), French (Intermediate level), Spanish (Basic knowledge)
Operating Systems	Microsoft Windows, Apple OS X
Programs	Typesetting (Apple iWork, L ^A T _E X, Microsoft Office) Molecular modeling (PyMOL, UCSF Chimera) Data processing (GraphPad Prism, Mathcad)

Other activities

Organizing and supervising holidays for physically and mentally handicapped persons with Insieme Luzern in collaboration with the Swiss civil defense.

Accordion (Handharmonikaorchester Solothurn)

Athletics (KTV Neuenkirch)

References

PD Dr. Carlos Ros	Prof. Dr. Christoph Kempf
Department of Chemistry and Biochemistry	Department of Chemistry and Biochemistry
University of Bern	University of Bern
Freiestrasse 3, 3012 Bern	Freiestrasse 3, 3012 Bern
Switzerland	Switzerland
+41 (0) 31 631 43 49	+41 (0) 31 631 43 31

Prof. Dr. José María Almendral del Río
Centro de Biología Molecular Severo Ochoa
Universidad Autónoma de Madrid
Cantoblanco, 28049 Madrid
Spain
+34 (0) 91 196 45 59